

**Symposium DD: Low-dimensional materials-synthesis, assembly, property scaling
and modeling**

Grant Number: N00014-07-1-0660

Contact personnel:

Donna Gillespie
Symposium Funding Administrator
Materials Research Society
506 Keystone Drive, Warrendale, PA 15086-7573
gillespie@mrs.org
724-779-3004

Masaru Kuno
251 Nieuwland Science Hall
Department of Chemistry and Biochemistry
University of Notre Dame
Notre Dame, IN, 46556
mkuno@nd.edu
574-631-0494

Funding requested: \$4,500

Duration of effort:

April 9-13, 2007

ONR contact:

Dr. Chagaan Baatar (Program officer)
Office of Naval Research
One, Liberty Center
875 North Randolph St. Suite 1425
Arlington, VA 22203-1995
703-696-0483
baatarc@onr.navy.mil

20080630 209

REPORT DOCUMENTATION PAGE					Form Approved OMB No. 0704-0188	
<p>The public reporting burden for this collection of information is estimated to average 1 hour per response, including the time for reviewing instructions, searching existing data sources, gathering and maintaining the data needed, and completing and reviewing the collection of information. Send comments regarding this burden estimate or any other aspect of this collection of information, including suggestions for reducing the burden, to Department of Defense, Washington Headquarters Services, Directorate for Information Operations and Reports (0704-0188), 1215 Jefferson Davis Highway, Suite 1204, Arlington, VA 22202-4302. Respondents should be aware that notwithstanding any other provision of law, no person shall be subject to any penalty for failing to comply with a collection of information if it does not display a currently valid OMB control number.</p> <p>PLEASE DO NOT RETURN YOUR FORM TO THE ABOVE ADDRESS.</p>						
1. REPORT DATE (DD-MM-YYYY) 06/24/2008		2. REPORT TYPE Final Technical Report		3. DATES COVERED (From - To) 2/23/2007 - 12/31/2007		
4. TITLE AND SUBTITLE Symposium DD: Low-Dimensional Materials - Synthesis, Assembly, Property Scaling, and Modeling				5a. CONTRACT NUMBER		
				5b. GRANT NUMBER N00014-07-1-0660		
				5c. PROGRAM ELEMENT NUMBER		
6. AUTHOR(S) Dr. Moosub Shim, University of Illinois-Urbana				5d. PROJECT NUMBER		
				5e. TASK NUMBER		
				5f. WORK UNIT NUMBER		
7. PERFORMING ORGANIZATION NAME(S) AND ADDRESS(ES) Materials Research Society 506 Keystone Dr Warrendale PA 15086				8. PERFORMING ORGANIZATION REPORT NUMBER		
9. SPONSORING/MONITORING AGENCY NAME(S) AND ADDRESS(ES) ONR Regional Office Chicago 536 S Clark St Rm 208 Chicago IL 60605-1588				10. SPONSOR/MONITOR'S ACRONYM(S) ONR		
				11. SPONSOR/MONITOR'S REPORT NUMBER(S)		
12. DISTRIBUTION/AVAILABILITY STATEMENT Distribution limitation - None						
13. SUPPLEMENTARY NOTES None						
14. ABSTRACT Attachments: Summary & Abstracts						
15. SUBJECT TERMS						
16. SECURITY CLASSIFICATION OF:			17. LIMITATION OF ABSTRACT None	18. NUMBER OF PAGES 81	19a. NAME OF RESPONSIBLE PERSON Donna J. Gillespie, Symposium Fund Administrator	
a. REPORT N/A	b. ABSTRACT N/A	c. THIS PAGE N/A			19b. TELEPHONE NUMBER (Include area code) 724-779-3004 Ext 202/gillespie@mrs.org	

Executive summary:

Low-dimensional materials such as nanocrystals, nanowires, and nanotubes are at the forefront of materials research. Novel physical and chemical phenomena observed in these systems allow us to envision a variety of next-generation technologies such as high-performance transistors for nano- and microelectronics, low-cost, high-efficiency photovoltaics, high-density magnetic storage media, nano-electromechanical systems and miniaturized biosensors. Fundamental challenges include synthesis of chemically and structurally well-defined nanoscale materials, developing methods of assembly, and establishing an understanding of how properties of isolated nano-objects change and scale as they are incorporated into functional architectures at multiple-length scales. Robust and verified theoretical methods and computational tools ranging from solid-state theory, surface science and computational quantum chemistry to theories that address multiple-length- and time-scale integration need to be developed in parallel with synthetic and experimental efforts.

This symposium will focus on advanced syntheses of nanoscale materials (e.g. heterostructures of nanoparticles and nanowires); directed and self assembly of functional architectures (e.g. bio-inspired assemblies and combined top-down/bottom-up patterning); properties of isolated nanoscale objects; how these properties change and scale (in relation to areas such as nanoelectronics, magnetism, photonics, photovoltaics, and bio-imaging); and computational applications and theoretical developments (related to the design, synthesis, properties and understanding of low-dimensional nanomaterial structures, assemblies and phenomena)

Session topics:

- Advanced synthesis of nanoscale materials (e.g. heterostructures, anisotropic shapes and multifunctional materials)
- Doping low-dimensional materials
- Directed and self assembly, and patterning
- Nano/bio interfaces and assemblies
- Electron transport in individual nanocrystals, nanowires, and nanotubes, and in their assemblies/networks
- Optical properties of nanoscale materials in complex/functional systems
- Quantum mechanical to atomistic to mesoscale modeling
- Interaction potentials
- Multiscale theories that address challenges of length- and time-scale integration

Invites speakers include:

Jerry Bernholc (NC State), William Buhro (Washington Univ. St. Louis), Marija Drndic (U. Penn), Venkat Ganesan (UT Austin), Valeriy Ginzburg (Dow Chemical), Bill Goddard (Caltech), Philippe Guyot-Sionnest (Chicago), Bob Hamers (U. Wisconsin), Peggy Hines (Evident Tech.) Taeghwan Hyeon (Seoul National), Heinrich Jaeger (Chicago), Yoshi Kawazoe (Tohoku Univ.) Victor Klimov (LANL), Brian Korgel (UT Austin), Todd Krauss (Rochester), Michael Mackay (Mich. St.) Alf Mews (Univ. Siegen), Ken Schweizer (UIUC), Horst Weller (Hamburg), Peidong Yang (UC Berkeley)

Symposium Organizers:

Moonsub Shim
University of Illinois, Urbana-Champaign
Dept. Materials Science and Engineering
mshim@uiuc.edu

Masaru Kuno
University of Notre Dame
Department of Chemistry and Biochemistry
Notre Dame Radiation Laboratory
mkuno@nd.edu

Xiao-Min Lin
Argonne National Laboratory
Materials Science Division and Chemistry Division
xmlin@anl.gov

Ruth Pachter
Air Force Research Laboratory
Materials and Manufacturing Directorate
Ruth.pachter@wpafb.af.mil

Sanat Kumar
Rensselaer Polytechnic Institute
Department of Chemical and Biological Engineering
Kumars5@rpi.edu

Final report:

I. Primary Objectives and Scope of the Symposium

The primary goal of this symposium was to bring together researchers in the growing field of nanoscale materials in order to promote synergy between modeling and experiments along with concurrent advances in materials synthesis and assembly.

Registration fee waivers and travel assistance provided by ONR enabled 19 students and 6 invited speakers (including 2 women faculty/scientists and 2 junior faculty members) to attend the conference.

II. Highlights: Research Activities and Findings

A total of 340 abstracts were submitted to this symposium. This was the largest number of participants for a given Spring MRS session. To accommodate as many researchers as possible, an additional joint session with symposium EE (Applications of Nanotubes and Nanowires) was organized. Over 130 oral presentations and over 140 posters resulted during the entire week of the conference.

Student Highlights:

- Funds from ONR provided meeting registration or travel reimbursements for 19 students. Most would have otherwise have had financial difficulties in attending the meeting.
- A large fraction of the oral and poster presentations were given by students. Numerous discussions were initiated by them during the question and answer sessions.
- A student presentation was highlighted by a MRS electronic newsletter, which described the meeting. A copy of the transcript as posted on the MRS website is provided below.

“Na Li of the Department of Mechanical Engineering and Materials Science at Duke University presented work that challenged the "line tension" model of nanowire growth and suggested a "chemical tension" model of vapor-liquid-solid (VLS) nanostructure growth. Her presentation was entitled "Chemical Tension in VLS Nanostructure Growth Process: From Nanohillocks to Nanowires." A nanohillock is a small fragment of a nanowire that results when growth stops prematurely. The line tension model uses Neumann's quadrilateral relation to describe the quasistatic stress balance scheme of nanowire growth. However, for a nanowire to attain a steady growth rate requires negative line tension, which Li says is only theoretically possible. Instead, her group has taken a different approach based on energetics, called the "chemical tension" model, in which minimization of ΔG of the liquid droplet is the controlling factor. At equilibrium, a balance is struck between static physical tension and dynamic chemical tension. Chemical tension thus becomes the driving force for a wire to grow in this model.”

Symposium Highlights

Researchers from various disciplines presented their progress in areas ranging from fundamental physics/chemistry to advances in nanomaterials applications. In the area of optical properties of nanoscale materials, Victor Klimov (LANL) presented Type-II band offset CdS/ZnSe core/shell semiconductor nanostructures for the purpose of manipulate exciton-exciton interactions. This has led to a new strategy for developing nanocrystal-based lasers. In a related topic, Philippe Guyot-Sionnest (U. Chicago) discussed effects of charges on the optical properties of semiconductor nanocrystals and their implications on fundamental processes governing carrier dynamics and photoluminescence. Within the context of 1D materials, Bill Buhro (Washington University) demonstrated charge trap-induced "blinking" of the emission from solution-based semiconductor nanowires. Analogous charges have also been shown to induce chemistry that can change the shape/morphology of nanostructures. In this respect, Carolina Novo (U. Melbourne) described the shape evolution in gold nanorods upon electron injection due to Rayleigh instability. Likewise, Vishva Ray (UT Arlington) presented strategies to exploit electrostatic interactions between charged nanoparticles and charge-patterned substrates to "funnel" nanoparticles into precise predetermined locations. Other directions in assembling and patterning nanoscale materials presented during the symposium included exploiting bubble expansion for large-area aligned nanowire deposition. This work was described by Guihua Yu (Harvard). Along the same lines, linear arrays of nanoparticles, generated by drying a solution of nanoparticles at the interface between a sphere and a flat substrate, was discussed by Zhiquan Lin (Iowa State). Prospects for nanoscale materials in future technologies were highlighted by Margaret Hines (Evident Tech.) who described the frontiers in large scale production of semiconductor nanocrystals and their incorporation into devices such as LEDs. Taeghwan Hyeon (Seoul National U) described the utilization of MnO nanoparticles for biomedical imaging where the contrast and resolution in non-destructive MRI images can be improved to a point where it is comparable to postmortem histology studies. The high resolution and contrast achieved by using magnetic nanoparticles in MRI may lead to breakthroughs in early detection of cancer, brain tumor, and other diseases.

III. Interactions/Networking /Training Experiences

There were 5 full days of oral presentation sessions with each session topic highlighted by one or two invited speakers. Invited talks were chosen to educate researchers about the state-of-the-art in nanoscale materials. The symposium also utilized three full evenings for poster sessions. Both oral and poster sessions were well-attended, providing opportunities for student presenters and attendees to interact and network with researchers from other fields.

IV. Contributions to Education and Outreach

Funds from ONR were used to cover the costs of meeting registration and/or travel reimbursements for 19 graduate students and 6 invited speakers. This includes 2 women faculty/scientists and 2 junior faculty members. For student aid, recipients were notified by email about this opportunity. They were chosen among the presenters based on their educational status (e.g. graduate student vs. postdoctoral) and financial needs. We have received feedback from several students indicating their appreciation for the opportunity.

Symposium audio/visual needs were also handled by graduate student symposium aids giving them additional opportunities to interact with invited speakers and other researchers in the symposium.

V. Contributions within the discipline

This symposium contributed to the dissemination of frontier research on nanoscale materials through numerous oral and poster presentations over 5 days. Topics ranged from fundamental optical properties of nanocrystal quantum dots and their syntheses to technological advances in utilizing nanoscale materials in optoelectronic devices. The joint session together with symposium EE provided many opportunities for researchers from various disciplines to interact and to initiate discussions, enabling future advances in the field.

VI. Contributions to other disciplines

Presentations on applications and devices based on nanoscale materials provided a forum for highlighting the impact of nanoscience and nanotechnology in other fields such as solar energy conversion and biomedical imaging.



Materials Research Society
The Materials Gateway

[Home](#) [Meetings](#) [MRS Meeting Archives](#) [2007 Spring Meeting](#) [Abstracts](#)

Symposium DD: Low-Dimensional Materials-- Synthesis, Assembly, Property Scaling, and Modeling

April 9 - 13, 2007

Chairs

Moonsub Shim

Dept. of Materials Science and Engineering
University of Illinois, Urbana-Champaign
1304 W. Green St.
Urbana, IL 61801
217-333-7361

Xiao-Min Lin

Materials Science Division and Chemistry Division Center for
Nanoscale Materials
Argonne National Laboratory
Bldg. 200, A-181
9700 S. Cass Ave.
Argonne, IL 60439
630-252-6289

Sanat Kumar

Dept. of Chemical and Biological Engineering
Rensselaer Polytechnic Institute
Rm. 132, Ricketts Bldg.
110 8th St.
Troy, NY 12180
518-276-3032

Masaru Kuno

Dept. of Chemistry and Biochemistry Notre Dame
Radiation Laboratory
University of Notre Dame
251 Nieuwland Science Hall
Notre Dame, IN 46556
574-631-0494

Ruth Pachter

Materials and Manufacturing Directorate AFRL/MLPJ
Air Force Research Laboratory
3005 Hobson Way
Wright-Patterson AFB, OH 45433-7702
937-255-9689



Symposium Support

The Air Force Office of Scientific Research, AFRL
The Dow Chemical Company
Evident Technologies
National Science Foundation
Office of Naval Research

Proceedings to be published online
(see Proceedings Library at www.mrs.org/publications_library)
as volume 1017E
of the Materials Research Society
Symposium Proceedings Series.

* Invited paper

SESSION DD1/EE1: Joint Session: Synthesis of Nanotubes and Nanowires
Chair: Jie Liu
Monday Morning, April 9, 2007
Room 2001 (Moscone West)

8:00 AM DD1.1/EE1.1

Controlling Growth of Carbon Nanotubes for Devices John Robertson, Stephan Hofmann, Mirco Cantoro and Guofang Zhong; Engineering, Cambridge University, Cambridge, United Kingdom.

Carbon nanotubes have unique properties which may lead to their use in high performance electronic devices such as vias, interconnects and FETs. However, these applications require a much better control of the growth process than presently exists. For Vias formed by a bunch of multi-walled nanotubes, the effective resistance must be reduced to 10 ohms. Unless the contact resistance is very low, this requires growth of very closely spaced MWNTs. MWNTs grown by PECVD or CVD are typically grown from a Ni or Fe which has been restructured into a nano-particle from which the nanotube nucleates. But this tends to restrict the site density. On the other hand, FETs require use of only semiconducting single wall nanotubes, which in effect requires some chiral selection, or post-growth separation, which is uneconomic. Both applications place temperature limits on the growth process. We have shown by recent work an improved understanding of the growth process which helps in each of these aspects, such as the ability to grow SNWTs at only 350C by purely thermal CVD [2], and the highest nucleation density and catalyst efficiency of vertically aligned SWNT mats [3]. 1 S Hofmann, et al, App Phys Lett 83 135 (2003); J App Phys 98 034308 (2005) 2 M Cantoro et al, Nanolett 6 1107 (2006) 3 G Zhong et al, Carbon 44 2009 (2006)

8:15 AM DD1.2/EE1.2

Combinatorial Control of Catalysts for Carbon Nanotube Growth: From Sparse Networks for Transparent Electrodes to Dense Forests for Mass Production Suguru Noda¹, Hisashi Sugime¹, Kei Hasegawa¹, Ryuhei Itoh¹, Shingo Morokuma¹, Kazunori Kakehi¹, Toshio Osawa¹, Shigeo Maruyama² and Yukio Yamaguchi¹; ¹Department of Chemical System Engineering, The University of Tokyo, Tokyo, Japan; ²Department of Mechanical Engineering, The University of Tokyo, Tokyo, Japan.

For single-walled carbon nanotubes (SWNTs), various applications have been proposed and intensively studied. To realize high-value-added devices such as integrated circuits, many development challenges still exist in the structural control from the chirality of individual SWNTs to the position and orientation of numerous short SWNTs. On the other hand, if the SWNTs can be grown at a low cost, other applications such as transparent conducting films may be realized with fewer innovations in processing technology. In this paper, we applied our combinatorial method [1,2] for catalyst screening and grew SWNTs on substrates at various areal densities and lengths. Co-Mo binary catalysts are known effective to grow SWNTs either from CO and C₂H₅OH. However, different values are reported as the optimum Co/Mo atomic ratio; 1/3 for the former [3] and 1/1 for the latter [4]. We grew SWNTs from C₂H₅OH at 1073 K and 0.4-4 kPa for 3-30 min on a catalyst library with orthogonal thickness profiles of 0.01-0.8 nm Co and 0.03-2 nm Mo. Both of those two regions proved catalytically active, and in addition, another region with a large Co/Mo ratio became active at 4 kPa after a few minute incubation time where nanotubes containing SWNTs grew rapidly. By controlling reaction and catalyst conditions, the areal density and length of nanotubes can be controlled. Films of bundled, networked nanotubes show optical and electrical properties depending on the structure. For example, a nanotube film on a quartz glass substrate showed a 85 % transmittance and a 8 kΩ/sq. sheet resistance, whereas a film with a larger nanotube length and a lower areal density showed a 92 % transmittance and a 2 kΩ/sq. sheet resistance. Properties of nanotube films can be tailored in this way. Fe/Al₂O₃ can rapidly grow SWNTs from C₂H₄ when a small amount of H₂O is added [5]. We applied our combinatorial method to this reaction system. The Fe/Al₂O₃ catalyst library grew nanotubes of various diameters and the nanotube yield was largely dependent on the nominal Fe thickness. Millimeter-thick films of nanotubes containing SWNTs were formed in 10 min after a complicated optimization among partial pressures of C₂H₄, H₂ and H₂O and temperature. Some of these films can be easily separated from the substrate, and this growth mode may be applied for the mass production of SWNTs. [1] S. Noda, et al., Appl. Phys. Lett. 86, 173106 (2005). [2] S. Noda, et al., Carbon 44, 1414 (2006). [3] J.E. Herrera, et al., J. Catal. 204, 129 (2001). [4] Y. Murakami, et al., Chem. Phys. Lett. 385, 298 (2004). [5] K. Hata, et al., Science 306, 1362 (2004).

8:30 AM DD1.3/EE1.3

Dependence of Carbon Nanotube (CNT) Length and Growth Rate upon Temperature in the Growth of CNT by Metal-catalyzed Chemical Vapor Deposition. Michael J. Bronikowski, Jet Propulsion Laboratory, California Institute of Technology, Pasadena, California.

Growth of carbon nanotubes (CNT) by metal-catalyzed chemical vapor deposition (CVD) upon flat silicon substrates is studied as a function of growth temperature. It is found that, at all temperatures, CNT grow at a constant rate for a certain amount of growth time, after which growth ceases; the product of the growth rate and the growth time gives the ultimate length of the CNT. Both the growth rate and the growth time are found to depend on the CVD temperature, and this dependence is such that the ultimate CNT length increases as temperature decreases, i.e., longer CNT can be grown at lower temperatures than at higher temperatures. This surprising and non-intuitive result reflects the interaction of competing factors affecting the CNT growth: the rate at which carbon is deposited and incorporated into CNT vs the rate at which catalytic metal particles become inactive. CNT bundles as long as one millimeter have been grown at temperatures as low as 600 C.

8:45 AM DD1.4/EE1.4

Control of Catalyst Nanoparticles for Selective CVD Growth of Carbon Nanotubes. Yunyu Wang¹, Bin Li¹, Zhiquan Luo¹, Li Shi², Zhen Yao³, Eugene Bryan⁴, Robert J. Nemanich⁵ and Paul S. Ho^{1,2}; ¹Microelectronics Research Center, The University of Texas at Austin, Austin, Texas; ²The Department of Mechanical Engineering, The University of Texas at Austin, Austin, Texas; ³The Department of Physics, The University of Texas at Austin, Austin, Texas; ⁴The Department of Materials Science and Engineering, North Carolina State University, Raleigh, North Carolina; ⁵The Department of Physics, North Carolina State University, Raleigh, North Carolina.

A proper control of size, density and morphology of catalyst nanoparticles is essential for selective growth of carbon nanotubes (CNT). In this study, catalyst nanoparticles were formed by depositing Fe thin films of 1.5 to 9 nm in thickness on a supporting layer. Different supporting materials including high surface tension tantalum (Ta), Palladium (Pd), Chromium (Cr) and low surface tension silicon dioxide (SiO₂) were used. The Fe nanoparticles were formed by annealing at 700 C on the supporting layer and their size, density and morphology were found to greatly depend on the supporting materials. In particular, Fe nanoparticles revealed a Volmer-Weber growth mode on SiO₂ but a Stranski-Krastanov mode on tantalum, which can be attributed to the different surface tension of the supporting layers and their interface with the catalyst particle. Chemical vapor deposition (CVD) of CNTs was conducted subsequently. It was found that the growth rate and growth mode are distinctly different on different supporting layers. Vertically aligned CNTs with density exceeding 10E 11 tubes per cm² can be formed using Fe nanoparticles properly deposited on a Ta substrate.

9:00 AM DD1.5/EE1.5

Synthesis and Structural Characterization of Aligned Carbon Nanotubes on Sapphire and Quartz Substrates Lewis Gomez¹, Bo Lei², Kounghmin Ryu², Alexander Badmaev², Xiaolei Liu², Steve Cronin² and Chongwu Zhou²; ¹Chemistry, USC, Los Angeles, California; ²Electrophysics, USC, Los Angeles, California.

Synthesis of massively aligned single-walled carbon nanotubes has stimulated significant interest due to their potential for integrated nanotube circuits and systems. Despite recent success on the synthesis, there is still a lack of study on the influence of the substrate on the structural and ultimately physical properties of the nanotubes. In this talk we will present our recent advance in aligned nanotube synthesis and also in-depth Raman characterization of the nanotubes obtained. The synthesis of aligned nanotubes was achieved using a chemical vapor deposition technique with Ferritin as the catalyst and a-plane sapphire and mistcut quartz as the substrates. Simultaneous control over the nanotube orientation and position has also been achieved by patterning catalyst at desired sites on the crystalline substrates. The nanotubes on a-plane sapphire were found to lie normal to the c-axis of the substrate, while the nanotubes on quartz followed the step edges of the miscut substrates. AFM and SEM microscopy combined with vibrational resonantly enhanced micro Raman characterization was proved to be a powerful tool to structurally characterize the samples at the single nanotube level. We use three different laser energies to determine diameter distribution and non-nanotube carbon impurities. The metallic to semiconducting ratio analysis of the carbon nanotubes revealed a metallic nanotube content of ~ 27%. Polarized Raman spectra of nanotubes showed a suppression of the C=C stretching mode when the laser electric field axis was perpendicular to the nanotubes principal axis. Furthermore, electrical properties on nanotubes produced on the different substrates were evaluated. Our results demonstrate that the surface molecular arrangement of the substrate as well as surface-carbon interactions play an important role in the properties of the synthesized nanotubes.

9:15 AM DD1.6/EE1.6

Influence of Hydrogen Level During the Growth Process on the Properties of Single-wall Carbon Nanotubes. Alexandru S. Biris^{1,2}, Alexandru R. Biris³, Dan Lupu³, Zhongrui Li², Enkeleda Dervishi^{1,2} and Viney Saini^{1,2}; ¹Applied Science, University of Arkansas at Little Rock, Little Rock, Arkansas; ²Nanotechnology Center, University of Arkansas at Little Rock, Little Rock, Arkansas; ³National Institute for Research and Development of Isotopic and Molecular Technologies, Cluj Napoca, Romania.

Single-wall carbon nanotubes were synthesized on a Fe-Mo/MgO catalyst by catalytic chemical vapor deposition from methane and with argon as a carrier gas. Controlled amounts (15, 30, 45, 60, 90 ml/min) of hydrogen were introduced in separate experiments along with the carbon source. The properties and morphology of the single-wall carbon nanotubes generated during these processes were monitored by transmission electron microscopy, Raman and UV-Vis-NIR spectroscopy, and thermogravimetric analysis. The nanotubes with the highest crystallinity were obtained when 60 ml/min of hydrogen was introduced in the reactor. By monitoring the radial breathing modes (RBM) in the Raman spectra of the single-wall carbon nanotube samples we observed a variation in the number and position of peaks with the flow level of hydrogen, indicating morphological changes of the catalyst systems.

9:30 AM DD1.7/EE1.7

High Yield Multiwall Carbon Nanotube Synthesis in Supercritical Fluids Danielle Kristin Smith, Doh C. Lee and Brian A. Korgel; Chemical Engineering, University of Texas at Austin, Austin, Texas.

Multiwall carbon nanotubes (MWNTs) were synthesized in supercritical toluene at temperatures ranging from 600 to 645 °C at 8.3 MPa using ferrocene, cobaltocene, nickelocene, Fe, and Co nanocrystals as catalysts. A continuous flow reactor was used to produce nanotubes with outer diameters of 10 - 50 nm and wall thicknesses of 5 - 20 nm. In this supercritical fluid synthesis, toluene served as both the solvent and the primary carbon source for nanotube formation. We also discovered that supplemental carbon sources, either hexane or ethanol (30 vol %), increased the yield of the carbon nanotubes relative to pure toluene by almost an order of magnitude. Additionally, catalytic amounts of water (0.75 vol %) minimized the formation of carbon filaments and amorphous carbon deposition. Cobalt and nickel precursors in addition to the use of a continuous flow reactor led to much higher yields than previous batch reactions in supercritical toluene. Using cobaltocene as a catalyst, with ethanol as a supplemental carbon source, gave the highest percentage of nanotubes in the product (70%) and the highest conversion of toluene to MWNTs (4%). Cobaltocene was also the best catalyst in terms of purity of the product with the highest proportion of carbon nanotubes produced relative to carbon filaments and amorphous carbon. These observations might be explained by examining the phase diagrams, which report higher carbon solubility into Co compared to Ni and Fe at temperatures of 600 to 650 °C. The MWNTs generated in this supercritical fluid system tended to exhibit bamboo morphology and appear to grow by a folded-growth mechanism with graphitic sheets wrapped around the seed metal particles. Many MWNTs exhibited significant defects in their graphitic layers, resulting in curly and kinked nanowires. In some cases where cobaltocene was used as a catalyst, the nanowire bending was consistent along the length of the nanotube, resulting in coiled nanotube formation, with the appearance of springs, hairpins, lassos, and coiled ropes. In future work, conditions might be identified that will enable SWNT synthesis.

9:45 AM *DD1.8/EE1.8

Synthesis and Applications of Classes of Non-carbonaceous Nanostructures. Stanislaus Wong, Department of Chemistry, SUNY Stony Brook, Stony Brook, New York; Condensed Matter Physics and Materials Sciences Department, Brookhaven National Laboratory, Upton, New York.

Nanoscale structures, such as nanoparticles, nanorods, nanowires, nanocubes, and nanotubes, have attracted extensive synthetic attention as a result of their novel size-dependent properties. Ideally, the net result of nanoscale synthesis is the production of structures that achieve monodispersity, stability, and crystallinity with a predictable morphology. Many of the synthetic methods used to attain these goals have been based on principles derived from semiconductor technology, solid state chemistry, and molecular inorganic cluster chemistry. We describe a number of advances that have been made in the reproducible synthesis of various non-carbonaceous nanomaterials, including alkaline earth metal titanates, alkali metal titanates, bismuth ferrites, iron oxides, ABO₄-type oxides, fluorides, as well as miscellaneous classes of ternary metal oxides, and comment on their associated applications and properties.

10:30 AM *DD1.9/EE1.9

Nanowires and Nanotubes Synthesized in Solution: Their Chemistry, Twins and Branching. Brian A. Korgel, Chemical Engineering, University of Texas at Austin, Austin, Texas.

Crystalline high aspect ratio semiconductor nanowires can be synthesized in solution using metal nanocrystals to seed their growth. Solution approaches have the potential for mass production of these new materials on the kg/day scale, yet the fundamental chemistry of these systems must be well understood for this to happen. In this talk, I will summarize what we currently understand about nanowire growth in solution by the supercritical fluid-liquid-solid (SFLS) and solution-liquid-solid (SLS) mechanisms. (1) We find that Si and Ge nanowires can be produced using alternatives to gold, such as nickel, cobalt and copper at growth temperatures well below their eutectic temperatures. These metals seed nanowire growth via the formation of solid-phase alloys, as opposed to a liquid-phase eutectic. (2) Small additions of impurities to the reaction can lead to dramatic differences in product morphology. In the case of Si, the addition of a small amount of water and oxygen impurity into the Cu nanocrystal-seeded growth of Si nanowires leads to silica nanotubes. In some cases, these nanotubes are coiled. (3) In some nanowire systems, we have observed a tendency for branched growth. Branching in ZnSe nanowires for example appears to be encouraged by the presence of twinning defects in the nanowires. (4) Twins appear to occur in many nanowire systems and are a very common extended defect in semiconductor nanowires. I will present a semi-quantitative model that describes the factors that lead to twinning and which metal/semiconductor systems allow and prevent twinning.

11:00 AM DD1.10/EE1.10

Alternative Catalysts For Si-Technology Compatible Growth Of Si Nanowires. Francesca Iacopi¹, Philippe M Vereecken¹, Nele Moelans², Bart Blanpain² and Hefin Griffiths³; ¹IMEC, Leuven, Belgium; ²MTM, Katholieke Universiteit Leuven, Leuven, Belgium; ³Oxford Instruments, Bristol, United Kingdom.

Au has been widely demonstrated in literature as an efficient metal catalyst for the growth of semiconducting nanowires [1]. Also metals such as Ag, Cu, Pd have been shown to be efficient catalysts for growth of Si whiskers [2]. Nevertheless, from a Si semiconductor technology point of view, most of those are undesired metals, either because their diffusion into bulk silicon leads to the formation of mid gap states [3], or because they react with Si, leading to uncertainties on the final stoichiometry of the precipitate. In order to allow a viable evolutionary path from the conventional planar CMOS technologies to 1D nanowire-based devices, alternative catalyst materials more compatible with Si and allowing nanowire growth at temperatures at least around or below 500°C need to be established. In this context, feasibility for growth of Si nanowires catalysed by Indium nanoparticles was investigated. Indium shows several advantages: does not react with Si, is compatible with Si technology (it is used as p-type dopant material), and is also a thermodynamically favourable catalyst for Si nanowire growth according to the Vapor-Liquid-Solid (VLS) theory. Indeed, the In-Si system has a low eutectic temperature (157°C) with low Si solubility (0.004%). On the other hand, Indium is not an efficient catalyst for the dehydrogenation reaction of SiH₄, reason why early attempts for Si nanowires growth with In nanoparticles were not successful [2]. Growth experiments were conducted in a Plasma Enhanced Chemical Vapour Deposition system onto (100) Si, previously electroplated with In nanoparticles with diameter ranging roughly between 200nm and 30nm. Slightly tapered Si nanowires were grown at rather high rate (~300nm/min) at 500°C, using silane as precursor gas and low RF power (5W). Tip growth was recognized from the almost spherical In particles observed on the top of the whiskers, in agreement with the VLS model. In addition to In, the efficiency of other Si-compatible metal catalysts such as Al, Sb, Ga is currently under investigation. The selection of the catalyst system will be extended to favourable alloys/compounds by means of thermodynamics calculations of ternary systems with Si. Feasibility for SiGe nanowire growth using the same catalysts will also be investigated. [1] R.S.Wagner, W.C.Ellis, Appl.Phys.Lett. 4 (5), pp.89-90, 1964 [2] G.A.Bootsma, H.J.Gassen, J.Crystal Growth 10, pp.223-234, 1971 [3] S.M.Sze, Physics of Semiconductor Devices, Wiley Interscience, New York, 1981

11:15 AM DD1.11/EE1.11

Plasma-stimulated Control of Silicon Nanowire Nucleation, Orientation and Growth Kinetics. Pavan Reddy K Aella^{1,4}, W. T. Petuskey^{1,4} and S. T. Picraux^{2,3,4}; ¹Department of Chemistry and Biochemistry, Arizona State University, Tempe, Arizona; ²Department of Chemical and Materials Engineering, Arizona State University, Tempe, Arizona; ³Los Alamos National Laboratory, Los Alamos, New Mexico; ⁴Science and Engineering of Materials Graduate Program, Arizona State University, Tempe, Arizona.

Plasma-enhanced chemical vapor deposition is shown to significantly alter the nucleation rate and activation energy for vapor-liquid-solid (VLS) growth of silicon nanowires compared to simple thermal growth, providing new control over nanowire morphologies and new insight into the rate-limiting mechanisms of VLS growth. Initially, catalytic gold films (0.5 - 2 nm thick) were thermally evaporated onto hydrogen terminated Si (100) substrates at room temperature in a UHV deposition system. Subsequently, Si nanowires were grown at 0.5 Torr in atmospheres of 10% SiH₄ in H₂ between 350 to 510°C and RF plasma powers of up to 7.5 W. Field emission SEM images show that thermally grown nanowires on Si (100) substrates nucleate and grow predominantly in <111> directions. In contrast, plasma stimulation significantly enhances the nucleation rate of smaller diameter <110> Si nanowires and also reduces coarsening of Au dots. A comparison of the growth rate vs. temperature for <111> and <110> nanowires shows a large reduction in the activation energy (from 0.74 to 0.26 eV) due to the plasma. The overall growth rate is also greatly enhanced, particularly at low temperatures. Growth rates at 350°C using plasma are an order of magnitude greater than for thermal growth. As temperature is increased there is greater thermal energy for silane dissociation and the effect of plasma becomes less important. Also the growth rate increases linearly with plasma power, which is similar to thin film growth. Under our low temperature LPCVD thermal conditions the predominant source gas is silane while in the case of plasma stimulation, additional dissociation of silane to SiH₃ and SiH₂ species occurs. These results demonstrate that the rate limiting step relates to the kinetics of silicon incorporation at the vapor-liquid interface and not at the liquid-solid interface. They also indicate a lower effective energy is required to drive nucleation under plasma stimulated conditions, presumably due to a plasma-induced increase in chemical potential. Finally, a two step growth method is demonstrated whereby initial plasma excitation nucleates <110> nanowires followed by thermal growth to preferentially form a high density of small diameter <110> nanowires on Si (100) surfaces, greatly limiting the large diameter <111> nanowire formation found under thermal growth conditions with identical Au seeding. This demonstrates the overall effect of the plasma on shortening nucleation times, favoring thinner wires, and thereby dominating the rest of the growth process.

11:30 AM DD1.12/EE1.12

Quantitative Determination of the Nucleation Kinetics of Si Nanowires. grown on Si₃N₄ substrates by the VLS mechanism Bong-Joong Kim¹, Suneel Kodambaka², Mark Reuter², Kathy Reuter², Eric Stach¹ and Frances Ross²; ¹Eric Stach, Purdue University, West Lafayette, Indiana; ²IBM Watson Research Center, Yorktown Heights, New York.

A quantitative understanding of nucleation and growth kinetics for nanowires grown using the VLS (Vapor-Liquid-Solid) process is important for

structural optimization. In order to achieve wafer scale integration of nanowires, we particularly need to understand the reliability of nanowire nucleation and its dependence on growth conditions. Although prior publications have addressed nucleation, a quantitative analysis of the nucleation mechanism has not been carried out to date. Here we report real time transmission electron microscopy measurements of the time required to nucleate Au-catalyzed Si nanowires on amorphous Si₃N₄ substrates by the VLS mechanism. We directly observed all the stages of Si nanowire nucleation, starting from solid, pure Au crystallites, transitioning to liquid Au-Si eutectic droplets as Si flux is supplied by exposing the specimen to disilane, and ending with the formation of a Si nucleus within the liquid droplet. We show that the nucleation time is proportional to the diameter of the Au-Si droplet, contrary to the expected behavior based on the Gibbs-Thomson effect. Furthermore, measurements of the nucleation rate as a function of temperature yield an activation energy for nucleation. We find that the rate limiting step is the thermally activated dissociative adsorption of disilane on the catalyst surface. Additionally, the in-situ analysis reveals that the nucleation rate is proportional to disilane pressure, which is directly correlated with the reactive sticking probability of an incident Si₂H₆ molecule. These measurements may help in designing processing steps to fabricate well-controlled VLS structures for electronic devices.

11:45 AM DD1.13/EE1.13

Self-assembled Tm Silicide Nanowires on Si(001) Studied by STM and TEM. Jiaming Zhang¹, M. A. Crimp¹, Yan Cui² and J. Nogami²;

¹Department of Chemical Engineering and Materials Science, Michigan State University, East Lansing, Michigan; ²Department of Materials Science and Engineering, University of Toronto, Toronto, Ontario, Canada.

Self-assembled rare earth (RE) metal silicide nanowires are promising for application in future nano interconnects and devices. Since the formation of epitaxial silicide nanowires by deposition of RE metals on Si(001) was first discovered, intense interest has been focused on the epitaxial growth mechanism of RE silicides on Si surfaces. Our recent work has shown that Tm silicides form epitaxial nanowires on Si(001). Unlike many of the other nanowire forming RE metals, which have several different polymorphic silicides at about the same stoichiometry, Tm forms three bulk silicides Tm₅Si₃, TmSi, and Tm₃Si₅ with very different compositions and crystal structures. The latter two phases the potential for nanowire formation.

Scanning tunneling microscopy (STM) shows many 3D nanowires with some larger square islands. However, the structures of the nanowires seem to be more complex than in the case of other RE silicides. Surface reconstructions on these indicate strain relief mechanisms within these wires. Plan-view and cross-sectional high resolution transmission electron microscopy (HRTEM) results will be used to correlate silicide crystal structure to island and nanowire morphology.

SESSION DD2:

Chairs: Sanat Kumar and Ruth Pachter
Monday Morning, April 9, 2007
Room 2003 (Moscone West)

8:00 AM *DD2.1

Origin of Molecular Stability and Magnetism Revealed by the Complete Solution of Many-electron Schroedinger Equation. Yoshiyuki Kawazoe, Kenta Hongo, Takayuki Oyamada, Yohei Maruyama and Hiroshi Yasuhara; Institute for Materials Research, Tohoku University, Sendai, Japan.

Based on the present supercomputer power, it is becoming possible to solve the many-body quantum mechanical equation exactly including exchange-correlation potentials. Recently we have revealed that the origin of the molecular stability and magnetism have completely been misunderstood in most of the standard textbooks. (1)Hund found his empirical rule on the maximum ground state spin state in 1925. After this interesting finding many researchers had tried to understand the reason and Slater explained this rule in 1929 by a perturbative approach based on the electron exchange. In most of the textbooks today still use this traditional explanation. However, Slater's explanation has been doubted theoretically by Davidson, Boyd, and other researchers by using Hartree-Fock level and better approximations. We have solved the many-body Shroedinger equation exactly with diffusion quantum Monte Carlo method (DQMC) and finally confirmed that the traditional Slater's explanation is invalid. The exact reason of the Hund's multiplicity rule is that the energy gain for maximum spin state is realized mainly by the electron-nucleus attractive interaction. (2)Another impact of this study is that we clarify the fundamental reason of stability of materials. When atoms gather to form molecules or crystals, energy gain is only achieved by the nucleus-electron attractive force, and electrons come closer to nucleus, the potential energy decreases, and the kinetic energy increases to realize stability of materials. This result proves that the Heitler-London model is invalid, where kinetic energy decreases when molecule is formed from atoms. These recent results indicate that the traditional models are wrong and we should solve the many-body quantum electron problem exactly including exchange-correlation potentials to design new materials with reliability.

8:30 AM *DD2.2

First Principles Structures and Properties of Nanotubes. William A. Goddard, Materials and Process Simulation Center, Caltech, Pasadena, California.

Combining Quantum mechanics with first principles derived reactive force fields (ReaxFF) it is now possible to make reliable predictions on complex structures incorporating one-dimensional nanotubes. We will report here results on two systems 1) metal-carbon nanotube contacts, 2) thermoelectric properties on nanowires and nanotubes, to illustrate the role of theory and computation in characterizing and optimizing such systems.

9:00 AM *DD2.3

Atomic Scale Design of Nanostructures Jerry Bernholc^{1,2}, W. Lu¹, M. Buongiorno Nardelli^{1,2}, V. Meunier², F. Ribeiro¹, S. Wang¹ and Q. Zhao¹;

¹Physics, NC State University, Raleigh, North Carolina; ²CSMD, ORNL, Oak Ridge, Tennessee.

Nanoscale and molecular electronics promises to revolutionize computing, sensing, and electronic warfare. However, molecular-scale control and manufacturing are difficult tasks, which require major advances to become practical in large-scale applications. The development of molecular scale devices and circuits can be greatly enhanced by predictive simulation of their components and by formulating design principles that will make molecular circuitry smaller, more efficient and more reliable. We will discuss three recent applications: (i) Nanotube-cluster systems, which behave as effective chemical sensors whose electrical response changes dramatically upon adsorption of small molecules onto the metal clusters, enabling

detection of minute quantities of adsorbants. (ii) We show that the celebrated Negative Differential Resistance (NDR) effects can be expected for a wide range of small organic molecules attached to semiconductor leads. For example, if benzene is suspended between Si leads, NDR occurs when its LUMO drops below the conduction band edge of the negative lead. For more complex molecules, such as porphyrins, which are candidates for multibit molecular memories, crossing of band edges by various molecular levels leads to multiple NDR effects. (iii) For organic self-assembled ferrocenyl monolayers on gold, NDR occurs due to crossing of the Fermi level by the molecular HOMO. In general, our results show that NDR must occur for surprisingly simple structures. This enables the design of molecule-based NDR devices based mainly on processing considerations, rather than the choice of specific molecules.

9:30 AM DD2.4

Modeling the Conductance of a Nanotube Bundle Connected to a Copper Surface Steven Compemolle^{1,2}, Geoffrey Pourtois², Bart Soree², Wim Magnus² and Arnout Ceulemans¹; ¹Laboratorium voor kwantumchemie, and INPAC - Institute for Nanoscale Physics and Chemistry, Katholieke Universiteit Leuven, Leuven, Belgium; ²IMEC, Leuven, Belgium.

Metallic carbon nanotubes (CNTs) are promising candidates to replace copper interconnects. Knowledge of the contact resistance between the metal and the CNT is therefore indispensable. Previous studies focused mainly on the conductance of a *single* CNT in contact with a metal. However, to optimize the conductance per unit of area a *bundle* of CNTs — as thin and closed-packed as possible — could be used. However, the impact of the small diameter and high packing density on the conductance per CNT are unknown. We present an *ab initio* study on the conductance of a closed-packed bundle of very narrow metallic CNTs vertically placed on top of a Cu(100) surface. The calculations are based on the Landauer-Büttiker formalism. The use of thin metallic CNTs is advantageous, since they can reach a higher intrinsic conductance compared to the wide-diameter metallic CNTs. Both the interface atomic configuration and the CNT packing density were varied. It is observed that the conductance does strongly depend on the exact atomic configuration. A too dense packing can occasionally, but not necessarily, lead to a strong suppression of the conductance per CNT.

10:00 AM *DD2.5

Equilibrium and Dynamics in Polymer-Nanoparticle Mixtures. Venkat Ganesan, Chemical Engineering, The University of Texas at Austin, Austin, Texas; Chemical Engineering, The University of Texas at Austin, Austin, Texas.

Mixtures of polymers and particles occur in a wide variety of applications. Traditional applications of polymers in such systems include their role as colloidal stabilizers, and in rheological modifiers. Many of these applications are characterized by the feature that the polymer size is much smaller than the size of the particle. However, more recent developments in nano- and biotechnology applications have moved the polymer-particle mixtures from the "colloid limit" to the "nanoparticle limit" where the polymer size is comparable to or larger than the size of the particle. This transition to the nanoparticle limit has brought forth new physical aspects and challenges. At the equilibrium level, the curvature of the particle now plays an important role in determining the interactions and phase behavior. At a dynamical level, conventional "continuum" wisdom no longer applies, and counterintuitive phenomena have been observed. This talk will focus on some recent work in our group which addresses the issue, "how does the equilibrium, dynamical and rheological aspects of nanoparticle-polymer mixtures differ from their colloidal counterparts?" It will be demonstrated that many aspects of colloidal physics is still applicable, albeit allowance must be made for polymer-particle, particle-particle and polymer-polymer interactions, particle curvature and the relative sizes of the polymer and particles. In essence, the theoretical predictions delineates the size scales at which the particles cross-over from behaving both in equilibrium and dynamics as a "particle suspension in polymers" to a "solvent for the polymers." Some applications of our findings to the context and experiments of protein-polymer mixtures and polymer nanocomposites will also be presented.

10:30 AM *DD2.6

Theory of Effective Interactions, Structure and Phase Behavior of Polymer Nanocomposites Kenneth S. Schweizer¹, Justin B. Hooper^{1,2} and Lisa Hall¹; ¹Materials Science, University of Illinois, Urbana, Illinois; ²Materials Science, University of Utah, Salt Lake City, Utah.

Microscopic polymer liquid state theory has been employed to study second virial coefficients, the potential of mean force (PMF), pair correlation functions, scattering patterns, and the miscibility of hard spherical nanoparticles in a dense polymer melt over a wide range of interfacial chemistry, chain length, and filler size and volume fraction conditions. A variable strength and range monomer-particle attractive potential is used to probe the material-specific competition between packing entropy and interfacial adsorption. As interfacial cohesion increases the nanoparticle organization evolves from contact depletion aggregation, to well dispersed sterically stabilized behavior associated with a thermodynamically stable polymer coating, to tightly-bridged particles. Near linear scaling of the PMF with the particle/monomer size asymmetry ratio is found, and the spatial range of the interfacial attraction is important in determining nanoparticle organization. Spinodal demixing calculations predict two types of phase separated states which bracket a miscibility window. For weak interfacial attractions an entropy-driven fluid-fluid phase separation occurs, while for strong cohesion an enthalpically driven network or complex formation type of demixing is predicted. The miscibility window at intermediate interfacial attraction strengths represents a compromise between energetic and entropic considerations. Its existence is delicate in the sense that the miscibility window systematically narrows, and is ultimately destroyed, as particle size and/or direct filler-filler attractions increase. The length-scale dependent real space statistical structure has been quantified via calculations of the intermolecular pair correlation functions and partial scattering structure factors. At high filler volume fractions interference between the polymer organization near nanoparticle surfaces results in significant modification of particle packing and degree of collective order. The presence of bound polymer layers in miscible nanocomposites results in microphase-separation-like features in the collective polymer structure factor at small wavevectors, and comparisons with the recent neutron scattering measurements of Kumar and coworkers will be presented. The implications of the theoretical results for the design of thermodynamically and/or kinetically well-dispersed polymer nanocomposites, and the formation of a nonequilibrium network-like material, will be discussed. The theory has also been generalized to treat the consequences of soft intermolecular repulsions, and nonspherical fillers of variable dimensionality including rod, disk and compact molecular-like shapes.

11:00 AM *DD2.7

Nanoscale Phenomena in Polymer - Nanoparticle Blends. Michael E Mackay, Michigan State University, East Lansing, Michigan.

In our previous work, we investigated the effect of polystyrene nanoparticles on the flow properties of entangled polystyrene melts. This is an ideal

system since the particle and polymer are chemically equivalent, and have a similar refractive index, thereby reducing if not eliminating dispersion forces. Thus, the system was thought equivalent to hard spheres dispersed in an entangled polymer melt. Two unusual phenomena were noted in these studies; the viscosity was reduced upon nanoparticle addition and the nanoparticles remained dispersed despite the interparticle gap being smaller than the polymer radius of gyration. The viscosity decrease is not easily explained and it appears as if it is related to introduction of free volume created by the vast surface area generated by the nanoparticles, which excludes the polymer molecules, and an effect which may be related to constraint release. This latter occurrence could be due to the nanoparticles eliminating entanglements due to their presence and allowing the polymer chain to relax more readily. Further study is required to fully understand this phenomenon. This leads to the key point, unless nanoparticles are well dispersed in polymer melts then one would not expect any unusual phenomena to exist. Furthermore, one would expect the equivalent of depletion flocculation to occur at moderate volume fraction since the interparticle gap becomes so small in nano-systems and this simply does not occur. We suggest the dispersion driving force is due to an enthalpy gain the nanoparticles experience. Consider the pure nanoparticle phase, the van der Waals forces effectively propagate over a distance of order δ , however, the interstices between the nanoparticles could be larger than this resulting in a reduced cohesive energy. Distances smaller than δ will of course experience interparticle interactions to delineate an area A_c , the covered area. So, there is an uncovered area ($A - A_c$), A is the area of a nanoparticle, that does not experience interparticle associations. This area is important, since, if the nanoparticles were to be dispersed, they would gain intermolecular contact with the polymer melt and so have an enthalpy gain. We believe this is the phenomenon that drives miscibility and allows nanoparticle dispersion. This is a true nanoscale phenomenon since if the nanoparticles are too small then there is no uncovered area while if they are too large then there are not enough of them per unit volume to cause a significant enthalpy gain for a given volume fraction. An optimum exists at a radius of approximately 3-5 nm. This nanoscale phenomenon and others will be discussed in the presentation to demonstrate that spherical nanoparticles do create unusual effects as long as they are well dispersed.

11:30 AM *DD2.8

Polymer-Inorganic Nanocomposites: Theoretical Studies of Thermodynamics and Phase Behavior Valeriy V. Ginzburg, The Dow Chemical Company, Midland, Michigan.

Polymer nanocomposites (PNC) represent a new class of materials that is being actively developed for a wide variety of commercial applications (automotive, packaging, cosmetics, electronics, etc.) Particular attention is paid to three main classes: (i) polymer/metal nanoparticle composites; (ii) polymer/carbon nanotube composites; (iii) polymer/clay nanocomposites. Significant successes have been achieved in making these systems yet our understanding of their behavior is still rather limited. In my talk, I will describe recent theoretical efforts aimed at the understanding of thermodynamics and phase behavior of PNC's. In particular, we will examine theoretical models describing (i) self-assembly of block copolymer/metal nanoparticle mixtures, and (ii) morphology of clay platelets in homogeneous polymer melts. We will see that the size and geometry of the nanoscale fillers play a crucial role in determining the morphology and phase behavior of the nanocomposite. It is shown that for the case of small (5–10 nm) nanoparticles, self-assembly can indeed guide the system towards thermodynamically stable morphologies (e.g., lamellar morphologies with particles segregated into one block or at the interfaces between lamellar domains). In the case of clays, on the other hand, thermodynamically advantaged morphology is often the "macrophase separated" state where clay platelets are segregated from the matrix; it becomes necessary, therefore, to be able to preserve the system in a non-equilibrium state (which is often difficult to do). Overall, theoretical predictions - while imperfect - could serve as good guidelines for the composite formulation design.

SESSION DD3/EE2: Joint Session: Synthesis of Nanotubes and Nanowires II

Chair: Jie Liu

Monday Afternoon, April 9, 2007

Room 2001 (Moscone West)

1:30 PM DD3.1/EE2.1

Growth of SiC Nanowires in Different Directions on Sapphire Substrates Qingkai Yu¹, Shin-Shem Pei¹, Jian Shi² and Hao Li²; ¹Univ of Houston, Houston, Texas; ²University of Missouri, Columbia, Missouri.

Free-standing SiC nanowires and SiC nanowires on R-plane sapphire substrates were grown by chemical vapor deposition. SiO vapor and various carbon sources are the precursors for the formation of SiC nanowires. The morphology and composition were characterized by SEM, TEM, AFM, and XPS. TEM results demonstrate that the nanowires have a core-shell structure. It was also found that the diameter of SiC nanowires influence the morphology of both free-standing SiC nanowires and the ones on sapphire substrates. The directions of SiC nanowires grown on R-plane sapphire substrates are affected by precursors, experimental conditions, and the substrates. At the end, the electrical properties and potential applications are also discussed.

1:45 PM DD3.2/EE2.2

Thermodynamics and Kinetics of Germanium Nanowire Nucleation and Growth Hemant Adhikari¹, Paul C McIntyre¹, Christopher E.D. Chidsey² and Ann F Marshall³; ¹Materials Science and Engineering, Stanford University, Stanford, California; ²Chemistry, Stanford University, Stanford, California; ³Geballe Laboratory for Advanced Materials, Stanford University, Stanford, California.

In 3-dimensional nanoelectronics, vertically aligned nanowires have been proposed to provide a solution to attain ultra high density nanoscale device arrays. We have demonstrated the growth of vertically aligned single-crystal germanium nanowires (GeNWs) at temperatures of 400°C or less by metal nanoparticle-catalyzed chemical vapor deposition. We found that temperatures close to bulk eutectic of Au-Ge are required for efficient nucleation of epitaxial nanowires on Ge substrates, but the subsequent growth of nanowires can be carried out at temperatures as low as 270°C. To understand the nucleation of nanowires from gold catalyst particles and to test whether the Vapor-Liquid-Solid mechanism is actually responsible for the growth of nanowires, it is important to understand the phase equilibrium between Au nanoparticles and germanium. Capillary effects, often represented by the Gibbs-Thomson pressure, increase the free energy of the nanoparticle catalyst and the nanowire relative to their bulk values and hence cause lower the eutectic temperature. NW nucleation, where the catalyst nanoparticle is initially in contact with a flat Ge surface, and NW growth, where it is in contact with a GeNW, are very different situations. We have calculated the equilibrium phase diagrams for both the Au-rich liquid nanoparticle in contact with flat Ge (nucleation) and Au-rich liquid nanoparticle in contact with nanowire (growth) cases. The Gibbs-Thomson pressure effect is estimated to be insufficient to stabilize a liquid at the temperatures at which we observe stable Ge NW growth. However, we have also derived limiting expressions for the metastable liquidus for the Au-Ge binary system when a nano-scale liquid droplet is supersaturated with Ge during GeNW growth. Results obtained from these calculations suggest that much larger undercoolings of a Au-Ge liquid are possible during Ge NW

growth, consistent with our experimental observations. Ex-situ heating and cooling behavior of germanium nanowires of different diameters (without Ge deposition) was observed inside a transmission electron microscope column. We noted that temperatures close to bulk eutectic were required for the Au tip of nanowire to melt and form a eutectic alloy with the GeNW during the heating cycle. But, when cooling from a high temperature, the liquid alloy remained stable for an under-cooling of the order of 100°C. These ex-situ TEM heating/cooling results suggest that a substantial undercooling of the liquid below the bulk eutectic temperature may also arise because of the barrier associated with nucleating solid Au. A critical assessment of the importance of the Au nucleation barrier versus Ge supersaturation of the Au-Ge catalyst particle in maintaining a liquid catalyst at large undercoolings will be presented.

2:00 PM DD3.3/EE2.3

Vapor-liquid-solid Growth of Ge Nanowires at Temperatures Below the Eutectic Temperature. Suneel Kodambaka^{1,2}, Jerry Tersoff¹, Kathleen B Reuter¹ and Frances M Ross¹; ¹Physical Sciences, IBM T. J. Watson Research Center, Yorktown Heights, New York; ²Materials Science and Engineering, University of California, Los Angeles, California.

Nanowires of semiconducting materials are conveniently grown via the vapor-liquid-solid (VLS) process, where material from the vapor is incorporated via a liquid catalyst, commonly a low-melting eutectic alloy. Wire growth can also occur in presence of a solid, rather than a liquid, catalyst via vapor-solid-solid (VSS) mechanism. Previous studies have shown that III-V compound semiconductor and elemental Ge nanowires can be grown using Au as the catalyst at temperatures far below the binary alloy eutectic temperature. While it is widely believed that the wire growth occurs via VLS process, the exact growth mechanisms and/or the nature of the catalyst have not been identified. In this talk, we will present in situ transmission electron microscopy (TEM) studies of Ge nanowire growth as a means to develop a fundamental understanding of the mechanisms governing the wire growth kinetics. We provide direct evidence that Ge wires can grow via VLS process in presence of a liquid catalyst at temperatures below the Au-Ge eutectic temperature. We also show that Ge wires can be grown via VSS processes at the same temperature and pressure. From real-time observation of pressure- and diameter-dependent changes in the catalyst shapes, we identify possible mechanisms for the existence of liquid phase catalyst at temperatures below the eutectic temperature. We expect that our results provide valuable insights into fundamental understanding of the nanowire growth kinetics and applicable to other material systems.

2:15 PM DD3.4/EE2.4

Growth of Boron Nanowires by Chemical Vapor Deposition Li Guo and Raj N. Singh; Chemical and Materials Engineering, University of Cincinnati, Cincinnati, Ohio.

Motivated by the extensive research on carbon nanotubes (CNTs), boron and its related nano-structures have attracted increasing interests for potential applications in nanodevices and nanotechnologies due to their extraordinary properties. B-related nanostructures are successfully grown on various substrates in a CVD process. The boron nanowires have diameters around 20-200 nanometers and lengths up to microns. Icosahedra B12 is shown to be basic building unit forming the B nanowires by Raman. The gas chemistry is monitored by the in-situ mass-spectroscopy, which helps to identify reactive species in the process. A nucleation controlled growth mechanism and VLS growth are proposed for the growth of these nanostructures. The role of the catalysts in the synthesis is also discussed.

2:30 PM DD3.5/EE2.5

Plasmon-assisted Local Growth of Individual Semiconductor Nanowires Linyou Cao^{1,2}, David N Barsic^{1,2}, Alex R Guichard^{1,2} and Mark L. Brongersma^{1,2}; ¹Department of Materials Science and Engineering, Stanford University, Stanford, California; ²Geballe Laboratory for Advanced Materials, Stanford University, Stanford, California.

Controlled growth of individual semiconductor nanowires (NWs) at well-defined and pre-specified locations will greatly simplify the integration of such NWs into device architectures. It can also prevent possible processing-induced damage to the nanowires common in conventional nano-fabrication process. Conventional chemical vapor deposition (CVD) growth typically produces many nanowires simultaneously in a high-temperature environment and device fabrication requires the use of complex post-processing methods. Here, we demonstrate a new technology capable of locally depositing heat in a pre-specified metal particle. To this end, a low power (~10mW), focused laser beam is used to illuminate a Au nanoparticle layer generated by evaporation and annealing. The laser wavelength is chosen to match the surface plasmon resonance frequency of the Au particles, such that the electromagnetic energy is efficiently converted to heat. Growth occurs when 2% SiH₄ in Ar gas is delivered to this heated area. The high temperature region is confined to the immediate vicinity of the heated particle with the environment remaining at room temperature. The observed results are in agreement with a thermal model that predicts the temperature distribution around an illuminated Au particle for a certain laser power density and spot size. This work could have a major impact on the field of nanoparticle catalysis and growth and enable new NW-based devices to be realized.

2:45 PM DD3.6/EE2.6

Growth Direction Control in Zinc Oxide Nanowires Husnu Emrah Unalan, Pritesh Hiralal, Yang Yang, Tim Butler, Nalin Rupasinghe, Ken Teo and Gehan Amaratunga; Electrical Engineering Division, Engineering Dept., University of Cambridge, Cambridge, United Kingdom.

Growth direction control of nanowires is essential in determining the integration density as well as positioning of the nano scale devices. In this work, we have utilized electric field during growth of zinc oxide (ZnO) nanowires by chemical vapor deposition for the control of growth direction. Both lateral and vertical growth results will be described. The alignment techniques used follow from those developed for deterministic growth of single walled [1] and multi walled [2] carbon nanotubes. Electric field inside the plasma sheath is exploited for vertical alignment, whereas an auxiliary DC is applied to generate the field for the lateral alignment. We have analyzed the as-grown ZnO nanowires with scanning electron microscopy, transmission electron microscopy, photoluminescence and electrical measurements. In brief, the work reported is a step towards integration of ZnO nanowires in nanoscale electronic and optoelectronic devices. [1] Y. Zhang, A. Chang, J. Cao, Q. Wang, W. Kim, Y. Li, N. Morris, E. Yenilmez, J. Kong, H. Dai, Appl. Phys. Lett 79 (2001) 3155. [2] M. Chhowalla, K. B. K. Teo, C. Ducati, N.L. Rupasinghe, G.A.J. Amaratunga, A.C. Ferrari, D. Joy, J. Robertson, W. I. Milne, J. Appl. Phys. 90 (2001) 5308.

3:15 PM DD3.7/EE2.7

Synthesis and Photoluminescence Properties of Ultrathin Alumina-coated ZnO Nanotubes Grown on Si Wafer. Chi-Sheng Hsiao, San-Yuan Chen and Wan-Lin Kuo; Department of materials science and engineering, National Chiao Tung University, Hsinchu, Taiwan.

The novel uniform ultrathin ZnO nanotubes with alumina nanoparticles coated were fabricated using a solothermal method at low temperature (95 degree centigrade) on a Si wafer. Rapid thermal annealing process was used to control light emission of the nanotubes. The morphology characteristic of the novel ultrathin alumina-coated nanotubes was investigated by a field-emission scanning electron microscope (FESEM) and high resolution transmission electron microscope (HRTEM). Moreover, the photoluminescence property of them was measured by 325 nm He-Cd laser. By controlling growth time and pH, the ZnO nanotubes with cross-sectional dimensions of 20 to 30 nm, lengths of 3-5 μm , and wall thickness of 5-10 nm can be obtained. These nanotubes can potentially be used in various devices, such as energy-storage devices, solar cells and gas sensors. The HRTEM result shows the lattice fringe of the ZnO nanowire is about 0.51 nm, corresponding to the (001) fringe perpendicular to the growth direction, which is consistent with that of the bulk wurtzite ZnO crystal. Moreover, alumina nanoparticles with diameter of 5-10 nm were coated on the modified ZnO nanotubes. Photoluminescence spectrum shows that strong blue light emission can be detected from the alumina-coated nanotubes. Furthermore, under the control of different temperature and atmospheres, the alumina-coated ZnO nanotubes could exhibit various light emissions, such as blue and yellow emissions that may be related to quantum size effect. As expected, it could be further developed for nano-sized white-light device. In conclusion, we have successfully synthesized uniform ultrafine alumina-coated ZnO nanotubes at low-temperature on Si wafer. Different emissions (white, blue, yellow) from the alumina-coated nanotubes can be obtained after annealing process that will be discussed in this work. Furthermore, the formation mechanism of the nanotubes will be analyzed by HRTEM observation and processing control.

3:30 PM DD3.8/EE2.8

Formation and Applications of Biphasic GaN Nanowires as a Function of Growth Parameters. Kaylee McElroy¹, Benjamin W. Jacobs¹, Andrew D. Baczewski¹, Virginia M. Ayres¹, Joshua B. Halpern², Mao Q. He², Mihail P. Petkov³, Martin A. Crimp¹ and Harry C. Shaw⁴; ¹College of Engineering, Michigan State University, East Lansing, Michigan; ²Department of Chemistry, Howard University, Washington D. C.; ³District of Columbia; ⁴NASA Jet Propulsion Laboratory, Pasadena, California; ⁵NASA Goddard Space Flight Center, Greenbelt, Maryland.

Biphasic homostructure nanowires represent a new class of waveguide structures with important possible applications in quantum transport [1]. Catalyst free GaN nanowire growth mechanisms [2] have resulted in GaN nanowires with a biphasic crystalline homostructure [3] where zinc blende and wurtzite phases are observed along the full length of the nanowire. The radial arrangement has been observed to vary from a fully enclosed coaxial biphasic structure to a side-by-side arrangement. The formation of these two structures was investigated as a function of growth temperature and ammonia flow during the growth process. The electronic structure of the nanowires was investigated with cathodoluminescence, which was used to quantitatively measure the wurtzite and zinc-blende bandgaps. The crystal structures of the nanowires were investigated with high resolution transmission electron microscopy. Selected area electron diffraction, and fast Fourier transforms of the images were used to identify the crystalline phases present. Both intact nanowires and cross sections made by focused ion beam were investigated. The elemental composition of the nanowires was investigated by energy dispersive spectroscopy and electron energy loss spectroscopy, with results indicating a 1:1 GaN stoichiometry. The electronic performance of the GaN nanowires in a three terminal transistor nanocircuit (NanoFET) configuration was investigated. NanoFETs were fabricated using electron beam lithography on an oxide layer with a highly doped silicon substrate acting as the global back gate. Two and four point probe measurements were carried out using the Zyvyx KZ100 Nanomanipulator System. Symmetric I-V traces indicated little or no leakage current. Direct contact nanoprob of an open end of the nanowire was also investigated. All electronic measurements indicated high current densities. The experiments also indicated that electronic transport may be phase dependent. The optoelectronic performance of the GaN NanoFETs was investigated. Results indicated UV sensitivity with no response to visible light, indicating the potential application of these GaN nanowire systems as UV-sensitive photodetectors. [1] B.W. Jacobs, V.M. Ayres, M.A. Tupta, R.E. Stallcup, A. Hartman, J.B. Halpern, M.-Q. He, M.A. Crimp, A.D. Baczewski, N.V. Tram, Q. Chen, Y. Fan, S. Kumar, L. Udpa, "Electronic Transport Characteristics of Gallium Nitride Nanowire-based Nanocircuits", 2006 6th IEEE Conference on Nanotechnology Proceedings, ISBN 1-4244-0078-3 [2] M. He, P. Zhou, S. N. Mohammad, G. L. Harris, J. B. Halpern, R. Jacobs, W. L. Sarney, L. Salamanca-Riba, J. of Crys. Grow. 231, 357 (2001) [3] V.M. Ayres, B.W. Jacobs, M.E. Englund, E.H. Carey, M.A. Crimp, R.M. Ronningen, A.F. Zeller, J.B. Halpern, M.-Q. He, G.L. Harris, D. Liu, H.C. Shaw and M.P. Petkov, "Investigation of Heavy Ion Irradiation of Gallium Nitride Nanowires and Nanocircuits", Diamond and Relat. Mater., Vol. 15, pp. 1117-1123 (2006)

3:45 PM DD3.9/EE2.9

Single-Crystalline Nanotubes of $\text{II}_3\text{-V}_2$ Semiconductors. Guozhen Shen, Yoshio Bando and Dmitri Golberg; Nanoscale Materials Center, National Institute for Materials Science, Tsukuba, Japan.

In recent years, considerable attention has been paid to 1-D nanostructures owing to their unique physical and chemical properties, and potential applications in nanoscale devices with diverse functions [1]. Semiconducting $\text{II}_3\text{-V}_2$ compounds are of great scientific and technological importance. Due to the large excitonic radii of these materials, they are expected to exhibit pronounced size quantization effects. The electrons in such a semiconductor will become confined in crystals much larger than for the analogous II-VI or III-V semiconductors. However, compared with the significant progress in 1-D nanoscale II-VI and III-V semiconductors, research on nanoscale $\text{II}_3\text{-V}_2$ semiconductors has been lingering far behind because of the lack of appropriate and generalized synthetic methodologies [2]. Herein, we report the first synthesis of single-crystalline $\text{II}_3\text{-V}_2$ nanotubes, Cd_3P_2 and Zn_3P_2 nanotubes, by thermal evaporation a mixture of ZnS (or CdS), P, and Mn_3P_2 powders in a vertical induction furnace [3] by a self-sacrificing template process, in which the in-situ formed Cd or Zn nanorods act as the self-sacrificing templates for the growth of nanotubes. By carefully controlling the experimental parameters, $\text{II}_3\text{-V}_2$ nanotubes based 1D heterostructures are also fabricated using this simple method [4]. After reaction, XRD results indicate the formation of pure Zn_3P_2 and Cd_3P_2 structures. The morphology and composition of the synthesized products were checked using SEM, TEM and EDS. The results reveal the formation of smooth Cd_3P_2 nanotubes with outer diameters of 80-250 nm and Zn_3P_2 nanotubes with outer diameters of 100-200 nm. All the nanotubes have circular cross-sections, open ends without any attached particles, uniform diameters along their entire lengths and very thin walls compared to hollow cavities. HRTEM images shows the clearly marked interplanar d-spacing of 0.35 nm for Cd_3P_2 and 0.33 nm for Zn_3P_2 , corresponding to that of the {202} lattice planes of tetragonal Cd_3P_2 and Zn_3P_2 , respectively. Besides the pure nanotubes, some partially filled nanotubes were also observed. Series of experimental results give a self-sacrificing template mechanism of these nanotubes. Cathodoluminescence (CL) properties of $\text{II}_3\text{-V}_2$ nanotubes were briefly studied here at 16 K. Zn_3P_2 nanotubes with wall thickness of ca. 10 nm, 20 nm and 45 nm, show emissions centered at about 491 nm, 711 nm, and 796 nm, respectively.

Great blueshifts were observed for the nanotubes with very thin wall thickness, which are caused by the quantum confinement. [1] (a) Xia, Y.; et al. *Adv. Mater.* 2003, 15, 353-389. (b) Shen, G. Z.; Chen, D. J. *Am. Chem. Soc.* 2006, 128, 11762. [2] Shen, G. Z.; et al. *Appl. Phys. Lett.* 2006, 88, 143105. [3] (a) Shen, G. Z.; et al. *Chem. Eur. J.* 2006, 12, 2987. (b) Shen, G. Z.; et al. *Appl. Phys. Lett.* 2006, 88, 243106. (c) Shen, G. Z.; et al. *Appl. Phys. Lett.* 2006, 88, 123107. [4] Shen, G. Z.; et al. *Angew. Chem. Int. Ed.* 2006, in press.

4:00 PM DD3.10/EE2.10

PLD Synthesis of Aligned Fe₃O₄ and ϵ -Fe₂O₃ Nanowires and Nanobelts. Jenny Ruth Morber¹, Yong Ding¹, Michael Stephan Haluska¹, Yang Li², J. Ping Liu², Zhong Lin Wang¹ and Robert Snyder¹; ¹Materials Science and Engineering, Georgia Institute of Technology, Atlanta, Georgia; ²Physics, University of Texas at Arlington, Arlington, Texas.

Though one-dimensional (1D) morphologies of many magnetic materials hold great promise to generate new applications and improve those currently filled by nanoparticles and quantum dots through enhanced properties, such as increased magnetic response, spin filter effects, and multiple species functionalization, development of these materials has been slow. For ferrite materials such as magnetite (Fe₃O₄) and the elusive ϵ -Fe₂O₃, this sluggish growth is most likely due to the problematic synthesis of these materials in 1D morphologies. We have demonstrated successful and controllable synthesis of both Fe₃O₄ and ϵ -Fe₂O₃ nanowires and nanobelts in high density through a pulsed laser deposition (PLD) synthesis technique. [1,2] These nanowires were shown to be single-crystalline and of high quality. Our PLD technique enables efficient synthesis of metastable phases without the necessity of templates or high vacuum conditions, through the ability to direct laser energy to heat engineered targets at a very high rate. The ϵ -Fe₂O₃ phased nanowires are of particular interest due to their coupling of spontaneous magnetization and electronic polarization seen in nanoparticles of this material, the only known morphology of ϵ -Fe₂O₃ until this time. Systematic experimentation reveals a basic parameter range for iron oxide nanowires grown by this synthesis, and show that the heat generated by the laser energy is the primary evaporation source, allowing great control over the synthesis process. Although some initial samples contained mixed phases, heat treatment provides an easy method to tweak composition while maintaining the nanowires' morphology. SQUID (superconducting quantum interference device) data on our samples shows interesting magnetic phenomena. [1] J. R. Morber, Y. Ding, M. Haluska, Y. Li, J. Ping Liu, Z. L. Wang, and R. L. Snyder, *J. Phys. Chem. B.* 2006, published online. [2] for more details: <http://www.nanoscience.gatech.edu/zwang/>

4:15 PM DD3.11/EE2.11

Pulsed-Potential Regimes for the Electrodeposition of Bismuth Telluride Nanowires in Porous Alumina. Lynn Trahey¹, Catherine R. Becker, Jeff Sharp² and Angelica M. Stacy¹; ¹Chemistry, University of CA, Berkeley, Berkeley, California; ²Marlow Industries, Inc., a Subsidiary of II-VI Incorporated, Dallas, Texas.

With the goal of synthesizing an optimal thermoelectric nanowire array, bismuth telluride has been electrodeposited into porous alumina templates using different pulsed-potential regimes. Pulsed-potential deposition allows for dense arrays with even nanowire growth fronts in high aspect ratio channels (2000:1) of homemade porous alumina. This work investigates the effects that different synthetic regimes have on the nanowire growth rates, template filling, preferred orientation, composition, and thermoelectric performance. Scanning electron microscopy is used to study the morphology and template filling of the arrays. X-ray diffraction is used to analyze the preferred orientation of nanowires that have not overgrown the top of the template. The bismuth telluride composition is assessed with electron microprobe analysis. Lastly, thermoelectric properties of some arrays will be presented in order to ascertain if there is enhanced efficiency with reduced dimensionality of the bismuth telluride material.

4:30 PM DD3.12/EE2.12

Microwave-assisted Rapid Synthesis of Silver Nanowires. Linfeng Gou and Jeffery M. Zaleski; Indiana University, Bloomington, Indiana.

We report the rapid, microwave-assisted aerobic synthesis of silver nanowires based on the polyol method. Benchtop dissolution of NaCl and AgNO₃ in ethylene glycol and subsequent heating using microwave irradiation (300W) in the presence of polyvinylpyrrolidone generates Ag nanowires in ~80% yield in 3.5 minutes. Upon purification, microscopy (TEM, SEM) and powder X-ray diffraction reveal a uniform array of crystalline Ag nanowires 45 nm x 4-12 nm. Wire formation is highly dependent upon the microwave heating power, time, and NaCl:AgNO₃ ratio due to the rapid heating process and the presence of O₂ as an etching coreagent. The nanowire formation mechanism, particularly the role of microwave irradiation as compared to the traditional heating techniques, will be presented. The microwave assisted preparation does not require any external seed crystals, precursors, or mechanical stirring, and is conducted under ambient O₂ conditions, leading to significant potential for the large-scale fabrication of Ag nanowires using this approach. Additionally, the rapid heating feature of microwave can be adapted to many hydrothermal/solvothermal approaches for preparing other 1-D nanostructures. Specific examples of these nanowire materials will be discussed.

4:45 PM DD3.13/EE2.13

Multicolor Nanolasers from Individual Multi-quantum Well Nanowire Heterostructures. Fang Qian¹, Yat Li¹, Silvija Gradecak¹, Hong-Gyu Park¹, Yong Ding², Zhong Lin Wang² and Charles M. Lieber¹; ¹Department of Chemistry and Chemical Biology, Harvard University, Cambridge, Massachusetts; ²School of Materials Science and Engineering, Georgia Institute of Technology, Atlanta, Georgia.

We demonstrate for the first time the rational growth of III-nitride based multi-quantum well (MQW) radial nanowire heterostructures, and room-temperature multicolor lasing in these free-standing nanowire structures. MQW nanowires were prepared by metal-organic chemical vapor deposition with a GaN core and InGa_xN_{1-x}/GaN MQW shell, where the indium composition in InGa_xN_{1-x} QW is used to tune emission wavelength. Cross-sectional electron microscopy studies reveals that MQW nanowires are single crystals with triangular shape, and high quality InGa_xN_{1-x}/GaN MQWs were observed on the {1-101} lateral facets. Optical studies show the MQW nanowire heterostructures exhibit strong photoluminescence consistent with bandgap emission from InGa_xN_{1-x} QWs, and that these structures function as Fabry-Pérot optical cavities. Excitation energy-dependent studies demonstrate a threshold for stimulated emission and well-defined lasing modes at distinct wavelengths ranging from 380nm to 480nm depending on indium composition. In addition, the observed laser threshold dependence on emission wavelength and MQW shell thickness was analyzed using three-dimensional finite-difference time-domain calculation, which provides key insight for further development of these nanowire MQW lasers, in terms of the coupling efficiency between the optical field and gain medium. The ability to achieve lasing from single-crystal MQW nanowire heterostructures suggests significant potential for nanoscale photonic systems, including the demonstration of multicolor nanoscale injection lasers.

SESSION DD4:
Chair: Ruth Pachter
Monday Afternoon, April 9, 2007
Room 2003 (Moscone West)

1:30 PM DD4.1

Limit of Coherency in Core-shell and Axially Heterogeneous Metallic and Semiconductor Nanowires via Molecular Dynamics. Arvind Arumbakkam¹, Yumi Park¹, Amritanshu Palaria² and Alejandro Strachan¹; ¹School of Materials Engineering, Purdue University, West Lafayette, Indiana; ²Electrical and Computer Engineering, Purdue University, West Lafayette, Indiana.

We use molecular dynamics (MD) with first principles-based force fields to characterize the heteroepitaxial integration of metallic and semiconductor wires. We consider axially heterogeneous and core-shell nanowires composed of platinum or silicon and a fictitious element that differs from Pt or Si only in its lattice parameter to characterize the maximum lattice mismatch that supports coherent (defect-free) structures. The lattice parameter of the fictitious element is increased in strain steps of 0.25% until interfacial coherency is lost. We characterize the limits of coherency for the two types of heterostructures and various orientations as a function of radius and length. Our results show that one dimensional structures can support enormous lattice mismatches (over 10%) while maintaining defect-free interfaces. The CMP decreases markedly with increasing radius and increasing length in the case of high aspect ratio axially heterogeneous wires. We perform an analysis based on relative displacement of nearest neighbor atoms to characterize the mechanisms of plastic relaxation at the CMP and the resulting defective structures. For the axially heterogeneous metallic case [111] oriented wires relax via partial dislocations with Burgers vector $1/6\langle 112 \rangle$ that glide on the interfacial plane; for [112] wires relaxation also occurs via $1/6\langle 112 \rangle$ partials on closed packed planes that make an angle of 19.47 degrees to the interface. In [110] cases we observe $1/6\langle 112 \rangle$ and $1/2\langle 110 \rangle$ slip on a close packed plane at an angle of 35.26 degrees to the interface. The relative orientation of the closed packed plane with respect to the interface governs the CMP; for axially heterogeneous metallic wires those oriented along [110] exhibit the largest limits of coherency. We foresee that our MD results will help determine the feasibility of integration of heterogeneous metallic and semiconductor nanowires.

1:45 PM DD4.2

One Dimensional Silicon Nanostructures: Atomic Level Structures and Properties from MD and DFT. Amritanshu Palaria^{1,2} and Alejandro Strachan²; ¹School of Electrical and Computer Engineering, Purdue University, West Lafayette, Indiana; ²School of Materials Engineering, Purdue University, West Lafayette, Indiana.

Understanding how material properties evolve when their size is reduced to the nanoscale and harnessing the new phenomena that may arise to achieve improved performance is a central challenge in many disciplines of science and engineering. With this in view, we propose a general strategy to predict the atomic level structure of one-dimensional nanostructures using a combination of ab initio electronic structure calculations and molecular dynamics (MD) with the reactive force field ReaxFF. The new strategy is applied to silicon and the electronic and thermo-mechanical properties of the resulting nanostructures are characterized. We use MD simulations to explore configuration space via an annealing procedure involving compression and tension cycles at various temperatures starting with simple ordered structures (nanotubes with pentagonal and hexagonal cross sections). The most promising configurations obtained during the MD simulations are further refined with density functional theory within the generalized gradient approximation. The new method predicts several low-energy nanotube-type structures of comparable stability; some of the resulting structures have been previously reported as low energy configurations while some are reported for the first time here. MD simulations of mechanical deformation of some low energy Si nanostructures show a novel behavior akin to superelasticity. We find that Si nanowires can support large tensile strain (over 20%) and recover their original structure once the load is removed. This phenomenon stems from structural transitions between different conformations. The electronic bandstructure of these low energy structures are also reported. First principles computational strategies such as the ones presented here, that enable the prediction of both the structure and behavior of nanosized materials are seriously needed and likely to play a key role in the design of next generation devices.

2:00 PM DD4.3

Electronic Structure of Silicon-Based Nanostructures Lok C Lew Yan Voon¹ and Gian Guzman-Verri²; ¹Physics, Wright State University, Dayton, Ohio; ²Centro de Investigaciones en Ciencia e Ingeniería de los Materiales, Universidad de Costa Rica, San José, Costa Rica.

We have developed a new unifying tight-binding theory that can model the electronic properties of recently proposed Si-based nanostructures [1,2], namely, Si graphene-like sheets and Si nanotubes. The electronic properties of silicene, Si (111), Si h-NT's and Si g-NT's were studied via a tight-binding approach. We derived sp^3s^* and sp^3 models up to first- (1NN) and second-nearest (2NN) neighbors, respectively. We compared the band structures of Si (111) and of silicene to the one of graphene. We expect Si (111) and silicene to be either semiconductors of band gap zero or metals. Electrons in the neighborhood of the K point should behave as Dirac massless fermions. However, the Fermi velocity v_0 in Si (111) (104 m/s) and in silicene (105 m/s) are smaller than the one in graphene (106 m/s). Silicon h-NT's and Si g-NT's were compared to carbon nanotubes (CNT's) as well. The band structure of Si h-NT's and of CNT's are similar to each other. In the case of zig zag semiconductor Si h-NT's, the gap is inversely proportional to the tube diameter, as in zig zag CNT's, nonetheless, for a given diameter, Si h-NT's will have a smaller gap. The magnitude of the effective masses is also inversely proportional to their diameter. However, for a given diameter, Si h-NT's have greater mass, which makes CNT's more suitable for transport properties. As far as Si g-NT's are concerned, we found that they follow Hamada's rule [3] as CNT's do, even though they show different hybridizations. Our calculations for all the Si-based materials considered here were compared to the ab initio calculations performed by Yang et al. [2]. When comparing silicene and Si (111), we found that the 2NN sp^3 model is in better agreement with Yang's band structures than the 1NN sp^3s^* model. For Si h-NT's, our band structures agree with the ones obtained by Yang et al. [2]: they all follow Hamada's rule. In contrast, they disagree for all Si g-NT's. Whereas our calculations show that these nanotubes also follow this rule, Yang's calculations do not. Work supported by an NSF CAREER award (NSF Grant No. 0454849), and by a Research Challenge grant from Wright State University and the Ohio Board of Regents. [1] J. Sha, J. J. Niu, X. Y. Ma, J. Xu, X. B. Zhang, Q. Yang and D. Yang, Silicon nanotubes. Adv. Mat. 14, 1219 (2002). [2] X. B. Yang and J. Ni, Electronic properties of single-walled silicon nanotubes compared to carbon nanotubes, Phys. Rev. B 72, 195426 (2005). [3] N. Hamada, S.I. Sawada and A. Oshiyama, New one-dimensional conductors: Graphitic microtubules, Phys. Rev. Lett. 68, 1579 (1992).

2:15 PM DD4.4

Study of Charged Exciton in Silicon Quantum Dot. Gian Franco Sacco, Paul von Allmen and Seungwon Lee; Jet Propulsion Laboratory, Pasadena, California.

The trion system (also called charged exciton), a bound state of two electrons and a hole or two holes and one electron, has received particular attention in the past few years due to the possible applications of such a system, ranging from single photon emitter which can be used in quantum cryptography, ultra-high density memory devices, mobile light emitters and probe for semiconductor material. Moreover the trion has been proposed as a key element in the fabrication of quantum gates allowing fast spin flip of an electron in a charged quantum dot. In this study we compute the lowest energies of a trion system for two Silicon quantum dots of radius 1.09 and 1.36 nm respectively (i.e. two and two and a half unit cell of radius) by using the configuration interaction method. We first obtain the electron and hole energies states using the tight binding method and then we construct a basis set of trion states with good spin quantum number and diagonalize the trion Hamiltonian. Because of the weak spin-orbit coupling in Silicon, trion states with different spin are not mixed. We find that the spin three half state is more bound than the one-half and we confirmed that the binding energy decreases as the size of the system increases. We get that the trion binding energy of the dot with radius 1.09 nm is 0.242 eV and 0.227 eV for the spin three-half and one-half respectively, while that of the dot with radius 1.36 nm is 0.295 eV for the spin three-half state and 0.261 eV for the spin one half-state. We finally compute the absorption cross section for a charged quantum dot excited into a trion state. We show that the spin three half state is a "dark" state, while the one half spin is a bright state.

2:30 PM DD4.5

Shape and Size Dependent Exciton Fine Structure of CdSe Nanocrystals. Qingzhong Zhao¹, Kwiseon Kim¹, Peter A. Graf¹, Alberto Franceschetti¹, Wesley B. Jones¹ and Lin-Wang Wang²; ¹National Renewable Energy Laboratory, Golden, Colorado; ²Computational Research Division, Lawrence Berkeley National Laboratory, Berkeley, California.

We investigate the exciton fine structure of CdSe nanocrystals using empirical pseudopotential calculations. We studied the shape and size effects by calculating the band-edge states of CdSe spherical quantum dots, elongated nanorods, and flattened nanodisks. Large scale electronic calculations consisting of 100–20,000 atoms with diameters ranging from 2 to 8 nm and lengths from 2 to 11 nm were performed. Band-edge states of semi-infinite 1D quantum wires and 2D quantum wells were also calculated. We used the empirical pseudopotential method and the configuration interaction method [1,2] to obtain the band-edge exciton fine structure. We find the experimentally observed dark-bright exciton state crossing [3]. We discuss its shape and size dependency.

3:15 PM DD4.6

Fully Ordered Array Of Subnano II-VI Semiconductor Wires Coordinated By Organic Molecules: Electronic And Optical Properties. Yong Zhang¹, Brian Fluegel¹, Angelo Mascarenhas¹, Lin-Wang Wang², Xiao-Ying Huang³ and Jing Li³; ¹Materials Science Center, National Renewable Energy Lab., Golden, Colorado; ²Computational Research Division, Lawrence Berkeley National Laboratory, Berkeley, California; ³Department of Chemistry and Chemical Biology, Rutgers University, Piscataway, New Jersey.

A new family of inorganic-organic hybrid crystals based on II-VI semiconductors has recently been synthesized. The success of synthesizing such materials represents two major advances in nanotechnology: (1) the ability to obtain fully ordered nanostructure arrays without any structural and chemical fluctuation typically found in other hybrid materials and nanostructures, and (2) the opportunity to explore the subnano region for both fundamental sciences and applications. These novel hybrid crystals are typically composed of subnano inorganic building blocks interconnected or coordinated by small organic molecules, and have been shown to exhibit numerous unusual electronic and optical properties.[1-3] They can be classified into three categories: 3-D, 2-D, and 1-D structures. In this presentation, we focus on the 1-D structure, that is, a fully ordered array of II-VI semiconductor (e.g., ZnTe) wires coordinated by organic molecules (e.g., pda = C₃N₂H₁₀). The wire is in fact a single chain of II-VI binary semiconductor in a wurtzite structure, thus it forms the smallest possible nanowire practically achievable. Because of the extremely small physical scale and thus exceedingly strong quantum confinement effect, the wire array has shown a huge bandgap shift near 2 eV, compared to the II-VI binary. Both electronic structure, calculated through first-principles density function, and experimental studies using various optical techniques will be presented. References: [1] X.-Y. Huang, J. Li, Y. Zhang, and A. Mascarenhas, JACS 125, 7049 (2003). [2] B. Fluegel, Y. Zhang, A. Mascarenhas, X.-Y. Huang, and J. Li, PRB 70, 205308 (2004). [3] Y. Zhang, G. M. Dalpian, B. Fluegel, Su-Huai Wei, A. Mascarenhas, X.-Y. Huang, J. Li, and W.-L. Wang, PRL 96, 26405(2006). Work supported by DOE, NREL LDRD, and NSF.

3:30 PM DD4.7

Switching Behavior in Silicon-Molecule-SWCNTs Devices: A Density Functional Theory Study Brahim Akdim and Ruth Pachter; AFRL/ML, Wpafl, Ohio.

Recently, a testbed for exploring the electrical properties of single molecules was fabricated [He, J., et al., Nat. Mat. 2006], in order to eliminate the possibility of metal nanofilament formation and to ensure that molecular effects are measured. Silicon and single-wall carbon nanotubes (SWCNTs) were used as electrodes for the molecular monolayer. These devices were found to exhibit a hysteresis in the current-voltage characteristics for π -conjugated molecules. In this work, in order to gain an understanding of the switching behavior, we present a density functional theory study (DFT), combined with the non-equilibrium Green's function formalism, for oligo(phenylene ethynylene) and its derivatives, as well as for the arylalkanes molecules bridged between a SWCNT and a Si slab. Conformational changes in the molecules, due to an applied field, and their interaction with SWCNT, will be reported. A detailed structural analysis, electronic structures, and the density of states near the Fermi level as a function of an applied field, will be outlined. In addition to the DFT results, the charge transport obtained by applying the non-equilibrium Green's function formalism will be discussed.

3:45 PM DD4.8

Multiscale Modeling of Low-Dimensional Quantum Nanostructures in Semiconductors. Vinod K. Tewary¹, David Read¹ and Bo Yang²; ¹Materials Reliability, National Institute of Standards & Technology, Boulder, Colorado; ²Mechanical and Aerospace Engineering, Florida Institute of Technology, Melbourne, Florida.

Currently there is a strong interest in modeling the characteristics of low dimensional quantum structures such as nanowires, quantum dots, quantum wells, etc., because of their potential application in powerful new devices. Modeling is needed for calculation of lattice distortions in and around nanostructures, interpreting measurements for their mechanical characterization, and for strain engineering of the nanostructures and their

self-assembled arrays. A precise knowledge of lattice distortion is necessary for quantum mechanical calculation of electronic wave functions in the core of the nanostructures to determine their electronic and optical characteristics. Conventional modeling techniques based upon continuum mechanics are not applicable to nanostructures because their properties are largely determined by their discrete atomistic structure and nonlinear and quantum effects in their core. A quantum nanostructure embedded in a host has to be modeled at the following scales: (i) the nonlinear core region (sub-nanometer), (ii) the region of the host around the core (nanometer), and (iii) free surfaces and interfaces in the host (macro). Modeling of these structures is thus a multiscale problem that requires linking of length scales. A nanostructure embedded in a host causes lattice distortion, which refers to atomic displacements in and around the nanostructure, and long-range strain and displacement fields in the host. Strain and displacement fields at a free surface of the host can be measured and used to characterize the nanostructure and verify the calculated atomic locations in the core. Strain field determines the elastic energy of the system and is partly responsible for the self-assembly and formation of arrays of the structures. Strain is a continuous variable whereas lattice distortion is a discrete variable that must be calculated by using a discrete lattice theory. Hence we need a multiscale model to calculate the lattice distortion at the atomistic scale and relate it to a measurable parameter such as strain at the macroscale. We have developed a computationally efficient multiscale model for calculation of strains and displacements in and around nanostructures, by integrating molecular dynamics with Green's functions. We use molecular dynamics at the core of the nanostructure to account for the nonlinear discrete lattice effects, and lattice statics Green's function for the host lattice. The lattice statics Green's function reduces asymptotically to the continuum Green's function, which links the atomistic scales to macroscales for interpretation of measurements. The model is applied to a Ge nanowire and a quantum dot embedded in a Si host containing a free surface. Numerical results will be reported for atomistic distortion in and around a nanostructure, its strain field at the free surface, and its elastic interaction with the surface.

4:00 PM DD4.9

Chemical Tension in VLS Nanostructure Growth Process: From Nanohillocks to Nanowires. Na Li¹, Ulrich Gösele² and Teh Yu Tan¹;

¹Mechanical Engineering and Materials Science, Duke University, Durham, North Carolina; ²Max-Planck Institute of Microstructure Physics, Halle, Germany.

We formulate a global equilibrium model to describe the growth of 1-d nanostructures in the VLS process by including also the chemical tension in addition to the physical tensions, i.e., surface energies. The chemical tension derives from the Gibbs free energy change due to the growth of a crystal layer of an elementary thickness. The system global equilibrium is arrived at via the balance of the static physical tensions and the dynamic chemical tension. The model predicts, and provides conditions for the growth of nanowires of all sizes exceeding a lower thermodynamic limit. The model also predicts the conditions distinguishing the growth of nanohillocks from nanowires. These predictions will allow verifying the model by future experiments specifically designed for this purpose.

4:15 PM DD4.10

Growth Mechanism of Group III-Nitride Nanorods Using Hydride Vapor Phase Epitaxy Yong Sun Won^{2,1}, Young Seok Kim², Olga Kryliouk²

and Tim Anderson²; ¹Guest Scientist, Metallurgy, MSEL, NIST, Gaithersburg, Maryland; ²Chemical Engineering, University of Florida, Gainesville, Florida.

A convincing mechanism for catalyst- and template-free InN and GaN nanorod growth using HVPE was proposed, featured with the random nanoparticle nucleation from stable gas phase oligomers ($[\text{Cl}_2\text{InNH}_2]_n$ or $[\text{Cl}_2\text{GaNH}_2]_n$) and the subsequent directional growth along the c-axis. The involvement of group III-trichloride (InCl_3 or GaCl_3) as a key intermediate required $\text{HCl}/\text{group III}$ ratio to be above 3 by stoichiometry. A combined study of equilibrium thermodynamics and computational thermochemistry suggested that the best growth zone of group III-nitride nanorods lies in the vicinity of the growth-etch transition. As for the GaN nanorod growth, a two-temperature approach was recommended due to the high activation barrier for GaCl_3 formation; high temperature for GaCl_3 formation and low temperature for GaN nanorod growth via the proposed mechanism. Theoretically resolved operation conditions - temperature and $\text{HCl}/\text{group III}$ ratio - for group III-nitride nanorod growth showed a good agreement with experimental results.

4:30 PM DD4.11

Composition and Strain Dependence of the Piezoelectric Coefficients in Semiconductor Alloys. Max Migliorato, Electronic and Electrical Engineering, University of Sheffield, Sheffield, United Kingdom.

In epitaxially grown semiconductors, the piezoelectric effect can be observed via the off diagonal strain tensors that exist in quantum wells grown on (111) substrates, quantum wires and quantum dots. Piezoelectric effects in such nanostructures have attracted a substantial amount of interest in recent years, and were identified as the source of experimentally observable optical anisotropies[1-3]. Previous work has considered only the first-order piezoelectric effects and employed either the experimental piezoelectric coefficients of bulk semiconductors or linear interpolations between two compounds. A recent study by Bester et al [4] has pointed out that neglecting the second-order effects leads to substantial errors in the calculations of quantities such as the piezoelectric field though their prediction do not found quantitative experimental validation. In this paper we will present an alternative approach [5] to calculating the first- and second-order piezoelectric coefficients. Our model is based on expressing the direct and dipole contributions to the polarization in terms of microscopic quantities that can be calculated by Density Functional Theory (DFT). The polarisation is decomposed into the direct and dipole contributions and these can be written in terms of Tight Binding expressions and elastic properties. Both the bulk and the strained values are calculated through Density Functional Perturbation Theory or DFT-LDA, effectively incorporating the second order effects in the strain into the expressions for the piezoelectric coefficients. We will show how our approach, which can be easily extended to any III-V semiconductor material, for the first time, fully explains the experimental data. Furthermore we can finally answer the 10 years old question of the validity of the piezoelectric coefficients framework, which first came to light in studies of InGaAs Quantum Wells grown on GaAs (111)B substrates[6]. 1 M. A. Migliorato, D. Powell, S. L. Liew, A. G. Cullis, M. Fearn, J. H. Jefferson, P. Navaretti, M. J. Steer, M. Hopkinson, J. Appl. Phys. 96, 5169 (2004) 2 G Bester and A Zunger, Phys Rev B 71, 045318 (2005) 3 O. Stier, M. Grundmann and D. Bimberg, Phys Rev B 59, 5688 (1999) 4 G Bester, X Wu, D Vanderbilt and A Zunger, Phys Rev Lett 96, 187602 (2006) 5 M.A. Migliorato, D. Powell, A.G. Cullis, T. Hammerschmidt, G.P. Srivastava, to appear in Phys Rev B 6 R.A. Hogg, T.A. Fisher, A.R.K. Willcox, D.M. Whittaker, M.S. Skolnick, D.J. Mowbray, J.P.R. David, A.S. Pabla, G.J. Rees, R. Grey, J. Woodhead, J.L. Sanchez-Rojas, G. Hill, M.A. Pate and P.N. Robson, Phys. Rev. B 48, 8491 (1993)

4:45 PM DD4.12

Modeling and Experimental Investigation of Nanometer Scale Cold Field Emitters For Multi-length Scale Integration Darrell L. Niemann^{1,2}, Bryan P. Ribaya^{1,2}, Norman Gunther¹, Mahmud Rahman¹, Cattien V. Nguyen^{1,3} and Joseph Leung²; ¹Electrical Engineering, Santa Clara University, Santa Clara, California; ²NASA Ames Research Center, Moffett Field, California; ³ELORET/NASA Ames Research Center, Moffett Field, California.

We develop a novel modeling technique based on Technology Computer Aided Design (TCAD) in parallel with experimental results to investigate the field emission properties of individual carbon nanotubes (CNTs). Particular emphasis is placed on the optimization of integrating CNT as an electron source in electron microscopy. CNT based field emitters are promising for field emission applications because of their inherently high brightness, low energy spread, and low operating voltages [1,2]. We demonstrate a robust computational methodology capable of investigating the large-scale integration of individual CNT field emitters, thus enabling multi-length scale structural optimization specifically for designing an efficient electron source. This paper presents experimental field emission data for two structurally well-defined cathode structures: one composed of a multi-walled carbon nanotube (MWNT), acting as a nano-scale emitter, attached to an etched Ni metal wire and the other composed of a MWNT attached to a flat Ni-coated Si microstructure. Although both incorporate CNTs with similar geometries, they exhibit quite different macroscopic turn-on fields of 1.6 and 2.5 V/ μm , respectively. The effect of overall cathode structure on the electrostatic fields at the tip of the nano-scale emitter is directly investigated by TCAD simulation. TCAD results for cathode structures analogous to those in experiments exhibit a trend similar to that observed experimentally. In order to achieve the typical microscopic turn-on field of 1x109 V/m at the nano-scale emitter tip, the two different structures require macroscopic turn-on fields of 1.4 and 2.4 V/ μm , respectively [3,4]. Furthermore, TCAD simulation results reveal that the magnitude of the microscopic field varies with the area of the supporting structure. This study demonstrates quantitatively that the supporting cathode structure effect must also be considered in the analysis of field emission properties of nanoscale emitters. Based on these results, TCAD is concluded to be an effective tool for investigating the multiple-length scale integration of nanoscale emitter. Such computer aided techniques enable the exploration of the challenges presented by large scale integration. 1. B. Ribaya, D. Niemann, N. Gunther, M. Rahman, C. V. Nguyen, Proc. IVEC/ IVESC, pp. 25-3-4, (2006). 2. N. de Jonge and J.-M. Bonard, Phil. Trans. R. Soc. Lond. A 362, 2239 (2004). 3. N. de Jonge, M. Allieux, M. Doytcheva, M.K. Philips, K.B. K. Teo, R.G. Lacerda, and W.I. Milne, Appl. Phys. Lett. 85, 1607 (2004). 4. J. Cumings, A. Zettl, M. R. McCartney, J. C. H. Spence, Phys. Rev. Lett. 88, 56804 (2002).

SESSION DD5: Properties of Nanocrystals
Chairs: Philippe Guyot-Sionnest and Moonsub Shim
Tuesday Morning, April 10, 2007
Room 2001 (Moscone West)

8:00 AM DD5.1

The Role of Particle Size Volume Fraction in Bimodal Metals for Optimized Mechanical Properties at Varying Temperatures. Tammy R Smith, Alla V Sergueeva, Umberto Anselmi-Tamburini and Amiya K Mukherjee; Chemical Engineering and Materials Science, UC Davis, Davis, California.

Despite thorough research on the link between microstructural features and mechanical properties, there has never been a systematic study about volume fraction dependence of strength and ductility on bimodal metals. Specimens are consolidated by spark plasma sintering nickel powder mixtures of two uniform particle sizes of 200 nm and 20 nm. Two mechanisms have been proposed that suggest that increased strength is not just a tradeoff for ductility with a larger fraction of small particles. In this study, mechanical tests are performed on specimen through a range of particle size compositions and temperatures. The strength and ductility as a function of particle size is mapped. The temperature at which the tensile behavior changes from strong and brittle to weaker and ductile is governed by the volume fraction. Fracture surface analysis reveals separate deformation mechanisms for individual particles in a single specimen. It is proposed that multiple simultaneous deformation mechanisms that arise from different particle sizes contribute to increasing strength without sacrificing ductility and vice versa.

8:15 AM DD5.2

Structural and Magnetic Properties of Self-Assembled Gold Nanoparticles in Alumina Thin Films Jeremiah T Abiade¹ and Dhananjay Kumar^{1,2}; ¹Mechanical & Chemical Engineering, North Carolina A&T State University, Greensboro, North Carolina; ²Oak Ridge National Laboratory, Oak Ridge, Tennessee.

Traditionally, gold has been a highly sought after material for use as jewelry or in commerce because of its lustrous appearance and scarcity in nature. However, recent studies on the properties of nanostructured gold particles, nanowires, and ultrathin films have generated widespread interest in Au for sensors and actuators and for catalysis. Reports of ferromagnetism in Au nanoparticles and thin films are even more intriguing because bulk Au is diamagnetic. To investigate the possibility of ferromagnetic-like properties in Au nanoparticles, we have deposited self-assembled Au nanoparticles of various sizes in nonmagnetic alumina thin films using pulsed laser deposition (PLD). X-ray diffraction (XRD), scanning transmission electron microscopy with z-contrast (STEM-Z), and vibrating sample magnetometry (VSM) were used to characterize the structural and magnetic properties of the samples. The size of the nanoparticles ranges from ~ 1 - 20 nm. Hysteresis is only observed in the magnetization versus field loops in the nanoparticle samples (< 10 nm) and is clearly present at 300 K. In this talk we will discuss the origin of the size dependent ferromagnetic characteristics in Au nanoclusters.

8:30 AM *DD5.3

Surface Functionalization of Semiconductor Nanostructures. Alf Mews, Ma Xuedan, Zhou Xiaoyin, Maxime Tchaya and Lars Birlenbach; Physical Chemistry, University of Siegen, Siegen, Germany.

The optical and electronic properties of semiconductor nanostructures are strongly related to their molecular surface modification. This is a direct consequence of the electronic interaction between the molecular surface ligands and the inorganic semiconductor particles. However, it is not known up to which extend localized surface levels or the quantized electronic levels of the particle interact with the molecular levels of the ligands. Here we present a detailed study of different nanoparticle-ligand combinations, which are investigated by a combination of optical spectroscopy and cyclic voltammetry (CV), respectively. This allows to measure the absolute energetic positions of the electronic NC- and ligand-levels by CV and compare them to the respective band-gaps and fluorescence intensities from the optical spectra. In addition we present different "functional" ligands, where the energetic levels are depending on the chemical environment. Finally we present results from single nanoparticle fluorescence spectroscopy to

get a deeper insight into the fluorescence dynamic of individual surface modified particles.

9:00 AM DD5.4

Hydroxyl-Quenching Effects on the Photoluminescence Properties of $\text{SnO}_2\text{:Eu}^{3+}$ Nanoparticles. Taeho Moon, Dae-Ryong Jung, Sun-Tae Hwang, Dongyeon Son, Jongmin Kim, Myunggoo Kang and Byungwoo Park; Materials Science and Engineering, Seoul National University, Seoul, South Korea.

For display devices, such as plasma display panel (PDP), field emission display (FED), etc., nanophosphors have potential advantages over traditional micron-sized phosphors. However, nanoparticles have generally showed poor luminescence efficiencies, and one possible reason for this is hydroxyl quenching due to the presence of some adsorbates during the synthesis of the nanoparticles. Hydroxyl-quenching effects were reported for rare-earth ions and nanoparticles suspended in water. However, reports on the characterizations of phosphor itself have been rare, and it is easily expected that hydroxyl quenching will largely depend on the thermal histories of the nanoparticles. The effects of hydroxyl quenching were examined on the photoluminescence properties of $\text{SnO}_2\text{:Eu}^{3+}$ nanoparticles. High-quality $\text{SnO}_2\text{:Eu}^{3+}$ nanoparticles were synthesized from SnCl_4 , EuCl_3 , and ethylene glycol ($\text{C}_2\text{H}_6\text{O}_2$) by a solvothermal method. The photoluminescence spectra showed a reddish orange emission, which gradually increased with the calcination temperature in the range from 700°C to 1000°C. As the calcination temperature varied, the change of the $\text{OH}^-/\text{O}^{2-}$ integrated-intensity ratios from XPS corresponded qualitatively with that of the photoluminescence intensities. The samples obtained after the hydrothermal treatment and after reheating, respectively, exhibited a decline and recovery of their emission intensities, and this behavior with XPS confirmed the hydroxyl-quenching effect. Corresponding Author: Byungwoo Park: byungwoo@snu.ac.kr

9:15 AM DD5.5

Synthesis and Photoluminescence of Mn-Doped Zinc-Sulfide Nanoparticles. Dongyeon Son, Dae-Ryong Jung, Jongmin Kim, Taeho Moon and Byungwoo Park; Materials Science and Engineering, Seoul National University, Seoul, South Korea.

Zinc sulfide (ZnS) is an important luminescence material with a wide band gap, and widely used in flat-panel displays, infrared windows, sensors, etc. Since the first paper of Mn-doped ZnS (ZnS:Mn) nanoparticles in 1992, many researchers have investigated the synthetic techniques, luminescence properties, and applications. However, there are few reports on the Mn-concentration effects with considering the crystallinity and capping elements. In this work, ZnS:Mn nanoparticles were synthesized using a liquid-solid-solution (LSS) method, as a simple synthetic route for preparing ~7 nm-sized monodisperse nanocrystals. The influence of doping concentration for optimum luminescence properties was studied with the actual Mn concentration, the non-uniform distribution of local strain, and the capping effect. The improved photoluminescence intensity of the 450°C-annealed samples with 1.0 at. % Mn doping is attributed to both the removal of water/organics and the enhanced crystallinity (reduced local strain). Corresponding Author: Byungwoo Park: byungwoo@snu.ac.kr

9:45 AM DD5.6

Parity Forbidden Transitions in PbSe Nanocrystals Jeffrey Peterson and Todd D. Krauss; Dept of Chemistry, University of Rochester, Rochester, New York.

Over the last 20 years, semiconductor nanocrystals (NCs) have enabled exciting visualizations of quantum confinement effects in low dimensionality materials, motivating both fundamental and technological investigations of their size-tunable electronic and optical properties. Using a simple "particle in a sphere" model and traditional selection rules, one can essentially understand the major features and the size-dependence of NCs' electronic structure. Due to their extremely large electron and hole Bohr radii, lead salt NCs (PbSe, PbS, and PbTe) can achieve levels of quantum confinement that are not possible in other materials and thus are ideal systems to study confinement effects. Indeed, their absorption spectra indicate a series of well defined and widely spaced energy levels that can be tuned throughout the near infrared spectral region. However, despite this spectral simplicity, theory continues to fail to explain the presence of a dipole-allowed transition at the second excitonic absorption feature in the spectrum. Interestingly, this second peak energy is accurately predicted if formally parity-forbidden transitions are allowed, although it remains unclear what causes such a strong symmetry breaking in the NC. Conversely, recent scanning tunneling spectroscopy investigations suggest that previous theoretical models are inaccurate and that the second absorption peak originates from an allowed transition. We will present investigations of PbSe NC electronic structure using two-photon photoluminescence excitation spectroscopy. The idler beam of an optical parametric amplifier pumped by a Ti:sapphire regenerative amplifier was used to excite, via a two-photon process, PbSe NC samples with (one-photon) absorption peaks between 1200-1450 nm. In all four sizes of PbSe NCs studied, the first two-photon allowed optical transition occurs at the energy of the second, one-photon absorption peak. Unlike one-photon excitation, two-photon processes formally allow mixed parity transitions. Thus, the two-photon excitation data provides direct evidence that the second absorption peak originates from a mixed parity transition. Accordingly, we assign this peak as a "1S-1P" transition. We propose that the molecular origin of this symmetry breaking is due to faceting of the NC faces, which can result in the creation of a permanent dipole in the NC and, thus, alters the wavefunction symmetry. We will present recent experimental and theoretical investigations relevant to this hypothesis. Similar parity-forbidden transitions have been observed in other materials. However, the parity-forbidden transition energies closely overlap with the allowed transition energies and are thus obscured due to "spectral congestion." In contrast, the wide spacing of transitions in PbSe NCs provides a striking example of this phenomenon and highlights the critical role of the NC surface reconstruction in determining their fundamental properties.

10:00 AM *DD5.7

New Paradigm for Nanocrystal Lasing Using Engineered Exciton-Exciton Interactions Victor I. Klimov, Chemistry Division, Los Alamos National Laboratory, Los Alamos, New Mexico.

Chemically synthesized semiconductor nanocrystals (NCs) are almost perfect emitters that combine size-controlled tunability of emission color with near-unity photoluminescence quantum yields. Paradoxically, despite these favorable light-emitting properties, NCs are difficult to use in optical amplification and lasing. Because of exact balance between absorption and stimulated emission in NCs excited with single electron-hole pairs (excitons), optical gain can only occur due to the NCs that contain at least two excitons. A complication associated with this multiexcitonic nature of light amplification is fast, picosecond optical-gain decay due to nonradiative, exciton-exciton Auger recombination. Here, we demonstrate a practical approach for obtaining NC optical gain in the single-exciton regime, which completely eliminates the problem of ultrafast Auger decay. Specifically, we develop core/shell hetero-NCs that produce efficient spatial separations between electrons and holes resulting in generation of a strong local

electric field. This field induces a giant (~100 meV) transient Stark shift of the absorption spectrum with respect to the luminescence line in singly excited NCs, which breaks the exact balance between absorption and stimulated-emission. We use this effect to demonstrate for the first time optical amplification in NCs due to single-exciton states.

10:30 AM DD5.8

Dopant-Carrier Exchange Interactions in Colloidal Doped Semiconductor Nanocrystals. Daniel R. Gamelin, Chemistry, University of Washington, Seattle, Washington.

The generation and manipulation of electron spins in magnetic semiconductor nanostructures is a central theme of the emerging field of spintronics. Carrier-dopant magnetic exchange interactions in diluted magnetic semiconductors provide the basis for many important magneto-electronic phenomena, including carrier-mediated ferromagnetism, magnetic polaron nucleation, and proposed spin-based quantum information processing schemes. This talk will describe our group's recent investigations into the use of photochemical carrier generation and magneto-optical spectroscopies to probe carrier-dopant interactions in colloidal diluted magnetic semiconductor quantum dots. Related references: (1) Norberg, N. S.; Parks, G. L.; Salley, G. M.; Gamelin, D. R. "Giant Excitonic Zeeman Splittings in Co²⁺-doped ZnSe Quantum Dots." *J. Am. Chem. Soc.*, 2006, 128, 13195-13203. (2) Liu, W. K.; Whitaker, K. M.; Kittilstved, K. R.; Gamelin, D. R. "Stable Photogenerated Carriers in Magnetic Semiconductor Nanocrystals." *J. Am. Chem. Soc.*, 2006, 128, 3910-3911. (3) Norberg, N. S.; Kittilstved, K. R.; Amonette, J. E.; Kukkadapu, R. K.; Schwartz, D. A.; Gamelin, D. R. "Synthesis of Colloidal Mn²⁺:ZnO Quantum Dots and High-TC Ferromagnetic Nanocrystalline Thin Films." *J. Am. Chem. Soc.*, 2004, 126, 9387-9398. (4) Schwartz, D. A.; Norberg, N. S.; Nguyen, Q. P.; Parker, J. M.; Gamelin, D. R. "Magnetic Quantum Dots: Synthesis, Spectroscopy, and Magnetism of Co²⁺- and Ni²⁺-Doped ZnO Nanocrystals." *J. Am. Chem. Soc.*, 2003, 125, 13205-13218. (5) Norberg, N. S.; Dalpian, G. M.; Chelikowsky, J. R.; Gamelin, D. R. "Energetic Pinning of Magnetic Impurity Levels in Quantum Confined Semiconductor Nanocrystals." *Nano Letters*, in press.

10:45 AM DD5.9

Effect of Er Doping on the Electronic and Optical Properties of Group IV Nanoparticles. Anthony van Buuren^{1,2}, Rob Meulenberg¹, Trevor Willey¹, April Montoya Vaverka^{1,3} and Lou Terminello¹; ¹LLNL, Livermore, California; ²Dept. of Natural Sciences, UC Merced, Merced, California; ³Department of Materials Science, UC Davis, Davis, California.

We have produced Er doped Si and Er doped Ge nanoparticles using an extension of a physical vapor deposition technique we have used to produce undoped nanoparticles. Using a dual evaporator the Si and Er can be independently resistively heated to their melting temperature. A He buffer gas is used to promote condensation of the supersaturated vapor and the nanoparticles are collected on a substrate sitting ~1 cm above the evaporators. The nanoparticle size and morphology are characterized in-situ using an atomic force microscopy (AFM). We have made doped Si or Ge nanoparticles ranging from 2-8 nm in diameter with Er concentration ranging from 0.02- 10. %. In addition, we can take the deposited Er doped nanoparticles and spin cast a silica sol-gel solution onto the nanoparticles. This is done to facilitate air stability of the nanoparticle as well to enhance the 1.54 micrometer PL from such materials. Our characterization capabilities are ideally suited to measuring the effects of chemical doping due to the element specific nature of our synchrotron based x-ray techniques. High Er doping concentration are found to reduce quantum confinement effects in the conduction band edge of the nanoparticles however for doping concentrations below 2% no effect on the nanoparticle band edges is observed. Also, using two different methods to determine the structure of the conduction band, a bulk sensitive photon in-photon out fluorescence mode or a surface sensitive electron mode, can allow us to gain an understanding of where dopant atoms reside in the nanoparticle. With doping of the nanoparticles we want to drive the broad emission from quantum dots into a narrower band and provide another tool to tailor the optical emission. This work was performed under the auspices of the U.S. Department of Energy by the University of California, Lawrence Livermore National Laboratory under contract W-7405-Eng-48.

11:00 AM DD5.10

Photoluminescence of Charged Colloidal Quantum Dot. Philippe Guyot-Sionnest and Praket Jha; University of Chicago, Chicago, Illinois.

Due to small sizes and quantum confinement, the optical properties of colloidal quantum dots are exquisitely sensitive to extra charges. As for electrochromic materials, the optical absorption is directly modified by state filling. The quantum dots are however rather unique in that the fluorescence yield is also strongly affected by dynamic interaction between excitons and charges via Auger and trapping processes. This is of great interest in the context of electrically driven light emission. With doubly charged CdSe dots, it was shown that the increased band edge transparency led to a reduced stimulated emission threshold.^[1] However, redox surface reactions were also observed to create non-radiative recombination centers that effectively quench the luminescence. The effects of the surface chemistry on the photoluminescence from charged dots will be described. ^[1] C. J. Wang et al, Light emission and amplification in charged CdSe quantum dots, *J. Phys. Chem. B* 108, 9027-9031 (2004)

11:30 AM DD5.11

Solution-Phase Single Quantum Dot Fluorescence Resonant Energy Transfer: Probing Nanoparticle-Conjugate Heterogeneity Thomas Pons¹, Igor L Medintz², Xiang Wang³, Doug S English³ and Hedi Mattoussi¹; ¹Optical Sciences Division, Code 5611, Naval Research Laboratory, Washington, District of Columbia; ²Dept. of Chemistry & Biochemistry, University of Maryland, College Park, Maryland; ³Center for Bio/Molecular Science and Engineering, Code 6900, Naval Research Laboratory, Washington, District of Columbia.

Luminescent semiconductor nanocrystals, or quantum dots (QDs), offer several advantages over traditional organic dyes for use in both in vitro assays and in vivo cellular and animal imaging. As methods are developed to conjugate biomolecules to QDs, and as these nano-assemblies find increasing applications in biological sensing and imaging, there is a growing need for characterization of QD-biomolecule conjugate heterogeneity. Compared to ensemble measurements, single molecule studies are able to resolve molecular scale heterogeneities in macroscopically homogeneous samples (e.g. a dispersion of nanoparticles). Here, we present a single particle QD-based fluorescence resonance energy transfer (spFRET) study that allows us to probe the heterogeneity in QD-dye labeled protein conjugates. We first show that QDs are compatible with spFRET detection by demonstrating the equivalence of single particle and ensemble measurement modalities in terms of derived average FRET efficiencies and separation distances between a central QD donor and dyes attached to specific sites on conjugated proteins. We then use spFRET data to demonstrate that the distribution of QD-protein conjugate valence follows Poisson statistics.¹ We finally apply spFRET to characterize heterogeneity in the interactions between single QD-maltose binding protein (QD-MBP) sensing assemblies with their target maltose. In particular, we show that in

a macroscopically homogeneous sample two distinct sensor populations coexist: one is composed of maltose-free QD-MBP conjugates and the other of QD-MBP-maltose complexes. The fraction of QD-MBP bound to its target varies with maltose concentration, and the binding constant derived from spFRET is consistent with the one derived from ensemble measurements. 1 T. Pons, I.L. Medintz, X. Wang, D.S. English, and H. Mattoussi, J. Am. Chem. Soc., ASAP (2006).

11:45 AM DD5.12

Indirect Excitation of Er in Si Rich SiO₂ Films - Defects vs. Nanocrystals. Oleksandr Savchyn¹, Forrest Ruhge¹, Pieter Kik¹, Ravi Todi² and Kevin Coffey²; ¹College of Optics and Photonics: CREOL & FPCE, University of Central Florida, Orlando, Florida; ²School of Electrical Engineering and Computer Science, University of Central Florida, Orlando, Florida.

Erbium doped silicon rich silica is currently investigated intensively as a gain medium for the fabrication of a silicon compatible laser. Erbium ions (Er³⁺) in SiO₂ exhibit an optical transition at 1.54 μ m that can provide optical amplification and gain. However due to the low absorption cross section, high pump powers and resonant excitation are generally required to achieve population inversion. One of the possible ways of increasing the erbium absorption cross section is by means of sensitization with silicon nanocrystals. It is well known that excitons confined in Si nanocrystals can efficiently excite erbium, enhancing the effective optical absorption cross section by orders of magnitude. Recently there has been substantial debate about the merits of including large nanocrystals, and several papers have suggested that many smaller clusters would provide better gain performance. This presentation discusses the results of an annealing study carried out to correlate the formation of Si nanocrystals with the efficiency of indirect excitation. Surprisingly, significant indirect erbium excitation is observed at annealing temperatures well below the temperature required to form Si nanocrystals. These results suggest that efficient Er sensitization could be obtained with reduced annealing temperatures and/or shorter annealing times. Samples with an Er concentration of 0.63 at.% and a Si excess concentration of 12 at.% were prepared using magnetron cosputtering from Si, SiO₂ and Er₂O₃:SiO₂ targets. The samples were subsequently annealed in N₂ or H₂:N₂ atmospheres at temperatures in the range of 300°C-1200°C. Indirect erbium excitation was observed at annealing temperatures as low as 300°C, and excitation spectroscopy in the range 350-700 nm revealed broadband Er sensitization. Reference samples that did not contain excess Si did not exhibit indirect excitation at any annealing temperature. When excited at 476 nm, maximum Er photoluminescence (PL) intensity was obtained for an annealing temperature of 500°C. At temperatures above 900°C a broad visible luminescence band with a peak in the range of 740 - 800 nm appears, indicating the formation of Si nanocrystals. Contrary to what might be expected, this is accompanied by a strong reduction of the indirectly excited Er photoluminescence intensity, suggesting that nanocrystal formation is accompanied by a significant reduction of the erbium active fraction. The implications of these results for Si based Er doped gain media are discussed.

SESSION DD6: Properties of Nanorods
Chairs: Alf Mews and Moonsub Shim
Tuesday Afternoon, April 10, 2007
Room 2001 (Moscone West)

1:30 PM *DD6.1

Surface Induced Localized Charge of Single Imperfect CdSe Quantum Rods Todd D Krauss¹, Rishikesh Karishnan⁴, Philippe Fauchet⁴, Zhiheng Yu³, Sara E Maccagnano², Joaquin Calcines¹, Julie Smyder¹ and John Silcox²; ¹Chemistry, University of Rochester, Rochester, New York; ²Applied Physics, Cornell University, Ithaca, New York; ³Physics, Cornell University, Ithaca, New York; ⁴Electrical and Computer Engineering, University of Rochester, Rochester, New York.

The photophysical properties of semiconductor nanoparticles as a function of their size have been the subject of much interest over the past decade. However, significantly less attention has been paid to the influence of shape, and in particular surface morphology, on these same properties. Unlike macroscopic materials, where the surface to volume ratio is negligibly small, in nanoparticles the detailed surface structure can have a significant influence on particle behavior and in some cases can lead to completely unexpected phenomena. We will present measurements of the local electrostatic properties of colloidal semiconductor quantum dots (QDs) and quantum rods (QRs), and their influence on their photophysical properties, down to the single particle level. In particular, electrostatic force microscopy (EFM) was used to determine that single CdSe quantum rods (QRs) have a permanent polarization surface-charge density, an unexpected observation for supposedly well-shaped, neutral dielectric particles. To investigate the source of the surface charge, we performed high-resolution surface morphology as well as high-resolution electron nanodiffraction studies with a scanning transmission electron microscope (STEM). Annual darkfield STEM imaging demonstrated that individual QRs show variations in thickness and shape, including extensive faceting of the nanoparticle surface. In addition, electron nanodiffraction patterns suggest that rotations exist between various "sections" of individual QRs, and that the rotation axes may form substantial angles with the c-axis. Thus, we conclude that CdSe QRs are imperfect single crystals, and that the surface charge seen in EFM results from the slight angle between the QR sides and the direction of their internal electric polarization. Interestingly, despite the large dipole moment expected for CdSe QRs, none was observed to within our instrument resolution. The unavoidable presence of permanently charged surfaces on CdSe QRs has the potential to impede the development of novel devices incorporating these materials, as it has been suggested that electric charge on CdSe QDs and QRs causes a quenching of nanoparticle fluorescence. To explore this relationship further, we will also present measurements of the charge magnitude and photoluminescence intensity (obtained simultaneously) for CdSe QDs.

2:00 PM DD6.2

Rayleigh Instability in Gold Nanorods. Carolina Novo and Paul Mulvaney; School of Chemistry, University of Melbourne, Melbourne, Victoria, Australia.

The energy and linewidth of the surface plasmon resonances in metal nanoparticles are strongly determined by the particle shape and size, as well as by the nature of the surrounding medium [1-3]. There is increasing evidence that such nanoscale structures are far more vulnerable to damage by heat and light than the respective bulk metals. Nevertheless, even if they are thermodynamically unstable, they may still be of practical utility if the materials are kinetically stable and unable to respond to external stresses. Rayleigh considered the importance of surface fluctuations on the mechanical stability of liquid droplets. He showed that as a small sphere fluctuates to form ellipsoids due to an external perturbation, there is a critical amplitude beyond which fission becomes possible [4-6]. Such charge induced fragmentation, sometimes called a Coulomb explosion, is well known for liquids and has been studied for over a century. To date, there have been no studies of Rayleigh instabilities in small solid particles. This

is partly because of the experimental difficulty in applying significant charge to metal nanorods and the expected slow response time of a solid to the induced stress. In this work we report for the first time clear evidence that nanorods will undergo shape changes in response to double layer charging. The addition of electrons to gold nanorods in water with aspect ratios ranging from 2 to 6 leads to an initial blue shift in the absorption spectrum due to the increasing plasma frequency of the electron gas. However, at longer times, the SPL band red shifts due to changes in particle morphology induced by the surface charge. The particles increase their faceting and develop pointed endcaps. The deformation of the particles is plastic and irreversible. In the case of extreme electron densities, fragmentation is fast enough to compete with redox reactions that would discharge the double layer, so the rods fragment spontaneously leading to the formation of clouds of much smaller spherical gold particles. Though charge induced fragmentation is known from gas phase studies of liquid drops, it has not been previously demonstrated for solids. Our finding that sodium borohydride and to a lesser extent ascorbic acid are capable of causing shape changes in small gold rods is consistent with these gas phase studies. It demonstrates that crystal structure and morphology may be controlled by chemical reactions occurring locally as well as by external perturbations. References 1. Nikoobakht, B. and El-Sayed, M.A. Chem. Mater. 2003. 15(10): p. 1957-1962. 2. Murphy, C.J., et al. J. Phys. Chem. B 2005. 109(29): p. 13857-13870. 3. Mulvaney, P. Langmuir 1996. 12(3): p. 788-800. 4. Rayleigh, F.R.S. Phil. Mag. Ser. 1882. 14(5), p. 184-186. 5. Chandezon, F., et al. Phys. Rev. Lett. 2001. 87(15), Art. No. 153402. 6. (a) Duft, D., et al. Nature 2003. 421(6919): p. 128-128. (b) Duft, D., et al. Phys. Rev. Lett. 2002. 89(8), Art. No. 084503.

2:15 PM DD6.3

Abstract Withdrawn

2:30 PM DD6.4

Synthesis and Characterization of Self-assembled (In,Ga)As Quantum Posts on GaAs. Jun He¹, Hubert J Krenner¹, Craig Pryor², Jinping Zhang¹, Yuan Wu¹, Dan Allen³, Chris Morris³, Mark Sherwin³ and Pierre M Petroff^{1,4}; ¹Department of Materials, University of California, Santa Barbara, Santa Barbara, California; ²Department of Physics and Astronomy, University of Iowa, Iowa City, Iowa; ³Department of Physics, University of California, Santa Barbara, Santa Barbara, California; ⁴Department of Electrical & Computer Engineering, University of California, Santa Barbara, California.

We demonstrate a method for the growth of height controlled (In,Ga)As quantum posts (QPs) on GaAs (100) using MBE deposition. The QPs consists of a very short quantum wire connected to a seed QD. QPs with a height of 23nm and 40nm have been analyzed by transmission electron microscopy (TEM) and scanning TEM (STEM), X ray dispersive (EDX) analysis and low temperature photoluminescence (PL). From the cross-sectional TEM micrographs, the self-assembled QPs structures are found to be dislocation-free and coherently strained with the GaAs matrix. The average In distribution along the QPs was obtained from the EDX analysis and a reference Ga_{0.15}In_{0.85}As quantum well. The seed QD composition is In_{0.5}Ga_{0.5}As. The QP average composition is found to be Ga_{0.55}In_{0.45}As. The QPs are embedded laterally in a Ga_{0.9}In_{0.1}As layers with a thickness corresponding to the QPs height and the QP is terminated by pure GaAs on both sides in the growth direction. We will present low temperature micro-photoluminescence (micro-PL) spectra on a single QP and ensembles of QPs. The observed micro-PL properties are drastically different from those of InGaAs QDs. As the pump power is increased, we do not observe state-filling corresponding to the subsequent filling of in-plane orbital (s, p, d,...) states and bi-excitons which are typical of conventional QDs nanostructures. In contrast, the sharp emission lines of the seed dot are accompanied by features at higher energies originating from carrier recombination in the QP. The energy and numbers of these lines is dependent on the QPs height. In order to attribute the observed signatures to transitions in the QP we computed the electron and hole levels using an 8 bands k.p effective mass model. We use the structural and composition information obtained from the TEM and EDX to calculate the full band structure of the QP. For this band structure the single particle levels for electrons and holes are calculated and used to analyze the observed PL characteristics of the QPs. In particular, a comparison between experiment and theory supports that electron states are fully delocalized over the entire QPs whereas bound hole levels can exist in the seed QD. The structure and optical properties of the self assembled QPs suggest that they could have important device applications since they can easily be integrated into band gap engineered heterostructures and combined with conventional self-assembled QDs. The QPs also provide an easy route for efficient electrical carrier injection into QDs. Finally, the QPs growth should be accessible to the wide variety the materials systems for which QDs have been demonstrated since their synthesis relies on a modified growth mode based on that of the well established self assembled QDs. * This research is sponsored through an NSF-NIRT grant and HJK acknowledges support by the Alexander von Humboldt Foundation

2:45 PM DD6.5

Local Electronic Property of ZnO Tetrapods Jong Soo Lee¹, Junghwan Huh², Gyu Tae Kim², Shareghe Mehraeen¹, Nigel Browning¹ and Sangtae Kim¹; ¹Chemical Engineering and Materials Science, University of California, Davis, Davis, California; ²Electrical Engineering, Korea University, Seoul, South Korea.

In recent years, a large number of one-dimensional nanostructures have been synthesized with precisely controlled chemical compositions, morphologies, and sizes using various synthesis methods for potential applications in a variety of nanoscale devices. These include transistors, memory devices, logics, chemical/bio-sensors and lasers. In view of various distinctive properties of ZnO (a direct bandgap of 3.37 eV at room temperature), nanodevices based on this material hold a lot of promises for, in particular, gas sensing, electronic, optoelectronic applications. ZnO-based nanodevices are also promising candidates for biological applications due to easy fabrication and friendly nature to living organisms. ZnO is also known to have a variety of nanostructures including three-dimensional (3-D) forms such as tetrapods. Unlike one-dimensional single crystalline nanostructures, a tetrapod has a junction at which four legs meet. The junction core can possibly have a different structure from those of the legs such that it may show different electrical behavior. By measuring a dc current flowing through two legs across the junction (leg-junction-leg), however, one cannot distinguish between electrical contribution of the junction and of the legs to the overall resistance. In this contribution, we report the local electrical behavior of a ZnO tetrapod measured at relatively high temperature (>300 C) using an ac impedance spectroscopy technique. The results of detailed structural analysis on the tetrapod using HR-TEM will be also presented.

SESSION DD7: Properties of Nanowires I
Chairs: Todd Krauss and Moonsub Shim
Tuesday Afternoon, April 10, 2007
Room 2001 (Moscone West)

3:30 PM DD7.1

Absorption Anisotropy of Aligned CdSe and CdTe Nanowires Aidong Lan, Vladimir Protasenko and Masaru Kuno; Chemistry and Biochemistry, Univ. of Notre Dame, Notre Dame, Indiana.

Thin (5-15 nm diameter) semiconductor CdSe and CdTe nanowires (NWs) that reside in the intermediate to weak confinement regime exhibit unique optical properties due to their one dimensional (1D) nature. Among them, their linear absorption is of great interest from both scientific and practical perspectives. Although NW absorption cross-sections are large, direct measurements of the optical absorption of single NWs remain a great challenge. If the corresponding absorption spectra of well-isolated wires can be measured, then their 1D nature can be significantly enhanced. Solution-based CdSe and CdTe nanowires are synthesized using a recently developed solution-liquid-solid (SLS) procedure with Au/Bi core/shell catalyst nanoparticles. The NWs exhibit high degree of crystallinity and uniformity as seen through transmission electron microscopy (TEM) characterization of representative ensembles. These wires have radii between 3- 7 nm, comparable with the corresponding bulk exciton Bohr radius of CdSe and CdTe (aB ~ 5.6 nm of CdSe and 7.5 nm of CdTe). NW inter-wire diameter distributions range from 25-30% with intra-wire distributions on the order of 6%. As an intermediate step towards single NW absorption measurements, we chose aligned NWs as a convenient system for direct absorption anisotropy studies. Positive AC dielectrophoresis (DEP) is employed to align CdSe NW ensembles between micro-fabricated gold electrodes. The nanowires rapidly assemble in the AC electric field owing to their large induced dipole. A confocal microscope directly probes the absorption of the aligned NWs using a fiber-based supercontinuum white light source. Absorption spectra in the range from 470 to 900 nm were collected as a function of the incident light polarization angle. The measurements show substantial absorption anisotropies. Specifically, the absorbance when the light polarization is parallel to the NW axis is an order of magnitude greater than absorbance with an orthogonal light polarization/NW axis configuration. In addition, the spectral dispersion of the absorption polarization anisotropy was probed over the full spectral range.

3:45 PM *DD7.2

Fluorescence Behavior of Colloidal Semiconductor Quantum Wires. John J. Glennon, Rui Tang, Richard A. Loomis and William E. Buhro; Dept. of Chemistry, Washington University, St. Louis, Missouri.

We are studying the fluorescence and fluorescence intermittency (blinking) of CdSe quantum wires by single-wire imaging and spectroscopy. Band-edge fluorescence intensities from CdSe wires are enhanced significantly by a reversible photobrightening process, and by exposure to certain surface-capping molecules. We have found that most wires exhibit a "twinkling" phenomenon, in which the fluorescence intensity in small, localized wire domains fluctuates independently of similar fluctuations in nearby domains. However, a persistent fraction of the wires exhibits synchronous blinking over large wire segments (lengths > 500 nm), or even over whole wires (lengths > 2 μ m). Significantly, the blinking dynamics follow inverse-power-law statistics comparable to previous findings for quantum dots, suggesting mechanistic similarities between dot and wire blinking. A new mechanism for the reversible photobrightening and blinking will be proposed that is based on the photochemical filling of surface trap sites. The new mechanism is supported by theoretical simulations, which will also be presented. The temperature dependence of the fluorescence behavior in CdSe and other quantum wires may also be presented.

4:15 PM DD7.3

Far-Field Imaging of Optical Second-Harmonic Generation in Single GaN Nanowires. Jim P Long¹, Blake S Simpkins¹, David J Rowenhorst² and Pehr E Perhsson¹; ¹Surface Chemistry, Naval Research Lab, Washington, District of Columbia; ²Materials Science and Technology, Naval Research Lab, Washington, District of Columbia.

The nonlinear optical (NLO) response of nanostructured materials is of current interest because of the need for active elements in nanophotonic applications, and because the nonlinear response itself can serve as a useful diagnostic for intense nanoscale plasmonic fields or for the nanostructure itself. A nanostructure of particular interest is the semiconducting nanowire (NW), which can serve as a "self-wired" nanoLED, laser, or photoconductive detector. Here we report an investigation of femtosecond-induced second-harmonic generation (SHG) in GaN NWs that correlates far-field microscopic imaging of the polarization-dependent SHG from individual NWs with electron backscattered diffraction (EBSD) from the same NWs. We find that far-field methods offer an approach for distinguishing the crystallographic orientations of these wurtzite NWs. Because the NLO response of materials depends on the excitation and emission polarizations relative to the crystallographic orientation, single-particle studies are especially valuable for not only avoiding the usual ensemble averaging over variances among individual nanostructures, but also the averaging over angle that can obscure underlying structure in the NLO response of individual particles. The use of far-field microscopic imaging to assess NLO properties of nanomaterials offers flexibility over more complex, albeit powerful, near-field scanning methods, and could serve as a fully optical in-situ diagnostic of crystallographic orientation in surveys of NW collections, in NWs under test, or even in NWs sealed in devices. While a full analysis of the SHG response would require a tedious electromagnetic treatment, we find that the main polarization features of the SHG from these 75-nm diameter NWs are adequately explained by neglecting surface contributions and treating the bulk crystal within the much simpler quasi-static approximation. In the quasi-static approximation, which should prove useful in describing many nanophotonic behaviors, one assumes that the NW transverse dimension is much less than the first and SH wavelengths (here, 860- and 430-nm respectively). Our data also emphasizes the importance of including the transverse depolarization effect, which reduces the component perpendicular to the NW of not only the pump electric-field, but also the 2nd-order polarization $P(2\omega)$.

4:30 PM DD7.4

Orientation-dependent Raman Spectroscopy of Single Wurtzite CdS Nanowires. Hai Ming Fan¹, Zhenhua Ni¹, Yuanping Feng¹ and Zexiang Shen²; ¹physics department, national university of singapore, Singapore, Singapore; ²Physics and Applied Physics, Nanyang Technological University, Singapore, Singapore.

We report the first successful polarized and orientation-dependent Raman measurement on single wurtzite structured CdS nanowires, an important class of photonics and optoelectronics material, with diameter down to 80 nm. The Raman measurements of individual CdS nanowires were performed using Renishaw InVia System and Jobin-Yvon T64000 system with different resonance laser energy. No surface enhancement technique was employed in our measurement to ensure the collections of the intrinsic Raman signals. The resulted resonance Raman spectra of nanowires are compared with that of bulk ribbon and theoretical predications. The results show the phonons with polarization in axis of nanowire are strongly affected by shape effect, which has a greater effect on first order phonons than second order phonons. But the effect of the crystal symmetry cannot be neglected and its contribution can be estimated by deviation from the theoretical curve of angular dependences based on shape effect. Whereas

the angular dependences of the phonons with polarization absented in axis of nanowire are independent from shape effect. The shape effect have been quantitatively modeled based on classical electromagnetic theory by treating nanowire as an infinite dielectric cylinder in a vacuum to estimate the altered electric field amplitude inside nanowire. The polarized E-P coupling of the nanowire was identified and attributed to confinement effect in one-dimension shape. The analysis of angular dependence reveals the interaction and interdependency of shape effect, crystal symmetry and resonance effects on Raman spectroscopy in the single-crystal nanowire. These results can also be applied for understanding phonon behaviors of most useful semiconductor nanowires with wurtzite structure, such as ZnO, CdSe etc.

4:45 PM DD7.5

Piezoelectric Nanowires Scott Mao¹ and C. Jiang²; ¹Department of Mechanical Engineering and Materials Science, University of Pittsburgh, Pittsburgh, Pennsylvania; ²Shenyang Interfacial Material Center, IMR, Shengyang, Liaoning, China.

An atomic force microscopy (AFM) is used to measure the effective piezoelectric coefficient (d_{33}) of individual Li doped ZnO nanobelt lying on conductive surface. Based on references using bulk ZnO and quartz, piezoelectric constant d_{33} of Li doped ZnO nanobelt is found to be frequency dependent and varies from 14.3pm/V to 26.7pm/V, which is much larger than that for the bulk single crystalline ZnO of 12.4pm/V. The results support the application of Li doped ZnO nanobelts as nano-scale sensors and transducers.

SESSION DD8: Poster Session: Assembly, Modeling and Applications
Chairs: Sanat Kumar, Masaru Kuno, Xiao-Min Lin, Ruth Pachter and Moonsub Shim
Tuesday Evening, April 10, 2007
8:00 PM
Salon Level (Marriott)

DD8.1

Freestanding Polymer Colloid Crystal Wires and Metal Reverse Colloid crystal Wires: Magnetic Field Directed Assembly Behavior Feng Li and John B. Wiley; Department of Chemistry and Advanced Materials Research Institute, University of New Orleans, New Orleans, Louisiana.

Polymer colloid crystal wires, metal reverse colloid crystal wires and their arrays have been successfully prepared in large-scale at low temperature. First, polystyrene colloid spheres are driven into the channels of porous glass membranes with a double-template approach and assembled into helical colloid crystal wires. Electrochemical deposition in the void of colloid sphere modified channels then produce metal reverse colloid crystal wire array. The composite of membrane, colloid spheres and metal reverse colloid crystal wire is finally annealed to make the polymer colloid spheres fuse together. After selective removal of template, polymer colloid crystal wires and metal reverse colloid crystal wires with helical structure have been realized. The magnetic field directed assembly behavior of Ni reverse colloid crystal wires have also been investigated.

DD8.2

Hierarchically Organized Nanocrystal Metamaterials Formed through Building Block Self-Assembly. Hongyou Fan^{1,2}, Adam Wright², John Gabaldon², Erik W Leve², Darren Dunphy², Jeffrey Brinker^{1,2}, Kevin Malloy², Thomas Sigmon² and Kai Yang²; ¹Sandia National Lab, Albuquerque, New Mexico; ²Chemical and Nuclear Engineering, University of New Mexico, Albuquerque, New Mexico.

Nanocrystals (NCs) exhibit unique size- and shape-dependent physicochemical properties arising from low dimensional quantum confinement effects and have been successfully used as building blocks for the fabrications of 2- and 3-dimensional NC arrays for the development of 'artificial solids' (or metamaterials) with new collective optical and electronic properties derived from the interaction or coupling of different NCs in an assembly. NC surface chemistry plays a key role in control of microstructures of the NC arrays such as mesophase (face-centered-cubic (fcc), diamond, etc), interparticle distance, etc. To date, work has mostly focused on the synthesis of NCs that are stabilized with alkane ligands (CH₃(CH₂)_nR, R=SH, NH₂, PO, etc). Self-assembly of these NCs and formation of ordered NC arrays are driven by hydrophobic (or van der Waal) interactions of interdigitated alkane chains between NCs. Here we report our recent progress in the synthesis of a new building block- NC-micelle and its use in formation of ordered, three-dimensional, NC arrays. NC-micelles were synthesized through encapsulation of organic monolayer (alkane chains) derivatized, hydrophobic NCs within the hydrophobic interior of surfactant/lipid micelles (Fan et al. Science 304, 567-571, 2004). This approach is simple, general, and can be used to synthesize water-soluble metal, semiconductor, and magnetic NC-micelles with different shapes. Through using varied surfactants, the flexible NC-micelle surface chemistry provides unique opportunity for subsequent self-assembly through hydrogen-bonding, charge interactions, etc. and formation of highly ordered nanocrystal arrays with controlled mesophase, orientation, and material forms (film, powder, particle). Integration and charge transport of NC/metal oxide arrays will be also presented. Sandia is a multiprogram laboratory operated by Sandia Corporation, a Lockheed Martin Company, for DOE under contract DE-AC04-94ALB5000

DD8.3

Ordered Monolayer Array of Gold Nanoparticles by Self-Assembly Process on Functionalized Solid Substrates Geun-Tae Cho, Hye Jin Nam, Ju Yeon Chang, Jong-Hyeon Lee and Duk-Young Jung; Chemistry, Sung Kyun Kwan Univ., Suwon, Gyeonggi-do, South Korea.

Two-dimensional arrays of gold nanoparticles were prepared in colloidal solutions by self-assembly of 3 nm diameter thiolate-capped colloidal gold particles onto glass, Si wafer and silica grid substrates having amine or thiol functional groups with high affinity for gold. The monolayer film formation involves an exchange, crosslinking, and precipitation among the gold nanoparticles and interparticle linker molecules with two different functionalities, 1,4-butanedithiol (BDT) and 11-mercaptoundecanoic acid (MUA). The amine or thiol functional groups were formed by a vapor deposition of 3-aminopropyltriethoxysilane (APTES) and 3-mercaptopropyltrimethoxysilane (MPTMS) on the substrates. TEM images reveal that the 3 nm diameter gold nanoparticles were assembled with an ordered monolayer on the amine functionalized silica grid, and excess particles were effectively removed from the substrate by ultrasonic treatment. AFM results show that the assembled nanoparticle films on glass surfaces have a uniform roughness of 0.7 nm when the MUA was used as an interparticle linker. The gold monolayers possess a set of features that make them very attractive for various applications, including chemical and biological sensors, devices and so on.

DD8.4**Abstract Withdrawn****DD8.5**

Lattice Engineering Synthesis of Heterostructured Metal Oxide Nanoparticle-Layered Titanate Nanohybrids. Tae Woo Kim and Seong-Ju Hwang; Division of Nano Sciences, Ewha Womans University, Seoul, South Korea.

We have synthesized porous nanohybrids of $\text{MO}_x\text{-Ti}_{1.83}\text{O}_4$ ($M = \text{Zn, Cr, etc}$) heterostructure through a reassembling of exfoliated titanate nanosheets and transition metal oxide nanoclusters. According to XRD, FE-SEM, and HR-TEM analyses, individual titanate nanolayers are interstratified with metal oxide nanoparticles in layer-by-layer way, leading to the formation of porous intercalation structure. N_2 adsorption-desorption isotherm and diffuse reflectance UV-vis analyses demonstrate that the present nanohybrids show expanded surface areas and modified band structures, which is due to the micro-/meso-porosity of these materials and the coupling between metal oxide components, respectively. These nanohybrids display an enhanced catalytic activity as well as a stabilization of the guest metal oxide. The present results highlight that the exfoliation-reassembling route can provide a very powerful way of developing novel heterostructured materials with promising functionalities.

DD8.6

The Sodium Salt Effects on the Layer-by-Layer Self-Assembled Carbon Nanotubes Multilayers Kye Ung Lee¹, Byung Tae Ahn¹, Mike C Petty² and Do Jin Kim³; ¹Department of Materials Science and Engineering, Korea Advanced Institute of Science and Technology, Daejeon, South Korea; ²School of Engineering and Centre for Molecular and Nanoscale Electronics, University of Durham, Durham, United Kingdom; ³Department of Materials Science and Engineering, Chungnam National University, Daejeon, South Korea.

Layer-by-layer (LbL) self-assembly is a template-assisted process in which charge reversal techniques using polyelectrolytes enable the deposition of films layer-by-layer. Layer-by-layer self-assembly is a powerful method to build ultrathin films and nanoparticles also could be incorporated in the thin film in the aids of polyelectrolyte. In this work, we will describe the building of thin film architectures incorporating carbon nanotubes (CNTs) with polyelectrolytes and salt effect on the building CNTs films. The CNTs are positively and negatively charged by coating strong polyelectrolytes, poly(styrene sulfonate) (PSS) and poly(diallyldimethylammonium) (PDAA), respectively. The side groups of polyelectrolytes could non-covalently interact with CNT wall by pi-pi interaction, etc. So CNTs with polyelectrolytes could be dispersed stably in water. With this treatment, stability of dispersion and solubility in water is improved. The presence of charged functional groups on the surface of the CNTs then allows consecutive thin film deposition to proceed via the electrostatic LbL method. The persistence length is a basic property quantifying the stiffness of a macromolecule of a polyelectrolytes. The persistence length of the polyelectrolyte chain should be one of the key parameters since it determines the chain's ability to wrap around the nanotubes, resulting in the deposition. The persistence length of polyelectrolyte can be controlled by changing the ionic strength of CNT suspension, due to screening of electrostatic repulsion between the polyelectrolyte backbone charges. The ionic strength of CNT suspension was changed by changing sodium salt concentration. The analysis of UV-Vis spectroscopy and ellipsometry showed that the higher ionic strength enhanced the deposition of CNTs. The adsorption state of CNTs with polyelectrolyte was studied using TEM and TGA. The self-assembly process was monitored using UV-Vis spectrophotometer, quartz crystal microbalance and ellipsometer. And the surface morphology of films was studied using SEM.

DD8.7

Directed Assembly of Colloidal Particles on a Complex Physicochemical Nano Template. Yong Hoon Kim¹, Juhyun Park², Pil J. Yoo¹ and Paula T. Hammond¹; ¹Department of Chemical Engineering, Massachusetts Institute of Technology, Cambridge, Massachusetts; ²Department of Materials Science and Engineering, Massachusetts Institute of Technology, Cambridge, Massachusetts.

A new approach to directly organize colloidal particles into patterned arrays using a nanostructured polymer template coated with a layer-by-layer assembled polyelectrolyte multilayer was introduced. In this approach, a template using a UV-curable photo polymer was coated with polyelectrolyte multilayers, followed by a contact printing of an oppositely charged polyelectrolyte monolayer. The resultant topological template with both positive and negative charges provided a finely defined chemical nano-pattern to guide selective deposition of colloidal particles onto the patterned surface upon Coulombic attraction. For example, when negatively charged dilute colloidal suspensions were placed on the template, the particles were selectively adsorbed within positively charged grooves or holes. It was confirmed that the charge interaction between particles and multilayer coated templates is the main effect for the selective assembly of colloidal particles on the substrate. We verified that the efficiency of particle assembly on the template decreases with reducing particle size due to concurrently weakened electrostatic energy. This approach can allow selective deposition of sub micrometer scaled particles on the surface, as well as controlling the cluster size and shape of colloidal particles, suggesting potential applications on two dimensional photonic devices and bio-sensors using bio-functionalized particles.

DD8.8

Hierarchical Co-Doped ZnO Hexagonal Rings and Plates Composed of Self-Assembled Hexagonal ZnO Nanorods Yi Jing Li, Chiu-Yen Wang, Ming-Yen Lu, Kun-Mu Li and Lih-Juann Chen; National Tsing Hua University, Hsinchu, Taiwan.

Co-doped ZnO hexagonal rings composed of single-crystal ZnO hexagonal nanorods were grown via a combined hydrothermal and electrochemical process. The unique hierarchical ZnO hexagonal rings are based on the integration of single-crystalline ZnO nanorods of hexagonal shape. The growth of the external and inner frames of hexagonal rings is concentric. The perfect hexagonal units are aligned along $\langle 0001 \rangle$ directions while the frame of the hexagonal rings are bounded with six $\{1-210\}$ planes. The composing ZnO units were found to be tightly connected and matched, which provides direct evidence for an oriented attachment growth mechanism. The cathodoluminescence peaks show a redshift about 237 meV and 423 meV of the band gap edge from that of the pure ZnO nanorods for 0.25% and 1% Co-doped ZnO nanostructures, respectively. Tuning of band gap by doping shall be beneficial for optical applications.

DD8.9

Formation of Highly Ordered Arrays of Dimples on Tantalum at the Nanoscale. Peter Kruse, Sherdeep Singh, Warren Barden, Subir Ghosh,

Mark Greiner and Hany El-Sayed; Chemistry, McMaster University, Hamilton, Ontario, Canada.

Given the current interest in nanostructured materials and nanoparticles, templates with monodispersed and highly ordered regular features are in high demand. As a result, researchers are studying systems such as porous metal oxides with the goal of developing new self-assembly techniques. Due to its outstanding properties, tantalum is an important material for mechanical, electronic and medical applications, but the ability to control its surface properties at the nanoscale has been largely limited to the growth of dense anodic oxides and, recently, porous oxides of poor order. Here we show that electropolishing of tantalum in concentrated acid mixtures can reproducibly lead to dimples tens of nanometers in diameter, regular in shape, monodispersed in size and arranged in highly ordered arrays which even transverse grain boundaries. After a single polishing step of less than ten minutes, dimples of 30 nm to 50 nm in diameter (a function of polishing voltage) and around 10 nm deep form a 2-dimensional structure consisting of tantalum metal covered in native oxide. Dimpled tantalum is ductile, high-melting, chemically inert and easily prepared. It can be safely used as a template or mould for nanostructure synthesis under extreme conditions, as demonstrated with a simple sputter coating and flame annealing procedure for gold nanoparticles. Due to their exceptional properties, we anticipate that these nanostructured tantalum surfaces will be suitable for a wide variety of applications in catalysis, combinatorial materials science, nanoparticle synthesis, biomedical devices, cast or die for nanopatterning of other materials etc.

DD8.10

2D Growth of Nanomeshes in 3D Colloidal Crystal Templates. Ji Zhou and Ming Fu; Material Science, Tsinghua University, Beijing, Beijing, China.

Novel two dimensional (2D) zinc oxide nanosheets with ordered pore periodicity are synthesized via a colloidal crystal template-assisted electrochemical deposition method. The nanosheets are derived from the electrochemical deposition of zinc hydroxide nitrate hydrate (ZHNH) into the interstices of colloidal crystal arrays and the subsequent removal of the templates under calcinations. The nanosheets follows a preferable crystallization orientation along (111) crystal face of colloidal crystals, indicating that their growth and orientation on the substrate are mainly directed by the colloidal template-induced crystallization process.

DD8.11

Exfoliation and Reassembling Route to Nanoparticle-Lamellar Oxide Hybrid: TiO_2 -Pillared Layered Manganate. Joo-Hee Kang¹, Seung-Min Paek² and Jin-Ho Choy¹; ¹Division of Nanoscience and Department of Chemistry, Ewha Womans University, Seoul, South Korea; ²School of Chemistry, Seoul National University, Seoul, South Korea.

Pillared layered solids are of considerable interest due to their potential applications as secondary lithium battery, electrochromic device, electrochemical sensor, and so forth. Of particular interest, layered manganese oxides show reversible Li ion insertion-deinsertion property, which is appropriate as promising electrode materials for lithium rechargeable batteries. Especially, the high surface area of electrode material could provide facile and effective access of lithium ions to all available sites, resulting in high enhancement of discharge capacity. In this study, we report a novel pillared architecture of colloidal manganate nanosheets with titania nanoparticles via exfoliation and reassembling technique. At first, the layered protonic manganese oxide, $\text{H}_{0.13}\text{MnO}_2$, was exfoliated in an aqueous solution of tetrabutylammonium (TBA) hydroxide, and then, the obtained exfoliated nanosheets of manganate were reassembled with titania nanoparticles which resulted in highly porous nanohybrid materials. According to the X-ray diffraction (XRD) analysis, TiO_2 -pillared MnO_2 (hereafter abbreviated as TMN-rt) with an interlayer distance of 10.2 Å, determined by subtracting 5.2 Å for the thickness of the manganate nanosheet from the basal spacing of 15.4 Å, is in good agreement with the mean size (ca. 10 Å) of TiO_2 nanoparticles, suggesting the monolayer arrangement of TiO_2 nanoparticles in the intersheet region. Moreover, the cross-sectional transmission electron microscopy (TEM) analysis clearly showed that highly ordered pillared structure along the crystallographic a-axis was successfully achieved even after the reassembling reaction, and the lattice expansion of TMN-rt was determined to be 1.55 ± 0.1 nm, which is well consistent with the XRD results. Furthermore, based on the Mn K-edge X-ray adsorption near edge structure (XANES) analysis, the absorption edge energy that can be assigned to transitions from the core 1s level to unoccupied 3d states of the pillaring material is remained unchanged, indicating that the valence states of manganese ions are almost the same. It is evident that the electronic structure and local symmetry of Mn ion were maintained even after exfoliation-reassembling reaction. Finally, preliminary electrochemical charge-discharge measurements indicated that the present nanohybrids showed the enhanced discharge capacity compared to the theoretical value of the physical mixture between TiO_2 and MnO_2 . Such results suggest that highly porous nanohybrid materials fabricated by pillaring method could be useful as a cathode material in lithium secondary batteries.

DD8.12

Controlling Size, Shape, and Distribution of Platinum Nanoparticles Electrodeposited on Carbon Supports. S.M.Shahinoor I. Dulal, Chang-Koo Kim, Wonjin Jeon and Chee Burm Shin; Chemical Engineering, Division of Energy Systems Research, Ajou University, Suwon, South Korea.

There is much research interest in carbon supported platinum nanoparticles, especially for their use as catalysts in fuel cells and sensors. A plenty of work has been done to prepare colloidal platinum nanoparticles by chemical reduction using borohydride or other reducing agents. Colloidal nanoparticles, however, need to be supported for their use as catalysts. On the other hand, direct electrochemical reduction of platinum ions on a support is a relatively convenient way to fabricate nanoparticle electrodes. There are some reports on the preparation of supported nanoparticle by electrochemical route. The catalytic activity of these nanoparticles has also been tested. However, the catalytic performance of nanoparticles is crucially dependent on their size and shapes. The dispersion of nanoparticles on the support as well as the support itself also has significant influence on the catalytic performance. Uniformly dispersed smaller particles with uniform size and shape are normally desired for enhanced catalytic activities. But it has been found that the sizes of electrodeposited particles vary significantly and particles tend to agglomerate, resulting in uneven distribution on the support surface. The current work aims to control the size and shape of particles and their distribution on catalyst support. In this work, platinum nanoparticles were grown on carbon support by an electrochemical deposition method from an electrolyte containing chloroplatinic acid. The characterization of the supported nanoparticles has been carried out by electrochemical technique and by XRD, SEM and AFM. The electrocatalytic property of the supported nanoparticles was also tested. We have deposited monodispersed and relatively uniform sized platinum nanoparticles on carbon support. The particles have been found very stable on the support surface. It has also been found that particles size and their distribution can simply be controlled by changing electrochemical parameters. The carbon supported platinum nanoparticle electrodes have shown electrocatalytic activities for electrooxidation of methanol (fuel cell fuel) and hydroquinone & phenol (pollutants in industrial waste).

DD8.13

Highly Mesoporous TiO₂ Nanohybrid as an Electrode for a Lithium Battery. Seung-Min Paek^{1,2}, Joo-Hee Kang³, Hyun Jung³, Young-Jun Lee², Seong-Ju Hwang³ and Jin-Ho Choy³; ¹Advanced Materials Applications, Battelle Memorial Institute, Columbus, Ohio; ²School of Chemistry, Seoul National University, Seoul, South Korea; ³Center for Intelligent Nano-Bio Materials, Ewha Womans University, Seoul, South Korea.

To fabricate mesoporous electrode materials with delaminated structure, the exfoliated layered titanate in aqueous solution was reassembled in the presence of anatase TiO₂ nanoparticles to induce a great number of mesopores and eventually a large surface area of TiO₂. No (010) peaks corresponding to the layered titanate appear in the X-ray diffraction patterns of reassembled nanohybrids, which suggests that the titanate nanosheets were randomly hybridized with TiO₂ nanoparticles without any self-restacking into layered phase. According to the high-resolution transmission electron microscopy images of these nanohybrids, the randomly oriented titanate nanosheets can be seen clearly along with TiO₂ nanosol particles with spherical images, indicating that the exfoliated nanosheets are indeed incorporated with anatase TiO₂ nanoparticles to form porous materials. From N₂ adsorption-desorption isotherms, these nanohybrids are fairly high in specific surface area and in mesoporosity for effective and facile lithium insertion-deinsertion reaction. The BET specific surface area of nanohybrid is greatly enhanced from 13 m²/g (layered protonic titanate) to 190 m²/g (nanohybrid) upon hybridization. Furthermore, the pore size can be tailored within mesopore range by adjusting the ratio between titanate nanosheet and TiO₂ nanoparticle. In this regard, the applicability of the present nanohybrid as an electrode material for lithium rechargeable battery has been investigated by monitoring the electrochemical intercalation of lithium. This study clearly demonstrates that the hybridization between layered titanate and TiO₂ nanoparticles gives rise to a remarkable enhancement of discharge capacity compared to the capacities of layered titanate, TiO₂ nanoparticle, and their physical mixture.

DD8.14

Electronic Properties of C-face and Si-face SiC 3C/4H Heterostructures and Devices. Jie Lu, Chris Thomas, Mvs Chandrashekhar and Michael Spencer; Electrical and Computer Engineering, Cornell University, Ithaca, New York.

SiC has been studied intensively due to its potential in high voltage, high power and high frequency devices. The lack of a heterojunction, however, has limited its application in RF applications, unlike its wide bandgap counterpart GaN/AlGaIn. SiC is a polytypic semiconductor, with the different polytypes having markedly different electronic properties. It is thus a highly promising material for creating various polytype heterostructures, which find application in HEMT devices. The 4H/3C heterostructure has been studied by Schwierz et al. Their work, however, relies on the availability of a 3C SiC substrate, which has not been commercialized. Furthermore, 4H cannot readily be grown on 3C. Crystal growth constraints force the metal gate of the heterostructure to be on the narrow-gap 3C side, which is the structure investigated. We calculate the variation in carrier density with Schottky barrier height, thickness of the 3C layer and doping level. Both C face and Si face structures are investigated. We predict a 2DEG at the interface on the C-face. On the Si-face, however, we predict an inversion-type 2 dimensional hole gas (2DHG). The carrier density of 2DEG/2DHG at the interface is found to be as high as 1e13/cm². We also discuss the implications of having the gate on the narrow-gap 3C side, as opposed to the wide-bandgap 4H side.

DD8.15

A New Route to the Production and Patterning of Highly Smooth, Nanometer Thin Zirconium Oxide Films. Karl Coleman and Scott Watson; Department of Chemistry, University of Durham, Durham, United Kingdom.

The development of next generation computer chips has focused upon the reduction of the physical dimensions of such devices, enabling the integration of a greater number of components per chip. However, the 'scaling down' of such technology is limited by, amongst other things, the thickness of the dielectric silicon oxide layer used. This limitation is the result of the dielectric becoming sufficiently thin that electron tunneling across the layer takes place, resulting in current leakage. One solution to this problem is to replace present dielectrics with alternative materials exhibiting a higher dielectric constant. One metal oxide which may meet such requirements is zirconium oxide, which has been demonstrated to be stable against silicidation and silicate formation to temperatures up to 1150 K. Several methods for the production of thin zirconium oxide films have been reported in recent years, including chemical vapor deposition, sol-gel synthesis, electron beam deposition and sputtering. Typically these processes have been used in the production of oxide films ranging from several to hundreds of nanometer thick with varying degrees of roughness. Here we discuss a new approach for the production of highly smooth, nanometer-thick zirconium oxide films, by deposition of Langmuir-Blodgett (LB) films of octadecylphosphonic acid (ODP-H₂), upon chemically modified silicon oxide supports, stabilized by Zr⁴⁺. In this study, we employ LB deposition / self-assembly cycles to produce 'hybrid bilayer' films consisting of a 'lower leaflet' of long chain alkyl molecules and an 'upper leaflet' of ODP-H₂ monolayer. The bilayer produced is subsequently stabilized by Zr⁴⁺ and the zirconium oxide film generated by annealing at 750 K. Methods of patterning the zirconium oxide and hybrid bilayer films will be discussed.

DD8.16

Development of a Bath And Optimization of Electrochemical Parameters for the Deposition of Platinum Nanoparticles on Graphite. S.M.Shahinoor I. Dulal, Tae Ho Kim, Hyeong Jin Yun, Chang-Koo Kim and Chee Burm Shin; Chemical Engineering, Division of Energy Systems Research, Ajou University, Suwon, South Korea.

Platinum nanoparticle electrodes find applications in fuel cells, sensor development, and industrial waste treatment. There are many ways to prepare platinum nanoparticles such as chemical reduction, sol-gel, electrodeposition, etc. Nanoparticles prepared by chemical reduction or sol-gel methods need to be supported on suitable surfaces for their use as catalytic electrodes while electrochemical deposition of platinum nanoparticles directly on a support is a cheap, convenient, and efficient way to fabricate electrodes. The uniform distribution of nanoparticles plays an important role in determining their catalytic activity. It is, however, very difficult to obtain evenly dispersed and uniformly sized nanoparticles using electrodeposition. In the present study, we have developed an experimental system and a methodology to electrodeposit platinum nanoparticles with relatively uniform size and shape directly onto a graphitic carbon substrate. Carbon has been found most suitable support for platinum nanoparticles for their use as catalytic electrodes in fuel cells. Deposition conditions have been determined and optimized by electrochemical experiments such as cyclic

voltammetry. We have been able to deposit nearly monodispersed and evenly distributed platinum nanoparticles onto the carbon support from a bath containing chloroplatinic acid. It has been found that the particle size and distribution can be controlled by changing bath compositions and electrochemical parameters. The catalytic property of the carbon supported platinum nanoparticle electrodes has also been tested for the oxidation of methanol and phenol.

DD8.17

Broadband Asymmetric Mirrors using Metal-dielectric Nano-composite Coatings Aiqing Chen, Keisuke Hasegawa and Miriam Deutsch; University of Oregon, Eugene, Oregon.

An asymmetric mirror is a planar layered optical device exhibiting difference in reflectance of light incident from either side, while its transmittance remains the same. This reflectance asymmetry is due to the different losses in the mirror (in form of absorption as well as scattering,) when the light impinged from opposite direction. Asymmetric mirrors have recently found use in specialized Fabry-Perot interferometer systems. One of the simplest structures for an asymmetric mirror is a thin metal film on a dielectric slab, embedded in a uniform dielectric. The design of asymmetric mirrors previously addressed typically employed a smooth thin metal film on a dielectric substrate or multi-layer thin film stacks. The optical characteristics of these mirrors, such as reflectance asymmetry and the associated bandwidth are typically constrained to a narrow range, due to a limited choice of materials. However, when one of these films is replaced by a semi-continuous and disordered nanocrystalline silver film, the optical response of the nano-composite system could change dramatically, i.e., increasing the reflectance asymmetry, while simultaneously its dispersion is minimized. We report on design and fabrication of broadband asymmetric mirrors using metal-dielectric nano-composite coatings. Basic dispersion engineering principles were applied to model a broadband and large reflectance asymmetry, which was then inverted to yield the effective permittivity. An effective-medium approach was then implemented to approximate the required optical response function in metal-dielectric nano-composites. These nano-composites with engineered permittivities were realized from semi-continuous and disorder silver films deposited on glass substrates using a variation of Tollen's reaction. The morphology and average thickness ranged from 20-50 nm were characterized under high resolution scanning electron microscope (SEM) and atomic force microscope (AFM). Optical reflectance and transmittance spectra from samples with filling fraction ranged from 10% up to 90% were obtained and properly normalized. Various degree of reflectance asymmetry and their strong dependence on the surface coverage were observed. Nevertheless, the transmittance always remained symmetric, even for rough films with high surface coverage. The most noticeable feature is the flat (non-dispersive) and strongly enhanced (five times larger than smooth thin film,) reflectance asymmetry in the visible and near infrared, which experimentally demonstrated our theoretical prediction of a broadband asymmetric mirror. Details of the physical mechanism of asymmetric mirrors, as well as their potential applications will be addressed.

DD8.18

Enhanced Tunneling through sub 30 Angstroms thick Gallium Nitride Cap Layers on Silicon Carbide for Low Contact Resistance Choudhury Jayant Praharaj, Intel Corporation, Santa Clara, California; (formerly with) Department of Electrical and Computer Engineering, (formerly with) Cornell University, Ithaca, New York.

We present numerical calculations of tunneling through ultra thin Gallium Nitride cap layers on p-doped silicon carbide, from the two-dimensional hole gas accumulation regime to the pure depletion regime. We demonstrate the predominance of thermionic field-emission of the split-off holes to the total carrier flux, despite their low occupation factors in the Fermi-Dirac statistics. The contribution of the heavy and the light holes is damped by the large potential barrier. We calculate the contributions of spontaneous and piezoelectric polarizations to the tunneling profile seen by the holes. An enhancement of two orders of magnitude is seen in the transmission probabilities for a 10 angstroms thick Gallium Nitride cap layer for holes very close to the valence band edge, compared to a barrier without any gallium nitride cap. The contact resistances are also calculated for the Gallium Nitride tunneling caps and more than two orders of magnitude lowering is seen with the ultra-thin caps. Larger cap widths induce Two Dimensional Hole Gases, but the advantages of hole accumulation are offset by the higher effective tunneling width. Our calculations are relevant to nanostructures and nanodevices involving heterojunctions between gallium nitride and silicon carbide, and provide the basis for low contact resistances with as-deposited metals. While our calculations focus on the regime of very high barriers to the metal of the order of 1.5 ~ 2 electron volts, where the method of ultra-thin caps is most useful, similar conclusions also hold for lower barrier widths

DD8.19

Nanogap Fabrication by Pd Hydrogen Embrittlement for Field-Emission Applications. Fu-Ming Pan¹, Chih-Hao Tsai¹, Kuan-Jung Chen¹, Cheng-Yang Kuo¹, Mai Liu² and Chi-Neng Mo²; ¹Dept. Mat. Sci. Eng., National Chiao Tung University, Hsinchu, Taiwan; ²Chunghwa Picture Tubes,Ltd, Taoyuan, Taiwan.

We have employed hydrogen embrittlement to fabricate nanogaps on line-patterned palladium thin films, and studied the field emission characteristics of the Pd electrodes separated by the nanogap. The Pd-H system forms two distinct hydride phases, α and β phases. The two phases may singly exist in a pure form or coexist in the Pd-H system depending on the H:Pd atomic ratio and the temperature. The transition from the α -phase to the β -phase is accompanied by a volume expansion resulting in a mechanical strain in the Pd-H system. Properly selecting the hydrogen uptake condition to induce the mechanical stress in the Pd thin film, we have successfully fabricated a nanogap on the Pd line pattern. The Pd line structure was prepared on the Pt bottom electrode. Both the Pd and Pt thin films were electron-beam-evaporation-deposited and patterned by optical lithography and lift-off method. The temperature of hydrogen uptake was a critical factor determining the separation between the Pd thin film electrodes, and a nanogap as small as 30 nm could be readily achieved. The Pd thin film electrodes showed satisfactory field-emission characteristics with a turn-on voltage of 30 V, which is defined as the bias voltage producing a field-emission current of 0.1 mA. Further surface treatment of the Pd electrodes can greatly improve field-emission properties. Light spots could be clearly observed on a phosphor plate when the propagating surface electrons on the Pd electrodes, induced by the field emission from nine nanogaps with a field-emission cross-section of $3.0 \times 0.03 \mu\text{m}^2$, were extracted to the plate.

DD8.20

Electrical Properties of a Single TiO₂ Nanotubes Depending on Annealing Ambient (vacuum and O₂) and Temperature. Sanghee Won¹, Kyunghun Jeong¹, Seunghye Ko¹, Dongkyu Cha², Moon J. Kim², Jiyoung Kim² and Jaegab Lee¹; ¹School of Advanced Materials Engineering, Kookmin University, Seoul, South Korea; ²Electrical Engineering, The Univ. of Texas at Dallas, Richardson, Texas.

In this work we have demonstrated the dependence of the electrical properties of a single TiO₂ nanotube on annealing temperatures and ambient. TiO₂ nanotubes (200nm in diameter) were fabricated with atomic layer deposition (ALD) on nano-template. The device of TiO₂ nanotubes made from individual TiO₂ nanotubes with focused ion beam (FIB) induced Pt electrode. FIB-deposited Pt contacts to TiO₂ nanotubes indicating ohmic contacts of Pt to TiO₂. Resistivity of the as-deposited TiO₂ nanotube was 1.5×10^5 ohm-cm which was increased 8.7×10^6 ohm-cm after O₂ annealing at 700C, and was also reduced 0.0072 ohm-cm after vacuum annealing at 700C. Annealing in reducing ambient produces defects, such as oxygen vacancy and Ti interstitial, which determine the properties of the TiO₂ resistivity. An oxygen vacancy makes 2 free electrons because of charge neutral. Dramatic decrease of the resistivity in vacuum-annealed TiO₂ nanotube is due to the generation of oxygen vacancy (approximately 4.3×10^{20} #/cm³). The presence of OH in the ALD TiO₂ nanotubes and strain effects from the crystallization at high temperature is responsible for the lower formation energy (60.48 kcal/mol) of oxygen vacancy which is lower than value of single TiO₂ (105 kcal/mol). The high resolution-TEM confirms the strain effect in the crystalline of at as-annealed TiO₂ nanotubes. In addition, HR-TEM show the crystallization of TiO₂ nanotubes during annealing in vacuum and in O₂ ambient, which was need to explain the measured electrical properties and the strains effects on the crystallization. This work was supported by the ERC(CMPS, Center for Materials and Processes of Self -Assembly) program of MOST/KOSEF(R11-2005-048-00000-0)

DD8.21

Dual-gate ZnO Nanowire FETs Aligned by Dielectrophoresis Seung-Yong Lee, Duk-II Suh, Tae-Hong Kim, Jung-Hwan Hyung, Ji-Eun Park and Sang-Kwon Lee; Dept. of Semiconductor Science and Technology, Chonbuk National University, Jeonju, South Korea.

1D system, for instance nanowires, nanotubes, and nanobelts presenting a fascinating distinctive features and hence representing themselves as a potentially ideal building blocks for nano-electronics and nano-optoelectronics devices. Here, we report that the fabrication and electrical characterization of high performance dual-gate ZnO field-effect transistors such as MOSFET and MESFET. The ZnO nanowires were prepared by AC dielectrophoresis (DEP) method for device alignment. The AC DEP was optimized with a bias voltage of $15 V_{pp}$ at a frequency of 1 kHz. The DEP results indicated that the number of aligned ZnO nanowires increased with increasing AC voltages and ZnO nanowires were well aligned on the metal electrodes (Ti/Au=20/70 nm). For better ohmic contacts to ZnO nanowires, an additional capping layer was formed on the top of the source and drain metals. From the transport measurements of our AC DEP prepared ZnO nanowire FETs, the estimated carrier mobility from the gate-modulation characteristics was on the order of ~ 16 cm²/Vs. The device performances of DEP prepared ZnO nanowire MESFET are also presented.

DD8.22

Fabrication and Characterization of high-efficiency ZnO Nanowire Dye-Sensitized Solar Cells with a Branched Structure Dul-II Suh¹, Seung-Yong Lee¹, J. Chun², Tae-Hong Kim¹, Chan-O Jang¹, O-Bong Yang² and Sang-Kwon Lee¹; ¹Dept. of Semiconductor Science and Technology, Chonbuk National University, Jeonju, South Korea; ²School of Environment and Chemical Engineering, Chonbuk National University, Jeonju, South Korea.

One-dimensional (1D) semiconductor nanowires are especially attractive building blocks for assembling nanometer scale electronic and photonic devices since the individual nanostructures function as both device elements and interconnects. Among the wide range of 1D semiconducting nano-materials, the 1D nanostructures of II-VI semiconductor ZnO acquired a special place because of its diversity in properties, such as direct wide band gap, large saturation velocity, high breakdown voltage and large exciton binding energy at room temperature. Here, we demonstrated the high efficiency dye-sensitized solar cells (DSSC) with a branched structure single-crystalline ZnO nanowire which were grown by two-step vapor-liquid-solid (VLS) process using a hot wall chemical vapor deposition (CVD). To maximize the dye absorption and improve the energy conversion efficiency, we used a branched structure ZnO nanowire in DSSCs. The open-circuit voltage, short-circuit current density, and energy conversion efficiency for a branched structure ZnO nanowire DSSCs were determined to be ~ 0.693 V and ~ 1.64 mA/cm², and $\sim 0.54\%$, respectively from current-voltage characteristics of ZnO nanowire DSSCs. Our results also indicated that current densities and efficiencies improved by increasing the high surface area for dye absorption in DSSCs.

DD8.23

Magnetic-field Dependence of Valley Splitting for Si Quantum Wells Grown on Tilted SiGe Substrates. Seungwon Lee and Paul von Allmen; Jet Propulsion Laboratory, Pasadena, California.

The valley splitting of the first few Landau levels is calculated as a function of the magnetic field for electrons confined in a strained silicon quantum well grown on a tilted SiGe substrate, using a parameterized tight-binding method. More specifically, the valley splitting arising from the effect of misorientation between the crystal axis and the confinement direction of the quantum well is investigated. In the absence of misorientation (zero substrate tilt angle), the valley splitting slightly decreases with increasing magnetic field. In contrast, the valley splitting for a finite substrate tilt angle exhibits a strong and non-monotonic dependence on the magnetic field strength. The valley splitting of the first Landau level shows an exponential increase followed by a slow saturation as the magnetic field strength increases. The valley splitting of the second and third Landau levels shows an oscillatory behavior. The non-monotonic dependence is explained by the phase variation of the Landau level wave function along the washboard-like interface between the tilted quantum well and the buffer material. The phase variation is the direct consequence of the misorientation. This result suggests that when the misorientation effect is dominant, the magnitude of the valley splitting can be easily tuned by controlling the Landau-level filling factor through the magnetic field and the doping concentration.

DD8.24

Abstract Withdrawn

DD8.25

Computer Simulation of Epitaxial Lateral Overgrowth. Hee-Soo Kim¹, Pil-Ryung Cha² and Hee Seok Park¹; ¹Central R&D Institute, Samsung Electro-Mechanics, Suwon, South Korea; ²School of Advanced Materials Engineering, Kookmin University, Seoul, South Korea.

A phase field model is developed to investigate the surface morphology of the growing crystal over the mask windows during epitaxial lateral

overgrowth (ELOG) process. Two kinds of models are considered: Model I which does not consider solute diffusion, and Model II with the diffusion of solute in the vapor phase. Anisotropy of the kinetic coefficient in the phase field equation is the most important factor to determine faceted morphology of the growing crystal. Computer simulations in two- and three-dimensions give reasonable crystal shapes. The high diffusivity of the solute makes the concentration distribution non-uniform, and then gives a detrimental effect on the planarity of the solid-vapor interface. Both of the hexagonal and circular mask windows results in almost same hexagonal cone shape of the crystal in three-dimensional calculation. Some other miscellaneous features, such as growth rate according to crystal orientation, and rotated anisotropy when the growth occurs inwards, are also discussed. The simulation in this study is believed to provide a good description of morphological and kinematical aspects of ELOG qualitatively and quantitatively.

DD8.26 TRANSFERRED TO DD.12

DD8.27

A Simple Phenomenological Model for Growth of Nanodots with "magical sizes" Stabilized by Quantum Size Effect. Heikki Ristolainen and Ismo T. Koponen; Department of Physical Sciences, University of Helsinki, Helsinki, Finland.

In the deposition of Pb on Cu(111) [1] and Si(111) surfaces [2] certain "magical heights" of the structures are found to be more stable than the other ones. It has been suggested that this unusual stabilization during the growth can be ascribed to the quantum size effect (QSE) controlling the size-selection of the height of the dots [3]. However, there have been only few attempts to relate the occurrence of the magical sizes to the kinetics of the growth. From the point of view of kinetics of the growth, there are two crucial processes of the growth: First, the adatoms need to be fed in to the uppermost layers from the wetting layer, even in cases for nanoclusters of having height of several atomic layers. Second, the nucleation and growth of new layers on top of existing layers. In order to gain insight on the interplay between the effective mass currents and the structure morphology, we have constructed a phenomenological model designed to take into account only the process of most central to the generic behavior. The model is based on the description of the growing multilayer structure in terms of total coverage of the layers. In order to adapt such models for our present purposes in describing the QSE growth we need to modify the model by taking into account the interlayer mass transport, affected by QSE. This is done within the framework of diffusion corrected simultaneous multilayer (DCSM) growth [4]. The model contains thus only two parameters related to the basic atomistic process; parameters quantifying the effect of QSE on interlayer mass transport and for the feeding current, respectively. The model reproduces many of the known features of the QSE on the nanodot growth. In particular, it describes how QSE causes a transition from the growth of "wedding-cake" type, moderately sloped structures growing in SM growth mode to the towers with perfectly sharp edges, growing in perfect layer-by-layer growth mode. In addition, the model demonstrates that in such system the growth of towers may become terminated in certain parameter regions, when only stable magic sizes result. Finally, based on the model calculations, we give a phase diagram for different possible morphologies. References [1] R. Otero, A.L. Vazquez de Parga, and R. Miranda, Phys. Rev. B 66, 115401 (2002). [2] A. Menzel, M. Kammler, E.H. Konrad, V. Yeh, M. Hupalo, M.C. Tringides, Phys. Rev. B 67, 165314 (2003). [3] M. Hupalo and M.C. Tringides, Phys. Rev. B 65, 115406 (2002). [4] Q. Fu and T. Wagner, Phys. Rev. Lett. 90 106105 (2003).

DD8.28

Calculation of Photosensitivity of Porous Silicon for Optoelectronic Devices. Liubomyr S Monastyrskii and Bogdan S. Sokolovskii; Electronics, Ivan Franko Natl Univ, Lviv, Ukraine.

Porous silicon structures are commonly used for creation of silicon photo- and light-emission diodes. An important advantage of such devices in comparison with ones based on A2B6 and A3B5 compounds is their ecological purity and rather low cost, as well as the well developed industry technology of silicon microchips. We have developed a new theoretical model of the photosensitivity of porous Si which takes into account the recombination of photocarriers at the surfaces of pores. The model is based on the processes of the carrier generation under illumination of the material, the ambipolar diffusion of carriers towards the internal surfaces, as well as the nonequilibrium carrier recombination in both the bulk of semiconductor and the surfaces of pores. By solving carrier transport equations with appropriate boundary conditions, the analytical relations for the photosensitivity of porous material have been obtained for the cases of the spherical and cylindrical shapes of pores. They describe the dependence of the porous Si photosensitivity on the mean sizes of pores and the distances between them, as well as on the surface recombination velocity. The photosensitivity of porous Si has been shown to decrease under increasing the porosity magnitude and the surface recombination velocity. The model developed may constitute a basis for an experimental method of determining the parameters of carrier recombination processes occurring at the internal surfaces of pores.

DD8.29

Permittivity in Molecular Nanorods Sinisa Vucenovic¹, Dusan Ilic², Jovan Setrajcic³, Vjekoslav Sajfert⁴ and Dragoljub Mirjanic¹; ¹Medical faculty, University of Banja Luka, Banja Luka, Bosnia and Herzegovina; ²Faculty of technical sciences, University of Novi Sad, Novi Sad, Yugoslavia; ³Department of Physics, Faculty of natural sciences, University of Novi Sad, Novi Sad, Yugoslavia; ⁴Technical faculty "Mihajlo Pupin", University of Novi Sad, Zrenjanin, Yugoslavia.

In this paper we have theoretically investigated and calculated energy spectra of Frenkel excitons (quasi particles compound of electron-holes pairs linked with Coulomb interaction) and optical properties (dielectric permittivity) in molecular nanorods, i.e. structures limited with two planes (x, y) and practically unlimited in z - direction. We have compared those results with energy spectra and permittivity for bulk (x, y and z direction without limitations) and thin film structures (one limited direction). Method of Green's function was used. Space boundaries and the disturbance of energetic parameters on boundaries are considered as perturbations. In dielectric permittivity calculation, we have used Djalozinski and Pitaevski formula. Compared with bulk structures where excitons could take continual energies in wide zone, thin films demonstrate very sharp selection rules in energy spectra and optical properties. In molecular nanorods, those selection rules and energy shifting are more significant, especially in directions perpendicular on nanorods axis.

DD8.30

Electron Energy Spectra of Single and Multiple AlGaIn/GaN Quantum Dots with Spontaneous and Piezoelectric Polarization Effects Choudhury Jayant Praharaj, Intel Corporation, Santa Clara, California; (formerly with) Cornell University, Ithaca, New York.

We present numerical calculations of electron energy spectra of single and multiple coupled quantum dots based on Aluminium Gallium Nitride / Gallium Nitride heterostructures. The effect of spontaneous and piezoelectric polarization on the confinement potential seen by the electrons is taken

into account through bound interface sheet charges. We also calculated the spectra without polarization effects for reference. For some quantum dot dimensions, the energy eigenvalues shift by several hundred meVs due to the polarization charges. We calculate the spectra for the two cases of box-shaped and cylindrical quantum dots. The latter case is an approximation to quantum dots with hexagonal-facet shapes recently reported in the literature. The quantum dots in our calculations are surrounded by vacuum in the lateral direction, but the same qualitative conclusions will hold if the dots are embedded in some material, as long as the barrier heights are large. For GaN vertical confinement of less than 30 angstroms, most of the bound states are associated with the lowest eigenvalue of the vertical confinement potential. This is also true for higher vertical confinement dimensions because the triangular potential seen by the electrons is the same for the lowest energy eigenstates. The electric field in the vertical direction is a strong function of the aluminium concentration in the AlGaIn layer. As the AlGaIn layer composition is varied from very high Al concentration to medium Al concentration, the spectra shift by several hundred meVs, referred to the onset of the continuous spectra. The transition frequencies between bound states and between bound and the lowest continuum states lie in the low to the high infra-red range, and can be varied over a wide range by both the dimensions and the barrier aluminium concentration. For the case of 4 coupled quantum dots formed by repeated AlGaIn/GaN heterojunctions, we find that the polarization-induced electric fields lead to excessive band-bending and as a consequence there are fewer bound states compared to the spectrum calculated without polarization effects.

DD8.31**Abstract Withdrawn****DD8.32**

Melting of Transition Metal Nanoclusters: Application to Carbon Nanotube Synthesis. Nikhil Joshi¹, Douglas E. Spearot^{1,2} and Deepak Bhat^{1,2}; ¹MicroEp Program, University of Arkansas, Fayetteville, Arkansas; ²Mechanical Engineering, University of Arkansas, Fayetteville, Arkansas.

The melting of nanosized Fe and Ni clusters has been studied using Molecular Dynamics (MD) simulations with an aim of studying the effect of cluster size on the melting point and characterizing the degree of solid versus liquid behavior at different temperatures. In addition, our objectives are to study the characteristics of carbon species absorption and adsorption in transition metal clusters and the effect on melting temperature as a function of carbon content in the cluster. These clusters would be utilized to grow single walled nanotubes (SWNTs). The study of these clusters would validate the vapor-liquid-solid (VLS) mechanism during the nucleation of carbon nanotubes from transition metal catalysts. This work forms the basis of a larger study on the nucleation of SWNTs on surfaces with ledges. The hypothesis of this work is the nucleation of SWNTs and the properties of SWNTs will be influenced by the surface features, such as ledges and crystal orientation. The MD simulations in this work utilize the Born-Mayer potential for Fe-Fe interactions, the embedded-atom method (EAM) potential for Ni-Ni and the Johnson potential for metal-carbon behavior. This work will present results for the variation of melting temperature with cluster size and carbon content for Ni and Fe nanoclusters. The details of carbon absorption and adsorption into transition metal clusters will provide an increased understanding of the carbon nanotube nucleation process via the VLS mechanism.

DD8.33

Tetrahedral Silver Nanoparticles Produced by Inert Gas Condensation: An Experimental/simulation Study. Miguel Angel Gracia Pinilla¹, Joel Antunez-Garcia¹, Alfredo Tlahuice-Flores¹, Carlos Fernandez-Navarro¹, Sergio Mejia-Rosales¹, Eduardo Perez-Tijerina¹ and Miguel Jose-Yacamán²; ¹Laboratorio de Nanociencias y Nanotecnología - Facultad de Ciencias Físico Matemáticas, Universidad Autónoma de Nuevo León, San Nicolás de los Garza, Nuevo León, Mexico; ²Chemical Engineering Department and Texas Advanced Materials Center, The University of Texas at Austin, Austin, Texas.

We report the synthesis of silver tetrahedral nanoparticles (NPs), produced by inert gas condensation followed by thermalization and condensation in a high pressure zone. The size of the NPs was controlled through the variation of the gas flow inside the condensation zone (Ar and He), magnetron power, and condensation zone length. We performed a morphological and structural characterization of the particles by atomic force microscopy, scanning electron microscopy, and high resolution transmission electron microscopy. The analysis shows that the shape of the obtained Ag NPs is tetrahedral, about 5 nm in height, and almost monodispersed in size. In order to validate the stability of tetrahedra at this range of sizes, we performed a set of molecular dynamics (MD) simulations of a 2925-atom Ag regular tetrahedron under different thermodynamical conditions, finding that even though the tetrahedral structure is not the most energetically favourable, the structure is stable enough to keep their main features even at temperatures close to the melting transition. From the simulations, we also found that, as the tetrahedral particle is heated, when the temperature is sufficiently high (around 700K), a surface reconstruction takes place in a fashion that allows the formation of atomic islands on the faces of the particle, which resemble those observed by AFM. Additionally, we made density functional theory (DFT) calculations for Ag₂₀ and Ag₃₅ tetrahedral clusters, and a large stability for this geometry was found; these results make possible a layer-by-layer growth scenario for the observed tetrahedral nanoparticles.

DD8.34**Abstract Withdrawn****DD8.35****Abstract Withdrawn****DD8.36**

Chains of Hydrocarbon Molecules Deposited onto Monolayer Steps on Si(100): A study of Adsorption and Conductance. Anna Mazzone, IMM Sezione di Bologna, Bologna, Italy.

In this study chains, formed by hydrocarbon molecules, deposited onto monolayer SA steps of the Si(100) surface are considered. The purpose of the calculations is a systematic description of the adsorption capability of the silicon steps in dependence of the type of the incident molecule and of the chain length. The study deals with both the electronic configuration of the deposited system and with its transport properties and the flat, dimerized surface is used as reference. The calculations are based on a semi-empirical Hamiltonian which is applied to the evaluation of the total

energy and of the conductance and this last quantity is obtained from the scattering theory. It has been found that, though the step is a weaker sink than the flat surface, adsorption is possible and the molecules are bonded to the step. The functional relationship between the binding energy, the type of the adsorbed molecule and the chain length is reminiscent of the intrinsic binding energy of the molecule itself and is therefore similar for the flat surface and for the step. The transmission function depends on the type of molecule and of the substrate and on the allowed energy levels of the deposited system. Depending on the channel type, a direct, or reverse, proportionality exists between the conductance and the binding energy.

DD8.37**Abstract Withdrawn****DD8.38**

A Combined Experimental and Theoretical Study of CdSe Nanocrystal Formation Haitao Liu^{1,2}, Jonathan S Owen¹, Jeffrey Grossman³ and A. Paul Alivisatos^{1,2}; ¹Department of Chemistry, University of California, Berkeley, California; ²Material Science Division, Lawrence Berkeley National Laboratory, Berkeley, California; ³Department of Physics, University of California, Berkeley, California.

The synthesis of CdSe nanocrystals using tri-n-alkylphosphine selenide and cadmium carboxylate in n-octadecene has been investigated by experiments and by density functional theory (DFT) calculations to examine the formation of CdSe from the precursors. Binding of tri-n-alkylphosphine selenide to cadmium carboxylate leads to the formation of a metastable complex. A carboxylate molecule then attacks the tri-n-alkylphosphine selenide in the complex to give a pentavalent phosphorus intermediate, which undergoes further reaction to break the P=Se bond and form the initial Cd-Se bond. Our results show that surfactant molecule such as carboxylic acid is also a reagent for the synthesis of CdSe nanocrystals. The activation parameters of the CdSe synthesis were calculated and compared with experimental results.

DD8.39

Simulating Light Emission in Silicon Nanocrystal Field Effect Light Emitting Devices. Robert J. Walters¹, Douglas Bell² and Harry A. Atwater¹; ¹Applied Physics, California Institute of Technology, Pasadena, California; ²Jet Propulsion Laboratory, Pasadena, California.

As a low dimensional material, silicon nanocrystals exhibit several fascinating properties including a size tunable emission energy, very high radiative quantum efficiency, and an improved oscillator strength for radiation. These properties recommend silicon nanocrystals as a potential CMOS compatible material for optoelectronics. Unfortunately, the oxide matrix that surrounds a nanocrystal and provides the quantum confinement is also an electrical insulator. This complicates the efficient electrical excitation of silicon nanocrystals. We have previously demonstrated that electroluminescence (EL) can be achieved in silicon nanocrystals within a "field effect light emitting device" (FELED) [1]. These devices resemble nanocrystal FLASH memory devices in which a roughly planar array of nanocrystals is embedded in the gate oxide of a transistor. We observe light emission at bipolar transitions in gate bias. Time resolved EL experiments show EL rise times of order 1 microsecond and EL decay times of order 10 microseconds. These measurements support a model in which excitons are formed by the sequential tunneling of complementary carriers into the nanocrystals. This is a surprising and unexpected result that can be better understood through simulation. Key challenges that must be addressed for this effort include the accurate modeling of both hole and electron tunneling, solving the electrostatics through the self-consistent Poisson-Schrodinger equation, and accounting for the decay processes of excitons in the nanocrystals. We will discuss our simulation of electroluminescence in a model system in comparison to our experimental results. [1] Walters et al., "Silicon Nanocrystal Field Effect Light Emitting Devices", IEEE JSTQE Silicon Photonics Issue, December 2006

DD8.40

Position Sensitive Growth of Mn Doped ZnO Nanowires on Si Substrate by CVD. Xiaomei Zhang¹, Yue Zhang¹, Yousong Gu¹, Xiaoyuan Zhan¹, Ruiping Gao² and Kexin Chen²; ¹Department of Materials Physics, University of Science and Technology Beijing, Beijing, China; ²National Natural Science Foundation of China, Beijing, China.

Position sensitive growth of Mn doped ZnO nanowires on Silicon substrate by chemical vapor deposition was discussed in this paper. The as-synthesized Mn-doped ZnO nanostructures were characterized by scanning electron microscope (Cambridge-360) and high resolution transmission electron microscopy (JELO-2010). The obtained outgrowth differing in morphologies and chemical constitution depended on the flowing of carrier gas of tube. A diagrammatic sketch of subarea growth was given and explained the growing process of the Mn doped ZnO nanostructures. Then one position sensitive growth mode on silicon substrate for in situ doping was built. Further microstructure analysis showed the obtained nanowire from nanowires'growing zone was single crystalline and has grown along the c-axis.

DD8.41

Initial Stages of the Formation of InAs/InP(001) Quantum Wires Studied by High-resolution Z Contrast Imaging. Sergio I Molina^{1,2}, Maria Varela¹, Stephen J Pennycook¹, David L Sales², Teresa Ben², Joaquin Pizarro³, Pedro Galindo³, David Fuster⁴, Yolanda Gonzalez⁴ and Luisa Gonzalez⁴; ¹Materials Science and Technology Division, Oak Ridge National Laboratory (ORNL), Oak Ridge, Tennessee; ²Departamento de Ciencia de los Materiales e IM y QI, Universidad de Cadiz, Puerto Real, Cadiz, Spain; ³Departamento de Lenguajes y Sistemas Informaticos, Universidad de Cadiz, Puerto Real, Cadiz, Spain; ⁴Instituto de Microelectronica de Madrid IMM-CNM, Madrid, Madrid, Spain.

The knowledge of the first stages of formation of self-assembled semiconductor nanostructures is very valuable to improve their design and to control their functional properties. In this communication we investigate the first stages of growth of self-assembled InAs quantum wires (QWRs) oriented along [1-10] grown by Molecular Beam Epitaxy (MBE) on InP (001) substrates. These are promising nanostructures to be used in light-emitting devices for the telecommunication industry. In a previous work [1] we observed by atomic force microscopy that before a dense array of QWRs covers the whole surface, isolated ≈ 200 nm long nanowires nucleate mainly at the step edges of the surface terraces. In this work we study the influence of these nucleation steps on the composition distribution and asymmetric shape observed in the QWRs [1-10] cross section [2] by high-resolution aberration-corrected Z contrast imaging, assisted by electron energy loss spectroscopy imaging. By analysing deconvoluted high-resolution Z contrast images, interfacial steps are observed to appear at the interface between InAs(P) nanowires and the InP surface. Compositional maps obtained from quantum wires by Z contrast imaging and spatially resolved electron energy loss spectra show the existence of

asymmetry in the As distribution in the wires nucleated at interfacial steps. Strain associated to interfacial steps has been calculated by finite element method and atomistic simulations. On the other hand, strain in the wire has been evaluated by applying the Peak Pairs method to high resolution Z contrast images. These results have contributed to improve the understanding of the quantum wire nucleation process. [1] David Fuster, Benito Alén, Luisa González, Yolanda González, and Juan Martínez-Pastor. Proc. XIVth International MBE Conference, Tokyo, September 2006. [2] Sergio I. Molina, Teresa Ben, David L. Sales, Joaquín Pizarro, Pedro L. Galindo, María Varela, Stephen J. Pennycook, David Fuster, Yolanda González and Luisa González, Nanotechnology, in press.

DD8.42

Electrical Characterization and Modeling of Geometry-dependent Resistivity Scaling in Single-walled Carbon Nanotube Films. Ashkan Behnam and Ant Ural; Electrical & Computer Engineering, University of Florida, Gainesville, Florida.

Due to their unique transport characteristics, 2D networks and 3D films of single walled carbon nanotubes have recently attracted significant research attention. In these materials, individual variations in nanotube diameter and chirality are ensemble averaged to yield uniform physical and electronic properties. Several significant applications of these networks and films have recently been demonstrated, such as thin film transistors, flexible electronics, sensors, and transparent electrodes for optoelectronics. Nanoscale study of percolating transport mechanisms in these films is essential for understanding and characterizing their performance in submicron devices. In this talk, we study the resistivity scaling in nanotube films as a function of nanotube and device parameters both experimentally and using simulations. We first characterize the resistivity of these films down to 200 nm lateral dimensions by fabricating standard four-point-probe structures. We find that the film resistivity starts to increase at device widths below 20 microns, and exhibits an inverse power law dependence on width with a critical exponent of 1.5 below a critical width of 2 microns. We then use quasi-3D Monte Carlo simulations to model and fit these experimental results. In these simulations, nanotubes are generated randomly on stacked 2D rectangular planes and the current continuity equations are applied at each tube-tube junction in order to calculate the resistivity of the film. In addition to fitting the experimental data, we also study the effect of four parameters, namely tube-tube contact resistance to nanotube resistance ratio, nanotube density, length, and alignment on resistivity and its scaling with device width. We observe stronger width scaling when the transport characteristics in the nanotube film are dominated by tube-tube contact resistance. We find that increasing the nanotube density decreases the absolute value of resistivity strongly, and results in a higher critical exponent and lower critical width. Increasing nanotube length also reduces the absolute value of resistivity, but increases both the critical exponent and the critical width. We also find that the lowest resistivity occurs for a partially aligned rather than perfectly aligned nanotube film. Furthermore, increasing the degree of alignment reduces both the critical exponent and critical width. We explain these observations, which are in agreement with previous experimental work, by simple physical and geometrical arguments. In conclusion, we show by experiments and simulations that resistivity of single-walled nanotube films depend strongly on nanotube and device parameters. This important effect needs to be taken into account when fabricating devices in which nanotube film transport characteristics play a vital role.

DD8.43

Ferroelectricity in Ultra-thin BaTiO₃ Films by LEED I-V and STS. Junsoo Shin^{1,2}, V. B Nascimento^{1,2}, S. V Kalinin^{2,3}, E. W Plummer^{1,2,3} and A. P Baddorf^{2,3}; ¹Physics, University of Tennessee, Knoxville, Tennessee; ²Materials Science and Technology Division, Oak Ridge National Laboratory, Oak Ridge, Tennessee; ³Center for Nanophase Materials Sciences Division, Oak Ridge National Laboratory, Oak Ridge, Tennessee.

BaTiO₃ thin films have been widely studied for applications in ferroelectric random-access memories and high-density capacitors because of their high dielectric constant and low leakage current. However, strong debate has recently erupted over the existence of a critical size for ferroelectricity. For a BaTiO₃ ferroelectric film sandwiched between two SrRuO₃ electrodes, ferroelectricity was observed down to 12.5 ML and a predicted to 6 ML by first-principle calculations. We have experimentally addressed polar ordering and polarization-dependent tunneling in in-situ ultra-thin BaTiO₃ films grown on SrRuO₃ electrode. Here, we explore ferroelectricity of several ultra-thin (< 10 ML) BaTiO₃ films grown by Pulsed Laser Deposition (PLD) at 700 °C in 10 mTorr O₂ pressure. The ferroelectric distortion and ferroelectric switching in the ultra-thin films were characterized in-situ by low energy electron diffraction (LEED) and scanning tunneling spectroscopy. These films provide a very sharp in-situ (1x1) LEED pattern, which suggests that several top atomic layers of BaTiO₃ films are well ordered in the tetragonal phase. Ferroelectricity of the films was investigated structurally by electron diffraction intensities (LEED I-V). Comparison with simulated LEED I-V of BaTiO₃ thin films, experimental data of 4 ML and 10 ML thick films indicate upward polarization and evidence of a polarized phase. Using electron tunneling through the ultra thin films with a scanning tunneling microscope, reversible polarization switching was observed on a local scale as a jump in the tunneling current. The combination of these two experiments reveals ferroelectric properties in ultra-thin BaTiO₃ films up to 4 ML. Research was sponsored by the Division of Materials Sciences and Engineering and the Center for Nanophase Materials Sciences, Office of Basic Energy Sciences, U.S. Department of Energy, under contract DE-AC05-00OR22725 with Oak Ridge National Laboratory, managed and operated by UT-Battelle, LLC.

DD8.44

Scaling of nanoporous materials: processing and mechanical properties Andrea Maria Hodge, Juergen Biener, Monika Biener, Octavio Cervantes and Alex Hamza; Nanoscale Synthesis and Characterization Laboratory, LLNL, Livermore, California.

Complex nanoscale structures such as nanoporous foams have shown potential for applications such as actuators and catalyst. Therefore, in order to utilize these materials for the next-generation nano-technologies there is a need to enhance our current understanding of scaling dimensions and their effect on the overall material behavior. Here we present a comprehensive study on scaling effects on both processing and mechanical behavior of nanoporous Au foams. The processing scale focuses on the dimensions of individual foam ligaments which range from 5 nm to 1 micron. Properties such as elastic modulus and yield strength are related as a function of the ligament length scale and compare to traditional macro-porous foams. Additionally, the foam surface to volume ratio at different length scales will be evaluated as a parameter for new catalytic materials. This work was performed under the auspices of the U.S. Department of Energy by University of California, Lawrence Livermore National Laboratory under contract of No.W-7405-Eng-48.

DD8.45

In situ Observation of Dewetting and Pattern Formation of Au and Ag Nanocrystalline Thin Films on Reconstructed c- and m-planes of

Sapphire. Joysurya Basu¹, Divakar Ramachandran¹, Ravishankar Narayanan² and C. Barry Carter¹; ¹Department of Chemical Engineering & Materials Science, University of Minnesota, Minneapolis, Minnesota; ²Materials Research Centre, Indian Institute of Science, Bangalore, Karnataka, India.

Controlled and site-specific growth of nanostructures has been a major challenge in design of nanomaterials. Various methods have been used to generate patterned substrates for subsequent nanostructure growth. It is known that dewetting of nanocrystalline thin films can be used to produce nanoscale islands of the film material, which can subsequently be used for nanostructure growth. The nature of the pattern obtained can be influenced by multiple factors including the film species, the substrate material and condition, as well as processing parameters. The major advantage of this technique, as opposed to lithography-based techniques, is that since the process involves heat treatment in a controlled atmosphere, it can be easily and economically scaled to large-volume production. However, usually competing processes occur simultaneously to produce the final nanopatterned substrate, and these are not well understood. Most studies to-date in this field have been performed ex situ, with post-treatment characterization by scanning probe microscopy. The modern transmission electron microscope (TEM) provides a clean, high-vacuum environment where in situ heating experiments can be carried out while simultaneously characterizing the film in imaging and diffraction modes. The in situ TEM technique enables exploration of the course of the dewetting process. In this work, dewetting of metallic thin films of Au and Ag on reconstructed c- and m-planes of sapphire has been carried out in situ in a TEM in order to study the nanopatterning process. The reconstructed sapphire surface structure depends on the sapphire crystal orientation. The pattern formed ultimately is dependent on the structure of this reconstructed surface, the thickness of the film, time and temperature of dewetting. Sputter-deposited thin films of both Au and Ag on c-plane sapphire, which were nanocrystalline in nature initially, underwent extensive grain growth prior to dewetting. In the case of an Au thin film on c-plane sapphire, during and after dewetting, large, irregular Au islands are formed and very fine droplets of gold, ~5 nm in diameter, are left behind mostly at the step edges. The dewetting of Au and Ag on reconstructed m-plane sapphire is different in nature. In the course of dewetting, continuous nanowire formation can be observed and at the end of the process, a pattern consisting of fine nanocrystals linearly arranged along the reconstruction ridges is formed. High-resolution microscopy, STEM with a HAADF detector and compositional analysis have been used to characterize the nanostructures in detail.

DD8.46

In situ TEM Study of Dewetting and Solid-state Reactions of Nanocrystalline Thin-film Oxides on Sapphire. Divakar Ramachandran, Joysurya Basu and C. Barry Carter; Department of Chemical Engineering & Materials Science, University of Minnesota, Minneapolis, Minnesota.

In situ transmission electron microscopy (TEM) allows one to use the microscope as an experimental laboratory in which physical processes can be recorded in real-time over a range of temperatures. In this type of experiment dewetting, solid-state reaction kinetics and reduction reactions can be observed in detail. The results can be analyzed to determine the reaction pathway. While elaborately modified TEMs have been described in the literature for creating specific reaction environments, these are usually not available in a conventional TEM. The unmodified TEM is also very useful for the study of solid-state reactions: it provides a clean, high-vacuum work place that is very well suited for the study of reactions involving ceramics at relatively high temperatures. However, in interpreting the results, the specific differences in the reaction parameters between ex situ and in situ experiments, it is particularly important to consider the near absence of trace atmospheric impurities and the presence of a steady stream of electrons through the volume under observation. The present paper compares the results from in situ experiments on oxide thin films on sapphire with those carried out ex situ. Results illustrate NiO and ZnO thin-films on sapphire of c- and m-plane orientations. Issues relating to film dewetting and spinel formation have been examined in relation to the reaction temperature; thin-film characteristics and the influence of the substrate orientation will be discussed. Reduction of the oxide to the metal is another possibility that further leads to the study of mobility of metal nanoparticles generated in situ on the sapphire surface. The in situ experiments have been carried out in a Tecnai T12 TEM operated at 120 kV and post in situ characterization has been carried out in a Tecnai F30 FEGTEM using both phase contrast and Z-contrast imaging modes.

DD8.47

Characterization of Ge Nanocrystal/SiO₂ multilayers Fabricated by Ion Beam Sputtering and Annealing. Seung Hui Hong¹, Do Kyu Lee¹, Sung Won Hwang¹, Phil Sung Jung¹, Suk-Ho Choi¹ and Kyung Joong Kim²; ¹College of Electronics and Information, Kyung Hee University, Yongin, Kyungkido, South Korea; ²Division of Advanced Technology, Korea Research Institute of Standards and Science, Daejeon, South Korea.

Ion beam sputtering deposition (IBSD) is a good candidate for the growth of Si or Ge nanocrystals (NCs) because it allows for the exact control of the oxygen composition and the individual layer thickness with sub-nm precision. In this work, Ge NCs have been fabricated by annealing the IBSD-grown Ge/SiO₂ multilayers and the relative film growth rate and amount of Ge and SiO₂ analyzed by x-ray photoelectron spectroscopy (XPS). The XPS data shows that Si 2p peak and O 1s peak increase with increasing annealing temperature (T_A) from 650 to 1050 °C, which indicates that Ge is isolated from GeO or GeO₂ phase during annealing. Transmission electron and scanning tunneling microscopies demonstrate the existence of Ge NCs of about 3~5 nm in SiO₂. The annealing condition and the thickness ratio of Ge/SiO₂ layers for the formation of Ge NCs were also optimized through photoluminescence (PL) measurements. When $T_A \geq 650$ °C, the PL peak appears at around 750 nm and its intensity increases up to 850 °C, but when $T_A \geq 950$ °C, it decreases. For metal-insulator-semiconductor (MIS) structures containing Ge NCs, C-V measurements were performed to study their nonvolatile memory properties.

DD8.48

Effect of Electron Irradiation on Nanogroove-networked Single-crystalline and Dendritic Polycrystalline Platinum Nanosheets. Masafumi Uota¹, Takumi Yoshimura^{2,1}, Takeshi Kuwahara², Daisuke Fujikawa^{2,1}, Hideya Kawasaki^{3,1}, Go Sakai^{2,1} and Tsuyoshi Kijima^{2,1}; ¹Japan Science and Technology Agency, Miyazaki, Japan; ²Applied Chemistry, Miyazaki University, Miyazaki, Japan; ³Applied Chemistry, Kansai University, Suita, Japan.

Increasing attention has been focused on nanoscale platinum particles for their potential applications as a catalyst in various fields such petroleum chemical processes and polymer electrolyte fuel cells. The catalytic reactivity of Pt nanoparticles depends on their sizes and shapes as well as the arrangement of surface atoms. It is therefore important to control the structural and morphological properties of Pt nanomaterials. Our recent studies demonstrated the fabrication of Pt nanotubes by the hydrazine reduction of H₂PtCl₆ within lyotropic mixed surfactant liquid crystals (LCs) of

polyoxyethylene (20) sorbitan monostearate (Tween 60) and nonaethyleneglycol dodecylether ($C_{12}EO_9$).¹ We also synthesized nanogroove-network structured single-crystalline nanosheets through the reduction of Na_2PtCl_6 with $NaBH_4$ using compositionally the same mixed surfactant LC templates.² Furthermore, we also found that the nanogrooved Pt loaded on carbon exhibit fairly high electrocatalytic activity for oxygen reduction reaction. It would be of importance to characterize in more detail the structurally and functionally unique Pt nanomaterials. An attempt was thus made to study the effect of electron irradiation on the structural properties of the nanogroove-network structured single-crystalline nanosheets and 2D-dendritic polycrystalline nanosheets. The nanogroove-network structured single-crystalline and the 2D-dendritic polycrystalline nanosheet samples were prepared using the Tween 60 based mixed- and single-surfactant LC templates as described elsewhere.¹ Electron irradiation experiments were carried out by using transmission electron microscopy (TEM). The as-grown samples of single-crystalline nanogrooved and 2D-dendritic polycrystalline nanosheets were characterized by nearly the same average groove-width or dendritic spacing of 1.3-1.4 nm. On exposure to electron beam for 20 min at the acceleration voltage of 200 keV, the nanogrooved nanosheets were morphologically little affected, but the dendritic ones were transformed into less branched polycrystalline structures with spacings distributed around ~ 1.7 nm. The shape transformation of the latter was found to occur by the combined mechanism of segmental migration and atomic diffusion. These observations indicate that the nanogrooved Pt nanosheets are highly stabilized by the grooved but crystallographically continuous Pt framework, leading to their extremely high thermo-resistance, in marked contrast to the polycrystalline dendritic structures constructed of crystallographically discontinuous linkages of nanoblocks. 1. T. Kijima et al., *Angew. Chem.*, 2004, 43, 228. 2. To be presented in this symposium.

DD8.49

Effects of Chirality and Diameter on Electron Transport Properties in Individual Semiconducting Carbon Nanotubes. M. Z. Kauser and P. P. Ruden; Dept. of ECE, University of Minnesota, Minneapolis, Minnesota.

Carbon nanotubes (CNTs) are recognized as structures with the potential to be key building blocks in future nano-scale electronic and optoelectronic devices [1]. The structure of a CNT is fully determined by a pair of integers, (n,m) . It is well established from theoretical calculations and scanning tunneling microscopy (STM) studies of CNTs that (n,n) CNTs with chiral angle $\theta = 30$ degree and the group defined by $(n-m) \bmod 3 = 0$ are metallic, while rest are semiconducting. It is to be expected that chirality should affect the properties of semiconducting CNTs. Previous theoretical efforts have focused on the understanding of transport in achiral, semiconducting, zigzag $(n,0)$ CNTs, based on analytical models [2] and Ensemble Monte Carlo (EMC) simulations [3,4,5]. Chiral (n,m) CNTs are rarely modeled, mainly due to their complicated electron and phonon dispersions associated with low symmetry. Recently we reported a technique to study chiral CNTs using EMC simulation and we found interesting effects of chirality and of group (defined by $(n-m) \bmod 3 = \pm 1$) on the transport properties of chiral CNTs with similar diameter [6]. In this paper, we explore the effects of chirality, group, and diameter on the electronic structure and transport properties of semiconducting CNTs. The electronic band structure is calculated based on a Tight Binding model along with zone folding. The high-field transport properties are simulated using EMC. The principal electron scattering mechanisms are due to coupling to longitudinal acoustic (LA), longitudinal optical (LO), and radial breathing mode (RBM) phonons. Both Normal and Umklapp scattering processes are considered. The low-field mobility is calculated using the momentum relaxation time approximation. The effects of chirality, group, and diameter on low-field mobility, saturation velocity, saturation electric field, and negative differential mobility are studied for all semiconducting CNTs usually investigated in experiments. Results show consistent trends of change in these properties with group, chirality, and diameter, which are attributed to changes in the electronic structure, especially the lowest subband effective masses. This study thus gives upper and lower bounds for key transport parameters for CNTs of known diameter but unknown chirality, which is the case typically encountered in experiments. References: [1] M. P. Anantram and F. Leonard, *Rep. Prog. Phys.* 69, 507 (2006). [2] V. Perebeinos, J. Tersoff, and P. Avouris, *Phys. Rev. Lett.* 94, 086802 (2005). [3] A. Verma, M. Z. Kauser, and P. P. Ruden, *J. Appl. Phys.* 97, 114319 (2005). [4] A. Verma, M. Z. Kauser, and P. P. Ruden, *Appl. Phys. Lett.* 87, 123101 (2005). [5] M. Z. Kauser, A. Verma and P. P. Ruden, *Physica E* 34, 666 (2006). [6] M. Z. Kauser and P. P. Ruden, *Appl. Phys. Lett.* 89, 162104 (2006).

DD8.50

Phonon Spectra and Thermodynamic Properties Of Crystalline Nanowires. Dusan Ilic¹, Sinisa Vucenovic², Stevo Jacimovski³, Vojkan Zoric³ and Jovan Setrajic³, ¹Faculty of Technical Sciences, University of Novi Sad, Novi Sad, Vojvodina, Yugoslavia; ²Faculty of Medicine, University of Banja Luka, Banja Luka, Republic of Srpska, Bosnia and Herzegovina; ³Department of Physics, Faculty of Sciences, University of Novi Sad, Novi Sad, Vojvodina, Yugoslavia.

Phonon spectra and allowed phonon states, as well as thermodynamic characteristics of nanowires of simple cubic crystalline structure, are analyzed using the method of two-time dependent Green's functions, adjusted to bounded crystalline structures. Poles of Green's functions, defining phonon spectra, can be found by solving of the secular equation. For different boundary parameters, this problem is presented graphically. The presence of boundaries as well as the change of boundary parameters leads to appearance of new properties of low dimensional structures (thin film and nanowire). The most important feature is that beside allowed energy zones (which are continuous as in the bulk structure), zones of forbidden states appear. Different values of boundary parameters lead to appearance of lower and upper energy gaps, or dispersion branches spreading out of bulk energy zone. The correlation with spectra of phonons in corresponding unbounded and thin film structures is maintained in the work. Determination of phonon spectra and allowed phonon energies has great importance for kinetic and thermodynamic properties of semiconductive nanostructures and devices. The temperature behavior of nanowire specific heat is compared to that of bulk structures and thin films. It is shown that at extremely low temperature nanowire and film specific heats are considerably lower than the specific heat of bulk sample. It was discussed what are the consequences of this fact to the thermal, conducting and superconducting properties of materials.

SESSION DD9: Properties of Nanowires II
Chairs: Marija Drndic and Masaru Kuno
Wednesday Morning, April 11, 2007
Room 2001 (Moscone West)

8:00 AM DD9.1

Determination of the Young's modulus of individual electrospun nanofibers by microcantilever vibration method. Philip A. Yuya¹, Yongkui Wen¹, Zheng Li², Joseph A. Turner¹ and Yuris A. Dzenis¹; ¹Engineering Mechanics, University of Nebraska-Lincoln, Lincoln, Nebraska; ²Mechanics & Engineering Science, Peking University, Beijing, China.

We report a technique for measuring the Young's modulus of a single electrospun nanofiber using the vibrations of two microcantilevers coupled with the nanofiber. The modulus is calculated from the resonant frequency shift resulting from the nanofiber. Polyacrylonitrile nanofibers (200 nm diameter) were collected during electrospinning and wrapped on two similar microcantilevers causing a shift in first resonance from 10.0 kHz to 19.4 kHz. Finite element analysis was used to analyze the frequency shift using images from a scanning electron microscope giving a modulus of the as-spun PAN nanofiber of 26.8 GPa. Prospects for exploiting this technique for high-throughput mechanical characterization of electrospun nanofibers are discussed. [Results supported by NSF].

8:15 AM DD9.2

Suspended Mechanical Structures Based on Elastic Silicon Nanowire Arrays. Alvaro San Paulo^{1,2}, Noel Arellano², Jose Antonio Plaza¹, Rongrui He², Carlo Carraro², Roya Maboudian², Roger T Howe³, Jeff Bokor² and Peidong Yang²; ¹Centro Nacional de Microelectrónica, Bellaterra, Spain; ²University of California at Berkeley, Berkeley, California; ³University of Stanford, Stanford, California.

The development of methods for the controlled assembly of semiconductor nanowires into well-ordered arrays is essential for both the implementation of electromechanical systems that exploit the unique properties of individual nanowires and for exploring novel fundamental properties of nanowires and nanowire arrays different from that of bulk macroscopic materials. In this contribution, we present the fabrication and characterization of mechanical structures composed of horizontally suspended, well-oriented and size-controlled Si nanowire arrays. By a novel bottom-up/top-down combined fabrication approach that integrates the vapor-liquid-solid synthesis of Si nanowires with standard microfabrication techniques, the nanowire arrays are horizontally grown between the sidewalls of prefabricated Si microstructures, which automatically provides an elegant solution to the problem of interfacing the nano and micro length scales. As a result, we obtain mechanical structures which in the simplest case consist of an array clamped to the sidewall of a supporting structure at one end and to a freely suspended micropaddle at the other, resembling a single clamped microbeam with a body composed of a uniformly dense, well-oriented and size-controlled nanowire array instead of bulk Si. These unique beam-like mechanical structures are used then to investigate the elasticity of the arrays by atomic force microscopy and finite element simulations. We provide both experimental evidence and theoretical description of important differences in the mechanical elasticity of mechanical structures composed of nanowire arrays with respect to equivalent bulk material structures. Under the application of a normal force by the tip of an atomic force microscope, it is found that multiple nanowire arrays consecutively linked by suspended spacers behave like a set of linear springs connected in series instead of an elastic beam as it could have been intuitively predicted. Moreover, the values that we obtain experimentally for the spring constants of the array-based mechanical structures are typically two orders of magnitude smaller than equivalent bulk material structures. The agreement between the experimental results and finite element simulations of the fabricated structures validates our conclusions. We believe that both our fabrication approach and the unique morphological and mechanical properties of the resulting nanowire arrays can open new perspectives in the development of a new generation of nanoelectronic and nanoelectromechanical systems with a wide range of applications. Surrounding gate horizontal nanowire array field effect transistors for nanoelectronics or biosensing, ultrasensitive piezoresistive transducers based on the giant piezoresistance effect observed in Si nanowires, or microcantilever-like platforms for physical, chemical or biological sensing are some examples discussed in our conclusions.

8:30 AM DD9.3

STM of Polydiacetylene Nanowires: Electrode Interactions and Stability . Rajiv Giridharagopal and Kevin F Kelly; Electrical and Computer Engineering, Rice University, Houston, Texas.

An alternative to the traditional silicon electronics paradigm is molecular electronics, wherein carefully-tailored single molecules operate as switching elements. Interconnecting such elements to form a circuit poses a unique challenge at this scale, particularly from an electronic structure viewpoint. Polydiacetylene nanowires have been proposed as a possible molecular wire because they can be easily formed on a monolayer surface, have a simple, linear structure, and exhibit enhanced conductivity when doped. These nanowires have been analyzed at the nanoscale using scanning tunneling microscopy (STM) and spectroscopy. Analysis shows that the nanowires exhibit a strong electronic interaction with the substrate. Polydiacetylene nanowires on different electrode materials such as graphite and molybdenum disulfide exhibit substantially different electronic properties. The substrate-dependent charge transfer behavior observed implies that the electrode material is critical for using polydiacetylene interconnects in molecular electronic devices. Additionally, the desorption of these nanowires due to the STM tip was investigated. Desorption can occur in segments or along the entire nanowire. In both cases, the surrounding monolayer order is fully restored almost instantaneously via a "molecular cascade" effect. Desorption underlies a critical stability issue in polydiacetylene nanowires, and the properties outlined here are also important for applications of polydiacetylene in other fields, such as bio-sensors.

8:45 AM DD9.4

Investigation of the Heterojunction Sharpness of Nanowhiskers by Analytical TEM Measurements. Daniela Sudfeld¹, Jochen Kaestner¹, Guenter Dumpich¹, Ingo Regolin², Werner Prost² and Franz-J. Tegude²; ¹Experimental Physics - AG Farle, University of Duisburg-Essen, Duisburg, Germany; ²Solid State Electronics Dept., University of Duisburg-Essen, Duisburg, Germany.

Semiconductor nanowhiskers excite a great research interest due to their intriguing growth features as well as a potential application in nano-scaled electronic and optoelectronic devices. For future device applications the abruptness of the interfaces of the heterojunctions is of fundamental importance [1]. High crystal quality single GaAs/InGaAs/GaAs and GaAs/GaP/GaAs nanowhiskers were grown by metal-organic vapour-phase epitaxy on (111)B GaAs substrates using the vapour-liquid-solid growth mode [2,3]. The diameter ranging between 10 and 100 nm of the nanowhiskers was defined by monodisperse gold nanoparticles deposited on the GaAs substrate. Energy-dispersive X-ray spectroscopy (EDS) measurements were performed with a FEI/Philips Tecnai F20ST microscope to investigate lateral and vertical transitions with extremely high resolution [4]. The investigations include (1) the segregation out of the gold seed particle, (2) the interface sharpness of group-III versus group-V transitions, and (3) lateral transitions attributed to a parasitic conventional layer growth forming a core-shell structure perpendicular to the growth direction. The results show that the group-III transitions exhibit long tails attributed to a memory effect of the group-III species in the Au droplet [5], while lateral sharp core-shell GaAs/InGaAs/GaAs heterojunctions were found. In contrast, the transition of the GaAs/GaP/GaAs whisker is much sharper due to a lacking memory effect of group-V species in the seed particle. These results provide important rules for an appropriate design of heterojunction nanowhisker devices. Acknowledgement: This work was supported by the DFG (SFB 445). References: [1] K. Hiruma et al., IEICE Trans. Electron., Vol. E77-C, No. 9 (1994). [2] R. S. Wagner and W. C. Ellis, Appl. Phys. Lett. 4, 89 (1964). [3] K. Hiruma, T. Katsuyama, K. Ogawa, M. Koguchi, H. Kakibayashi and G. P. Morgan Appl. Phys. Lett. 59, 431 (1991). [4] D. Sudfeld, I. Regolin, J. Kästner, G. Dumpich, V. Khorenko, W.

Prost, and F. - J. Tegude; Phase Transitions 79, no. 9-10 (2006) in print. [5] I. Regolin, D. Sudfeld, S. Lüttjohann, V. Khorenko, W. Prost, J. Kästner, G. Dumpich, C. Meier, A. Lorke, and F. -J. Tegude; special issue of Journal of Crystal Growth (2006), accepted.

9:00 AM DD9.5

Size Effect of TiO₂ Nanotubular Structures on Their Electrical Properties Sihyeong Kim, Bokyoung Ahn, Changdeuck Bae and Hyunjung Shin; School of Advanced Materials Engineering, Kookmin University, Seoul, South Korea.

Electrical properties of TiO₂ nanotubes with different wall thicknesses and diameters were investigated. TiO₂ nanotubes with the range from 1 to 100 nm of the wall thickness were deposited using atomic layer deposition (ALD) onto porous templates of polycarbonate (PC) and anodic aluminum oxide (AAO)[1]. To investigate electrical properties of TiO₂ nanotubes formed in the porous templates, we constructed devices of Pt (top electrode of 200 nm in diameter)/TiO₂ nanotubes in the porous templates/Pt (bottom electrode). I-V characteristics of PC templates without any coating of TiO₂ as control experiments exhibit typical insulating behavior of polymeric materials. I-V/C-V characteristics of the devices with TiO₂ nanotubes were measured. While the Schottky behaviors were common to both TiO₂ nanotubes of 50 and 200 nm in diameter, it was found that the barrier height of Schottky diode decreased with decreasing the diameters of nanotubes. Effects due to the size in nanometer scale in diameter as well as the wall thickness on their electrical properties are discussed. Acknowledgement This work was supported by the Center for Nanostructured Materials Technology of the Korean Ministry of Science and Technology (M105K0010026-06K1501-02610). [1] H. Shin, D.-K. Jeong, J. Lee, M. M. Sung, J. Kim, Adv. Mater. 2004, 16, 1197.

9:15 AM DD9.6

Measuring Thermal Conductivity and Electrical Breakdown of GaN Nanowires Elaine Lai, Reese Jones, George Wang, Richard Anderson, Bhavin Rokad and Alec Talin; Sandia National Labs, Livermore, California.

Sandia National Labs, Livermore, CA 94550 We report on the measurement of temperature, thermal conductivity, and eventual breakdown associated with Joule heating of individual GaN nanowires. Individual GaN nanowires with Ni/Au ohmic contacts are electrically heated under steady state conditions, while their temperature is determined by the wavelength of the band edge peak using micro-photoluminescence. We find that the extracted temperature is linearly related to the electrical power supplied to the nanowire. Breakdown occurs at a power range of 4 mW - 105 mW, depending on nanowire dimensions, and at a temperature range of 550K - 900K. Based on the temperature measurements, thermal conductivity was extracted using finite element modeling and compared to published bulk values for GaN. Sandia is a multiprogram laboratory operated by Sandia Corporation, a Lockheed Martin Company, for the United States Department of Energy's National Nuclear Security Administration under Contract No. DE-AC04-94AL85000.

SESSION DD10: Assembly, Patterning and Collective Properties I
Chairs: Heinrich Jaeger and Masaru Kuno
Wednesday Morning, April 11, 2007
Room 2001 (Moscone West)

9:45 AM *DD10.1

Nanoparticle Electronics: Controlled Nanocrystal Assembly and High-resolution Device Fabrication on Silicon Nitride Membranes using Transmission Selectron Beams. Marija Drndic, Michael Fischbein, Claudia Querner and Zonghai Hu; Physics and Astronomy, University of Pennsylvania, Philadelphia, Pennsylvania.

Nanocrystals are tunable crystals a few nanometers in size, exhibiting a range of quantum phenomena at room temperature. Efforts to explore nanocrystals unite the frontiers of chemistry, physics and engineering, and open up new applications ranging from electronics to biology. In this talk, I will discuss the assembly of spherical and rod-like CdSe and PbSe semiconductor nanocrystals into electronic devices, their electronic properties and the basic mechanisms of charge transport, both in the limit of large arrays and the limit of only a few quantum dots. I will show how local charge transport behavior can be directly imaged by electrostatic-force microscopy and correlated to nanopatterns observed with transmission electron microscopy. I will also describe a new and highly flexible method based on transmission-electron beams to controllably ablate metal films to produce intricate metal geometries and fully integrated devices with sub-10 nm features on top of silicon nitride membranes. Arbitrary metal patterns may be "carved out" on insulating membranes with sub-nanometer accuracy by ablating evaporated metal films with the 0.5 nm diameter beam of a high-resolution transmission electron microscope. In situ imaging of the ablation action allows for real-time feedback control. Specific examples presented here include nanogaps, nanorings, nanowires with tailored shapes and curvatures, and multi-terminal devices with nanoislands or nanoholes between the terminals. These nanostructures are fabricated at precise locations on a chip and seamlessly integrated into large-scale circuitry. The combination of high resolution, geometrical control and yield make this fabrication method highly attractive for many applications including nanoelectronics, superconductivity, nanofluidics and molecular translocation.

10:15 AM DD10.2

ENFilADIng: An Innovative Route to Nanowire Growth and Interfacing. Bret N. Flanders and Birol Ozturk; Physics, Oklahoma State University, Stillwater, Oklahoma.

We present a recently developed approach to nanowire fabrication and interfacing with external circuitry, termed Electrochemical NanoFilament Assembly and Directed Interfacing (ENFilADIng). Depositing salt solution over a pair of on-chip electrodes and applying an alternating voltage across the electrode-gap induces the growth of individual metal nanowires between the electrode tips (1). High resolution transmission electron diffraction measurements on wires grown from indium acetate and hydrogen tetrachloroaurate indicate that these nanowires are composed of single-crystalline indium and gold, respectively. Furthermore, precise control over the nanowire-diameter is attained through the frequency ω of the alternating voltage that induces the ENFilADIng process. For indium wires, increasing ω from 0.5 to 3.5 MHz increases the growth velocity of the wires from 11 to 78 $\mu\text{m/s}$ and reduces their diameter from 770 to 114 nm. Gold wires exhibit diameter-tunability that extends well below 100 nm. Thus, it is possible to tune the wire diameter from the microscale down to the nanoscale. We will report on mechanistic understanding that we have developed regarding the diameter-tunability aspect of this technique. Additionally, by the feedback-controlled application of the alternating voltage, where the feedback signal is the cross-gap current, it becomes possible to terminate the applied voltage once the wire has bridged the electrode gap, but before the alternating voltage drives damaging currents through the nanowires. This approach yields electrode-nanowire-electrode

assemblies with resistances of $223 \pm 26 \Omega$, reproducibility that would not be possible were the voltage terminated manually. This combination of capabilities—the growth of single crystalline nanowires with precisely controlled diameters and reproducible interfacing with external circuitry—enables interrogation of the intrinsic transport properties of metallic nanowires. An area of particular interest is the contribution of surface scattering mechanisms to the total resistivity, an effect that is expected to increase with decreasing diameter. Progress on this investigation will be reported. (1) Talukdar, I.; Ozturk, B.; Mishima, T. D.; Flanders, B. N. *Appl. Phys. Lett.* 2006, 88, 221907.

10:30 AM DD10.3

Electron Transport Properties of Solution-Processed Semiconducting Quantum-Wire Solids. Debdeep Jena¹, Amol Singh¹, Vladimir Protasenko², Huili Xing¹ and Masaru Kuno²; ¹Electrical Engineering, University of Notre Dame, Notre Dame, Indiana; ²Chemistry and Biochemistry, University of Notre Dame, Notre Dame, Indiana.

Charge transport properties of solution-synthesized PbSe, CdTe, and CdSe quantum wire solids are studied experimentally. The quantum-wire solids, analogous to previously reported quantum-dot solids, are formed by dense networks of connected nanowires. The semiconducting nanowires are synthesized by the solution-liquid-solid (SLS) technique. The general growth procedure leverages advances in the synthesis of semiconducting nanocrystals - ~2 nm diameter low melting metallic nanoparticle catalysts are used to promote 1-D crystallization in the presence of coordinating surfactants such as trioctyl phosphine oxide (TOPO). The nanoparticles are introduced with a group-VI precursor (for example TOP-Se for CdSe and PbSe wires), along with ligand-coordinated metal ions (CdO with octanoic acid for CdSe). The resulting nanowires are 5-10 nm in diameter, and several microns long. Prior to transport studies, optical absorption/emission and photoconductive studies are performed on the nanowires, verifying their semiconducting nature, and revealing their optical bandgaps, which are blue-shifted corresponding to their bulk gaps due to quantum confinement effects. High-resolution TEM images reveal that the nanowires are highly crystalline, and the diameter variation in a typical yield is 25-30%, and the intrawire diameter variations are of the order of 5%. The diameters of the nanowires (<10nm) are smaller than twice the respective bulk exciton Bohr radii. Ohmic contacts are fabricated by controlled annealing of metal-quantum wire solid-metal structures. Temperature-dependent conductivity measurements are performed on the structures. As opposed to the closely related quantum-dot solids where charge transport occurs by Mott's variable range hopping above a critical temperature and through Coulomb-blockade effects for low temperatures, the transport in the quantum-wire solids is clearly observed to be by band-transport ($\sigma \sim \exp[-E_g/2kT]$) with the activation energy corresponding precisely to half the bandgap of the semiconductor. This form of transport is observed for all three types of nanowires : PbSe, CdTe, and CdSe. The activation energies are in close agreement with the complementary optical absorption/emission and photoconductivity measurements ($E_g = 0.27$ eV, 1.6 eV, & 1.9 eV respectively for PbSe, CdTe, and CdSe nanowires). This provides the first demonstration that the solution-synthesized nanowires are nearly intrinsic, with very few density of dopant atoms (less than the respective thermally generated intrinsic carrier concentrations). Band-transport in such quantum-wire solids makes them attractive for a number of applications - they provide an alternative approach to various device architectures (FETs, photodetectors). Being solution-processed, they are cheap and scalable, and well suited for large-area devices on virtually any substrates without limitations imposed by lattice mismatch in epitaxial growth.

10:45 AM DD10.4

Precise Nanoparticle Placement via Electrostatic Funneling* Vishva Ray, Hong-Wen Huang, Ramkumar Subramanian, Liang-Chieh Ma, Choong-Un Kim and Seong Jin Koh; The University of Texas at Arlington, Arlington, Texas.

One of the key requirements toward the realization of nanoscale devices and sensors is the capability to place nanoscale building blocks on exact locations on the substrate. We have developed a wafer-scale scheme called "electrostatic funneling", which guides charged colloidal nanoparticles onto targeted locations with nanoscale precision. We have demonstrated a placement precision of 6 nm using one-dimensional guiding structure patterned on 200 mm silicon wafer. In this approach, the electrostatic guiding structures were fabricated by selectively charging the substrate using self-assembled monolayers (SAMs) of organic molecules in aqueous solution. The merit of this technique is that nanoscale precision can be realized with guiding structures that can be fabricated using conventional CMOS technology with dimensional control of only ~100 nm. The effectiveness of this technique has also been demonstrated for various other geometries such as 0-dimensional arrays and three-dimensional step structures with gold nanoparticles of diameter 20, 50, 80, and 200nm. We have also calculated the underlying electrostatic interaction energies between nanoparticles and charged substrates using DLVO theory and found very good agreement with experimental observations. Our calculations show that a 20nm gold nanoparticle is subjected to a lateral force of $1E-7$ to $4E-7$ dynes when the nanoparticle-surface distance is less than 100 nm and this strong lateral force is responsible for the guided placement of nanoparticles. We envision that this electrostatic guiding scheme can also be applied to the precise placement of other nanoscale building blocks such as nanowires, carbon nanotubes, DNAs, and proteins. An application to fabrication of single electron devices utilizing guided nanoparticle placement will also be discussed. *Supported by ONR (N00014-05-1-0030), NSF CAREER (ECS-0449958), and THECB (003656-0014-2006).

11:00 AM DD10.5

Strain-induced Self-assembled Oxide Nanostructures from Chemical Solutions. Marta Gibert Gutierrez¹, P. Abellan¹, C. Moreno¹, F. Sandiumenge¹, R. Huehne², T. Puig¹ and X. Obradors¹; ¹Institut de Ciència de Materials de Barcelona ICMAB-CSIC, Bellaterra, Catalonia, Barcelona, Spain; ²Institute for Metallic Materials, IFW-Dresden, Dresden, Germany.

Self-assembling and self-organizing processes are a common phenomenon in nature that show a high potential for the preparation of nanostructures in surfaces based on epitaxial growth through the control of interfacial energies. Such methodologies have already been widely investigated in the semiconductor field; however, its application in oxide materials has been scarcely investigated. Nevertheless, they constitute a promising strategy for the preparation of new magnetic, ferroelectric, electronic, optical and superconducting devices. In the present work, we present an innovative study of the generation of interfacial self-assembled oxide (BaZrO₃, CeO₂, Ce_{0.9}Gd_{0.1}O_{1-y}) epitaxial nanoislands based on chemical solution deposition (CSD). This methodology has been rarely used for the generation of nanostructures, in spite its high potential for the growth of low-cost large scale nano-structures. Through a detailed study of the kinetic and equilibrium processes leading to system's evolution (nucleation, growth, ripening and coalescence), we demonstrate the high and promising potential of CSD for the generation and tuning of size, morphology, density and distribution of the resulting oxide interfacial nanostructures. RHEED analysis have identified the epitaxial orientation relationship between the nanoislands and the underneath substrate. Accordingly, we have successfully grown templates with self-assembled oxide nanodots, nanowalls and nanorods. Typical dimensions for the nanodots are ~ 7 nm medium height, ~ 45 nm equivalent diameter and a medium density of ~ 60-80 nanodots/ μm^2 . Such fine tuning is done through the control and modification of lattice mismatch, solution's characteristics and growth conditions (temperature, atmosphere and time). The influence of those parameters on the resulting self-assembled oxide nanoscale interfacial structures will be presented. * This work

has been supported by the European Union and Spanish national funds (HIPERCHEM project, NMP4-CT2005-516858, MAT2003-01584 and MAT2005-02047).

11:15 AM DD10.6

Direct Assembly of Quantum Confined Nano-particles. Ingo Plueme^{1,2}, Klemens Hitzbleck², Ivo W. Rangelow⁴, Jan Meijer³ and Hartmut Wiggers²; ¹Experimental Physics, University of Duisburg-Essen, Duisburg, Germany; ²Institute of Combustion and Gasdynamics, University of Duisburg-Essen, Duisburg, Germany; ³RUBION, Ruhr-Universität Bochum, Bochum, Germany; ⁴Institute for Micro- and Nanoelectronics, Technische Universität Ilmenau, Ilmenau, Germany.

Advances in nanoparticle technology enable the production of new types of electronic devices, catalytic systems and complex functional surface coatings. For most of these applications, random deposition or self-assembled arrangement of the particles on surfaces are sufficient. However, an increasing number of potential applications such as single electron transistors and quantum computers require exact placement of single nanoparticles with sub-10 nm resolution and specific size. Till date, techniques that provide an exact online placement of countable and size-selected nanoparticles for functional devices have not been reported. For this purpose a cluster-jet system, based on a gas-phase nanoparticle synthesis source, connected to a focussing collimator system has been developed. The objective of this technique is to assemble countable single nanoparticles with spatial resolution of 10 nm or below onto a pre-structured substrate. In the first stage of this system, nanoparticles in the size regime between 3 and 10 nm are synthesized in a low-pressure microwave plasma reactor. This reactor has the unique advantage of generating particles with defined size distribution, structure, morphology and low degree of agglomeration due to coulomb repulsion during particle formation and growth. Separated single particles are extracted by means of a particle laden molecular beam. A mass filter consisting of a particle mass spectrometer (PMS) coupled to the reactor is used to select nanoparticles of a specific size, according to their mass, charge and kinetic energy. In order to achieve the designated lateral resolution, the particle laden beam will be collimated by electromagnetic lenses and focused onto a pierced AFM-tip. Operation of the focusing mechanism and tip preparation have been successfully performed separately and are currently being adapted to the use in the cluster-jet system. After completion, this technique is intended to enable the assembly of nanoparticles in almost any desired two-dimensional structure onto a substrate.

11:30 AM DD10.7

Lipid Nanotubes as Scaffolds for Selective Deposition of CdS Nanodots Yong Zhou¹ and Shimizu Toshimi^{1,2}; ¹SORST, Tsukuba Central 5, Japan Science and Technology Agency (JST), Tsukuba, Ibaraki, Japan; ²Nanoarchitectonics Research Center (NARC), Advanced Industrial Science and Technology (AIST), Tsukuba, Ibaraki, Japan.

In recent years, there has been much interest in using lipid nanotubes (LNTs) to modulate the growth of a large variety of inorganic nanomaterials including metal, semiconductor, and magnetic particles [1]. In this presentation, we report LNTs as scaffolds to selective deposition of CdS nanodots (NDs) on the surfaces, in the hollow cylinder, and in the bilayer membrane walls of the nanotubes with different techniques. Firstly, the dense helical arrays of CdS NDs, which are aligned one-by-one and side-by-side, form on the surfaces of the self-assembled LNT template from the binary components, glycolipid, N-(11-cis-octadecenoyl)- β -D-glucopyranosylamine (1) and aminophenyl- β -D-glucopyranoside (2) as an additive [2]. The formation mechanism greatly differs from precedent examples that utilize residual helical marks on the surfaces of LNTs and nanoribbons or organic templates with a helical morphology. Here, we functionalized the glycolipid nanotube of 1 by incorporation of 2 through the self-assembly. This functionalization process enabled us to create active binding sites, which trace the chiral molecular packing of the nanotube. Consequently, the helical nucleation and growth of the CdS NDs took place on the template surfaces. Secondly, one-dimensional (1-D) confinement of CdS NDs was made in the hollow cylinder of the LNT from 1 as a scaffold. We have used two paths to realize the 1-D arrangement of the CdS NDs in the LNT. One is that the LNT was dispersed into aqueous solutions of water-soluble CdS NDs, and then the fluidic NDs diffuse into the hollow cylinder of the LNT via capillary force. The other is that the solution of a CdS precursor diffuses into the LNT, followed by in situ formation of CdS NDs in the nanochannels of the LNT. Furthermore, calcination of the CdS-NDs-encapsulated LNT enabled us to obtain single-crystalline CdS nanowires. Thirdly, we first report in situ direct growth of the CdS NDs in the bilayer membranes of a self-assembled peptide LNT. We used the synthetic lipid, the sodium salt of 2-(2-(2-tetradecanamidoacetamido) acetamido) acetic acid (3) that can self-assemble in aqueous solutions into a hollow cylindrical structure in the presence of Cd²⁺. Upon exposure to H₂S vapor, the Cd²⁺ in the Cd²⁺-complexed LNT were released as a result of competitive binding of the proton to the COO⁻ group, resulting in the formation of H⁺-induced LNT. The released Cd²⁺ subsequently reacted with S²⁻ to initiate CdS nuclei, and finally grew into the CdS NDs in all over the lipid bilayer membranes of [3]. The present three processes typically represent effective steps to artificially control the crystal orientation and morphology on bio-inspired substrates. References [1] Shimizu, T.; Masuda, M.; Minamikawa, H. Chem. Rev. 2005, 105, 1401. [2] Zhou, Y.; Ji, Q.; Masuda, M.; Kamiya, S.; Shimizu, T. Chem. Mater. 2006, 18, 403 [3] Zhou, Y.; Kogiso, M.; He, C.; Shimizu, Y.; Koshizaki, N.; Shimizu, T. Adv. Mater. (in revision).

11:45 AM DD10.8

High Resolution DNA Arrays by Supramolecular Nanostamping Ozge Akbulut¹, Jin-Mi Jung², Ryan Bennett³, Robert Cohen³, Anne Mayes¹ and Francesco Stellacci¹; ¹DMSE, MIT, Cambridge, Massachusetts; ²Materials Science and Engineering, KAIST, Daejeon, South Korea; ³Department of Chemical Engineering, MIT, Cambridge, Massachusetts.

The emerging need for miniaturizing devices makes biomolecules great candidates not only for serving as a template but also as a structural component. In order to exploit DNA as well as other biomolecules, we need to find ways to produce high resolution bio-arrays. Although many methods to serially fabricate such arrays have been developed, no clear strategy on how to scale the production efficiency up has been presented. In the quest for fast soft material stamping processes able to produce chemically complex bio-devices, a recent method, Supramolecular Nanostamping (SuNS) has been demonstrated. It replicates DNA-made nanoscale features effectively from one surface to another keeping the DNA information. [1, 2] A layer of single stranded DNA molecules is immobilized on a surface. When this layer is treated with its complementary DNA molecules, which contain specific end groups, due to the supramolecular forces double helices are formed on the surface. The specific end groups of complementary DNA molecules target to bond covalently to a secondary surface. When the master and the secondary surface come into contact, complementary DNA molecules attach to the secondary surface through their end groups and stays there after dehybridization upon heating. Namely, SuNS duplicates the DNA arrays via harnessing the reversible hybridization reaction of complementary DNA molecules. Here we employ a convenient bottom-up approach to obtain ordered arrays of DNA with 10-20 nm features spaced by 70 nm. The master is formed by self-assembly of DNA on gold nanoparticles obtained from the gold-modified polystyrene-*b*-poly(2-vinylpyridine) (PS-*b*-P2VP) micellar block copolymer. [3] References

1)Yu, AA., Savas, TA., Taylor GS., Guiseppe-Elie A., Smith, HI., Nano Letters, 2005, 5, 1061. 2)Lin, H., Sun, L., Crooks, RM., J. Am. Chem. Soc., 2005, 127, 11210. 3)Lu, JQ & Yu, S., Langmuir, 2006, 22, 3951.

SESSION DD11: Assembly, Patterning and Collective Properties II
 Chairs: Bret Flanders and Masaru Kuno
 Wednesday Afternoon, April 11, 2007
 Room 2001 (Moscone West)

1:30 PM DD11.1

Drying Mediated Self-Assembly of Nanoparticles from a Sphere-on-Flat Geometry. Zhiqun Lin and Jun Xu; Materials Science and Engineering, Iowa State University, Ames, Iowa.

Self-assembly of nanoparticles via irreversible solvent evaporation has been recognized as an extremely simple route to intriguing structures. However, these dissipative structures are often randomly organized without controlled regularity. Herein, we show a simple, one-step technique to produce concentric rings and spokes consisting of quantum dots and gold nanoparticles with high fidelity and regularity by allowing a drop of nanoparticle solution to evaporate in a sphere-on-flat geometry. The rings and spokes are nanometers high, submicrons to a few microns wide, and millimeters long. This technique, which dispenses with the need for lithography and external fields, is fast, cost-effective and robust. As such, it represents a powerful strategy for creating highly structured, multifunctional materials and devices.

1:45 PM DD11.2

One-Nanometer-Scale Size-Controlled Synthesis and 2D Self-Assembly of Monodisperse Gold Nanoparticles. Sang-Kee Eah and James Ian Basham; Department of Physics, Applied Physics, and Astronomy, Rensselaer Polytechnic Institute, Troy, New York.

We developed a simple, fast, and highly reproducible chemical synthesis method for colloidal gold nanoparticles, which are monodisperse in size with diameters of 3, 4, 5, 6, 7, 8, and 9 nm. Gold nanoparticles smaller than 3 nm are made in water by reducing gold ions with sodium borohydride molecules, and then they are transferred to toluene after being coated with ligand molecules of 1-dodecanethiol. One-nanometer-scale size control is demonstrated simply by adjusting the heating time of the gold nanoparticles solution at the boiling temperature of 1-dodecanethiol. These monodisperse gold nanoparticles self-assemble into three-dimensional and two-dimensional (2D) superlattices of hexagonal close-packing order. We will present a 2D monolayer of gold nanoparticles as large as completely covering the whole surface of a 3 inch silicon wafer. The monolayer of gold nanoparticles is composed of nearly perfect 2D superlattice domains, whose size can be larger than 20 μm . To our best knowledge this monolayer and its 2D superlattice domains of nanoparticles are the largest ones ever reported. The 2D self-assembly is done simply by evaporating toluene droplets of gold nanoparticles together with water droplets without need of any special equipment. Conditions for reproducibly forming such large monolayers and 2D superlattice domains of nanoparticles will be discussed in addition to the mechanism of this 2D self-assembly method for nanoparticles. Currently we are working on generalization of this synthesis and 2D self-assembly method to other kinds of nanoparticles and 2D self-assembly of binary nanoparticles superlattices varying the size combination and the mixing ratio.

2:00 PM *DD11.3

Dried to Order: Metal Nanocrystal Superlattices Self-Assembled from Solution Heinrich Jaeger, James Franck Institute, University of Chicago, Chicago, Illinois.

This talk will give an overview of the properties of nanocrystal superlattice structures that can be self-assembled by drop drying. The first part discusses the main assembly mechanisms as well as extensions and techniques to produce (quasi-) one-dimensional, two-dimensional and three-dimensional structures. Close-packed monolayers can be produced that extend over millimeters and exhibit near-perfect long-range order over tens of square microns. The superlattices self-assemble directly onto solid substrates, can drape themselves over prefabricated electrode structures, and require no transfer or further processing. I will focus on results obtained with 6nm diameter, dodecanethiol-capped gold nanocrystals, but the self-assembly process has general applicability. By controlling the process conditions, ordered monolayer arrays with inter-particle spacing less than 1nm have been produced. The second part of the talk discusses the remarkably robust electronic transport properties of the self-assembled structures. Strong Coulomb blockade effects in the presence of quenched charge disorder give rise to highly nonlinear current-voltage characteristics. Inside the Coulomb blockade regime, the residual zero-bias conductance results from multiple co-tunneling events. The third part will look at the mechanical properties of metal nanoparticle monolayers freely suspended over micron-sized holes.

2:30 PM DD11.4

Fabrication, Optimization and Modeling of Highly Ordered Assemblies of Monodisperse Metallic Nanostructure Arrays. Aniketa Shinde^{2,1}, Chulsu Jo², Jiun Pyng You¹, Ju Hyeon Choi¹, Ruqian Wu¹ and Regina Ragan²; ¹CheMS, UC Irvine, Irvine, California; ²Physics & Astronomy, UC Irvine, Irvine, California.

Metal nanostructures have demonstrated extraordinary properties: the capacity for single molecule detection in plasmon resonance biosensors, chemical sensitivity and higher performance in catalytic processes than their bulk counterparts, and the transport of electromagnetic energy along particle chains in optical circuits. One of the most significant challenges to technical developments that capitalize on unique properties of metal nanostructures is the fabrication of nanostructure arrays with monodisperse size, shape and high density using low cost and high throughput technique. We will present a unique Si-compatible fabrication process for dense ordered arrays ($\sim 10^{11} \text{ cm}^{-2}$) of metal nanostructures with monodisperse size and shape, over large area ($> 1 \text{ mm}^2$), and having feature size and inter-particle spacing unattainable with state of the art electron beam lithography. Noble metal deposited via physical vapor deposition on a nanowire template combined with reactive ion etching produced noble metal core-shell nanowire and nanoparticle arrays with mean feature size of approximately 8 nm. Hexagonal rare earth disilicide nanowires, such as DySi_2 and ErSi_2 , are used as self-assembled nanowire templates on Si(001). Dense arrays of parallel DySi_2 and ErSi_2 nanowires having lengths greater than 1 micron and widths less than 5 nm have been fabricated and characterized on vicinal Si(001) previously. Scanning tunneling microscopy has shown that platinum (gold) forms clusters on the ErSi_2 (DySi_2) nanowire surfaces, and scanning electron microscopy backscattered images have shown that noble metal preferentially aggregates on the nanowire surfaces as opposed to the Si substrate. Noble metal coverage is used to select nanoparticle versus nanowire arrays after RIE. In the case of nanoparticles, a narrow size distribution of less than 1 nm and

inter-particle spacing of approximately 10 nm is obtained by our process. Few studies have been done on the theory behind the formation of the nanowire templates as well as the phenomena of preferential aggregation of noble metal on nanowire surfaces. Thus, theoretical modeling is combined with scanning probe microscopy in order to gain a deeper understanding of thermodynamics and kinetics driving nanostructure formation. We will also present ongoing work that uses VASP, an ab initio software package, to simulate RESi_2 crystal structures as well as metal atoms on nanowire surfaces. Our preliminary calculations for bulk YSi_2 have been found to be in close agreement with experiment and other theoretical studies. Our goal is to understand assembly mechanisms in order to optimize structure and make our process applicable to other material systems.

2:45 PM DD11.5

Templated Growth of Complex Hybrid Nanostructures Erik D. Spoeke, Thomas Sounart, Julia W.P. Hsu and James Voigt; Sandia National Laboratories, Albuquerque, New Mexico.

We have investigated the synthesis and characterization of multicomponent nanocrystalline hybrid materials and films. Nanoscale materials present unique optical, electrical, and structural properties with significant technological implications. Such unique properties are strongly dependent on the chemical and structural composition of these materials. We have explored synthetic strategies to create hybrid materials whose chemical and structural composition may be controlled on multiple organizational levels. Utilizing a multistage solution-phase growth process, we can create hierarchical zinc oxide (ZnO) nanostructures. Using these nanoconstructs as templates, we create unique hybrid structures whose final form and properties may be controlled through the introduction of bio-inspired crystal growth modifiers such as amino acids and engineered peptides. Combining this multistage, solution-phase growth approach with these organic tools facilitates controlled, directed nanostructure formation, interfacing functional materials such as cadmium sulfide or silica nanoparticles with zinc oxide nanorods. Extending the formation of these structures to form micropatterned films, we further demonstrate the hierarchical nature of the materials created using this multi-stage synthesis and assembly strategy. These methods for the growth of complex nanostructures represent powerful potential tools in the development of new materials systems. Sandia is a multiprogram laboratory operated by Sandia Corporation, a Lockheed Martin Company, for the United States Department of Energy's National Nuclear Security Administration under Contract DE-AC04-94AL85000.

3:00 PM DD11.6

Quantum Dot Microrods. Arya Ghadimi, Ludovico Cademartiri, Reihaneh Malakooti and Geoffrey A. Ozin; Chemistry, University of Toronto, Toronto, Ontario, Canada.

The recent developments in nanocrystal self-assembly have garnered a great deal of attention in part because such assemblies exhibit novel and useful combinations of properties. For instance, these assemblies may possess structurally significant size and mechanical stability in conjunction with photoluminescence characteristic of their quantum-confined constituents. However, synthesis of self-supporting nanocrystal assemblies is quite challenging: typically nanocrystals' original properties cannot be retained in the final assembly due to the harsh treatments necessary to preserve mechanical stability after the removal of the supporting template. Here we demonstrate a general approach for the fabrication of flexible, self-supporting microrods composed of densely packed nanocrystals which retain their properties throughout the assembly process. Furthermore, the nanocrystal building blocks show a remarkable tendency to self-assemble into large, highly-ordered domains within the microrods. Nano-channel anodized alumina was used as a template to synthesize microrods from PbS quantum dots and Bi_2S_3 nanorods. The nanocrystal assemblies were subsequently consolidated by the recently discovered process of nanocrystal plasma polymerization. The selective removal of the alumina template yielded flexible, self-supporting microrods composed of individual nanoparticles. In the case of PbS, the microrods exhibited photoluminescence comparable to that of pristine colloidal nanoparticles. PbS self-supporting nanotubes have also been demonstrated. The method and the results discussed here are important to the study of nanocrystal self-assembly and plasma polymerization in confined spaces, and the development of hierarchical nanocrystal-based architectures in which the geometry and the length scale are coupled to the overall functionality. The generality and versatility of this method add to its potential for creating purpose made micron-scale structures exhibiting nano-scale properties.

3:30 PM DD11.7

Hierarchically Organized Nanoparticle Mesostructure Arrays Formed through Hydrothermal Self-Assembly. Hongyou Fan^{1,2}, Adam Wright², John Gabaldon², Bruce Burckel¹, Jeffrey Brinker¹, Ryan Tian¹ and Jun Liu¹; ¹Sandia National Lab, Albuquerque, New Mexico; ²Chemical and Nuclear Engineering, University of New Mexico, Albuquerque, New Mexico.

Building block self-assembly is one of the efficient methods to the fabrication of nanostructured materials. Nanoparticles with controlled size, shape, and composition have been successfully used as building blocks for the fabrications of 2- and 3-dimensional nanoparticle arrays (or mesophases) for the development of 'artificial solids' (or metamaterials) with collective optical and electronic properties. Nanoparticle surface chemistry plays a key role in control of microstructures of the nanoparticle arrays such as mesophase (face-centered-cubic (fcc), diamond, etc), interparticle distance, etc. To date, work has mostly focused on the synthesis of nanocrystals that are stabilized with alkane ligands ($\text{CH}_3(\text{CH}_2)_n\text{R}$, $\text{R}=\text{SH}$, NH_2 , PO , etc). Self-assembly of these NCs and formation of ordered nanocrystal arrays are driven by hydrophobic (or van der Waal) interactions of interdigitated alkane chains between each nanocrystals. In this presentation, we report a new self-assembly pathway that leads to supported and hierarchically organized gold nanoparticle mesostructure arrays on solid substrates such as glass slide, thermal oxide, photopolymer film, and mica (Wright, A. et al Chem. Mater. 2006, 18, 3034-3038). We synthesized nanoparticle micelles through encapsulation of monodisperse hydrophobic nanoparticle within the hydrophobic core of surfactant micelle. The nanoparticle micelle provides unique surface chemistry for further self-assembly and formation of highly ordered nanoparticle metamaterials. Using the nanoparticle micelle as a building block (Fan H. et al Science 2004, 304, 567-571), hierarchical gold nanoparticle mesostructure arrays were prepared by a hydrothermal nucleation and growth process through self-assembly of nanoparticle micelles and organosilicates under basic conditions. Depending on the substrates used, the shape, order, and orientation of the gold nanoparticle mesostructure during nucleation and growth exhibit distinct features. Transmission electron microscopy and X-ray diffraction results revealed that gold nanoparticles were organized as a face-centered cubic mesostructure with precisely controlled interparticle spacing. Optical characterization using UV-vis spectroscopy shows a characteristic surface plasmon resonance band resulted from the ordered nanoparticle arrays. This method provides new means for colloidal self-assembly and for the fabrication of platforms for surface enhanced Raman scattering-based sensors and electric and optical nanodevices with enhanced thermal, chemical, and mechanical robustness. Sandia is a multiprogram laboratory operated by Sandia Corporation, a Lockheed Martin Company, for DOE under contract DE-AC04-94ALB5000

3:45 PM DD11.8

General Approach to Large Area Films of Aligned Nanowires and Carbon Nanotubes via Bubble Expansion Guihua Yu¹, Anyuan Cao² and Charles M. Lieber^{1,3}; ¹Chemistry, Harvard University, Cambridge, Massachusetts; ²Mechanical Engineering, University of Hawaii at Manoa, Honolulu, Hawaii; ³Division of Engineering and Applied Sciences, Harvard University, Cambridge, Massachusetts.

Central to many electronic device-based applications of nanowires (NWs) and carbon nanotubes (NTs) is the development of methods that enable organization over large areas with controlled orientation and density. Herein, we report a general and flexible method involving bubble expansion of homogeneous suspensions of NWs and carbon NTs to produce large area films. Studies demonstrate that the NWs and carbon NTs are well aligned within the films, and that density can be readily controlled by starting suspension concentration. The nanomaterial-embedded bubble films can be conformably transferred to a variety of substrates, including crystalline wafers and flexible plastics, and also suspended across open frames. In addition, measurements show that percolation threshold is readily exceeded to yield electrically conducting carbon NT films and that large scale NW field-effect transistor (FET) arrays can be easily fabricated on over large plastic substrates. The simplicity, scalability and generality of this approach offers substantial promise for exploring new structures containing large arrays of NWs and NTs, and for enabling applications of these nanomaterials.

4:00 PM DD11.9

Nano-Polymers. Gretchen A DeVries¹, Frajovon R. Talley² and Francesco Stellacci¹; ¹DMSE, MIT, Cambridge, Massachusetts; ²Howard University, Washington D.C., District of Columbia.

Nanoparticles will spontaneously aggregate into two- and three-dimensional structures, but to date they lack the ability to bond together in a directional manner to generate more complex structures. Anisotropic assemblies of nanoparticles possess unique properties that are not generally accessible by isotropic arrays of particles. The scope of potential scientific and technological applications for nanoparticles would be vastly enlarged by the introduction of a method to break the interaction symmetry of nanoparticles, thus inducing valency and directional interparticle interactions. Ligand-coated metal nanoparticles are particularly promising for this aim, because the ligands can be used as handles for directed assembly while simultaneously offering an easy way to manipulate the physical properties of the nanoparticles. We have demonstrated the ability to direct the assembly of metal nanoparticles into one-dimensional chains by taking advantage of molecularly defined defect points in the ligand shell located at diametrically opposed positions on the nanoparticle. Placing molecules with a reactive end group, such as a carboxylic acid, at these polar defect points generates "divalent" nanoparticles that can be reacted with diamine terminated molecules to generate linear chains of nanoparticles covalently held together through amide bonds. Here we discuss the assembly of these nanoparticle chains into structurally robust self-standing nanoparticle films that possess unique mechanical and electrical properties. Additionally, we present a detailed kinetic and thermodynamic characterization of the molecularly defined defect points that enable the generation of these chains and films. We demonstrate that the polar defect points are thermodynamically unique sites within the ligand shell and possess a significantly higher reactivity than other sites on the nanoparticle. A thorough understanding of the thermodynamic equilibrium governing place exchange at these defect points is essential for the controlled assembly of one-dimensional nanoparticle chains.

4:15 PM DD11.10

Silica Nanoparticles Three Dimensional Assembly: an Integrative Chemistry Approach toward Designing Opal-Like Silica Foams Renal Backov and Florent Carn; CNRS-Universite Bordeaux-I, Pessac, France.

Designing new porous materials in a monolithic form with framework involving hierarchical pore system while tailoring the macroscopic void spaces is an emerging area of technological interest toward heterogeneous catalysis, separations, artificial bone structure, thermal and/or acoustic insulation, ion-exchange operation. In addition to the micro- and/or mesoscale organization, shaping porous solids in the form of monolith with tailored macropore morphologies associated with a tunable surface roughness are also important factor that influence the suitability for potential applications. In this context of reaching specific functions, the integrative chemistry concept has been proposed recently and his offering a widespread materials with higher order architecture can be obtained by using soft matter macroscopic template such as biliquid[1] or air-liquid foam[2]. We describe here a low cost and effective way of preparing hierarchically organized porous silica monolith arising from an air-liquid foam structure transcription by colloidal crystallisation. The opal-like skeleton provide a tunable surface roughness by using different size of silica colloidal particles while the macropore morphology (i.e. pore wall thickness, pore wall length) can be tune by a continuous control over the foam's liquid fraction and the gas bubble size during the mineralization process. Moreover open or closed pore structure can be reached upon the foam's liquid fraction and the colloidal particle size involved during the foaming process. This work[3] extends the recently reported study[4] on the preparation of SiO₂ foam using molecular precursor. Herein, mimicking natural microstructure of super-hydrophobic leaves, the use of colloidal particle allows shaping the surface roughness leading thus to amplified the surface hydrophobic character. Furthermore, predominantly closed cell materials are needed for thermal insulation and open interconnected materials are required for uses involving fluid or gas transport such as filters and catalysts. 1- F. Carn, A. Colin, M.-F. Achard, H. Deleuze, E. Sellier, M. Birot, R. Backov, J. Mater. Chem., 2004, 14, 1370. 2- F. Carn, A. Colin, M.-F. Achard, H. Deleuze, C. Sanchez, R. Backov, Adv. Mater., 2005, 17, 62. 3- F. Carn, P. Massé, S. Ravaine, H. Deleuze and R. Backov, Langmuir (submitted). 4- F. Carn, A. Colin, M.-F. Achard, H. Deleuze, R. Backov, Adv. Mater., 2004, 6, 140.

4:30 PM DD11.11

Tailoring "Internal" Microstructure of Functional Inorganic Nanopatterns. Suresh Kumar Donthu^{1,2}, Zixiao Pan^{1,2} and Vinayak P David^{1,2}; ¹Materials Science and Engineering, Northwestern University, Evanston, Illinois; ²International Institute for Nanotechnology, Evanston, Illinois.

Dimensionally constrained material systems are at the forefront of current materials research because of their novel and often enhanced physical, chemical and biological properties. Remarkable progress has been made in recent years for synthesizing dimensionally constrained monolithic single crystalline structures such as nanorods and nanobelts. However, some recent reports^{1,2} suggest that "internal" microstructural inhomogeneities such as grain boundaries and porosity in such structures can further enhance their performance metrics such as gas sensitivity, for example. These results, coupled with the maxim that "microstructure is a material's DNA" underscore the need for novel approaches to enable tailoring of the "internal" microstructure of constrained nanopatterned systems and their characterization. We have recently developed an enabling nanopatterning technique termed as soft-electron beam lithography (soft-eBL)^{3,4} which utilizes liquid precursors (e.g., sol) as the material source for patterning variety of materials and composites with dimensional control down to 30 nm. Among several advantages, soft-eBL is capable of patterning structures on almost any substrate - single crystals, fragile ultra-thin membranes and insulators. We have exploited these unique attributes of soft-eBL to fabricate nanopatterns of simple and complex functional oxides with well-defined "internal" microstructure. For example,

diameter of cobalt ferrite and barium titanate discs on strontium ruthenate substrate can be tuned to control the number of grains per patterned disc - even down to converting each disc into its single crystal form⁵. As another example, we show that by controlling the width of ZnO nanopatterned lines on an amorphous substrate, it is possible to define the number of grains per unit line length, such as a beaded (or a bamboo) structure where a single grain spans the entire line width⁶. The presentation will highlight these unique attributes of soft-eBL and demonstrate its efficacy for true "internal" microstructural engineering of constrained nanopatterned systems. * E-mail: v-dravid@northwestern.edu References: 1. Wang et.al, J. Am. Chem. Soc., 2003, 125, 16176 2. Jiang et.al, J. Mater. Chem., 2004, 14, 695 3. Donthu et.al, Nano Lett., 2005, 5(9), 1710 4. Z. Pan et.al, Small, 2006, 2, 274. 5. Z. Pan et.al, Nano Lett., 2006, 6, 2344 6. Donthu et.al, Adv Mater, Accepted Aug 2006

4:45 PM DD11.12

MOCVD Behaviors of Two-sized InGaAs Ordered Nano-bar Arrays Grown Selectively on a GaAs Substrate. Benzhong Wang and Soo-Jin Chua; Opto-and Electronic Systems Cluster, Institute of Materials Research and Engineering, Singapore, Singapore.

Nanosphere lithography was used to form a nanoscaled SiO₂ template on a GaAs substrate. Especially, a simple method for fabricating nanopatterns with multi feature sizes within one step has been invented. These nanopatterns, as a template, can be used to grow selectively ordered nanostructures arrays such as quantum dots, quantum bars with different feature sizes in one step. Two sized InGaAs nano-bar arrays have been successfully grown on a GaAs substrate by MOCVD. In this report, we described the technique for fabricating multi-sized nanopatterns. MOCVD behaviors of InGaAs nano-bars onto such patterns were also discussed. Nanoscaled semiconductor structures with highly ordered arrangement are currently in high demand for variety of applications including low-dimensional structures such as quantum dots, quantum bars and quantum wires. Besides this, 2D photonic crystals (2DPCs) are also desired due to its possibility in manipulating photons. However, how to fabricate 2DPCs with quantum structures in economic ways is still a big challenge. In this paper, we present a simple, inexpensive and high throughput technique for fabricating nano-hole arrays with multi-feature sizes within SiO₂ film deposited on a GaAs substrate. These patterns have been used to grow semiconductor nanostructures by MOCVD. Two sized arrays of InGaAs nano-bars have been successfully grown on the GaAs substrate in one step. The basic idea of this technique is: i), forming areas with different thicknesses within the SiO₂ film by normal photolithography; ii) self-assembling close-packaged bilayers of polystyrene (PS) spheres on the patterned SiO₂ film; dry etching the SiO₂ through the interspaces between the PS spheres until the etching of the SiO₂ in the thickest areas down to the GaAs substrate. During the dry etching, we chose such etchants that not only etch the SiO₂, but also the PS material, resulting in tilted sidewalls of the SiO₂ openings. Therefore, the holes formed in the thinner SiO₂ areas are enlarged when the holes formed in the thicker SiO₂ areas just reach the substrate. Therefore, nanopatterns formed on the thicker areas of the SiO₂ have small features. The Features of the nanopatterns such as hole's diameter, periodicity and the ratio of the hole's diameters formed in different areas are easy to be controlled by using different sized PS spheres and thicknesses of the SiO₂ film. iii), after removing PS spheres, nanostructures of semiconductor can be deposited selectively. In this presentation, we describe structural features and the optical properties of two sized arrays of InGaAs nano-bars grown on a GaAs substrate by MOCVD. In this presentation, we also discuss selective growth behaviors of semiconductors when the growth area down to nano-scale.

SESSION DD12: Poster Session: Synthesis and Characterization I

Chairs: Sanat Kumar, Masaru Kuno, Xiao-Min Lin, Ruth Pachter and Moonsub Shim

Wednesday Evening, April 11, 2007

8:00 PM

Salon Level (Marriott)

DD12.1

Imaging and Nanopatterning in Liquids: in situ Studies of Electron Beam Induced Catalytic Deposition of Ag on TiO₂ Nanowires from Aqueous Solutions Natalia Kolmakova¹, John Bozzola² and Andrei Kolmakov¹; ¹Physics, SIUC, Carbondale, Illinois; ²IMAGE Center, SIUC, Carbondale, Illinois.

The combination of nm-scale resolution capacity of Scanning Electron Microscopy and innovative QuantomiX WETSEM technique is demonstrated to be a practical solution for immediate in situ real time high-resolution imaging of chemical processes taking place on the surfaces of nanostructures in liquids or high pressure conditions. In our report, electron beam induced catalytic reaction of metal deposition out of aqueous solution was studied on the surface of fully hydrated TiO₂ nanowires. This approach has excellent perspectives for not only in situ imaging and in vivo prompt analysis of the nano- and meso- objects in chemistry, physics and bioscience but also for nanofabrication and rational functionalization of nanostructures in liquids and different gas environment.

DD12.2

Polarization Photo-sensitivity of Randomly Oriented CdSe and CdTe Nanowires. Vladimir Protasenko¹, Gabor Galantai¹, Huili(Grace) Xing², Debdeep Jena² and Masaru Kuno¹; ¹Chemistry and Biochemistry, University of Notre Dame, Notre Dame, Indiana; ²Electronic Engineering, University of Notre Dame, Notre Dame, Indiana.

One dimensional (1D) semiconductor nanowires (NWs) poses features potentially attractive for polarization sensitive devices. Namely, the 1D nature of NWs enables band transport of photo-generated carriers along their lengths minimizing cross-wire charge hopping. An interesting prediction is the presence of "polarization memory" in randomly oriented NW arrays. In this model the orientation of metal contacts formed on the top of NW layer actually determines the polarization sensitivity of the photocurrent; the maximum current is detected when the light polarization is normal to the electrodes. When charges are photo-generated at distances from electrodes comparable with NW length the photocurrent polarization anisotropy deteriorates due to carriers hopping between differently oriented NWs. We explored this model by measuring the photocurrent anisotropy for randomly oriented CdSe and CdTe NWs optically excited by linearly polarized light. These NWs have average diameters ranging from 5-15 nm with ~6% corresponding intrawire diameter variations. In addition, they are often more than 1-10 µm long, and TEM micrographs show that the wires are highly crystalline. When the NWs are excited by linearly polarized light at distances less than a few microns from the Au electrodes the photo-generated current depends strongly on the polarization orientation of the incident light. The current polarization anisotropy measured near the electrodes reaches 10-20% dropping to 3-4% at 10-20 µm away from metal contacts. Smaller anisotropy numbers at larger distances suggest the involvement of hopping events for carriers traveling from excitation spot to the metal electrodes. When the NWs are dielectrophoretically aligned between electrodes the anisotropy rises to 30-35% near contacts and drops ~2 times at the middle of ~50 µm wide gap. Therefore for aligned NWs the direct carrier transport is favorable. Our measurements provide clear evidence that even randomly oriented NW arrays can serve as polarization sensitive devices. The highest anisotropy of the photocurrent is achieved when the distance between metal contacts is comparable with the NW

length. We believe that our findings can significantly reduce production cost of light polarization sensors because of extreme detector simplicity.

DD12.3

One-dimensional Necklace of Metal Nanoparticles that Exhibits Coulomb Blockade at Room Temperature. Jennifer Kane, Vivek Maheshwari and Ravi Saraf; University of Nebraska-Lincoln, Lincoln, Nebraska.

One-dimensional (1D) nanostructures are attractive materials for fabricating electronic devices because the structure serves both as a device and circuit element to integrate external power source and extract the signal. Carbon nanotubes and Si wires have been shown as functional 1D nanomaterials that work as electronic devices and provide circuitry. Basic logic circuits, a neural cell network device, and a variety of chemical and biochemical sensors have been developed using nanotubes and nanowires. Necklace of nanoparticles is another highly versatile avenue to build 1D nanostructures where both the chemistry of the nanoparticle and particle diameter can be tailored. To date, necklace of nanoparticles have been self-assembled using isolated DNA chains, peptide nanofibrils, microorganisms, block copolymers, and polyelectrolyte films as scaffolds. However, the electrical conductivity of these structures has not been demonstrated. Here we present an approach to self-assemble a necklace of Au nanoparticles onto a chain of (flexible) polymer wherein the particles are then cemented with an inorganic material. The electrical properties of the cemented necklace show a coulomb blockade at room temperature. Interestingly, the blockade is over 1 V compared to 50 mV for a single particle. Furthermore, the blockade voltage blue-shifts as temperature decreases. We will present the fabrication process and explain the observations in terms of a simple model.

DD12.4

Size-dependent Quantum Efficiency and Radiative Lifetime of Si Nanocrystals Embedded in SiN_x Films. Jae-Heon Shin¹, Chul Huh¹, Kyung-Hyun Kim¹, Jongcheol Hong¹, Gun Yong Sung¹, Yong-Hwan Kim², Yong-Hoon Cho² and Joong-Kon Son³; ¹IT-Convergence Technology Research Div., Electronics and Telecommunications Research Institute, Daejeon, South Korea; ²Department of Physics, Chungbuk National University, Cheongju, South Korea; ³Photonics Program Team, Samsung Advanced Institute of Technology, Suwon, South Korea.

We have measured the photoluminescence (PL) decay times and the light-emission quantum efficiencies of several-sized nanocrystal silicon (nc-Si) quantum dots (QDs) embedded in SiN_x films in-situ grown by plasma enhanced chemical vapor deposition. The measured PL decay times of 4.1-, 3.0-, and 2.7-nm-sized nc-Si QDs are about 0.24, 1.1, and 2.8 ns, respectively. These ultra-fast decay times show strikingly different characteristic comparing with Si nanocrystals in SiO_2 matrix, of which the decay times are of the order of 1 ~ 100 μs . For more exact discussions, we determined pure radiative lifetimes (τ_r 's) of the three samples with the help of internal quantum efficiency data since τ_r equals to the PL decay time divided by the internal quantum efficiency. The determined τ_r of 4.1-, 3.0-, and 2.7-nm nc-Si QDs in SiN_x matrix are about 0.56, 0.37, and 0.20 μs , respectively. Still fast and nearly size-independent characteristic of the radiative recombination rate do not agree well with quantum confinement effect.

DD12.5

Abstract Withdrawn

DD12.6

Deformation of Top-Down and Bottom-Up Metallic Nanowires. Austin Miles Leach¹, Matt McDowell¹ and Ken Gall^{1,2}; ¹Materials Science and Engineering, Georgia Institute of Technology, Atlanta, Georgia; ²George Woodruff School of Mechanical Engineering, Georgia Institute of Technology, Atlanta, Georgia.

In terms of fabrication, nanowires may be separated into two genres, top-down and bottom-up. Top-down implies the extraction of nanowires from a bulk material in a material removal approach, while bottom-up classifies nanowires that have been grown through chemical or molecular assembly. The fabrication methods differ in the crystallographic pathway traversed en route to a minimum energy, equilibrium structure. In general, the equilibrium structure of a metallic nanowire is characterized by two crystallographic features: the lattice orientation along the nanowire length and the orientation of the free surfaces. In both fabrication genres, for nanowires of face-centered-cubic structure, the most energetically favorable axial orientation lies along the $\langle 110 \rangle$ direction. The difference in top-down and bottom-up fabrication is realized in the internal structure and orientation of the nanowire free surfaces. For example, chemical growth of silver nanowires commonly results in five-fold twinned, pentagonal nanowires with $\{100\}$ surfaces; where as electron-beam irradiation of thin films (a top-down approach) may result in nanowires with a rhombic cross-section formed by four $\{111\}$ surfaces or a truncated-rhombic cross-section arising from a combination of $\{100\}$ and $\{111\}$ surfaces. As the dimensions of a material are reduced to the nanometer scale, the dependence of material properties on material structure is greatly enhanced. In this work, we relate the physical structure of experimentally observed, inherently stable top-down and bottom-up silver nanowires to mechanical properties. Using atomistic simulations, we probe the tensile deformation behavior of rhombic and truncated-rhombic nanowires, representative of top-down fabrication and five-fold twinned, pentagonal nanowires representing bottom-up fabrication. Our results demonstrate that the mechanical properties and operant deformation mechanisms in metallic nanowires are strongly dependent on the cross-sectional geometry and internal structure of the nanowires. We also investigate the size dependence of the mechanical properties of the nanowires ranging from 1-25 nanometers in diameter, a phenomenon that is readily explained by the differences in physical structure of the top-down and bottom-up nanowires. This work has application not only for the design of future nanometer scale devices, but also provides a fundamental understanding of the effects of physical structure on the mechanical behavior of nanometer scale materials.

DD12.7

Optical Properties of III-metal Nanoparticles/semiconductor Systems. Pae C Wu¹, Maria Losurdo^{1,2}, Tong-Ho Kim¹, Giovanni Bruno² and April S. Brown¹; ¹Electrical and Computer Engineering, Duke University, Durham, North Carolina; ²Institute of Inorganic Methodologies and of Plasmas - CNR and INSTM, Bari, Italy.

Coupling of surface plasmon resonant (SPR) metal nanoparticles with semiconductor materials, both inorganic and organic, is of great interest for photonic device enhancement, biosensing, and chemical sensing. Characterization of the SPR response of metal nanoparticles coupled with either

semiconductor/active regions or organic layers can be used to understand the system-level optical properties of these complex, hybrid structures. Currently, Au nanoparticles are ubiquitous for biosensing plasmonic technologies because of their chemical stability and IR-vis resonance range. Herein, we report on low-dimensional systems based on III-group metal nanoparticles coupled with semiconductors, which can be used for vis-UV applications. Using the particle plasmon resonance as an internal parameter from which we can discern the behavior of the entire complex system, we are able to characterize the optical behavior of metal nanoparticles coupled with semiconductor substrates and capped with both inorganic and organic materials. We discuss and present data on tuning the optical response of Ga and In nanoparticles deposited on semiconductors including Si, GaN, 4H-SiC (Si- and C-face) and ZnO by molecular beam epitaxy (MBE). The nanoparticles were deposited at room temperature to prevent interfacial reactions and intermixing. Real-time monitoring of the pseudodielectric function (ϵ) using in situ real-time spectroscopic ellipsometry (UVISEL-Jobin Yvon) in the extended 1.5-6.5eV photon energy range enables observation of the kinetic evolution of the surface plasmon resonance of the nanoparticle/semiconductor system during deposition. We show correlation between particle geometry and the splitting of the surface plasmon resonance between longitudinal (low energy) and transverse (high energy) modes, which results from the anisotropic dielectric environment induced by the semiconductor and spherical asymmetry of the nanoparticles. We also describe how the optical response of nanoparticles/semiconductor systems also depends on the polarity of the substrate - (Si- vs C-polar SiC, Ga-polar vs N-polar GaN and Zn- vs O-polar ZnO). As an example, deposition of both Ga and In nanoparticles onto both Si- and C-face 4H SiC substrates revealed a strongly damped transverse mode on the Si-face substrate compared to the C-face suggesting the polarization of the Si-face substrates attenuates the collective oscillations of the free electron density within the Ga and In nanoparticles. Additionally, a layer of a-Si:H or organic semiconductors of the PPV family has been deposited on top of nanoparticles to realize inorganic semiconductor-nanoparticles-organic/inorganic semiconductor hybrid structures for photovoltaics. The a-Si:H layer has been deposited by PECVD; the organic PPV-derivate films have been deposited by spin-coating. The modification of the optical response of these hybrid systems as a function of the top layer and of the PPV-polymer is discussed.

DD12.8

Enhanced Optical Properties of Au/ZnO core/shell Nanocrystals. Myung-Ki Lee and Yun-Mo Sung; Materials Sci. & Eng., Korea University, Seoul, South Korea.

In this study spherical-shape Au@ZnO core/shell nanocrystals were synthesized using a two-step solution phase method. The diameter of the Au core was ~3 to 5 nm and the thickness of the ZnO shell was ~0.5 to 3 nm. Special care was taken to precisely control the thickness of the ZnO shell varying the concentration of the precursor and surfactant in solution. Their nanostructures were identified using X-ray diffraction (XRD), high-resolution transmission electron microscopy (HRTEM), and selected area electron diffraction (SAED). Also, their optical properties were measured by UV-visible absorption and photoluminescence (PL) spectroscopy techniques. The Au@ZnO core/shell nanocrystals showed enhanced PL emission intensity compared to ZnO nanocrystals without Au core, most probably due to the transfer of a number of free electrons from the Au core to the ZnO Shell, caused by surface plasmon resonance (SPR) phenomena. Also, they showed strong PL emission dependence on the ZnO shell thickness. As the thickness of the ZnO shell increases, the intensity of the PL peaks become strong, indicating the increase in the crystallinity of the ZnO crystals. The red-shift in the PL peaks was observed with the increase of the ZnO shell thickness due to the quantum confinement effect of the shell. XRD and SAED patterns showed the nature of the ZnO shell was cubic up to its thickness of ~1 nm, and beyond this value it became wurtzite. The crystalline structural change in the ZnO shell did not affect the energy band gap of the core/shell nanocrystals.

DD12.9

Multi-Phase Titania Nanoparticles for High-Performance Photocatalyst Yun-Mo Sung and Jun-Su Park; Materials Sci. & Eng., Korea University, Seoul, South Korea.

Ti nanoparticles were synthesized by the inert gas condensation (IGC) method under a helium convection gas atmosphere. X-ray diffraction (XRD) and high resolution transmission electron microscopy (HRTEM) analysis results show that the nanoparticles (sample 1) accumulated on a liquid-nitrogen cooled cold finger were partially crystalline Ti, while those (sample 2) accumulated on a room-temperature cold finger were almost completely amorphous. Differential scanning calorimetry (DSC) scan curves show the crystallization exothermic peak temperatures of 444 and 448 °C for the samples 1 and 2, respectively. The sample 1 heat treated at 400 °C for 2 h (sample 1-H) shows formation of anatase (~80 vol %) and rutile (~20 vol %) as major phases with trace of metallic Ti phase, while the sample 2 heat treated (sample 2-H) shows formation of anatase with strong non-crystallinity. The pre-existing crystalline Ti phase in the sample 1 plays a critical role in determining the phase formation behavior of the nanoparticles during heat treatments. Thanks to the high anatase crystallinity, the sample 1-H shows higher photocatalytic properties than the sample 2-H, also probably due to the surface plasmon resonance of Ti phase as well as its fine particle size, the former could show even better photodecomposition efficiency than Degusa P-25®.

DD12.10

Characterization and Preparation of the ITO Target which Make use of Various Sizes of Tin Oxide. Ji-Hoon Rhee, Myung Geun Song, Pil-Sang Yun, Kyung Koo Jeong, Yun Ju Cho and Ju Ok Park; Nano Materials Lab, Samsung Corning, Suwon, South Korea.

Precipitation is a normal method for the preparation of tin dioxide due to lower cost and easier control than other methods. However, it is difficult to control particle size and distribution which significantly affect the electrical properties of ITO target. In this study, temperature which can be considered as one of factors to control particle size and distribution was tried to be controlled in two steps. The sintered density of the ITO target and particle size and distribution of tin dioxide were characterized by the Brunauer-Emmett-Teller (BET) and Scanning Electron Microscope (SEM) and Thermal Gravimetry Analysis (TGA) and Differential Scanning Calorimetry (DSC). The particle size of complete powders in aqueous solution was also measured by scattering method (Horiba LA-910). The electrical properties of the prepared ITO target were monitored in terms of particle size and distribution of tin dioxide. In this study, a structure and density of the prepared ITO target strongly depend on particle size as well as particle size distribution of tin dioxide. Additionally, the electrical properties showed the correlation with the sintered density of the ITO target. These results indicated that the lower particle size and distribution of tin dioxide in the ITO target, the better electrical properties of the ITO target such as sintered density and electric conductivity.

DD12.11

Photoreflectance Spectroscopy in InAs/GaAs Heterostructures Jun Oh Kim^{1,2}, Sang Jun Lee², Sam Kyu Noh², Kyu-Seok Lee³ and Jung Woo Choe¹; ¹Physics and Applied Physics, Kyung Hee University, Yongin, South Korea; ²Quantum Dot Technology Laboratory, Korea Research Institute of Standards and Science, Daejeon, South Korea; ³Electronics and Telecommunication Research Institute, Daejeon, South Korea.

Photoreflectance (PR) spectroscopy has been widely used for the characterization of semiconductors. Due to its derivative nature, the PR technique is a powerful tool to investigate the band structure of semiconductor heterostructures. Here, we report on room-temperature PR spectra of InAs quantum dots (QD)/GaAs and InAs WL/GaAs heterostructure grown on semi-insulating (SI)-GaAs substrates by using molecular beam epitaxy (MBE). Showing a major GaAs bandgap feature, the both structures reveal distinctive PR signatures associated with the confined subbands of WL with and without QDs at the energy region below the GaAs bandgap. For InAs quantum dots (QD)/GaAs samples, an oscillatory feature is also observed in the energy range below the bandgap of GaAs, which is due to the interference effect of reflected light beams, one reflected from the interface of GaAs/SI-GaAs substrate and the other reflected from the InAs-QD/GaAs heterointerface. A non-zero offset value of the PR interference indicates that the refractive index of the GaAs epilayer containing InAs QDs is modulated by a modulation laser light. On the other hand, InAs WL/GaAs heterostructures grown on SI-GaAs substrates do not show such oscillations, whereas Franz-Keldysh oscillations (FKO) are observed in the energy region above the GaAs bandgap, indicating that the GaAs cap grown on the InAs WL is subjected to a built-in electric field.

DD12.12

Fabrication and Optical Properties of Nanocrystalline ZnO Composite Films on Si Substrates. Young-Hwan Kim¹, Woon-Jo Cho², Seong-Il Kim¹ and Yong Tae Kim¹; ¹Semiconductor Materials and Devices Laboratory, Korea Institute of Science and Technology, Seoul, South Korea; ²Nano Device Research Center, Korea Institute of Science and Technology, Seoul, South Korea.

Optoelectronic materials compatible with silicon substrates are important from the viewpoint of practical applications for silicon photonics. In this work, we have fabricated nanocrystalline ZnO composite films on Si(100) substrates and these films showed a strong cathodoluminescent property. The nanocrystalline ZnO composite film was fabricated by rf sputtering of ZnO and Si targets simultaneously and rapid thermal annealing process. The composition of the film and post-annealing temperature were found to be crucial to fabricate the nanocrystalline ZnO composite films. The film composition was controlled by changing the area ratio of Si and ZnO targets and the as-deposited films were post-annealed at the temperatures of 400–1000 °C for 3 minutes in a nitrogen atmosphere. The high-resolution TEM analysis showed that the nanocrystalline ZnO composite film could be obtained by annealing the film with Zn/Si ratio=1.6 at 700 °C. This film contains nanocrystals with a size of ~5 nm, which could be identified as ZnO from electron diffraction pattern. The nanocrystalline ZnO composite film exhibited a strong and broad cathodoluminescence (CL) peak around 395 nm with a FWHM of ~180 nm. However, the film with Zn/Si ratio greater than the optimized value was found to have a ZnO film structure with many structural defects and exhibited the similar optical properties to those of ZnO film. The formation of ZnO nanocrystals in our composite film was confirmed by using energy dispersive x-ray spectroscopy and electron energy loss spectroscopy. The origin of the strong and broad CL peak around ~395 nm from the nanocrystalline ZnO composite film, leading to a possible application to a UV lighting source, will be discussed analytically. This work is supported by the Korea Institute of Science and Technology under Contract No. 2E19520.

DD12.13

Electrical Characteristics of HgTe Nanocrystal-based Thin-film Transistors Fabricated on Flexible Plastic Substrates. Jaewon Jang, Dong-Won Kim, Kyoungah Cho and Sangsig Kim; Korea University, Seoul, South Korea.

Transparent and flexible thin film transistors (TFTs) with channel layers composed of sintered HgTe nanocrystals were fabricated on poly-ether-sulphone (PES) substrates. In order to overcome the restriction of adhesion between HgTe nanocrystals and PES substrates, UV/ozone treatment was employed to the surface of PES substrates. HgTe nanocrystals were spin-coated on UV/ozone-treated PES substrates. The TFTs fabricated in this work after sintering the nanocrystals at 150 degree celsius exhibit p-channel ones. When the substrate is flat, a representative TFT reveals an on/off current ratio of 164, a gate threshold voltage (VT) of 0 V, and a field-effect mobility of 1.6 cm²/Vs. And, when the substrate is bent until the bending radius of the substrate reaches 0.5 cm which corresponds to a strain of 2.0% the HgTe thin film experiences, the TFT exhibits an on/off current ratio of 266, a VT of 0 V, and a field-effect mobility of 1.0 cm²/Vs. The fabricated TFTs on the UV/ozone-treated PES substrates have a higher mobility than organic p-channel TFTs investigated previously in other research groups.

DD12.14

Boundaries Between MgO Smoke Particles. Julia Deneen Nowak and C. Barry Carter; Chemical Engineering and Materials Science, University of Minnesota, Minneapolis, Minnesota.

Highly oriented nanoparticles are particularly suitable for study in the transmission electron microscope (TEM) because the surface facets can provide a certain a priori knowledge about the particles. Magnesium oxide (MgO) nanocubes are also suited for such a study because of the ease with which they can be produced and their crystal structure is well understood. When Mg metal is burned in air the reaction $2\text{Mg} + \text{O}_2 \rightarrow 2\text{MgO}$ produces a 'smoke' which consists of small particles of MgO. The particles produced are typically perfect cubes with edge lengths on the order of a few tens of nanometers and exhibit almost exclusively (100) faces. The smoke can be collected directly on an amorphous support film for investigation in the TEM. MgO is an ionically bonded crystal with the rocksalt structure. It has previously been found that special boundaries form when two cube particles come into contact. If the mis-orientation between two crystals takes a particular value, a special low-energy configuration can occur; special high-angle twist boundaries in MgO, first investigated in the early 1970s, are predicted by the coincidence site lattice (CSL) model. The CSL model, used to describe the unique angles of misorientation between the two crystals, predicts four low-energy twist boundaries in MgO: $\Sigma 5$, $\Sigma 13$, $\Sigma 17$, and $\Sigma 25$ though these are not all equally likely in practice. These pairs of bonded MgO cubes are particularly instructive for investigating CSL boundaries because the angle of misorientation between two particles can be measured directly in the TEM if the particles are oriented properly with respect to the electron beam. In addition to twist boundaries, MgO smoke particles also make contact along the cube edges and at the cube corners. The ionic nature of the MgO produces a local charge at the corners and edges of MgO smoke cubes where the coordination is different than that of the bulk. This study uses the TEM to examine the various types of boundaries between nanocubes of MgO and investigates the role of coordination in these unique contacts.

DD12.15

Structural and Magnetic Characteristics of Self-Assembled Nickel Nanoparticles in CeO₂ Thin Films Adero Paige¹, Jeremiah Abiade¹, Dhananjay Kumar¹ and A. K. Majumdar²; ¹North Carolina A&T State University, Greensboro, North Carolina; ²S.N. Bose National Centre for Basic Sciences, Kolkata, India.

Nanomagnetism has many applications in current technology, such as magnetic recording. The study of the characteristics of nanoparticles is extremely important, because particle size and shape determine magnetic properties such as coercivity and blocking temperature. In this experiment, pulsed laser deposition (PLD) was used to produce composite materials composed of nickel (Ni) nanoparticles and cerium oxide (CeO₂) thin films. The CeO₂-Ni composites were deposited onto silicon (100) and sapphire (c-plane) substrates. Magnetic measurements were performed using the vibrating sample magnetometry (VSM) option of a physical properties measurement system (PPMS). The results show samples made on silicon substrates have a higher blocking temperature (TB), but lower coercivity values than the samples deposited onto sapphire. X-Ray diffraction and transmission electron microscopy were used to obtain structural characteristics of the samples. The nickel particle size was determined to be ~ 18-20 nm for samples deposited on both substrates. In this talk, we will discuss the effect of nanoparticle size, shape, and crystallographic texturing on the resulting magnetic properties of self-assembled magnetic nanoparticles in a CeO₂ thin film matrix.

DD12.16

In situ Synchrotron Absorption Experiments and Modelling of the Growth Rates of Electrochemically Deposited ZnO Nanostructures.

Bridget Ingham^{1,2}, Benoit Illy³, Jade Mackay⁴, Stephen White¹, Shaun Hendy^{1,5} and Mary Ryan³; ¹Industrial Research Limited, Lower Hutt, New Zealand; ²SSRL, Stanford Linear Accelerator Center, Palo Alto, California; ³Department of Materials, Imperial College, London, United Kingdom; ⁴School of Chemical and Physical Sciences, Victoria University of Wellington, Wellington, New Zealand; ⁵MacDiarmid Institute for Advanced Materials and Nanotechnology, Wellington, New Zealand.

ZnO is known to produce a wide variety of nanostructures that have enormous scope for optoelectronic applications. Using an aqueous electrochemical deposition technique, we are able to tightly control a wide range of deposition parameters (Zn²⁺ concentration, temperature, potential, time) and hence the resultant deposit morphology. By simultaneously conducting synchrotron x-ray absorption spectroscopy (XAS) experiments during the deposition, we are able to directly monitor the growth rates of the nanostructures, as well as providing direct chemical speciation of the films. In situ experiments such as these are critical to understanding the nucleation and growth processes of such nanostructures. We present recent results from in situ XAS synchrotron experiments demonstrating the growth rates as a function of potential and Zn²⁺ concentration. These are compared with the electrochemical current density recorded during the deposition, and the final morphology revealed through ex situ high resolution electron microscopy. The results are indicative of two distinct growth regimes, and simultaneous changes in the morphology are observed. These experiments are complemented by modelling the growth of the rods in the transport-limited case, using the Nernst-Planck equations in 2 dimensions, to yield the growth rate of the volume, length, and radius as a function of time.

DD12.17

Fabrication and Applications of Se-coated CdSe Nanowires Prepared by Chemical Treatments and Molecular Surface Engineering. Ngai Sze Lam, Ka Wai Wong and Quan Li; Physics, The Chinese University of Hong Kong, Hong Kong, China.

Hybrid systems of II-VI semiconductor (e.g. CdSe, ZnSe) nanostructures and organic/biological materials have been proved to be pivotal in various nanomaterial-based electronics, optoelectronics, biosensors, and microelectromechanical systems due to their extraordinary quantum-sized effects and synergistic coupling effects arising from the inorganic, organic and/or biological partners. Many novel researches have shown that different types of these hybrid systems can enhance the conversion efficiency of solar cells and photovoltaic cells, allow more efficient charge separation, electron transport and optical absorption, and modulate the photoluminescence that was found to be extremely useful and applicable in biosensing technologies. In particular, one dimensional (1D) semiconducting nanostructures such as nanowires and nanotubes should possess more unique and superior properties than the spherical nanocrystals because of their uni-directional channels for charge transport. The success of fabricating hybrid systems based on 1D semiconducting nanostructures is hinged on the subtle molecular surface engineering of the 1D nanostructures in a controllable manner, that allows for delicate tuning of properties (optical, electronic and electrical) and effective subsequent manipulation and assembly of these 1D nanostructures for the formation or manufacture of more sophisticated hybrid nanodevices and nanosystems. In the present study, molecular surface engineering was performed on CdSe nanowires (NWs) made from thermal deposition. It was found that through delicate control of acid treatments, ultra-thin Se coating (<30 Å) can be formed around the CdSe NWs as revealed by XPS and SIMS. This Se coating acts several important roles for different purposes. First, it provides a viable surface for effective anchorage of organic and biological compounds upon subsequent chemical treatments. It was observed that the optical properties of the capped CdSe NWs can be tuned and adjusted by the surface functionality added. Second, it acts as a passivation layer protecting the integrity of inner CdSe NW core from oxidation and degradation, which are commonly observed for semiconducting nanocrystals. Lastly, the Se-coating serves as a sacrificial layer which can be thermally desorbed, leaving a fresh CdSe NW with thinner diameter. The above outcomes can potentially facilitate the fabrication of NW-based photovoltaic or biosensor hybrid systems with a better understanding in the surface composition and optical behavior of the surface engineered 1D CdSe NWs.

DD12.18

CNT Growth by Direct-Writing Wu Yu-Tsung and Tri-Rung Yew; National Tsing Hua University, Hsinchu, Taiwan.

This paper presents the formation of carbon nanotubes (CNTs) using KrF excimer pulse-laser direct-writing. This laser energy approach irradiates deposited amorphous carbon with Ni catalyst underneath for carbon nanotube (CNT) transformation from carbon species catalyzed by Ni. The effect of process parameters including pulse energy, frequency, and pulse duration on CNT formation will be investigated. The CNT formation mechanism will be also discussed. Scanning electron microscopy (SEM), transmission electron microscopy (TEM), and Raman spectrum will be utilized to characterize the physical properties of CNTs. The advantage of this direct-writing approach for CNT formation is its positioned growth for future potential interconnect and field effect transistor application.

DD12.19

Rational Synthesis of P-type Zinc Oxide Nanowire Arrays Bin Xiang¹, Pengwei Wang², Xingzheng Zhang², Shadi Dayeh¹, David Aplin¹, Cesare Soci¹, Dapeng Yu² and Deli Wang¹; ¹Department of Electrical and Computer Engineering, University of California, San Diego, La Jolla, California; ²Electron Microscopy Laboratory, School of Physics, Peking University, Beijing, China.

We report the synthesis of the high-quality p-type ZnO NWs using a simple chemical vapor deposition method, where phosphorus pentoxide has been used as the dopant source. Single crystal phosphorus doped ZnO NWs have growth axis along the <001> direction and form perfect vertical

arrays on a-sapphire. P-type doping was confirmed by photoluminescence measurements at various temperatures and by studying the electrical transport in single NWs field-effect transistors. Comparisons of the low temperature PL of unintentionally doped ZnO (n-type), as-grown phosphorus doped ZnO, and annealed phosphorus doped ZnO NWs show clear differences related to the presence of intra-gap donor and acceptor states. The electrical transport measurements of phosphorus doped NW FETs indicate a transition from n-type to p-type conduction upon annealing at high temperature, in good agreement with the PL results. The cross NW ZnO homojunction nano-LED and core-shell heterostructure device will be also discussed. The synthesis of p-type ZnO NWs enables novel complementary ZnO NW devices and opens up enormous opportunities for nanoscale electronics, spintronics, optoelectronics, and medicines.

DD12.20

Fabrication Of Piezoelectric Lead Zirconate Titanate Nanotubes By Spin Coating Of Sol-Gel Solution Using Porous Alumina Membranes. Sang Don Bu, Jongok Kim, Yong Chan Choi and Jin Kyu Han; Physics, Chonbuk National University, Jeonju, South Korea.

Piezoelectric nanotubes hold promise for applications in a variety of nanotechnological devices because these polycrystalline nanotubes can be strained when an electrical voltage is applied, and vice versa. Each tube could be triggered individually to release a small quantity of ink for ink-jet printing, or to deliver drugs into a patient. Sensor, actuator and data-storage applications are also possible. We report the fabrication of high aspect ratio (up to 400:1) piezoelectric $\text{Pb}(\text{Zr}_{0.52}\text{Ti}_{0.48})\text{O}_3$ (PZT) nanotubes by a spin-coating process of putting a sol-gel solution into a porous alumina membrane (PAM). PAMs with a pore diameter of about 50 nm were prepared in-house using a well-known two-step anodization procedure [1]. Sol-gel precursor solutions were also prepared in-house using a traditional sol-gel method in order to control the pH, mole concentration, viscosity, and composition of the sol-gel precursor solutions. PZT nanotubes were synthesized in PAM nanopores by a spin coating deposition technique described previously [2]. Briefly, a PAM was placed on a lab-made Teflon support, which was placed on a spin coater chuck, where the Teflon support was designed for the sol-gel precursor solution to flow well through the membrane pore. The precursor solution was dropped on the PAM using a micro pipette. It was then spin-coated at 1000 to 5000 revolutions-per-minute for 120 sec. High aspect ratio piezoelectric PZT nanotubes have been successfully fabricated. Field emission scanning electron microscopy (FESEM) images show that PZT nanotubes are well packed inside the pore of a PAM. Scanning transmission electron microscopy (STEM) analysis along with energy dispersive X-ray spectroscopy (EDS) mapping investigation of the nanotubes confirms the presence of lead, zirconium, and titanium. A field emission transmission electron microscopy (FETEM) image of a freestanding PZT nanotube shows that its outer diameter and length are estimated to be 50 nm and several microns, respectively. Further investigation reveals that PZT nanotubes have a wall thickness of 3 nm to 10 nm and consist of crystallites with a size in the order of 2-3 nm. The d-spacings for the rings in the electron diffraction pattern are 2.89 Å, 2.52 Å, 2.12 Å, 1.78 Å, 1.52 Å, and 1.39 Å. It suggests that our PZT nanotubes are a mixture of perovskite and pyrochlore phases. The majority of the tube is comprised of the perovskite PZT phase with a tetragonal structure [JCPDS 33-0784]. Our current concerns are the phase transformation from pyrochlore to perovskite and the electrical and electromechanical properties of a single PZT nanotube. [1] J. Kim, Y. C. Choi, K.-S. Chang, and S. D. Bu, *Nanotechnology* 17, 355 (2006). [2] Y. C. Choi, J. Kim, and S. D. Bu, *Mater. Sci. Eng. B* 133, 245 (2006).

DD12.21

Synthesis of Unit Oriented MWNTs on SiO₂ Particle. Junming Xu and Huibin Qin; College of electronic information, Hangzhou Dianzi University, Hangzhou, Zhejiang, China.

Random dispersed carbon nanotubes have been researched greatly, nanometer-size catalyst particles apart to each other on the support are always needed to act as catalyst, it always need a complex processing, such as sol-gel method. Otherwise, Aligned carbon nanotubes have also been researched greatly. It always need very thin metal film or catalyst islands acted as catalyst on substrate. The process is also complex and costing, such as PVD method. Local aligned carbon nanotubes that have the condition between random dispersed CNTs and whole aligned CNTs are not ever reported. Here a simple method are investigated to such unit oriented CNTs. Fe_2O_3 film was prepared on the surface of SiO_2 particle by mixing them with certain $\text{Fe}(\text{NO}_3)_3$ ethanol solution and baking. It was found that this metal oxide film can act well to synthesize carbon nanotubes by CVD method. The size and shape of SiO_2 particle affect the local structure of carbon nanotubes. If the SiO_2 particle is micron size and flake shape (named as M- SiO_2), unit oriented carbon nanotubes are synthesized, they grow perpendicularly to plane of every particle of SiO_2 . When replacing N- SiO_2 (nano-sized SiO_2) powder to M- SiO_2 as support, carbon nanotubes are randomly dispersed, but yield is increased. The carbon nanotubes were observed by TEM, the results shown they have bamboo-shape structure when NH_3 is in reaction gases. NH_3 is proved to have great influence to the CNTs growth. It can promote the crack of Fe_2O_3 , reduction of Fe_2O_3 and keeping catalyst higher activity for CNTs growth.

DD12.22

Controlled Synthesis of Single-Crystal Organic Nanowires of Cu-Phthalocyanine by Organic Vapor-Phase Deposition (OVPD) Method Kai Xiao¹, Jing Tao², Ilia Ivanov¹, Alex Puzetky¹, HoNyung Lee², Stephen Pennycook² and David Geohegan^{1,2}; ¹Center for Nanophase Materials Sciences, Oak Ridge National Laboratory, Oak Ridge, Tennessee; ²Materials Science and Technology Division, Oak Ridge National Laboratory, Oak Ridge, Tennessee.

Metal phthalocyanine is one of the promising organic compounds for possible applications in electrooptical devices, photoconducting agents, photovoltaic cell elements, nonlinear optics, electrocatalysis, and other optoelectronic devices. Several metal-substituted phthalocyanines have been widely investigated. Among the metal substituted phthalocyanines, copper (II) phthalocyanine (Cu-Pc) has attracted great attention for many years because of its combination of high thermal and chemical stability and outstanding optical and electronic properties. Hence Cu-Pc has been widely applied in gas sensors, xerography, optical disk, catalysis, electro-chromic display, organic solar cells, OLEDs, OFETs, and data storage devices. Cu-Pc is also expected to be a candidate material for optical detectors and non-linear optics with more tunable absorption band and lower cost than its inorganic counterparts. However, to date Cu-Pc has not been available in the form of well-controlled nanowires for new nanoscale applications which could take advantage of one-dimensionality to greatly enhance the performance of many currently existing devices. In this paper, the controlled synthesis of single-crystal organic nanowires of Cu-Pc by organic vapor-phase deposition are reported. The size, morphology and crystal structure of the Cu-Pc nanowires were principally determined by the substrate temperature. The transformation of the crystal structure of Cu-Pc nanowires with increasing substrate temperature from the alpha-phase of the orthorhombic crystal to the thermally stable beta-phase of the monoclinic crystal was studied by SEM, HRTEM, SAD, XRD and optical absorption spectroscopy. This well-controlled synthesis of Cu-Pc nanowires is very important for their application in electrical and optoelectronic devices, such as organic photovoltaic cells, organic light-emitting diodes, field-effect transistors, memories and gas sensors. This research was conducted at the Center for Nanophase Materials Sciences, which is sponsored at Oak Ridge National Laboratory by the Division of Scientific User Facilities, U.S. Department of Energy, managed by UT-Battelle, LLC, for the U.S. Department of Energy under contract DE-AC05-00OR22725.

DD12.23

Synthesis and Properties of Boron Nitride Nanotubes, Nanowires and Nanorods. Ying Chen, Hua Chen, Jun Yu, Yongjun Chen and Hongzhou Zhang; Department of Electronic Materials Engineering, The Australian National University, Canberra, Australian Capital Territory, Australia.

Quasi-one-dimensional boron nitride nanomaterials such as BN nanotubes, BN nanowires, BN nanorods, and BN whiskers have different nanostructures but uniform electronic band gaps independent of their diameters and chiralities. Their quantum confinement effects in these low-dimensional materials can enhance their optical emission substantially by inducing an indirect-to-direct conversion of the optical transition. Different nanostructures and dimensions have different emission behaviors. Therefore, one-dimensional BN nanomaterials are likely to find further applications in optoelectronics. We report an effective approach for controlled and patterned growth of the BN nanotubes [1, 2], BN nanowires [3, 4] and conical boron nitride nanorods [5, 6] as well as describe their optical, chemical, and thermal properties. Relationships between the different nanostructures and corresponding properties will be discussed. [1] J. Yu, Y. Chen, et al, Chemistry of Materials, 17 (2005) 5172. [2] H. Chen, Y. Chen, et al. Chemical Physics Letters 42(2006) 315. [3] YJ Chen, H. Zhang, Y. Chen, Nanotechnology, 17 (2006) 786. [4] YJ Chen, et al, Nanotechnology, 17 (2006) 2942 [5] H. Zhang, et al, Physical Review B, 74 (2006) 045407 [6] H. Zhang, et al, Applied Physics letters, 88 (2006) 093117.

DD12.24 TRANSFERRED TO DD3.11/EE2.11**DD12.25**

Synthesis and Transport Properties of Vapor-liquid-solid Grown Si_{1-x}Ge_x Nanowire. Sung Jin Whang¹, Sung Joo Lee¹, Wei Feng Yang¹, Hai Chen Zhu¹, Han Lu Gu¹, Byung Jin Cho¹ and Yun Fook Liew^{2,1}; ¹ECE, National University of Singapore, Singapore, Singapore; ²Data Storage Institute, Singapore, Singapore.

Semiconductor nanowires are emerging as a powerful building block for novel nanoscale device applications. There have been considerable studies on the synthesis/characterization of Si, Ge and heterostructured nanowires and their applications for electronic, photonic and bio devices. Si_{1-x}Ge_x has potential advantages of higher carrier mobility and the possible band-gap engineering at different concentration of Ge. Unlike 2-dimensional Si_{1-x}Ge_x films, it is expected that single crystalline 1-dimensional Si_{1-x}Ge_x nanowire via vapor-liquid-solid (VLS) mechanism can avoid geometrical defects induced from lattice mismatch between bulk Si_{1-x}Ge_x and Si substrate, since Au-catalyzed Si_{1-x}Ge_x nanowire will be synthesized from Au-Si-Ge alloy, which is predicted from low eutectic temperature in ternary alloy phase diagram. In this work, we report a successful synthesis of single crystalline homogeneous ~26 nm Si_{1-x}Ge_x nanowires grown by VLS mechanism and its microstructures and performances of MOSFET were studied. SiH₄ and GeH₄ gases were simultaneously introduced into CVD reaction chamber to grow Si_{1-x}Ge_x nanowire and the partial pressure of GeH₄ was kept at 0.12 Torr for 10 min. A study on the effects of temperature on nanowire growth showed that single crystalline homogeneous ~26 nm Si_{1-x}Ge_x nanowires without amorphous sheath layer can be obtained at 430 degrees Celsius. HRTEM images and EDS analysis show that Si_{1-x}Ge_x nanowires have single crystal structure with growth direction of (111) and atomic percentage (~ 16.5%) of Ge concentration is uniform within nanowire. It is also found that the minimum temperature required to initiate the nanowire growth is ~ 400 degrees Celsius, significant reduction in density and length of nanowires are observed at lower temperatures. In contrast, growth temperatures higher than 450 degrees Celsius result in 8~10 nm amorphous outer layer surrounding Si_{1-x}Ge_x core layer, probably due to the uncatalyzed deposition of amorphous Ge at outer shell of nanowire. Higher concentration of Ge (31.97 at. %) and oxygen were detected at outer layer. Back gated MOSFET was fabricated by using ALD-grown 10 nm HfO₂ as a gate dielectric and TaN/Ta as a gate electrode on Si substrate. Pd was deposited on Si_{1-x}Ge_x nanowire to form source/drain. Undoped amorphous layer-free Si_{1-x}Ge_x nanowire transistor exhibits p-MOS operation with Ion/Ioff = 1E4 and sub-threshold swing of 120mV/dec.

DD12.26

General Route to Template-Directed Gas-Phase Fabrication of Oxide Nanotubes Changdeuck Bae¹, Bokyoung Ahn¹, Moonchul Kang¹, Jiyoung Kim², Myung M. Sung³ and Hyunjung Shin¹; ¹School of Advanced Materials Engineering, Kookmin University, Seoul, South Korea; ²Department of Electrical Engineering, University of Texas, Dallas, Texas; ³Department of Chemistry, Hanyang University, Seoul, South Korea.

We present a high-throughput, one-step procedure for fabricating oxide nanotubes. Our approach combines template-directed atomic layer deposition (ALD) [1] with a micro-contact printing technique, allowing precise control over the dimensions of the nanotubes as well as one-step fabrication of free-standing oxide nanotubes. Metal oxide nanotubes made from TiO₂, ZrO₂, and Al₂O₃ with high aspect ratios of up to ~300 have been fabricated. Notably, two different types of membranes are employed as templates, track-etched polycarbonate and anodic aluminum oxide (AAO). We discussed that the nanopore sizes in growing those ALD layers play central role between growth rate and surface stress. The surface chemistry of selective ALD onto the templates is also addressed. Furthermore, it is speculated that bundles of oxide nanotubes are formed by strong capillary forces generated and exerted during dissolution of the surrounding AAO template in the fabrication of the oxide nanotubes. Acknowledgement This work was supported by the Center for Nanostructured Materials Technology of the Korean Ministry of Science and Technology (M105K0010026-06K1501-02610). [1] H. Shin, D.-K. Jeong, J. Lee, M. M. Sung, J. Kim, Adv. Mater. 2004, 16, 1197.

DD12.27

Self-Assembled Fluorocarbon Template for Growth of Nano-Scale Platinum. Sang Hwui Lee, Zhengchun Liu, J. Jay McMahon and Jian-Qiang Lu; CIE, RPI, Troy, New York.

A self-assembled fluorocarbon template for platinum (Pt) nanostructure growth is demonstrated. This novel approach to realize metal nanostructures uses a fluorocarbon thin film made by reactive ion etching (RIE) of SiO₂ followed by platinum sputtering. Fluorocarbon residues are generally considered as undesirable materials during the RIE of silicon or SiO₂. However, under the conditions studied here, fluorocarbon nano-scale rings are spontaneously formed with typical dimensions as ~50nm of diameter, ~10nm wall thickness, and ~50nm high during the RIE of SiO₂ with trifluoromethane (CHF₃) and oxygen. These ring structures are used as a template for metal nanostructure growth. Pillar-like Pt nanostructures up to 100nm in height and 50nm in diameter are grown on the template simply by a sputterer of low-cost thin film coater in 3 minutes; with increasing sputtering time, Pt nanorod bundles are formed. The morphology and growth mechanism of fluorocarbon nano-rings and platinum nano-pillars will

be discussed in detail. This work provides a simple approach to metal nanostructure growth for applications, such as fuel-cell using Pt nanorods as catalyst.

DD12.28

Single-Crystalline Bismuth Telluride Nanowires Grown by a Stress-induced Method Jinhee Ham, Wooyoung Shim, Seunghyun Lee and Wooyoung Lee; Department of Materials Science and Engineering, Yonsei University, Seoul, South Korea.

High-efficient thermoelectricity requires materials with a large figure of merit, ZT , defined by $ZT = \sigma S^2 T / \kappa$, where σ is the electrical conductivity, S the thermoelectric power, and κ the thermal conductivity. However, due to the interdependence of σ , S , and κ , the optimization of thermoelectricity remains challenging. It is well known that there are two approaches to enhanced ZT value. One is to utilize quantum confinement effects of nanostructures, providing an opportunity to individually control σ and S , and thus to promote ZT [1] because of increase of the density of states (DOS). The other is to reduce κ without having an effect on σ and S by using semiconductors of high atomic weight such as bismuth telluride (Bi_2Te_3) with much lower atomic vibration frequencies [2]. In this work, we present a new method to grow high-quality, single-crystalline Bi_2Te_3 nanowires for use as a thermoelectric material with high ZT . $\text{Bi}_x\text{Te}_{1-x}$ ($x = 0.35 \sim 0.55$) thin films were grown on an oxidized Si substrate using a co-sputtering system with a Bi (99.999%) and a Te target (99.99%). For the growth of $\text{Bi}_x\text{Te}_{1-x}$ nanowires, the co-sputtered films were transferred to a furnace for heat treatment in the temperature range 300 - 450°C. Scanning electron microscopy (SEM) and high-resolution transmission electron microscopy (HRTEM) were employed for the structural characterizations of the nanowires. Interestingly, uniform and straight Bi_2Te_3 nanowires with high aspect ratios were found to grow on the surface of the co-sputtered films after heat treatment. The growth of the Bi_2Te_3 nanowires is attributable to the relaxation of stress, originating from a thermal expansion mismatch between the film and the substrate. This mismatch is due to the large difference in the coefficient of thermal expansion of $\text{Bi}_x\text{Te}_{1-x}$ ($\sim 19 \times 10^{-6}/^\circ\text{C}$), SiO_2 ($0.5 \times 10^{-6}/^\circ\text{C}$) and Si ($2.4 \times 10^{-6}/^\circ\text{C}$). Elemental mapping profiles show the uniform distribution of Bi and Te along the length of a nanowire with $d = 100$ nm without appreciable segregation. The composition of $\text{Bi}_x\text{Te}_{1-x}$ nanowires were found to be adjusted by tailoring the composition of co-sputtered films from $x = 0.35$ to 0.55. A HRTEM study reveals that the Bi_2Te_3 nanowire with $d = 100$ nm grown along the $\langle 110 \rangle$ direction is high-quality single crystalline. The diffraction pattern recorded perpendicular to the long axis of the nanowire can be indexed to the hexagonal lattice of Bi_2Te_3 ($a = 4.43\text{\AA}$, $c = 29.91\text{\AA}$) with $[001]$ zone axis. The Bi_2Te_3 nanowires were found to have diameters ranging from 50 nm to 500 nm depending on the thickness of the co-sputtered $\text{Bi}_x\text{Te}_{1-x}$ films, indicating that the diameter of Bi_2Te_3 nanowires is controllable. Our results demonstrate that single-crystalline Bi_2Te_3 nanowires can be grown by the stress-induced method, providing a motivation for exploring the high-efficiency thermoelectric properties of single-crystalline Bi_2Te_3 nanowires.

[1] Y. Lin et. al., Phys. Rev. B 62, 4610 (2000) [2] A. Majumdar, Science 303, 777 (2004)

DD12.29

Nitrogen Mediated Synthesis of Au/Carbon Nanotubes Weon Ho Shin, Seong Ho Yang and Jeung Ku Kang; MSE, KAIST, Daejeon, South Korea.

Recently, transition metal nanoparticles dispersed carbon nanotubes have been considered as promising materials for potential applications such as hydrogen storage media, sensing materials, catalysts, or electronic devices. These applications require deep understanding of the nature of metal particle-carbon nanotubes interaction to achieve hybrid materials for desirable properties. For bio-sensing materials and catalysts, gold metal have been widely used due to its excellent stability of chemical and physical attack. Here, we report the interaction between carbon nanotubes and gold particles through density functional calculations. Calculations reveal that there is no interaction between pristine carbon nanotube and a gold atom. In this context, we introduced nitrogen atoms as extrinsic defects, which can substitute carbon atoms with graphitic like or pyridine like structure, resulting high binding energy between Au atom and nanotube. To compare with these theoretical results, we dispersed gold nanoparticles on carbon nanotubes and nitrogen doped carbon nanotubes. Nitrogen atoms could increase reactivity of carbon nanotubes, resulting more uniform distribution than pure carbon nanotubes. These hybrid materials can enhance catalytic or bio-sensing properties.

DD12.30

Pinching of Alkoxide Jets - a Route for Preparing Nanometre Level Sharp Oxide Fibres. Tanel Tatt¹, Kristjan Saal¹, Ilmar Kink¹, Uno Maeorg², Runno Lohmus¹ and Ants Lohmus¹; ¹Lab. Of Low Temperatures, Institute of Physics, Tartu, Tatu, Estonia; ²Department of Organic Chemistry, Institute of Organic and Bioorganic Chemistry, Tartu, Estonia.

Pinching phenomenon is used to shape jets of $\text{Sn}(\text{OBu})_4$ based viscous oligomeric melts into nanometre level sharp oxide needles. Influence of viscosity of the liquid, humidity of surrounding environment, and pulling speed on formation of the needles is investigated. Optimal conditions enable reproducible preparation of needles that have tip radii down to 15-25 nm, i.e. in the range that is of considerable interest for many nanotechnological applications.

DD12.31

Electron-beam Induced Growth of Silica Nanowires and Silica/Carbon Heterostructures Francisco Sola, Oscar Resto, Azlin Biaggi-Labiosa and Luis F Fonseca; Physics, University of Puerto Rico, San Juan, Puerto Rico.

A novel synthesis of silica nanowires and silica/carbon heterostructures by electron beam irradiation on porous silicon films was investigated. The method allows us to monitor the growth process in real time at atomic scales. Depending on the electron dose we obtain nanowires with diameters in the range of 15-49 nm and lengths up to 500 nm. We found that the adequate electron dose was between 10^3 - 10^5 nm⁻² s⁻¹. Additional electron dose causes plastic and failure deformations in the silica nanowires. A growth model consistent with our findings is presented that involves the flow of mass from the substrate to the nanowire driven by the local electric fields. Heterostructures showing a nanopalm-like shape are obtained after exposing the silica nanowire to poor vacuum conditions in which carbon aggregation from the surrounding gas is promoted by the local electric fields enhanced at the tip of the silica wires.

DD12.32**Ex-situ Doping and Characterization of Silicon Nanowires.** Sarang Ingole¹, Pavan Aella¹, Teresa Clement¹, E. Akhadov² and S. T. Picraux^{2,1};¹School of Materials, Arizona State University, Tempe, Arizona; ²Center for Integrated Nanotechnologies, Los Alamos National Laboratory, Los Alamos, New Mexico.

We demonstrate the application of a solid state diffusion-based approach for electrical doping of vapor-liquid-solid (VLS) grown silicon nanowires. Electrical doping of silicon nanowires is essential for their application in nanoscale devices. In-situ doping during VLS growth has been shown by several groups as one technique for doping nanowires, however it has been observed that it can have undesired effects on morphology of nanowires thereby limiting application in some cases. Therefore it is technologically important to develop/investigate alternative techniques for electrical doping of nanowires. We have thus explored ex-situ approaches based on solid-state diffusion, a well established technique in current device manufacturing technology. In the present study we report proximity doping with a spin-on boron dopant source for electrical doping of VLS grown silicon nanowires. This is a two stage process where the first stage (pre-deposition) involves annealing the nanowire sample placed in proximity of a dopant source in the range 850-950°C. Here the spin-on dopant spun onto a sacrificial substrate acts as a controlled dopant source. During this stage boron from the dopant source is introduced into the nanowires. In a second stage (drive-in) nanowire samples are heated at 975°C without the spin on dopant source present. This results in further diffusion of boron into the nanowires. Secondary ion mass spectroscopy (SIMS) carried out on these doped nanowires confirmed the presence of boron for various concentrations and Transmission Electron Microscopy (TEM) shows that the structural integrity is maintained after this high temperature doping process without introduction of extended defects. Electrical characterization measurements are carried out in order to extract the resistivity and determine the approximate dopant concentrations. Preliminary two point probe measurements indicate total resistance of these nanowires in the range of ~104 Ohms. In order to separate contact resistance from actual resistance of nanowire, Electron-beam lithography (EBL) is being utilized to write four-probe contact arrangements. Present results show the feasibility of this technique for electrically doping nanowires and semiconductor nanostructures in general.

DD12.33**Fabrication of Thermal Reduced Ag Nano-wires with Titanium Dioxide.** Hsien-Tse Tung¹, Cheng-Wei Yen¹, Tzu-Hsuan Kao¹, Jenn-Ming Song², Chang-Shu Kuo¹ and In-Gann Chen¹; ¹Materials Science and Engineering, National Cheng-Kung University, Tainan, Taiwan; ²Materials Science and Engineering, National Dong Hwa University, Hualien, Taiwan.

It have been reported [1] recently that silver nano-wires could be synthesized by the thermal reduction of an aqueous silver nitrate solution (AgNO₃) on the surface of titanium dioxide (TiO₂) prepared by electron-beam evaporation. In this study, two modified methods were developed to fabricate the Ag nano-wires. The first method is to dip AgNO₃ solution on anatase TiO₂ films prepared by reactive sputtering on Si substrate. The second method is to prepare AgNO₃ solution mixed with nano-sized anatase TiO₂ powders and dip on Si substrate. After thermal reduction treatment at 300°C, Ag nano-wires with diameter about 10² nanometers and length about 5- 50µm can be produced using both methods. The electrical properties of the Ag nano-wires produced were measured by a two-armed nano-manipulator in a SEM. Preliminary electrical conductivity measurements of the Ag nano-wires varied in the range of 10³ to 10⁷ µΩ-cm with a trend of inverse proportion to the Ag nano-wire diameter. And the Ag nano-wires produced by AgNO₃/TiO₂ solution exhibits a higher resistivity of about 3.1×10⁸ µΩ-cm than the samples with sputtered TiO₂. Possible reaction mechanism of Ag nano-wires and the different electrical performance will be discussed in this presentation. This research is supported by National Science Council under the contract of No. NSC95-2120-M-006-003 [1] T. K. Chen, W. T. Chen, M. C. Yang, and M. S. Wong, J. Vac. Sci. Technol. B Vol. 23, No. 6 (2005)

DD12.34**Selective Area Growth of ZnO Nanowires on Group III Oxide Nanowires/nanoparticles using Implantation-assisted Technique and MOCVD.** Kwong Chun Lo, Hui Wang and Ho Pui Ho; Electronic Engineering, The Chinese University of Hong Kong, Hong Kong, Hong Kong.

We report the selective area synthesis of gallium oxide (Ga₂O₃)/indium oxide (In₂O₃) nanowires on gold patterned gallium arsenide (GaAs)/indium phosphide (InP) substrate by ion implantation. The GaAs/InP substrate was first treated with implantation of carbon ions and then followed by coating the surface with a 40nm thick gold film. After rapid thermal anneal (RTA) at 750-950°C for 30 seconds, Ga₂O₃/In₂O₃ nanowires/particles were found on gold patterned surface and nanoparticles of gold were found at the tip of the nanowires. The nanowires with diameters of 50-500nm were examined by Raman spectroscopy, scanning electron microscopy (SEM), transmission electron microscopy (TEM), Photoluminescence (PL) and cathodoluminescence (CL). Subsequently MOCVD growth of ZnO nanowires on the Ga₂O₃/In₂O₃ nanowires was conducted. The size of ZnO nanowires depends on the size of gold nanoparticles and Ga₂O₃/In₂O₃ nanowires. ZnO nanowires grow from the gold nanoparticle, suggesting that a vapor-liquid-solid (VLS) mechanism was involved.

DD12.35**Mesoporous Nanowires and Nanotubes Prepared from a Confined-Passembly-template Assisted Electrodeposition.** Hongmei Luo¹, Yunfeng Lu² and Quanxi Jia¹; ¹Superconductivity Technology Center, Materials Physics and Applications Division, Los Alamos National Laboratory, Los Alamos, New Mexico; ²Chemical and Biomolecular Engineering, University of California, Los Angeles, Los Angeles, California.

One-dimensional (1D) nanostructures, especially nanowires and nanotubes (generally defined as hollow nanowires) have become the focus of intensive research owing to their potential applications. For sensor and catalyst applications, mesostructured nanowires and nanotubes are often needed, where tunable pore size and higher surface area are necessary. Here we report that a confined-assembly-template assisted (CATA) electrodeposition can be used to prepare mesoporous metal Pt, Pd, Co, Ni, and semiconductor ZnO nanowires and nanotubes. The overall diameter and length of 1D nanowire or nanotube are defined by the cylindrical pore channels of the porous membrane. Surfactant liquid crystals confined in pores are used to generate mesoporosity and to control the texture of nanowire or nanotubes. As compared to solid nanowires and nanotubes, the mesoporous nanowires and nanotubes exhibit unique properties. For example, mesoporous cobalt nanowires show much higher coercivity.

DD12.36

Synthesis of Pyramidal Lead Sulphide (PbS) Thin Films by Employing Liquid-liquid Interface. Dongbo Fan, Peter John Thomas and Paul O'Brien; School of chemistry, University of Manchester, Manchester, United Kingdom.

Lead sulphide (PbS) is a direct semiconductor with narrow bandgap (approximately 0.41 eV at 300 K) and large exciton Bohr radius (18nm at room temperature). It has emerged as a good candidate for many applications. For examples, PbS thin films have been used in near-IR communication, optical switches and IR detectors for their good photoconductivity in the near-IR region [1]. It has also been applied in investigate quantum confinement effect and electroluminescence device such as light emitting diode owing to its size tunable band gap [2]. Since the dependence between photoconductivity on morphology of PbS thin films and the prediction of special optical properties of PbS in nanoscale were reported [3], various different physical and chemical synthetic approaches have been developed to prepare PbS thin film with special morphologies. In this presentation, we demonstrate the liquid-liquid interface reaction technique (LLIRT) to grow PbS pyramidal nanocrystal, which subsequently, tend to be scalable forming particulate film by chemically driven self-assembly. X-Ray diffraction pattern reveals crystalline nature of thin film with cubic phase and the SEM images indicate the interesting uniform pyramidal morphology owned by thin films. The LLIRT method has been demonstrated an efficient approach for obtaining self-assembled metal, semiconductor nanoparticles and nanocrystalline thin films [4]. Now, it enabled us to generate legend free, self-stabilized, non-template, non-surfactant, highly monodisperse pyramidal super-nanostructure at the interface in a facile environmental condition. It is worthwhile to note that, till date, only several materials with a pyramidal morphology were reported [5]. References: [1] a) R. S. Kane, R. E. Cohen, and R. Silbey, 1996, Chem. Mater. 8, 1919-1924. b) R. S. Kane, R. E. Cohen and R. Silbey, J. Phys. Chem., 1996 (100) 7928. [2] I. Chakraborty and S. P. Moulik, Journal of Nanoparticle research, 2004 (6) 233-240. [3] a) G. P. Kothiyal, B. Ghosh and R. Y. Deshpande, J. Phys. D: Appl. Phys., 13 (1980) 869-73. b) L. Banyai, Y. Z. Hu, M. Lindberg and S. W. Koch, Physical Review B, 1988 (38) 8142-8153 [12] a) W. H. Binder, Angew. Chem. Int. Ed. 2005, 44, 5172-5175. b) H. W. Duan, D. Y. Wang, D. G. Kurth, and H. Möhwald, Angew. Chem. Int. Ed. 2004, 43, 5639-5642. c) C. N. Rao, G. U. Kulkarni, V. V. Agrawal, U. K. Gautam, M. Ghosh and U. Tumkurkar, J. Coll. Inter. Sci. 289, 305-318. [13] a) R. Oga, S. Yamamoto, I. Ohzawa, Y. Fujiwara, Y. Takeda, Journal of Crystal Growth, 237-239 (2002) 239-243. b) H. Jia, Y. Zhang, X. Chen, J. Shu, X. Luo, Z. Zhang and D. Yu, Appl. Phys. Lett. 2003, 82, 4146-4148. c) B. Muller, et al. J. Vac. Sci. Technol. B, 2001, 19, 1715.

DD12.37

Polyol Mediated Design of Core-Shell Pd-on-Au Bimetallic Nanoparticles. Domingo Ferrer¹, Alejandro Torres-Castro¹, Xiaoxia Gao¹, Selene Sepulveda-Guzman¹ and Miguel Jose-Yacamán^{1,2}; ¹Chemical Engineering, The University of Texas at Austin, Austin, Texas; ²Texas Advanced Materials Center, Austin, Texas.

The possibility of controlling the structure and the chemical composition of particles at the nanoscale level has an enormous importance for both basic science and technological applications. Metal nanostructures play a significant role in many important areas such as catalysis, photonics, magnetism, and imaging. In fact, bimetallic (or multimetallic) catalysts have long been valuable for in-depth investigations of the relationship between catalytic-activity and catalyst-particle structure. In this work, we report the synthesis of Pd-on-Au nanoparticles with a core-shell configuration, where a well-defined outer palladium shell embeds a gold core. The bimetallic Pd/Au nanoparticles were obtained by the successive reduction of their corresponding metallic salts in presence of poly(N-vinyl-2-pyrrolidone), using the polyol method. A narrow size distribution, centered at 3.4 nm was observed in the fabricated nanoparticles. The structure and elemental distribution of the nanoparticles was determined by transmission electron microscopy, high-angle annular dark field (HAADF) and energy dispersive X-ray spectroscopy (EDX). The observation of UV-VIS spectra showed that by increasing the amount of Pd on the Pd-on-Au nanoparticles, the surface plasma resonance (SPR) peak absorbance decreased in intensity, indicating the formation of Pd-shell on the Au-core. Core/shell-structured bimetallic nanoclusters often display higher catalytic activity than the corresponding monometallic nanoclusters. The colloidal Pd-on-Au dispersions described here might exhibit outstanding catalytic properties as catalysts.

DD12.38

Highly Water-Soluble Monodisperse Magnetic Iron Oxide Nanocrystals. Yadong Yin, Jianping Ge and Yongxing Hu; Chemistry, University of California, Riverside, Riverside, California.

High quality magnetic iron oxide colloidal nanocrystals have been synthesized using a high temperature precipitation procedure. These nanocrystals possess high crystallinity, narrow size distribution, and excellent water solubility. The surface of the nanocrystals is coated with a layer of carboxylate groups which allow convenient conjugation with biomolecules. By changing the synthetic condition, the size of the nanocrystals can be tuned from a few nanometers to above a hundred nanometers, with reasonably narrow size distributions. In addition to some biomedical applications of these nanoparticles, we will also discuss their self-assembly behavior under the external magnetic field.

DD12.39

Mixed-Surfactant-Templated Synthesis of Nanogroove-Network Structured Platinum Nanosheets and Their Electrochemical Characterization. Tsuyoshi Kijima^{1,2}, Takumi Yoshimura^{1,2}, Go Sakai^{1,2}, Shusaku Isohata¹, Masafumi Uota², Hideya Kawasaki^{3,2} and Daisuke Fujikawa^{1,2}; ¹Applied Chemistry, Miyazaki University, Miyazaki-city, Japan; ²CREST, Japan Science and Technology Agency, Miyazaki, Japan; ³Applied Chemistry, Kansai University, Suita, Japan.

Nanoscale platinum particles have attracted particular attention because of their potential use as catalysts in various fields such as fuel cells. The catalytic reactivity of Pt nanoparticles used for these applications depends on their structural properties such as size, shape, and the arrangement of surface atoms. Various methods have been therefore developed for controlling the structural properties of Pt nanoparticles and fabricating unconventional Pt nanostructures such as nanorods, nanotubes, and 2D mesoporous solids. Our recent study also demonstrated the synthesis of Pt nanotubes by the reduction of H_2PtCl_6 with hydrazine in lyotropic mixed surfactant LCs of polyoxyethylene (20) sorbitan monostearate (Tween 60) and nonaethyleneglycol dodecylether (C_{12}EO_9).¹ In this paper, we report that the borohydride reduction of Na_2PtCl_6 confined to compositionally the same mixed surfactant LCs yields single-crystalline Pt nanosheets with a nanogroove-network structure, together with their fairly high electrocatalytic activity for oxygen reduction reaction (ORR) upon loading on carbon. In the typical reaction, Na_2PtCl_6 , C_{12}EO_9 , Tween 60, and H_2O at a prescribed molar ratio were mixed at 60°C and then cooled to 20°C. The cooled LC material was reduced with an aqueous solution of NaBH_4 (SBH). AFM, TEM and HRTEM observations revealed that the resulting solids are identified as nanogroove-network structured single crystalline Pt nanosheets of ~3.5 nm thick and 50-60 nm diameter. The nanosheets have pseudo 2D irregular Pt networks in which Pt nanoleaves of ~2.6 nm wide and 2-4 nm

long are loosely interconnected with their crystallographic alignment to form an irregular network of nanogrooves ~ 1 nm in width. In contrast, the $C_{12}EO_9$ -based single surfactant system yielded an aggregate of featureless nanoparticles and the Tween 60-based single system led to a 2D-aggregate of Pt nanoleaves loosely linked but with their different orientations. FT-IR analysis suggested that the stearate species produced by the hydrolysis of Tween 60 serve as a capping agent responsible for the growth of sheet-like Pt nanoparticles. The mixtures of Pt-salt containing LC and carbon powder (VXC72R) were prepared and then treated with an aqueous solution of SBH at various SBH/Pt molar ratios. The carbon supported Pt products thus obtained were characterized for the electrocatalytic ORR by cyclic voltammetry in 0.5 M H_2SO_4 saturated with dissolved oxygen. It was found that the nanogroove-structured Pt/C obtained at high SBH amounts shows fairly high electrocatalytic activity for ORR, in contrast to non-grooved Pt nanoparticles/C obtained at low SBH amounts, although the loading amounts of Pt for both Pt/C are almost the same. 1. T. Kijima et al., *Angew. Chem.*, 2004, 43, 228.

DD12.40

Understanding Shape Control in Nanoparticle Synthesis. Jeremy J Gray¹, Danxu Du², David Srolovitz³ and Christine A Orme¹; ¹Chemistry, Materials and life sciences, Lawrence Livermore National Laboratory, Livermore, California; ²Department of mechanical and aerospace engineering, Princeton University, Princeton, New Jersey; ³Department of Physics, Yeshiva University, New York, New York.

Recent research has shown that biologically inspired approaches to materials synthesis and self-assembly, hold promise of unprecedented atomic level control of structure and interfaces. In particular, the use of organic molecules to control the production of inorganic technological materials has the potential for controlling grain structure to enhance material strength; controlling facet expression for enhanced catalytic activity; and controlling the shape of nanostructured materials to optimize optical, electrical and magnetic properties. In this work, we use organic molecules to modify metal crystal shapes towards understanding the metal-organic interactions that lead to nanoparticle shape control. Using in situ electrochemical AFM (EC-AFM) as an in situ probe, we study the influence of a variety of organic molecules on Ag island growth during electrochemical deposition on Ag(100). The results show that, depending on the organic molecule used, the Ag islands can develop into a wide-range of unique well-defined shapes. To understand the shape evolution of the Ag islands, we utilize electron backscatter diffraction (EBSD) in conjunction with microscopic ellipsometry to characterize the facet-specific binding of the organic molecules to polycrystalline Ag. This work was performed under the auspices of the U.S. Department of Energy by University of California, Lawrence Livermore National Laboratory under Contract W-7405-Eng-48. The project 06-LW-090 was funded by the Laboratory Directed Research and Development Program at LLNL.

DD12.41

Microwave Assisted Synthesis of Iron Oxide and Mixed Iron Oxide Nanoparticles. Jason G. Parsons¹, C. Luna¹, C. Botez², J. Elizalde², J. Peralta Videz¹ and J. L. Gardea-Torresdey¹; ¹Chemistry, University of Texas at El Paso, El Paso, Texas; ²Physics, University of Texas at El Paso, El Paso, Texas.

Microwave assisted synthesis is not a new concept in chemistry. However, we have shown that iron oxide and mixed iron oxide nanoparticles synthesized using this technique can be tuned depending on the temperature of the synthesis, the initial moles, and the reaction time. We have synthesized iron oxide particles of varying sizes from the titration of sodium hydroxide into different iron salts, which include iron(III) chloride, iron(III) nitrate, and iron(II) chloride followed by microwave irradiation. The results have shown that at 100 degree C iron oxyhydroxide compounds were synthesized from iron(III) or iron oxyhydroxide chloride starting materials within 30 minutes of reaction time. However, using iron(II) chloride as starting material, we have found that magnetite is synthesized at 100 degree C. We have also found that at temperatures higher than 150 degree C, all the starting materials produced Iron(III) oxide. Through XRD analysis using the Scherer equation we have been able to tune the size of the particles formed from approximately 80 nm to 325 nm with pure phases being synthesized. In addition, we have found an increase in the average size of the nanoparticles being synthesized with a smaller mole ratio of the iron from dilution after the addition of the hydroxide to the iron(III) starting solution, at the same temperature. Furthermore, we have also found that the shorter the reaction time of the materials exposed to the microwaves results in small particles being synthesized. Finally, we have also performed SEM analysis of these nanoparticles to further corroborate the sizes calculated from the XRD analysis. XRF analysis has also been used to verify the purity of the final synthesized materials. The XAS analysis of the synthesized nanoparticles will also be presented.

DD12.42

Synthesis and Characterization of Nanoscale ZnO and MgO. Peter Yaron¹, Zhengwei Pan², Andi Barbour¹ and J. Z. Larese^{1,2}; ¹Chemistry, University of Tennessee, Knoxville, Tennessee; ²Oak Ridge National Laboratory, Oak Ridge, Tennessee.

We will discuss recent synthetic, thermodynamic, electron microscopic and neutron scattering investigations that probe the topological, adsorption and chemical properties of MgO and ZnO nanometer sized particles. Using a novel, patented process we find that pure and doped metal oxides can be produced in large quantities with well-defined crystal habitat. Thermodynamic investigations quantify the binding energies for various gaseous and liquid thin films. Electron microscopy studies are used to identify that numerous shapes including cubes, rods, plates and tetrapods can be selectively produced. We will discuss the potential use of these nanostructured materials as catalysts, gas sensors and storage devices, and well as optoelectronic/solar cells. This work is supported by the Division of Materials Science, Office of Science, Basic Energy Sciences under contract DE-AC05-00OR22725 and the NSF under DMR-0412231.

DD12.43

Formation of Silver Nanostructures on MgZnO hexagonal and Cubic Alloys Shiva S Hullavarad and Nilima V Hullavarad; Office of Electronic Miniaturization, University of Alaska, Fairbanks, Alaska.

With potential applications in many fields from fundamental science to engineering technology, multi-dimensional (MD) metal nanostructures such as nanowires, nanoshells, and nanotubes have been very popular topics of research. They have been used to experimentally probe the effects of quantum confinement on electronic, magnetic, and other related properties, and they could be used as active components or interconnects in fabricating electronic, photonic, and sensing devices. Silver nanowires are particularly interesting to explore because bulk silver exhibits the highest electrical and thermal conductivities among all metals. Other modern applications of silver nanowires have also been discovered in many fields including catalysis, electronics, photonics, and photography. In this study, we present the formation of silver nanowires, nano shells and nano rods

by the thermal reduction of an aqueous silver nitrate solution on the surface of Magnesium Zinc Oxide ($\text{Mg}_x\text{Zn}_{1-x}\text{O}$) multiphase alloy thin films. $\text{Mg}_x\text{Zn}_{1-x}\text{O}$ is a strategically important semiconductor material, which potentially has wide applications in wireless communications, optoelectronics, including ultraviolet diode lasers and sensors, and MEMS technology. MgZnO is realized by alloying MgO with ZnO and by varying the Mg composition, the band gap can be tuned from 3.3 eV to 7.8 eV for wurtzite and cubic structured $\text{Mg}_x\text{Zn}_{1-x}\text{O}$, extending the cut-off wavelength from UV-A (320-400nm) to UV-B (280-320 nm) and UV-C (200-280 nm) regions. This material is of significant importance for various applications in flame sensors, UV index monitors and missile plume detection. The silver nanowires are characterized by Transmission Electron microscopy and Selective Area Diffraction methods. In this context, the formation of silver nanostructures on MgZnO alloy films is technologically important as it would lead in to the potential area of nano metallic contacts to emerging oxide electronic materials.

DD12.44

Probing and Tuning the Chemistry and Structure of Nanocrystalline Cerium Oxide. Satyanarayana VNT Kuchibhatla^{1,2}, Ajay S Karakoti¹, Sudipta Seal^{1,3}, Mark H Engelhard², Donald R Baer² and Thevuthasan Suntharampillai²; ¹Advanced Materials Processing and Analysis Center, University of Central Florida, Richland, Washington; ²Environmental Molecular Sciences Laboratory, Pacific Northwest National Laboratory, Richland, Florida; ³Nanoscience and Technology Center, University of Central Florida, Orlando, Florida.

Nanocrystalline oxide materials are receiving considerable research attention with possible applications in many areas including: sensors, solar cells, protective coatings, and fuel cells. Cerium oxide has exceptional oxygen storage capacity associated with the ability to switch between 4+ and 3+ oxidations states. Many studies have examined the change in oxidation state and lattice parameter as a function of the size of ceria nanostructures. With an increasing interest in the functional materials such as cerium oxide for novel bio medical applications, it is quite essential to have a thorough understanding of the material behavior under different environments. The impact of synthesis media, storage, ageing needs to be addressed. A major focus of this work has been the synthesis of cerium oxide nanoparticles using room temperature, green chemical methods in different media that can be directly used in various applications. Synthesis was carried in DI water, Poly (ethylene glycol) and other solvents. Nanoparticle suspensions were aged at different temperatures in as synthesized condition and the behavior was monitored as a function of time. UV Visible spectroscopy (UV - Vis) and X-ray photo electron spectroscopy (XPS) have been used to determine the oxidation state variation in the ceria nanoparticles. High Resolution Transmission Electron Microscopy (HRTEM) has been used to probe the morphology, size and structure of the nanoceria. The optical properties of the ceria nanoparticles have been studied using UV - vis and photoluminescence spectroscopy. In addition to excellent colloidal stability in specific media, we have also found a variety of time and environmental effects on the oxidation state of the ceria nanoparticles. The nanoparticles were found to form highly crystalline polyhedral agglomerates and one dimensional nanostructures under different ageing conditions through oriented self assembly. Important observations from this research and their significance will be described.

DD12.45

Synthesis and Characterization of Variable Pore Size, Ordered Cylindrical Nanopores in Alumina. Michael Felty¹, Paige Landry¹, Andi Barbour¹ and J. Z. Larese^{1,2}; ¹Chemistry, University of Tennessee, Knoxville, Tennessee; ²Oak Ridge National Laboratory, Oak Ridge, Tennessee.

We report on our synthesis and characterization of well-defined, close packed, cylindrical channels in an alumina matrix. These materials have been systematically produced using an anodization process that provides the ability to tune the pore size while retaining the long-range hexagonal pattern. Characterization of these materials includes electron and scanning microscopies, x-ray diffraction and volumetric adsorption. We expect to employ these materials in the study of gas storage and quantum confinement. Numerous theories predict a dramatic change in the physical properties of gases and liquids constrained to spatial dimensions that are on the order of several nanometers. Modeling studies of gas adsorption within these channels will be presented if time permits. This work is supported by the Division of Materials Science, Office of Science, Basic Energy Sciences under contract DE-AC05-00OR22725 and the NSF under DMR-0412231.

DD12.46

Nanoscale Site-Selective Nucleation and Growth on Planar and Colloidal Surfaces Changdeuck Bae and Hyunjung Shin; School of Advanced Materials Engineering, Kookmin University, Seoul, South Korea.

Self-assembly of small objects offers a powerful route for constructing functional, multidimensional structures, but the individual components being used is monotony or large. At nanoscale, selectively decorating the surfaces of the self-assembling objects could open a great deal of opportunity for their applications. We studied the site-specific heterogeneous nucleation and growth of inorganic materials at sub-100 nm length scale from organic templates on planar surfaces. The results suggest that high difference of surface energy between growing and surrounding surfaces leads to the complete site-selectivity. We also showed that this bottom-up approach can be applied to high curved surfaces (i.e., microspheres) in order to produce dielectrically anisotropic colloidal building blocks. Furthermore, we investigated the optical properties of the selectively grown nanodots arrays on both planar and colloidal surfaces in terms of photonic band gap.

DD12.47

Fabrication of Doped ZnO(Mn, Co) Nanostructures with Room Temperature Ferromagnetism by Chemical Vapo Deposition. Jingjing Liu, Amber West, Minghui Yu and Weilie Zhou; Advanced Materials Research Institute, New Orleans, Louisiana.

Mn and Co doped ZnO diluted magnetic semiconductor (DMS) nanostructures were prepared by direct reaction of zinc with manganese chloride powder and cobalt acetate, respectively, under oxygen environment using chemical vapor deposition (CVD) method. Several kinds of nanostructures, such as nanowire arrays, bowls/cages, and nanoneedles were obtained. The morphologies and crystal structures of the as-synthesized nanostructures were characterized using field emission scanning electron microscopy (FESEM), transmission electron microscopy (TEM), and x-ray diffraction spectroscopy (XRD). Superconducting quantum interference device (SQUID) measurement shows that the doped nanowire arrays, nanocrystalline bowls/cages and cactus-like nanoneedles have ferromagnetic ordering above room temperature. The fabrication of spintronic nanotransistors will be also discussed.

DD12.48

Position-controlled Heteroepitaxial Growth of InAs Nanowires on Lattice-mismatched Substrates by Selective Area Metalorganic Vapor

Phase Epitaxy. Katsuhiro Tomioka, Junichiro Takeda, Ling Yang, Shinjiro Hara, Junichi Motohisa and Takashi Fukui; Graduate School of Information Science and Technology and Research Center for Integrated Quantum Electronics, Hokkaido University, Sapporo, Japan.

Semiconductor nanowires have been attracting much attention as elemental components of electronic devices because they are one of the innovative materials to overcome a limit of scaling-rule. In this work, we report a position-controlled heteroepitaxial growth of highly uniform InAs nanowires on lattice mismatched substrates by selective-area metalorganic vapor phase epitaxy (SA-MOVPE). The crystal growth in SA-MOVPE proceeds in facet growth mode only within the predetermined mask opening regions. This is a promising method to achieve well position-controlled growth of nanowires. Mask pattern with circular opening of various diameters and pitches was formed on 20 nm SiO₂ deposited InAs(111)B, InP(111)B, GaAs(111)B and Si(111) substrates by electron beam lithography and wet chemical etching. Growth was carried out at 540°C for 20 min. The source materials were trimethylindium (TMIn) and arsine (AsH₃). The partial pressure of TMIn and AsH₃ were 1.25×10^{-4} and 4.87×10^{-7} atm. Prior to the growth, removal of native oxides for InAs, InP and GaAs was performed at ~ 600°C for 5 min under an AsH₃ flux. In the case of Si(111), surface was cleaned at ~ 920°C for 5 min in hydrogen ambient. InAs nanowires grown in these optimized conditions on InAs(111)B substrates had hexagonal pillar shaped structure surrounded by {110} vertical facets and (111)B surface and the growth direction was <111>B. Vertical InAs nanowires and their arrays were also successfully grown on InP(111)B and GaAs(111)B substrates. The growth rate of the nanowires was inversely proportional to the square of opening diameters independent of the substrate, which was attributable to the diffusion of growth species from mask to the opening region. High resolution TEM images showed that the crystal structure of InAs nanowires grown on InAs(111)B, InP(111)B and GaAs(111)B substrates were zinc-blende including 60°-rotated twin structure with the average period of several monolayers. The appearance of twin is probably caused by high growth rate. Position-controlled InAs nanowires were also successfully grown on Si(111) substrates. The growth mode of InAs nanowires on Si(111) differs from those on substrates described above. The directions are two types. One is normal to the surface; the other is ~ 20°-tilted to the substrate. The fraction of the latter type was ~ 5% for the whole nanowires grown on Si(111) substrates. This difference can be explained by the termination of the surface prior to the growth and the non-polar nature of Si. When the group-V atoms terminate dangling-bonds on Si surface, the growth direction is normal to the plane as similar to that of (111)B surface of III-V semiconductors. While, the direction can be tilted when the surface is terminated with group-III atoms because the terminated surface is (111)A-like surface. In fact, the growth direction of InAs nanowires on InAs(111)A substrates is one of the three equivalent <111>B which is ~ 20° tilted to the surface.

SESSION DD13: Devices and Applications of Low Dimensional Materials I

Chairs: Robert Hamers, Margaret Hines and Xiao-Min Lin

Thursday Morning, April 12, 2007

Room 2001 (Moscone West)

8:00 AM DD13.1

Architectural Design, 1-D Walls, 3-D Plumbing, and Interior Design en route to Multifunctional Nanoarchitectures Debra R. Rolison and Jeffrey W. Long; Surface Chemistry Branch, Naval Research Laboratory, Washington, District of Columbia.

Rate-critical applications require facile transport of reactant and charge carriers for high performance [1]. Aerogels and ambigels, which are sol-gel-derived ultraporous, aperiodic nanoarchitectures, unite high surface area for heterogeneous reactions with a continuous, porous network for rapid diffusional flux of molecules. Response times to gas-phase analytes are >10 times faster than those of the same chemistry expressed as a xerogel [2,3]. The surface area is expressed by "walls" that are defined by the nanoscopic, covalently bonded, one-dimensional solid network of the gel. The vast open, interconnected space characteristic of a building is represented by the interpenetrating nanoscopic pore network ("3-D plumbing"). Combining the 1-D interconnected nanoscopic solid with the 3-D interconnected nanoscopic pore network creates nanoarchitectures that yield high performance in rate-critical applications. In one example, the nanoarchitecture imposes electrical pathways along the low-dimensional network to yield macroscopic diffusion lengths for transport of ions from over a temperature range from ambient to 600°C. An architectural viewpoint provides a powerful metaphor to guide the chemist and materials scientist in the design of aerogel-like nanoarchitectures and in their physical and chemical transformation into multifunctional objects that yield high performance for rate-critical applications. [1] D.R. Rolison, *Science* 299 (2003) 1698. [2] N. Leventis, I. Elder, D.R. Rolison, M.L. Anderson, C.I. Merzbacher, *Chem. Mater.* 11 (1999) 2837. [3] J.M. Wallace, J.K. Rice, J.J. Pietron, R.M. Stroud, J.W. Long, D.R. Rolison, *Nano Lett.* 3 (2003) 1463. [4] M.S. Doescher, J.J. Pietron, B.M. Dening, J.W. Long, C.P. Rhodes, C.A. Edmondson, and D.R. Rolison, *Anal. Chem.* 77(2005) 7924. [5] C. Laberty-Robert, J.W. Long, E.M. Lucas, K.A. Pettigrew, R.M. Stroud, and D.R. Rolison, *Chem. Mater.* 18 (2006) 50.

8:15 AM DD13.2

Fabrication and Transport Characterization of Embedded Vertical Ge Nanowires Paul W. Leu¹, Terry Hou², Kyeongjae Cho³ and Paul McIntyre²; ¹Mechanical Engineering, Stanford University, Stanford, California; ²Materials Science, Stanford University, Stanford, California; ³Physics, University of Texas at Dallas, Dallas, Texas.

Germanium nanowires (NWs) are a promising material for electronic and photonic devices due to the high carrier mobilities of Ge and the low temperatures required for Ge NW growth. We demonstrate an approach to integrate <111> Ge NWs into vertical arrays suitable for programmable interconnects and sensors. The transport properties of these Ge NWs as a function of length and diameter are characterized by experiments and theory. Ge NWs are grown vertically from Au catalysts dip coated onto a degenerately doped <111> Si substrate. SiO₂ is conformally deposited by plasma enhanced chemical vapor deposition around the vertical NWs to isolate and provide mechanical stability to the wires, followed by chemical mechanical polishing to planarize the structure. The tips of the NWs are exposed and can be contacted and electronically characterized through the deposition of top metal layer contact or with a conductive atomic force microscope. We compare trends in the experimental electrical transport properties of Ge NWs with simulation results from a Non-Equilibrium Green's function technique within an sp³d⁵s* tight-binding approximation.

8:30 AM DD13.3

Magnetic Separation and Water Treatment with Monodisperse Fe₃O₄ Nanocrystals. John Thomas Mayo¹, Cafer Yavuz¹, William Yu¹, Arjun Prakash², Joshua Falkner¹, Sujin Yean³, Lili Cong³, Heather Shipley³, Amy Kan³, Mason Tomson³, Douglas Natelson⁴ and Vicki Colvin¹; ¹Chemistry, Rice University, Houston, Texas; ²Chemical and Biomolecular Engineering, Rice University, Houston, Texas; ³Civil and Environmental Engineering, Rice University, Houston, Texas; ⁴Physics and Astronomy, Rice University, Houston, Texas.

Magnetic separations can be applied to diverse problems, such as household water purification and the simultaneous separation of complex

mixtures. High-surface area and monodisperse magnetite (Fe₃O₄) nanocrystals were shown to respond to low fields in a size-dependent fashion. The particles apparently do not act independently in the separation but rather reversibly aggregate through the resulting high-field gradients present at the surfaces. Using the high specific surface area of Fe₃O₄ nanocrystals that were 12 nanometers in diameter, we reduced the mass of waste associated with arsenic removal from water by orders of magnitude. Additionally, the size dependence of magnetic separation permitted mixtures of 4- and 12-nanometer-sized Fe₃O₄ nanocrystals to be separated by the application of different magnetic fields.

8:45 AM DD13.4

Biological Applications of Phase Separated Gold Nanoparticles. Oktay Uzun, Darrell Irvine and Francesco Stellacci; Department of Materials Science and Engineering, Massachusetts Institute of Technology, Cambridge, Massachusetts.

The endo-lysosomal escape of drug or gene carriers is crucial for enhancing the effectiveness of delivering their load and executing their function in cytosol, especially the contents that are susceptible to lysosomal degradation. Current vectors that enable the endo-lysosomal escape of their loads such as DNA are limited by their toxicity and by their ability to carry only limited classes of therapeutic agents. An efficient and nontoxic carrier to deliver desired materials specifically into the cell is needed. Recently, we have developed a molecular system, known to phase separate into domains of random size and shape, form highly ordered phases with size (~ 0.5 nm) when assembled on surfaces with a radius of curvature smaller than 10 nm that are highly resistant to nonspecific protein adsorption. These particles can be tailored for a specific application and potentially be used as synthetic gene-delivery agents or for diagnostic Computed Tomography (CT) contrast agents.

9:00 AM *DD13.5

Directed Assembly and Real-time Detection of Nanowire Bridges for Direct Digital Sensing Robert J. Hamers¹, Bo Li¹, Lu Shang¹, Joe Beck¹ and Ed Perkins²; ¹University of Wisconsin, Madison, Wisconsin; ²Army Environmental Lab, Vicksburg, Mississippi.

We are investigating the use of electrical fields combined with biomolecular recognition events to create new types of hybrid nano-bio devices. By coupling AC dielectrophoresis with a flow, nanowires can be controllably guided along electrodes into a gap. AC impedance measurements show that nanowire bridging and un-bridging events can be detected in real time. This combination provides a pathway toward automated assembly of nanoscale structures. By combining this manipulation with biomolecular recognition, it is possible to create devices that are essentially chemically- or biologically-actuated "fuses", in which a recognition event includes cleavage of a nanowire bridge. We demonstrate the real-time detection and such a nanowire "unbridging" event as a proof-of-principle.

9:30 AM DD13.6

A Self-Assembled, Nanoparticle Based Tactile Sensor with Sensitivity & Resolution of Human Finger. Vivek Maheshwari and Ravi Saraf; Chemical Engineering, University of Nebraska Lincoln, Lincoln, Nebraska.

Sensation of touch, primarily the determination of stress distribution over the area of physical contact between the sensor and the object surfaces, is critical for advancement of minimum invasive surgical procedures. It gives a surgeon the "touch sensation" to decipher, for example, cancer tissue and gallstone using signals from a tactile sensor. Moreover, there is increasing interest in developing humanoid robots that can sense shapes, textures, hardness and further manipulate complex objects which are not readily possible by vision alone. Touch (or tactile) sensors are usually made as micro-electromechanical systems, or else by integrating chip with electronic circuit and strain sensitive materials, such as magento-resistive ceramics, piezoelectric polymers, and strain sensitive conducting elastomers. The spatial resolution of current large-area tactile sensor (greater than 1 cm²) lags by over an order of magnitude compared to human finger. Using metal and semiconducting nanoparticles ~100 nm thick, large area thin-film device is self assembled such that the change in current density through the film and the electroluminescent light intensity are proportional to local stress. Both lateral and height resolution of texture are comparable to human finger, an improvement by a factor of ~50 over current technologies. Furthermore, a sensitivity of 9 KPa is well within the 10 to 40 KPa range that a human finger applies to sense texture and shape. The stress image can be constructed by directly imaging the electroluminescence on a CCD or by mapping the current density over the surface of the device. The device is based on the principle of electron tunneling and is capable of imaging stress distribution with a spatial resolution of ~20 μm and height resolution of <5 μm, comparable to the ~40 μm and ~2 μm resolution of a human finger. The fabrication requires no lithography and the transduction of stress distribution is virtually continuous at 100 nm scale. The device is self-assembled, consisting of alternating layers of Au (10 nm) and CdS (3 nm) nanoparticles separated by dielectric layers (DL), composed of polyelectrolyte. Being a solution based assembly process it allows fabrication of the device over geometric surfaces with ease. We expect to image tissue hardness with resolution at cellular level which will give us the ability to detect cancer initiation and growth at cell level.

9:45 AM DD13.7

Glycine-coated Single Walled Carbon Nanotube Field Effect Transistors (SWNT-FETs) for Alcohol Specific Sensor Applications. Hyun Jae Song and Hee Cheul Choi; chemistry, Pohang University of Science and Technology, Pohang, Kyungbuk, South Korea.

With its unique electronic and electrical properties, single walled carbon nanotube field effect transistor (SWNT-FET) has been widely investigated as a nanoscale platform for chemical and biological sensing. Regardless of sensing mechanisms such as charge injection or Schottky barrier modulation as proposed by several groups, the fundamental requirement for the development of selective sensor is to discover and immobilize "probe" molecules which bind to guest molecules with high specificity. Different from the antigen-antibody interaction in biological systems, in the case of gas sensing, false signals are easily generated from unexpected adsorption of mixed gas species unless they are effectively discriminated by proper probe molecules. We introduce glycine as a probe molecule for alcohol specific sensing. As the simplest amino acid, glycine has been spontaneously adsorbed on single walled carbon nanotubes (SWNTs) to form into self-assembled nanoclusters. Self-clustering of glycine is believed to be initiated by natural but highly specific interactions between carbon nanotubes and amine groups of glycines. The field effect transistor (FET) devices coated with glycines as a signal transducer have detected alcohols, such as isopropanol (IPA) and ethanol with selectivity against water and acetone. Upon the adsorption of both IPA and ethanol, the glycine-coated SWNT-FET devices have exhibited metal-like transport behaviors (on/off ~ 1) while the original and glycine-coated devices show conventional p-type characteristics (on/off ~10³). Simulation studies have revealed that such significant changes in transport property commence from the decreased effective electric field that SWNTs may experience. Such a gate field shielding phenomenon is believed to occur because individual SWNTs are wrapped with alcohols, which play as an another dielectric layer than 500 nm thick SiO₂ underneath dielectric layer.

10:30 AM DD13.8

Schottky, p-n Junction and Light Emitting Diodes Employing (In,Ga)N Nanorod Heterostructures. Parijat Pramil Deb^{1,2}, Hogyoung Kim^{4,2}, Yexian Qin^{4,2}, Roya Lahiji^{4,2}, Mark Oliver^{1,2}, David Ewoldt^{1,2}, Ron Reifenger^{4,2} and Timothy Sands^{2,1,3}; ¹Materials Engineering, Purdue University, West Lafayette, Indiana; ²Birck Nanotechnology Center, Purdue University, West Lafayette, Indiana; ³Electrical Engineering, Purdue University, West Lafayette, Indiana; ⁴Physics, Purdue University, West Lafayette, Indiana.

The lateral relaxation of lattice misfit strain in heterostructures grown on nanoscale substrates substantially increases the range of lattice misfit and overlayer thickness that can be accommodated without the introduction of extended defects. In the case of (In,Ga)N, nanoheteroepitaxy offers the possibility of increasing the maximum InN mole fraction or the InN quantum dot size that can be accommodated in quantum confined structures, thereby promising a broader range of emission wavelengths from GaN-based LEDs. However, to realize devices utilizing nanostructures, it is imperative to investigate the electrical properties of individual nanorod devices, and compare their characteristics to both nanorod arrays and to devices based on conventional thin-film heterostructures. Conductive atomic force microscopy (CAFM) is a powerful tool for investigating both the morphology and the electrical behavior of individual nanorod devices. CAFM was used to make Schottky and ohmic contacts to n and p-type GaN nanorods, respectively, grown on unintentionally doped n-type GaN. The current-voltage (I-V) characteristics obtained from the CAFM study were compared to those from large-area contacts made by metal deposition over the exposed tips of ~110000 nanorods. For CAFM Schottky diodes to n-GaN nanorods, the barrier height was reduced and the ideality factor increased relative to a planar contact to n-GaN without nanorods. The difference in Schottky barrier I-V characteristics can be attributed to enhanced tunneling current due to the reduction of the barrier width in the presence of a nanoscale contact. The nanorod p-n junction diodes exhibited a dramatic reduction in the ideality factor as compared to planar diodes grown under similar conditions. The improvement in junction characteristics may be attributed to the absence of dislocations in the nanorods. The reverse breakdown voltage was found to be larger for large-area contacts to an array of p-n junction nanorods compared to I-V characteristics measured from single p-n junction nanorods by CAFM. The possibility of fabricating dislocation-free light-emitting nanorod heterostructures with self-organized (In,Ga)N axial quantum dot arrays will be highlighted, and their application to phosphor-free white light emitters will be discussed. This material is based upon work supported by the Department of Energy under Award Number DE-FC26-06NT42862 and by the National Science Foundation (ECS-0424161).

10:45 AM DD13.9

Lead Chalcogenide Nanowires and Hyperbranches for Multiexciton Generation Solar Cells Yi Cui, Jia Zhu and Hailin Peng; Stanford University, Stanford, California.

Incorporating multiexciton generation (MEG) into solar cells can potentially increase the power conversion efficiency dramatically. MEG been demonstrated in lead chalcogenide nanocrystals by Klimov and Nozik. Here we report the synthesis and measurements on lead chalcogenide nanowires towards MEG solar cells. We show that nanowire and hyperbranched network structures can be synthesized via a vapor-liquid-solid (VLS) growth. The epitaxial growth can be achieved using cheap NaCl substrates. The electron transport and MEG measurements in these nanowires will be discussed.

11:00 AM *DD13.10

Quantum Dot Synthesis - The Journey from Milligram to Kilogram. Margaret A. Hines, Evident Technologies, Troy, New York.

Methods to produce high quality quantum dots have been rooted in the literature for well over a decade. Originally they required reagents that were expensive and dangerous to handle. The methods evolved and now utilize significantly cheaper and easier to handle reagents making large scale production and commercial manufacture of quantum dots readily feasible. In turn, applications harnessing QD technology are no longer academic demonstrations but rather on the frontline of product development throughout industry worldwide. Evident Technologies is a forerunner in the manufacture of quantum dots and in the research and development of products for the life sciences, security and markings, and LED/displays markets. In this talk I will present an industrial perspective of quantum dot synthesis. The challenge is not merely an issue of scaling but extends to consistently producing high quality materials that meet product specifications across an array of applications. Accordingly, we are utilizing the insight gained from the scale-up of current products in the development of new quantum dot materials.

11:30 AM DD13.11

Growth and Characterization of InAs Quantum Dot Enhanced Photovoltaic Devices. Seth Hubbard¹, Ryne Raffaele¹, Ross Robinson¹, David Wilt² and Sheila Bailey²; ¹Physics, Rochester Institute of Technology, Rochester, New York; ²Photovoltaic and Space Environment Branch, NASA Glenn Research Center, Cleveland, Ohio.

Recent proposals have pointed to alternate approaches to improving solar cell efficiency using low dimensionality nanostructured materials. Insertion of low dimensional heterostructures (i.e., quantum dot arrays) into the intrinsic region of a single junction p-i-n solar cell may lead to formation of an intermediate band. Theoretical studies have predicted such an approach could yield a photovoltaic efficiency near 63%. In this paper, Organometallic Vapor Phase Epitaxy (OMVPE) was used to: first, optimize InAs quantum dot (QD) growth on GaAs; and secondly, grow GaAs PIN solar cells with the optimized QDs. The effects of substrate offset, QD growth temperature, and V/III ratio were studied using photoluminescence spectroscopy (PL), PL mapping, and atomic force microscopy (AFM). Higher growth temperatures resulted in improved QD density and PL intensity. The V/III ratio also had a strong effect on the uniformity of QD nucleation across the wafer, with a lower V/III ratio resulting in improved distributions in size and coherence. The optimal QDs had a size and density of $7 \times 40 \text{ nm}$ and $5(\pm 0.5) \times 10^{10} \text{ cm}^{-2}$, respectively. PL spatial maps show the QD size (peak PL wavelength) and coherence (PL intensity) across the 2" wafer varied by 0.3% and 16 %, respectively. Quantum dot arrays with 5 layers were grown using the optimized growth conditions. A 10 nm GaAs spacer layer was grown between each dot layer. The PL peak for the stacked dots was centered near 1.08 eV, indicating a slight decrease in dot size. PL mapping showed a wavelength (dot size) and intensity (coherence) distribution across the wafer of 2.5% and 24%. In addition to the standard stack of 5 QD layers, a strain compensated version was also grown. In this case, a 1nm GaP strain compensated layer was inserted into the 10 nm GaAs spacer layer. PL peak wavelength was still centered near 1.08 eV and the mapping showed a wavelength uniformity of 2.5%. However, PL intensity was doubled in magnitude and the uniformity improved to 11%. Four GaAs PIN solar cells were then grown: (1) a standard PIN cell without QDs, (2, 3) cells with both 1 and 5 layers of QD in the i-region, and (4) and a cell with 5 layers of strain compensated QDs in the i-region. An array of 1 cm² solar cells was fabricated on each type of wafer, IV curves were collected under AM0 conditions, and the spectral response was measured from 300-1100 nm. The spectral response for each QD cell clearly shows

sub bandgap conversion, indicating adsorption due to the QDs. Unfortunately, the 1 and 5 layer uncompensated QD solar cells show degraded efficiency. However, the strain compensated QD cell shows clear efficiency and power improvements over either of the 1 and 5 layer uncompensated QD cells, as well as the subgap conversion. In addition to the efficiency, the other solar cell performance metrics will be discussed for both the baseline and QD cells.

11:45 AM DD13.12

Silicon and Silicon-Germanium Nanorod and Nanorod Array Synthesis for Solar Cell Applications. Brendan M. Kayes, Michael A. Filler, Morgan C. Putnam, Michael D. Kelzenberg, Julie S. Biteen and Harry A. Atwater; Applied Physics, California Institute of Technology, Pasadena, California.

Silicon and silicon-germanium nanorod arrays have the potential to enable low-cost, high efficiency solar cells via efficient radial minority carrier collection in materials with low minority carrier diffusion lengths [1]. This can be achieved by creating an optically thick array of nanorods aligned normal to a substrate in which each nanorod has a radial pn junction, enabling light absorption along the entire rod length but minority carrier collection along the rod minimum dimension in the radial direction. Silicon and silicon-germanium nanorods for photovoltaic applications have been grown by a vapor-liquid-solid (VLS) chemical vapor deposition (CVD) process on silicon and germanium substrates from 5% silane or germane diluted in argon using both gold and indium as catalysts. Catalyst particles were formed either by lithography or by partial de-wetting of vapor-deposited films of the catalyst material to form droplets with diameters of tens to hundreds of nanometers. Via lithographic catalyst particle patterning, silicon nanorods were grown with diameters of 100 nm to microns and lengths of microns to tens of microns. Dense arrays of silicon nanorods highly-aligned normal to the substrate were achieved with substrate temperatures of 500-550°C and a total pressure of 1 Torr. Varying flow rate between 40 and 200 sccm was found to have relatively little effect on the results. Silicon-germanium nanorods were also prepared by initially growing silicon nanorods and switching to a germane source, as well as reducing the substrate temperature to 300°C, halfway through the deposition process. Photoluminescence (PL) decay lifetime measurements acquired at 1125 nm for silicon nanorod arrays prepared using gold catalysts indicate a minority carrier lifetime on the order of 1 μ s. Four-point probe measurements performed on individual nanowires indicate that nominally undoped 1 μ m diameter rods grown by CVD synthesis have a resistivities of 2.5 k Ω -cm, corresponding to an electrically-active doping concentration of approximately 10^{13} cm⁻³, while boron-doped rods grown using a silane/trimethylboron (141 ppm) mixture yielded resistivities on the order of 0.1 Ω -cm, corresponding to an electrically-active doping concentrations greater than 10^{17} cm⁻³. Photoconductivity was observed in individual nanowires illuminated at 514 nm. [1] Kayes, Atwater, and Lewis, J. Appl. Phys., 97, 114302 (2005).

SESSION DD14: Devices and Applications of Low Dimensional Materials II

Chairs: Yi Cui and Xiao-Min Lin
Thursday Afternoon, April 12, 2007
Room 2001 (Moscone West)

1:30 PM *DD14.1

Nanowire Building Blocks for Photonics & Electronics Peidong Yang, University of California, Berkeley, California.

Nanowires are of both fundamental and technological interest. They represent the critical components in the potential nanoscale electronic and photonic device applications. Achieving high level of synthetic control over nanowire growth allows us to explore some of their very unique physical properties. For example, semiconductor nanowires can function as self-contained nanoscale lasers, sub-wavelength optical waveguides, frequency converters and photodetectors. It was also discovered that the thermoconductivity of the silicon nanowires can be significantly reduced when the nanowire size in the 20 nm region, pointing to a very promising approach to design better thermoelectrical materials for energy conversion. In this talk, I will outline our recent efforts in the direction of using nanowires for photonics, electronics and energy conversion applications.

2:00 PM DD14.2

New Maskless Process for Directed Assembly of Nanowire Electrical Contacts. Sarang Ingle¹, Pavan Aella¹, S. J. Hearne² and S. T. Picraux^{3,1}; ¹School of Materials, Arizona State University, Tempe, Arizona; ²Center for Integrated Nanotechnologies, Sandia National Laboratories, Albuquerque, New Mexico; ³Center for Integrated Nanotechnologies, Los Alamos National Laboratory, Los Alamos, New Mexico.

A new approach to electrically contacting semiconducting nanowires is presented. Studies of silicon nanowires for novel field-effect transistor elements and chemical/biological sensors have shown promising results. However every study that exploits electrical control of nanowire properties first requires the establishment of good electrical contact to the nanowire. Previous approaches have shown that electron beam lithography is very useful in establishing metal-nanowire contacts for exploratory studies, but this technique is slow and hence not suitable for mass fabrication. While there have been other techniques reported that are promising for mass assembly of electrical contacts to nanowires onto a device platform, they require either a post nanowire assembly photolithography step which increases cost and processing complexity, or a specific substrate orientation which may not always be possible when nanowires are to be integrated onto a chip with other devices. Thus new techniques that are easy to integrate, low cost and involve minimum additional time are needed for integration of nanowires onto device platforms. In the present work we report a maskless process for establishing metal contacts to silicon nanowires. In the first step of our process nanowires are aligned using dielectrophoresis between pairs of planar metal electrodes that have been photolithographically defined on top of oxidized silicon substrate. After alignment the nanowires are held in place by the Van der Waals attraction with the electrodes. In order to get good electrical contacts to the two ends of such nanowires one needs to deposit metal on top of them. One way to achieve this is to perform a photolithography step followed by metal deposition. However present work renders such a photolithography step unnecessary and therefore we call it a maskless process. This is achieved through the use of electroplating, which is routinely used in the semiconductor industry. The prefabricated metal electrodes act as selective sites for metal deposition during electroplating with the ends of the nanowires becoming encapsulated by the plated metal. We demonstrated this process using electrodeposited nickel on electrically doped Si nanowires. Good coverage and control for nanowires aligned between Au/Cr pre-deposited electrodes was achieved and post-electroplating annealing resulted in low contact resistances (~10 k Ω m). The results are promising for development of a general mass-level integration technique for nanostructures on device platforms.

2:15 PM DD14.3

High Performance Silicon Nanowire Transistors by the Self-assembling "Grow-in-Place" Approach. Yinghui Shan and Stephen J. Fonash;

Center for Nanotechnology Education and Utilization, The Pennsylvania State University, University Park, Pennsylvania.

High performance silicon nanowire (SiNW) transistors have been fabricated by our novel nanochannel-template-guided self-assembling "grow-in-place" approach. Our approach offers the ability of synthesizing self-positioned/self-assembled SiNWs in place, for SiNW device fabrication, directly from the Si source gas. The pre-defined nanochannel template in this approach "nurses" and guides the SiNW vapor-liquid-solid (VLS) growth, giving control of nanowire size, number, inter-wire spacing, position and orientation. With the grown SiNWs fixed by the channels of the permanent templates, transistors are then easily made, in position, from these well-controlled, self-positioned and self-assembled "grow-in-place" nanowires by simple photolithography, without any "grow-and-place" difficulties; i.e., there are no nanowire collecting, picking, handling, assembling and integrating steps in our process. As a demonstration, we report on the performance of single SiNW field effect transistors, configured as top gate structures with core-shelled thermal SiO₂ as the dielectric layer. The application of our approach is not limited to SiNW. Other nanowire or nanotube devices of different materials can be fabricated through our approach by using different precursor gases, catalysts and growth conditions. Our nanowire transistor "grow-in-place" fabrication approach is mass-manufacturable and environmentally benign since only the exact number of nanowires needed is fabricated and the fabricated nanowires are always fixed by the guiding channels of the permanent template structure.

2:30 PM DD14.4

Ultra-large Scale Directed Assembly of Single-walled Carbon Nanotube Devices. Aravind Vijayaraghavan, Sabine Blatt, Matti Oron-Carl, Frank Hennrich, Horst Hahn and Ralph Krupke; Institut für Nanotechnologie, Forschungszentrum Karlsruhe, Karlsruhe, Germany.

Despite the rapid progress in understanding the electronic transport behavior of single-wall carbon nanotubes and their numerous potential applications in nano-electronics, the fabrication of nanotube devices still remains the biggest obstacle in the way of practical realization of their enormous potential. In this presentation, we demonstrate the use of A/C dielectrophoresis to fabricate individual nanotube devices on a large scale. We have achieved densities of 3 - 4 million devices/cm², which is many orders of magnitude greater than anything that is possible with other methods. This density is comparable to the current level of microelectronics complexity, namely Ultra-Large Scale Integration (ULSI). We also show an added advantage of this technique, in that it is a self-limiting process, allowing only an individual nanotube to deposit between the electrodes for each device, which is highly desirable for controlled device fabrication. We include finite-element simulations of the dielectrophoretic force experienced by the nanotube, in order to illustrate this self-limiting behavior. In addition to these primary achievements, we also present a new, two-layer metallization technique, which surrounds the ends of the nanotubes in metal. This is unlike other fabrication techniques where the nanotube lies either on top or underneath the metal only. By this method, we provide a robust and reliable way significantly reduce the metal-nanotube contact resistance. Systematic electrical characterization of our devices is also presented. The techniques and discussions presented here are not merely limited to carbon nanotubes. In fact, dielectrophoresis is a universal phenomenon observed in a number of nano-scale objects like nano-wires, nano-particles, and even biological molecules and cells. The results in the presentation have universal appeal as they can be adapted and extended to form large-scale systematic electrical contacts to any number of such nano-scale objects. Dielectrophoresis can also be used to fabricate other nanotube structures, such as thin conducting films, and also to separate nanotubes according to their electronic properties (see contribution "Upscaling dielectrophoretic nanotube separation and probing dielectrophoretic force fields" by S. Blatt et al.)

2:45 PM DD14.5

Schottky-Barrier Si Nanowire MOSFET: Effects of Source/Drain Metals and Gate Dielectrics. Weifeng Yang, Sung Jin Whang, Sung Joo Lee, Haichen Zhu, Hanlu Gu and Byung Jin Cho; ECE department, SINDL, NUS, Singapore, Singapore.

Bottom up grown 1-dimensional semiconductor nanowires have recently been emerging as powerful building blocks for novel nanoscale device applications. In this work, we fabricated and studied the performance of Schottky-Barrier Si nanowire MOSFETs. Vapor-liquid-solid grown Au-catalyzed Si nanowires (10~20 nm) were dispersed on various gate dielectrics (ALD-grown HfO₂, Al₂O₃, thermal SiO₂) formed on TaN/Ta stack, which was deposited on Si substrate as a back gate electrode. After patterning the source/drain contact by E-beam lithography, different metals (Pd, Ni, Ti, Yb) were deposited by E-beam evaporation, followed by lift-off process. The distance between source and drain electrode is typically ~ 1 μ m. First, p-type behavior was observed from undoped Si nanowire MOSFETs: accumulation and transport of hole carriers from source through channel and higher conduction with more negative gate voltage (V_g). The clear difference in drain current (I_d) was also observed for different source/drain metals. Much higher I_d and I_{on}/I_{off}, and better gate controllability from high work function metals (Pd, Ni) suggest that the carrier transport in Si nanowire MOSFETs are dominated by Schottky barrier at source side. High I_{on}/I_{off} ratio as 1E5 was achieved from Si nanowire MOSFET with Pd source/drain electrode and 20nm ALD- HfO₂. This transistor also exhibited small changes in I_d-V_g curves at different drain voltage (V_d), implying that the Schottky barrier for hole at the source side is insignificant so that the increase in I_d due to drain voltage induced band-bending can be reduced, while significant increase in I_d and degraded subthreshold slope with increasing V_d was observed for MOSFETs with Ti and Yb source/drain electrodes. Subthreshold transport characteristics of Schottky-Barrier Si nanowire MOSFETs will be determined by the interface quality between Si nanowire and gate dielectrics and/or Schottky barrier height between Si nanowire and source/drain metals. Low subthreshold slope as 80mV/decade was obtained from Si nanowire MOSFETs integrated with ALD-HfO₂ and ALD-Al₂O₃ gate dielectric.

3:00 PM DD14.6

Modeling the Carrier Mobility in InAs Nanowire Channel FET. Werner Prost, Quoc-Thai Do, Ingo Regolin, Kai Blekker and Franz-Josef Tegude; Solid-State Electronics Department, University Duisburg-Essen, Duisburg, Germany.

Selectively doped InAs nanowires exhibit excellent material properties including a low contact resistance and very high current density [1]. However, the determination of carrier type, carrier concentration, and carrier mobility is a difficult task for any nanowire. While the contact and wire resistance can both be determined by applying multiple contacts and transmission line type measurements, detailed transport data remain uncertain. We report on the extraction of a full set of transport data such as carrier type, density, and mobility by adopting experimental nanowire field-effect transistor device data to a MISFET device model. InAs:Si nanowires were grown by the vapour-liquid-solid growth mode in a LP-MOVPE. Colloidal Au nanoparticles of 50 nm in diameter were deposited on the InAs (100) substrate surface as seed particles prior to the growth. The seed particles were annealed at 600 °C for 10 minutes under nitrogen and tertiarybutylarsine flow in order to form an Au-In alloy and to remove the oxide. N-InAs nanowhiskers were grown at a temperature of T_g = 400 °C for 10 minutes with a constant V/III ratio of 6 with N₂ as a carrier gas. Trimethylindium was used as group-III precursor, tertiarybutylarsine as group-V precursor, and di-tert-butylsilane was used for the n-type doping. Numerous field-effect transistor (FET) were fabricated using the grown InAs nanowires with a diameter of d = 50 nm as a channel. A wide range of SiNx insulation layer thickness of h = 20 nm to 90 nm, and gate length of LG = 1 μ m to 3 μ m were realized. The devices exhibit a very high current density of up to I_D = 8E6 A/cm² and also a very high maximum transconductance of up to gm/d = 3.5 S/mm. The I-V data of the fabricated FET were analysed at

low drain bias in order to reduce the effect of extrinsic resistances. With these I-V data obtained from a wide range of experimental device parameters a good proof of the validity of the selected long channel MISFET model became feasible. For this model, the determination of the capacitance of the partly wrapped gate requires careful consideration and was carried out by electrostatic field simulation software based on the finite difference method. After determination of the gate capacitance, the carrier mobility remains as the solely parameter to fit experimental modeled device data. This way, the electron mobility in InAs nanowires forming a FET channel is evaluated to $\mu = 13,000 \text{ cm}^2/\text{Vs}$. [1] Bryllert T; Wernersson L E; Froberg L E; Samuelson L; IEEE Electron Device Letters, 27 (2006) 5, p. 323-5 [2] Mohny S E; Wang Y; Cabassi M A; Lew K K; Dey S; Redwing J M; Mayer T S; Solid-State Electronics 49(2005) 227-232.

SESSION DD15: Synthesis and Characterization of Nanoscale Materials I
Chairs: Masaru Kuno, Moonsub Shim and Peidong Yang
Thursday Afternoon, April 12, 2007
Room 2001 (Moscone West)

3:30 PM *DD15.1

Synthesis and Characterization of Ultrathin Nanorods, Nanowires, and Nanoribbons of Oxides and Chalcogenides Taeghwan Hyeon^{1,2}, Taekyung Yu^{1,2}, Kwangjin An^{1,2}, Sang-Hyun Choi^{1,2}, Jung Ho Yu^{1,2} and Jin Joo^{1,2}; ¹School of Chemical and Biological Engineering, Seoul National University, Seoul, South Korea; ²National Creative Research Center for Oxide Nanocrystalline Materials, Seoul National University, Seoul, South Korea.

Uniform-sized ultra-thin nanorods and nanowires of lanthanide oxides were synthesized via non-hydrolytic sol-gel reactions. Ceria (CeO₂) nanowires with a uniform diameter of 1.2 nm and a length of 115 nm were synthesized [Angew. Chem. Int. Ed. 2005, 44, 7411]. We synthesized novel tadpole-shaped nanowires consisted of spherical head with a diameter of 3.5 nm and wire-shaped tail with a diameter of 1.2 nm and length of 27 nm. We synthesized uniform rectangular shaped samaria nanowires with uniform cross-section dimensions of 1.1 nm × 2.2 nm [J. Am. Chem. Soc 2006, 128, 1786]. Uniform sized pencil-shaped CoO nanorods with an extraordinary wurtzite ZnO crystal structure by the thermal decomposition of a cobalt-oleate complex [J. Am. Chem. Soc 2006, 128, 9753]. The simultaneous phase- and size-controlled synthesis of TiO₂ nanorods was achieved via the non-hydrolytic sol-gel reaction of continuously delivered two titanium precursors using two separate syringe pumps [J. Phys. Chem. B 2006, in press]. We reported low temperature solution-phase synthesis of one-dimension (1-D) quantum confined CdSe nanoribbons with uniform and ultrathin thickness of 1.4 nm [J. Am. Chem. Soc 2006, 128, 5632]. Very interestingly, the room temperature photoluminescence spectrum of the CdSe nanoribbons showed a sharp peak at 2.74 eV (451 nm) with an unprecedented narrow band of a full width at half-maximum (FWHM) of as small as 70 meV (11 nm). We successfully doped Mn(II) ions into the 1.4 nm thick CdSe nanoribbons. We synthesized the Cu-In sulfide heterostructured nanocrystals from the thermal decomposition of a mixture of Cu-oleate and In-oleate complex in dodecanethiol. By varying the reaction temperature and time, we were able to synthesize Cu-In sulfide nanocrystals with acorn, bottle, and larva shapes [J. Am. Chem. Soc 2006, 128, 2520].

4:00 PM DD15.2

Growth and Properties of Superconducting Anisotropic Lead Nanoprisms Xiao-Min Lin¹, Helmut Claus², Ulrich Welp², Igor Beloborodov², Laura Adams³, Wai-Kwong Kwok², George Crabtree² and Heinrich Jaeger³; ¹Center for Nanoscale Materials, Argonne National Lab, Argonne, Illinois; ²Materials Science Division, Argonne National Laboratory, Argonne, Illinois; ³The James Franck Institute, University of Chicago, Chicago, Illinois.

Anisotropic shaped Pb nanoprisms were synthesized using high temperature polyol reduction of lead acetylacetonate through a kinetically controlled synthesis. Transmission electron microscopy studies showed the majority of the prisms grows along {111} planes while nanowires grow in various directions. SAED on single prism revealed the anisotropic growth is due to twinning in the growing nuclei. Magnetic measurements showed a large magnetic hysteresis that is due to the penetration and pinning of magnetic vortices. The flux trapping behavior could be due to type-I intermediate state caused by a large shape induced demagnetization factor or a possible transition from type-I to type-II superconductor due to finite thickness of the prisms.

4:15 PM DD15.3

Cetyltrialkylammonium Bromide Mediated Growth of Gold Nanorods and Bipyramids Chia-kuang (Frank) Tsung^{1,2}, Xiaoshan Kou², Jianfang Wang² and Galen D Stucky¹; ¹Chemistry and Biochemistry, University of California Santa Barbara, Santa Barbara, California; ²Department of Physics, Chinese University of Hong Kong, Shatin, Hong Kong.

Gold nanorods have been prepared in high yields using a one-step seed-mediated process in aqueous cetyltrialkylammonium bromide solutions in the presence of silver nitrate. In order to explore the effect of the head group size on the growth of nanorods and to have better control of the synthesis, surfactants (cetyltrialkylammonium bromide) with different head groups have been used to synthesize gold nanorods. The diameters of the nanorods range from 3 to 11 nm, their lengths are in the range of 15 to 350 nm, and their aspect ratios are in the range of 2 to 70. These Au nanorods are single-crystalline and oriented in either the [100] or [110] direction under transmission electron microscopy imaging, irrespective of their sizes. The systematic study of the synthesis of gold nanorods indicates unambiguously that the average aspect ratios of the Au nanorods generally increase and the nanorod growth rates decrease as the cationic surfactant head group becomes larger. To the best of our knowledge, this is the first report on the preparation of single-crystalline Au nanorods that have aspect ratios larger than 15 using wet-chemistry methods. Furthermore, by using penta-twinned seeds instead of single crystal seeds during the synthesis, gold nano bipyramids can be synthesized. Transmission electron microscopy characterizations reveal that the gold bipyramids are penta-twinned. The diameters and lengths of the bipyramids are also tunable by varying the amount of the seeds and using surfactants with different head groups and the longitudinal plasmon wavelength of the bipyramids ranges from 700 nm to 1300 nm. It is interesting to note the sharp and intense of the extinction peak generated by longitudinal surface plasmon mode of the gold bipyramids. Compared with gold nanorods, the sharpness and intensity extinction peak has stronger potential for application in bio imaging and signal enhancement.

4:30 PM DD15.4

Plasmonic and Structural Effects in the Growth of Ag Triangular Nanoplates Tulio Rizzuti Rocha^{2,1}, Herbert Winnischofer³, Eduard Westphal⁴, Socrates Dantas², Douglas Galvao² and Daniela Zanchet¹; ¹Laboratório Nacional de Luz Síncrotron, Campinas, São Paulo, Brazil; ²Universidade Estadual de Campinas, Campinas, São Paulo, Brazil; ³Universidade Federal do Paraná, Curitiba, Paraná, Brazil; ⁴Universidade Federal de Santa Catarina, Florianópolis, Santa Catarina, Brazil.

The shape control of metallic nanoparticles has been a subject of intensive research in the past few years because it provides an alternative way, in addition to size, to tune the properties of a metal. In this work, we present solid experimental evidences corroborated by computational simulations of the important role of surface plasmons (SP) and structural defects in the growth mechanism of photochemically synthesized Ag triangular nanoplates (TNPs). The use of incident radiation with different wavelengths revealed that two different growth processes are present: an initial slow growth (stage I), when small TNP are formed and a second rapid anisotropic growth (stage II), which begins when the surface plasmon resonance (SPR) peak of the growing TNPs becomes resonant with the incident light. The correlation of the reaction kinetics, followed by *in situ* Ag⁺ concentration measurements, with the morphological evolution, obtained by transmission electron microscopy (TEM) and ultraviolet-visible spectroscopy, allowed us to clearly demonstrate the enhancement of the photochemical reaction by excitation of SP of the growing particles, as evidenced by the change in the reaction rate. Our results pointed out that SP excitation plays an important role defining the final length of the nanoplates during stage II, and therefore providing an efficient size control mechanism, but it does not seem to be the main driving force of the anisotropic growth. To further understand the stage I and the origin of the anisotropic growth in this system, detailed structural characterizations were performed in the early stages of the synthesis. In the initial seeds, several particles containing many parallel twins or stacking faults in the <111> direction were observed, as indicated by X-ray powder diffraction and high resolution TEM (HRTEM). The same structure was also present in all of the TNP after irradiation. The HRTEM observation of intermediate stages revealed that TNP are formed in the early stages of the synthesis by epitaxial anisotropic deposition of Ag photoreduced atoms over the defective seeds present in the initial solution. The use of Au seeds confirmed the effect of structural defects in the growth process and also provided instructive insights about the role of the capping molecule. Finally, the use of seeds with different distribution of crystalline structures had a striking effect in the final product, pointing out the important role of structure in the shape control mechanism. Additionally, energetic calculations using a realistic potential to describe the metal particles were performed to evaluate the structural effects in the growth process and the preferential growth of anisotropic particles during stage I.

4:45 PM DD15.5

Kinetically Controlled Synthesis of Pd Nanoplates and Nanorods: Two Anisotropic Shapes with Tunable Plasmonic Properties Yujie Xiong and Younan Xia; Chemistry, University of Washington, Seattle, Washington.

The surface plasmon resonance (SPR) peaks of Pd nanoparticles (usually below 10 nm in size) are typically located in the UV region, which makes them more difficult to probe due to strong absorption of glass and most solvent at these wavelengths. In this presentation, I will demonstrate that the SPR peaks of Pd nanostructures can be tuned into the visible region by growing them into anisotropic shapes such as nanoplates and nanorods. As shown by Wulff construction, the thermodynamically favored shape of Pd is cubooctahedron which can be produced via a fast reduction of Pd precursor. We have recently developed three different approaches to control the reduction/growth kinetics and thus obtain Pd nanoplates and nanorods: i) to slow down the reduction by coupling with oxidative etching, ii) by using a mild reducing agent for the synthesis of triangular and hexagonal nanoplates; and iii) by introducing some anionic species that selectively adsorb onto certain facets and change relative surface energies of different facets for the synthesis of nanorods. By controlling the ratio of edge length to thickness of nanoplates or the aspect ratio of nanorods, their SPR peaks could be tuned to the visible and near-IR region. The synthetic strategies have also been extended to Ag and Au. It is expected that the present work will enable us to manipulate the SPR peaks of metal nanostructures and open the door to new applications in the visible and near infrared regions.

SESSION DD16: Poster Session: Synthesis and Characterization II
Chairs: Sanat Kumar, Masaru Kuno, Xiao-Min Lin, Ruth Pachter and Moonsub Shim
Thursday Evening, April 12, 2007
8:00 PM
Salon Level (Marriott)

DD16.1

Abstract Withdrawn

DD16.2

Solvothermal Synthesis and Self-assembly of One-Dimensional FePt and Fe₃O₄ Nanoparticles Min Chen^{1,2} and Hongyou Fan¹; ¹Advanced Materials Lab, Sandia National Laboratories, Albuquerque, New Mexico; ²Center for Micro-Engineered Materials, University of New Mexico, Albuquerque, New Mexico.

One-dimensional magnetic nanoparticles are promising for advanced applications in photonic, electronic, and data storage devices because of their anisotropic structures in nanoscale domain. We present here the solvothermal synthesis of one-dimensional FePt nanoparticles from simultaneous decomposition of Fe(CO)₅ and reduction of Pt(acac)₃ in an organic solvent. Low heating rate favored the formation of smooth nanorods. By simply increasing the heating time, the FePt nanowires with a length up to a few hundred nanometers were formed. Similarly, decomposition of Fe(CO)₅ produced Fe₃O₄ nanorods and nanowires. As prepared, one-dimensional Fe₃O₄ nanoparticles were amorphous. Upon annealing under protection of nitrogen gas at a temperature of 400 °C, the crystalline Fe₃O₄ nanorods were formed. The effect of annealing temperature on the crystal structures and magnetic properties of one-dimensional FePt and Fe₃O₄ nanoparticles will be discussed.

DD16.3

Single-crystalline Si Nanotip Array Fabricated Using Si-based Porous Anodic Alumina Template. GaoShan Huang¹, XingLong Wu¹ and Paul K. Chu²; ¹National Laboratory of Solid State Microstructures and Department of Physics, Nanjing University, Nanjing 210093, China; ²Department of Physics and Materials Science, City University of Hong Kong, Kowloon, Hong Kong.

Si-based SiO₂ nanoislands can be obtained by anodizing Si-based aluminum film in a 0.3 M sulfuric acid solution under a constant voltage of 25 V, with the help of monitoring current-time curve. Nanoislands were observed at the bottoms of nanochannels of Si-based porous anodic alumina membrane. The morphology and composition of this nanoisland array were characterized using atomic force microscope (AFM), x-ray photoelectron spectroscopy (XPS), and Fourier transfer infrared spectrum. The results indicate that the nanoislands consist of silicon dioxide, while the 25-nm height of the SiO₂ nanoisland can be determined by XPS depth profile. According to the growth model of the SiO₂ nanoislands, a Si nanotip exists at each triple point of the SiO₂ nanoisland array. After a series of experiments, we established appropriate experimental conditions to completely remove the surface SiO₂ nanoislands and to exposure the underneath single-crystalline Si nanotips, which have the same crystal orientation as that of the starting wafer. Obviously, the density and ordering of the Si nanotips inherit those of previous SiO₂ nanoislands. AFM measurement demonstrates that these single-crystalline Si nanotips with a very sharp end have uniform bottom diameters of 20-30 nm and heights of ~20 nm. Most importantly, this array shows an excellent field emission property with a low turn-on field of 8.5 V/ μ m (defined as the electric field to extract a current density of 10 μ A/cm²) and a homogenous emission area. The obtained Fowler-Nordheim plot is linearly dependent, indicating that the emission current arises from the quantum tunneling effect. Based on our experimental results, we can roughly estimate the field enhancement factor (β) to be as large as 1100 for current single-crystalline Si nanotip array. The favorite field emission property of the single-crystalline Si nanotip array is considered to be intimately connected with its unique geometrical structure, perfect surface composition, and good contact with underlying Si substrate. This kind of Si nanotip arrays can be expected to have important applications in nanoelectronic devices.

DD16.4

Sol Gel Synthesis of Ge Nanophases in Silica Matrix. Norberto Chiodini, Sergio Brovelli, Alessandro Lauria and Alberto Paleari; Dip. di Scienza dei Materiali, Università di Milano-Bicocca, Milano, Italy.

Communication technology has created a high demand for optoelectronic functional units able to generate, to modulate and to process optical signals. Whereas a plurality of solutions for the processing of optical signals already exists, up to now there are no satisfying devices to transform electrical into optical signals within integrated circuits. Looking for alternative light-emitting materials, Si-nanoclusters in silica are of interest because they offer the possibility to avoid the disadvantage of an indirect Si band gap [1]. Other semiconductive nanophases, such as Ge, Sn and also wide band gap semiconductor like SnO₂ [2] dispersed in silica, are recently under investigation for such a purpose as well. Typical methods of synthesis of Si and Ge nanocluster in glass materials are from CVD or ion implantation. In this work we show a new sol-gel synthesis of elemental Germanium nanophase in silica matrix phase separated from germanium-doped silica xerogel. Silica xerogel with different Ge concentration are synthesized by sol-gel method. Elemental Ge is obtained during sintering procedure by a suitable reducing atmosphere and so phase separated. Characterization was carried out by means of micro-Raman spectroscopy, I.R. spectroscopy, X-ray diffraction [2,3] and TEM, showing cubic Ge nanophases. Light emission activity due to recombination centers in the glass matrix is also investigated to verify the feasibility of light emitter devices. Bibliography: 1) L. Pavesi, L. Dal Negro, C. Mazzoleni, G. Franzoi & F. Priolo; "Optical gain in silicon nanocrystals"; Nature 408, pp. 440-444, November 2000 2) N. Chiodini, A. Paleari, M. Romagnoli, "Nanostructured SnO₂ - SiO₂ glass ceramic: a competitor for Si nanodots in silica" SPIE vol. 5925 (2005) 3) F. Pezzoli, Lucio Martinelli, E. Grilli, M. Guzzi, S. Sanguinetti, M. Bollani, H.D. Christina, G. Isella, H. von Kanel, E. Wintersberger, J. Stangl, G. Bauer; "Raman spectroscopy of Si_{1-x}Gex epilayers"; Materials Science and Engineering B 124-125, pp 127-131 (2005) 4) X. L. Wu, T. Gao, X. M. Bao, F. Yan, S. S. Jiang, and D. Feng; "Annealing temperature dependence of Raman scattering in Ge-implanted SiO₂ films"; J. Appl. Phys. 82, 2704 (1997)

DD16.5

Surface Modification of Si Nanocones Fabricated by Porous Anodic Aluminum Oxide Templation. Te-Ming Chen¹, Jui-Yi Hung¹, Fu-Ming Pan¹, Shieh-Chuan Wu² and L. Chang¹; ¹Dept. Mat. Sci. Eng., National Chiao Tung University, Hsinchu, Taiwan; ²National Nano Device Laboratories, Hsinchu, Taiwan.

Anodic aluminum oxide (AAO) has a highly ordered hexagonal pore arrangement, and has been widely used as a template for nanostructured materials fabrication, such as carbon nanotubes. Using AAO as a template in conjunction with reactive ion etch, we have prepared Si nanocones with an arrangement in compliant with that of the AAO. To prepare the AAO template, an Al film 2 μ m thick was first thermally evaporated on a sputter-deposited TiN layer of 30 nm in thickness. The Al film was anodically oxidized in an oxalic acid electrolyte at room temperature, and the finished AAO pores had a pore diameter about 60 nm. During the preparation of the AAO pore channels, the underlying TiN layer was anodically oxidized as well in the late stage of the AAO anodization forming titanium oxide nanodots. The TiO_x nanodots were then used as the hardmask for dry-etching the remaining TiN and the Si substrate, thereby transferring the AAO hexagonal arrangement pattern to the Si substrate leading to the formation of the well-ordered Si nanocone array. To improve field emission properties of the Si nanocones, we have deposited an iridium oxide layer by electrodeposition or an ultra thin a-carbon layer by microwave plasma chemical vapor deposition on the nanocones. The two types of modified Si nanocones showed improved field emission properties as compared to the as-prepared Si nanocones. Details in fabrication and field emission characteristics of the surface-modified Si nanocones will be discussed.

DD16.6

Post-annealing Induced Formation of ZnO Nanowires on the ZnO Films in the N₂O Ambient. Ping-Yuan Lin¹, Wei-Tsai Liao¹, Kuo-Yi Yan¹, Chia-Chi Chang¹, Jyh-Rong Gong¹, Jian-Hao Lin² and Tai-Yuan Lin²; ¹Department of Physics, National Chung Hsing University, Taichung City, Taiwan; ²Institute of Optoelectronic Sciences, National Taiwan Ocean University, Keelung, Taiwan.

Zinc oxide (ZnO) has received great attention because of its direct wide band gap nature ($E_g = 3.3$ eV at room temperature) and large exciton binding energy of ~ 60 meV which is larger than that of GaN[1]. In addition, ZnO is thermally and chemically stable in air. Various applications have been proposed for ZnO including gas sensors[2] and ultraviolet (UV) photonic devices[3]. Recently, ZnO nanowires have been studied extensively using different growth approaches including metal-mediated growth. In this paper, we report the preparation of ZnO nanowires by post-annealing ZnO films in the N₂O ambient at elevated temperatures. ZnO films were grown on (0001) sapphire substrates by atomic layer deposition (ALD) using diethylzinc (DEZn) and nitrous oxide (N₂O) in an inductively heated reactor operated at atmospheric pressure. In this case, purified nitrogen gas was used as the carrier gas. Low-temperature(LT) ZnO buffer layers having various thicknesses were deposited at 400 C followed by subsequent growth of ZnO films at 600 C. The ZnO films were then post-annealed at 1000 C in the N₂O flow. Under certain growth conditions, ZnO nanowires were formed on the post-annealed ZnO samples. Based on scanning electron microscopic (SEM) observations, it was found that ZnO embryos were

nucleated on the as-grown ZnO film and grew into ZnO nanowires during thermal annealing. Room temperature (RT) photoluminescence (PL) spectrum of the ZnO nanowires shows strong ultraviolet (UV) near band edge emissions at 3.27 eV with a typical full width at half-maximum (FWHM) of 130 meV and quenched green luminescence at 2.8 eV. 10 K PL spectrum of the best ZnO nanowires only exhibits excitonic emissions with the dominant emission being located at 3.394 eV having a FWHM of 5 meV. [1] A. Mang, K. Reimann and St. Rübenacke, Solid state Commun. 94 (1995) 251. [2] N.J. Dayan, S.R. Sainkar, R.N. Karekar, R.C. Ayer, Thin Solid Films 325(1998) 254. [3] Z.K. Yang, G.K.L. Wong, P. Yu, M. Kawasaki, A. Otono, H. Koinuma, Y. Segawa, Appl. Phys. Lett. 72 (1998) 3270.

DD16.7

Controlled Synthesis of Highly Branched TiO₂ Nanowire Heawon Chung^{1,2}, Young-wook Jun¹, Mi-yun Kim¹ and Jinwoo Cheon^{1,2}; ¹Department of Chemistry, Yonsei University, Seoul, South Korea; ²Nanomedical National Core Research Center, Yonsei University, Seoul, South Korea.

Anisotropic shape control of nanoparticles is of considerable importance due to their novel characteristics. Particularly in titanium dioxide, there are several notable synthetic methods among previous findings, but their shape is not methodically regulated nor their crystalline phase can be systematically varied. Here we demonstrate the synthesis of titanium dioxide of branched multipod nanowire structures via simple nonhydrolytic colloidal growth process. By controlling the introduction point of oxygen generating molecular precursor, two different crystalline phases rutile and anatase simultaneously form in one-pot; in consequence material shapes can be tuned from nanorod to branched nanowire structure. The length of nanowires can be varied from 20 nm to 200 nm and branched structures are typically bipods and tripods. We'll discuss the mechanism of multi-branched TiO₂ growth in detail along with photochemical properties associated with the anisotropy.

DD16.8

Biosynthesis of CdS and ZnS nanoparticles by two different Fungus Luis Reyes¹, Idalia Gomez¹, Teresa Garza¹ and Patricia Zambrano²; ¹Facultad de Ciencias Químicas, UANL, San Nicolás de los Garza, Nuevo León, Mexico; ²Facultad de Ingeniería Mecánica y Eléctrica, UANL, San Nicolás de los Garza, Nuevo León, Mexico.

The development of synthetic processes for sulfide nanomaterials is an issue of considerable topical interest. While a number of chemical methods are available and are extensively used, the collaborations are often energy intensive and employ toxic chemicals. On the other hand, the synthesis of inorganic materials by biological systems is characterized by processes that occur at close to ambient temperatures and pressures, and at neutral pH. In this paper we show that CdS and ZnS nanoparticles may be produced at room temperature intracellularly by challenging the fungi, *Fusarium* and *Penicillium* sp., with mixtures of cadmium and zinc salts. Extracellular hydrolysis of the anionic metal complexes by cationic proteins secreted by the fungi results in the room-temperature synthesis of crystalline CdS and ZnS nanoparticles that exhibit a signature of agglomeration same as assembly in sizes already of 2 micrometers. X-Ray diffraction and SEM microscopy with EDAX analysis let us to confirm the obtention of CdS and ZnS nanoparticles by this route of synthesis.

DD16.9

Templated Growth of Semiconductor Nanostructures Using Block Copolymer Lithography Seth Taylor¹, Azar Alizadeh¹, David Hays¹, Kasi Krishnan¹, Chris Keimel¹, Lauraine Denault¹, Rosalyn Neander¹, Ken Conway¹, Oliver Boomhower¹, Sanjay Krishna², Andreas Stintz², Jay Brown², Edit Braunstein³ and Colin Jones³; ¹GE Global Research, Niskayuna, New York; ²University of New Mexico, Albuquerque, New Mexico; ³Lockheed Martin, Orlando, Florida.

Semiconductor nanostructures hold great potential for achieving new capabilities in optoelectronics, field emission, and various sensing and detection technologies, but their applications to date have been limited by processing challenges and scale-up issues. Templated growth of semiconductor quantum dots through a nano-patterned mask allows for precise control over dot size, shape, spacing and uniformity, and is therefore a promising route for fabricating large arrays of quantum confined structures. Here, we report on the templated growth of sub-20 nm InAs nanostructures using molecular beam epitaxy (MBE) in concert with block copolymer lithography. Atomic force microscopy, SEM, and high resolution TEM have been used extensively to characterize nanostructure morphology as a function of different growth parameters, and to further quantify quantum dot size, spacing, uniformity and areal density. Using reactive ion etching to form an oxide mask from a block-copolymer template, we demonstrate a dense and highly uniform array of quantum-confined and optically-active InAs dots on GaAs. Correlations are drawn between the optoelectronic performance of the quantum dots, as measured by photoluminescence (PL) spectroscopy at various temperatures, and their internal (defect) structure as revealed by HRTEM. We discuss the potential for this processing technique to overcome some of the fundamental limitations posed by Stranski-Krastanow-based self-assembly approaches for quantum dot formation.

DD16.10

Size and Shape Control of Nickel Nanoparticles. Yi Yang, Yang Xiang, Chandra Khadilkar and Aziz Shaikh; Ferro Corporation, Independence, Ohio.

Nanocrystalline nickel powders, spherical or spiky shapes with the size of 10 to 100 nm, were prepared through chemical reduction of their corresponding metal salts under suitable conditions. Transmission electron microscopy (TEM), scanning electron microscopy (SEM), x-ray diffraction (XRD), BET method and thermal gravimetry (TG) were used to characterize the nickel nanoparticles prepared at various conditions. The carbon and oxygen contents and tab densities of the nano-nickel powders were also measured.

DD16.11

Scalable Synthesis of Silver Nanocubes in Less than a Minute under Microwave irradiation Subrata Kundu and Ravi F Saraf; University of Nebraska, Lincoln, Department of Chemical & Biomedical Engineering, Lincoln, Nebraska.

Shape control synthesis of inorganic nanostructures has received considerable attention in recent years because of applications in catalysis, optics, microelectronics and magnetism and medical diagnostics. A wealth of chemical methods have been developed for the synthesis of metal nanostructures that have well-controlled shapes, such as, wires, rods, disks, cubes, belts, plates, prisms and branched multipods. Faceted nanostructures, such as cubes can provide properties distinct from spherical nanoparticle, for example, pinning of the magnetic domains to attain

ferromagnetic properties at nanoscale, catalysis and SERS-based sensing that are lost in spherical shape due to thermal fluctuation. Furthermore, the ordered self-assembly cubes can be used as a templates to make superlattices for high density storage applications. Noble metal nanoparticles (NPs) such as silver with cubic shape used as a template formation of gold nanoboxes and iron nanocubes used as the building block of magnetic superlattices. Typically, current synthesis methods to make nanocubes have processing long time, high temperature and requiring multiple steps that may be challenging to translate to mass scale production. Recently, microwave (MW) as a heat source has been applied to the rapid synthesis of metallic nanoparticles due to uniform heating for the reaction solution, giving a size and shape controlled synthesis as compared to thermal convection. Here, we demonstrate a new approach for the rapid synthesis of silver nanocubes by a simple microwave irradiation approach. The formation of cubes is exclusive with very few spherical or other shaped particles. The synthesized nanocubes of Ag are stable for at least 2 months with no appreciable change in dimensions. The present approach we described here for connecting nanomaterials into desired shapes and thereby tuning their optoelectronic properties may find wide application in nanotechnology particularly in nanoelectronics and plasmonics.

DD16.12

Crystallography of the Catalytic System of Small Metallic Gold Particles Supported on Coexisting Titania Phases. Amado F. Garcia-Ruiz, Physics, UPIICSA-IPN, México, D. F., Mexico; Institute of Physics, UNAM, México, D. F., Mexico; CCADET, UNAM, México, D. F., Mexico.

A. Morales and X. Bokhimi. Institute of Physics. The National University of Mexico (UNAM), A. P. 20-364, 01000 México, D. F., Mexico. A. Garcia-Ruiz. UPIICSA-COFAA. The National Polytechnic Institute (IPN). Té 950, Iztacalco, 08400 México, D. F. Mexico. R. Zanella. Center of Applied Sciences and Technological Development (CCADET). The National University of Mexico (UNAM), A. P. 70-186, 04510 México, D. F., Mexico. Synthesis of titania to get a high concentration of brookite coexisting with rutile and anatase were tried out by two ways. In the first way, an aqueous solution of titanium butoxide with hydrochloric acid was treated hydrothermally at the synthesis temperature, between 90 C and 200 C, with several molar ratios H_2O/HCl and a fix ratio $HCl/TiBu$. In the second way, coexisting titania polymorphs were prepared by sol gel, starting from an acidic solution, nitric acid for obtaining anatase or rutile as dominant phase or hydrochloric for obtaining brookite as predominant, and aggregating titanium butoxide for get, annealing at 90 C, a precipitate of titania. The specimens obtained in this second way were utilized as support to prepare catalysts Au/TiO_2 and $Au/Ce-TiO_2$ with 5 wt% Au and 12 % cerium concentration, also by sol gel. Samples were characterized by X-ray diffraction, which allowed to refine the crystalline phases of titania using the Rietveld method for obtaining the concentration and the lattice parameters of the three polymorphs, as well as the size and the morphology of the crystallites. For the samples obtained in the first method, these parameters were obtained as function of the ratio H_2O/HCl and also of the synthesis temperature. The results showed that the synthesis with the ratio H_2O/HCl equal to 20 and the temperature of 120 C is the ideal one in order to get the maximum of the brookite concentration. The morphology and the average size of the crystals obtained by means of the refinements are in good accord with the corresponding observed values in the micrographs generated by HRTEM. For the catalysts, with titania support obtained by the second way, the Rietveld refinements provided also crystallographic features of the metallic gold phase. The gold crystallite size and morphology depended on the titania polymorph used as support: when it was anatase the gold crystallite had their smallest dimension perpendicular to their (111) planes, while for brookite and rutile it was perpendicular to the (200) planes. The large amount of structural defects in the support worked as particle pinning centers of the gold crystallites, hindering production of larger crystallites. The refinement allowed to extract the contribution of the metallic gold to the X-ray diffraction pattern of the catalyst. When anatase and brookite were doped with cerium their crystallite size decreased and their structural defects increased. For anatase, all the cerium was incorporated favoring the formation of smaller gold crystallite.

DD16.13

One-Step Microwave Preparation of Well-defined Polymeric Nanoparticles Zesheng An^{1,3}, Wei Tang¹, Craig J. Hawker^{1,2,3} and Galen D Stucky^{1,2,3}, ¹Chemistry, UCSB, Santa Barbara, California; ²Materials Research Laboratory, UCSB, Santa Barbara, California; ³Mitsubishi Center for Advanced Materials, UCSB, Santa Barbara, California.

Well-defined colloidal polymeric nanoparticles are important in advanced biomedical and optical technologies. We report a facile microwave methodology to prepare narrowly disperse, crosslinked polymeric nanoparticles at high solids content through surfactant-free emulsion polymerization process. The nanoparticle size was controlled by using crosslinkers with enhanced reactivity through a one-step microwaving process, significantly simplifying the nanoparticle synthetic process. The successful size control was realized by confining the crosslinking to intraparticle crosslinking rather than interparticle crosslinking. We also discovered that the superheating/dielectric heating effect associated with microwave irradiation could be utilized to effectively reduce the nanoparticle size.

DD16.14

Abstract Withdrawn

DD16.15

Enhanced Near UV Emission from Sunflower-like Nanostructures Composed of SiOx Nanorods with Spotty SnO2 Nanoparticles Kum M. Li, Yi-Jing Li, Ming-Yen Lu, Jr-Hau He and Lih-J. Chen; Department of Materials Science and Engineering, National Tsing Hua University, Hsinchu, Taiwan, Republic of China, Hsinchu, Taiwan.

Sunflower-like nanostructures composed of SiOx nanorods with spotty SnO2 nanoparticles have been synthesized in large quantities via a thermal evaporation and condensation method. The size of absorbed SnO2 nanoparticles can be controlled by adjusting the flow of O2. The peculiar nanostructures exhibit intense near UV emission in cathodoluminescence measurement. By controlling the size of the SnO2 nanoparticles on the SiOx nanorods, the intensity of near UV emission of 398 nm can be enhanced. The nanostructures are potentially applicable as near UV emitters.

DD16.16

III-VI Compound Semiconductor Indium Selenide (In2Se3) Nanowires: Synthesis and Characterization Xuhui Sun, Garrick Ng, Thuc Dinh Nguyen and Bin Yu; Ames Center for Advanced Aerospace Materials and Devices, NASA Ames Research Center, Moffett Field, California.

Indium Selenide (In2Se3), a very interesting compound semiconductor of A2IIB3VI family, is of great interest due to its polymorphism and the related metal-ion defect structure. In2Se3 has attracted substantial attention as a promising semiconductor material for several different applications

such as photovoltaic solar cell, optoelectronics, and ionic battery. In particular, In_2Se_3 has been recently used as a programmable material in phase-change random access memory (PRAM). We report for the first time the synthesis of one-dimensional indium selenide (In_2Se_3) nanowire (NW), an III-VI group compound semiconductor nanostructure with potential applications in data storage, solar cells, and optoelectronics. Nanoscale gold particles were used as catalysts and growth was also demonstrated using indium as self-catalyst. The growth mechanism is confirmed to be vapor-liquid-solid process by in-situ heating experiments in which In and Se were found to diffuse back into the gold catalyst bead forming a Au-In-Se alloy that was molten at elevated temperatures. The physical morphology, chemical composition, and crystal structure of the as-synthesized In_2Se_3 NWs were analyzed by scanning electron microscopy (SEM), energy dispersive X-ray spectroscopy (EDS), and high-resolution transmission electron microscopy (HR-TEM). The as-synthesized In_2Se_3 NWs are single crystal of the β -phase hexagonal structure with lattice constant a of ~ 4.0 Å, and c of ~ 19.2 Å. The most (90%) nanowires are grown preferably along the $\langle 110 \rangle$ crystallographic direction and another 10% show $\langle 001 \rangle$ growth direction. The electrical resistivity of the In_2Se_3 NW was also measured.

DD16.17

Syntheses, Structures and Magnetic Properties of 1D Metallomacrocyclic Complexes. Mi Hyang Jeong, Ju Chang Kim and Young Soo Kang; Chemistry, Pukyong National Univ., Busan, South Korea.

1D metal systems with antiferromagnetic intrachain interactions have been extensively studied. However, 1D metallomacrocyclic systems with intrachain ferromagnetic interactions are considerably rare. The metallomacrocyclic complexes bridged by chromate, molybdate or tungstate ligands can mediate ferromagnetic interactions between the metal centers due to the magnetic orbital overlap through the bridge. In this presentation, we discuss syntheses, structures and magnetic properties of molybdate- and tungstate-metallomacrocyclic complexes which show ferromagnetic interactions.

DD16.18 TRANSFERRED TO DD17.2

DD16.19

Characterization of Carbon Nanotubes Grown by a Non-Metal Catalyst Method Shantee Houston, Gail Brown, Bill Mitchel and John Boeckl; Wright Patterson Air Force Base/Air Force Research Laboratory, Wright-Patterson, Ohio.

Carbon nanotubes (CNTs) have been formed on both the Si and C-face of both 4H and 6H SiC substrates, by sublimation of Si from SiC at elevated temperatures. There is no purification process needed to remove metal from the CNTs after growth, because a metal is not used in the growth process. After subjecting the SiC sample to temperatures ranging from 1400° – 1700°C in a vacuum furnace (10-2–10-5 torr), oxidation caused SiC to decompose and Si sublimed from the substrate. The remaining carbon atoms left on the surface are the nucleation site for the CNTs; the air in the chamber catalyzes the formation of carbon nanotubes. Characterization of the CNTs grown using this method was performed using: scanning electron microscopy (SEM), transmission electron microscopy (TEM), atomic force microscopy (AFM), and Raman spectroscopy. The SEM showed that CNTs grow at a faster rate on the C-face than on the Si-face of the substrate; and the use of the TEM concluded that the pressure in the vacuum furnace has an effect on the CNT growth. All characterization techniques showed a growth of both multi-walled and single-walled CNTs.

DD16.20

The Significance of Catalyst to Hydrocarbon Ratio in the CVD Synthesis of Multiwalled Carbon Nanotubes Gregg S. B. McKee and Kenneth Scott Vecchio; Materials Science and Engineering Program, University of California, San Diego, La Jolla, California.

The vapor-phase catalytic chemical vapor deposition (cCVD) synthesis of multi-walled carbon nanotubes (MWNT's) shares many similarities with the synthesis of vapor grown carbon fibers (VGCF). It has been shown that the catalyst to hydrocarbon feed ratio determines the fiber diameter and aspect ratio of VGCF. As a result of the similar growth processes, it might be expected that the same would apply to the cCVD growth of MWNT, potentially enabling a more direct dimensional control over what is often an empirical synthesis technique. It is also probable that an ideal catalyst/carbon ratio exists which would allow the synthesis of nanotubes of an optimal structure resulting from minimal defect density and maximum chemical stability. This work will examine the significance of the catalyst to carbon ratio in these respects and will establish an optimum ratio allowing for the creation of low-defect nanotubes with high chemical stability. Temperature Programmed Oxidation (TPO) analyses on nanotubes synthesized using varying catalyst/carbon ratios will be described and their results compared with Raman spectra obtained from each sample. It is expected that these methods will indicate an ideal ratio for the synthesis methods used. The results of a TEM survey of the nanotube population will be described which indicate the dimensional dependence of the nanotubes upon the catalyst/carbon ratio.

DD16.21

One step synthesis and densification of Nanocrystalline NbSi_2 - Si_3N_4 Composite by High-Frequency Induction heated Combustion In-Jin Shon¹, Hyun-Kuk Park², In-Kyoon Jeong³, In-Yong Ko⁴ and Jin-Kook Yoon⁵; ¹Advanced Materials, Chonbuk University, Jeonju, Jeonbuk, South Korea; ²Advanced Materials, Chonbuk University, Jeonju, Jeonbuk, South Korea; ³Advanced Materials, Chonbuk University, Jeonju, Jeonbuk, South Korea; ⁴Advanced Materials, Chonbuk University, Jeonju, Jeonbuk, South Korea; ⁵Metal Processing Research Center, Korea Institute of Science and Technology, Seoul, Seoul, South Korea.

Dense nanostructured 4NbSi_2 - Si_3N_4 composite was synthesized by high-frequency induction-heated combustion synthesis (HFIHCS) method within 1 minute in one step from mechanically activated powders of NbN and Si. Simultaneous combustion synthesis and densification were accomplished under the combined effects of an induced current and mechanical pressure. Highly dense 4NbSi_2 - Si_3N_4 composite with relative density of up to 98% was produced under simultaneous application of a 60 MPa pressure and the induced current. The average grain size and mechanical properties (hardness and fracture toughness) of the composite were investigated. The average grain sizes of NbSi_2 and Si_3N_4 phases in the composite were about 90 and 25nm, respectively. The average hardness and fracture toughness values obtained were 680 kg/mm² and 3.1MPa m^{1/2}, respectively. The lack of reported data on NbSi_2 - Si_3N_4 makes difficult to make direct comparisons, but based on reported data on NbSi_2 coating, an approximate comparison shows that the present results exhibit a lower hardness and higher toughness.

DD16.22

Ultrafast Pulsed Laser Ablation as a Method for Synthesis of Nanocrystals Bing Liu¹, Zhendong Hu¹, Yanbin Chen², Xiaoqing Pan² and Yong Che¹; ¹IMRA America Inc., Ann Arbor, Michigan; ²Department of Materials Science and Engineering, University of Michigan, Ann Arbor, Michigan.

Near infrared (1 μ m) ultrafast pulsed laser is used to ablate pure metal and metal alloy targets in a vacuum chamber. We find that by optimizing the ablation conditions, as a direct result of ultrafast laser ablation, crystalline nanoparticles can be abundantly produced without intermediate nucleation and growth processes. Combining with different background gases, versatile structural forms can also be obtained for the nanocrystals. Using metal nickel as a sample material, we have produced Ni/NiO core/shell nano-spheres and NiO nano-cubes. We also study the production of alloy nanoparticles, which has been challenging in fabrication. We demonstrate production of nanoparticles containing up to three metal elements using ultrafast laser ablation. The laser ablation process is investigated using an ion probe in real-time. Nanoparticle samples are examined using atomic force microscopy and high resolution transmission electron microscopy for morphological, structural, and chemical analysis. This study provides a simple physical method for generating nanoparticles with a narrow particle size distribution, a high particle yield, versatile chemical compositions and structural forms.

DD16.23

Paramagnetic Polynuclear Transition Metal Clusters with Redox Active Ligands Derived from TTFs. Lahcene Ouahab, Kostyantyn Gavrylenko, Yann Le Gal, Olivier Cador and Stephane Golhen; Chemistry, UMR CNRS 6226 University of Rennes 1, Rennes, France.

Developpement of molecular electronics depends strongly on the developpement of functional molecules and molecule-based materials. Therefore, current trends in this last field include nanoscience, functional single molecules such as single molecule magnets, single chain magnets and single molecule conductor, and multifunctional materials. In particular, designing molecule-based materials, which possess synergy or interplay between two or more properties such as electrical conductivity with magnetism or spin cross-over ..., is currently a challenging target and it has been attracting great interests from chemists and physicists for both application to devices or for fundamental science. Preparation of paramagnetic transition metal complexes where the redox active ligands such TTFs are coordinated to spin carrier is a very promising alternative to achieve conducting (or superconducting) magnets through interaction between d spins and mobile electrons.¹ We present in this contribution a new route for the synthesis of homometallic and heterometallic polynuclear transition metal complexes as well as their crystal structures, cyclic voltametry and magnetic properties.² The first trinuclear complexes of this kind are shown in the figure and it constitutes a first step towards high spin single molecules with redox active ligands. Current target is to study the behaviour and properties of this kind of nonoscale molecules (~4nm) on surfaces.
1. L. Ouahab, T. Enoki, Eur. J. Inorg. Chem., 931, (2004) 2. K.S. Gavrilenko, S.V. Punin, O. Cador, S. Golhen, L. Ouahab, V.V. Pavlishchuk, J. Am. Chem. Soc., 127, 12246 (2005).

DD16.24

Fabrication Gold Nanorattles from AucoreAgshell Templates Hao Ming Chen and Ru -Shi Liu; Department of chemistry, National Taiwan University, Taipei, Taiwan.

This investigation describes the formation of a gold nanorattle with a pure metal shell by varying experimental parameters. The galvanic replacement reaction between silver and chloroauric acid was adopted to prepare hollow gold nanoparticles. This approach is extended to produce nanorattles of Au cores and Au shells by starting with AucoreAgshell nanoparticles as templates. The effect of temperature on the nanostructure of the final product is also considered. The composition of the shell in nanorattles can be controlled by varying the reaction temperature (to form pure gold or gold-silver alloy, for example). X-ray absorption fine structure spectroscopy is conducted to elucidate the fine structure of these nanoparticles. Partial alloying between the Au core and the Ag shell is elucidated observed by extended X-ray absorption fine structure (EXAFS).

DD16.25

The Effect of Ge Layers on the Kinetics of NiSi₂ Islands Formation Ling-Hui Wu and Cho-Jen Tsai; Material Science and Engineering, National Tsing Hua University, Hsinchu, Taiwan.

The effects of a Ge layer on the kinetics of NiSi₂ islands formation in Ge/Ni/Si (100) structure were investigated. It was observed that the nucleation and growth of NiSi₂ islands were impeded with increasing thickness of the Ge layers. A Si (100) wafer was cleaned using standard RCA process and dipped into a diluted HF solution. The substrate was further sputtered cleaned using an Argon ion beam for 1 minute before film deposition. One monolayer (ML) of Ni and an amorphous Ge cap layer (5, 10, 15, 20ML) were deposited on Si substrate. The samples were then ex-situ annealed at 400-800 oC. The formation temperature of NiSi₂ phase is 500 oC and 580 oC for the Ge layer of 5 ML and 20ML, respectively. The samples were ex-situ characterized using field emission scanning electron microscopy and transmission electron microscopy to study the microstructure and to identify the formation temperature of the NiSi₂ phase. The reaction process started with the dissolution of the Ni atoms into the amorphous Ge layer. Next, solid phase epitaxy of the Ge layer followed. The Ni atoms were expelled from the crystallized region and redistributed in the amorphous region. Until the concentration of Ni in the amorphous Ge layer exceeded the solubility limit, the Ni atoms diffused through the crystallized Ge layer and reacted with the Si to form NiSi₂ phase. The kinetics of the NiSi₂ phase formation is, thus, governed by the rate of solid phase epitaxy. The rate of solid phase epitaxy is impurity dependent. For the same amount of Ni to redistribute in the amorphous Ge cap layer, the thinner Ge layer has higher Ni concentration, which increases the rate of solid phase epitaxy. Besides, in this experiment, the interface between the amorphous layer and the Si substrate is probably mixed due to the ion beam bombardment. Therefore, compared with the pure Ge layers, the solid phase epitaxy in this experiment occurs at the higher temperature. If the amorphous Ge layer has higher Ni concentration, the segregation of Ni in amorphous Ge can reach its solubility limit at smaller thickness of the crystallized Ge. The nucleation of the NiSi₂ phase would occur earlier for an amorphous Ge with higher Ni concentration than that with lower Ni concentration. For thicker Ge cap layer, because the concentration of Ni in the amorphous Ge layers is lower, the nucleation of the NiSi₂ island would occur at a higher temperature. Hence, the appearance of the NiSi₂ phase is kinetically retarded. This experiment demonstrates that the nucleation and growth of NiSi₂ islands are controlled by using a Ge layer with different concentration of Ni atoms. It is a new method to form silicides, which is different from the oxide mediated epitaxy or the nitride mediated epitaxy.

DD16.26

New Palladium Nanomaterials for Catalysis : Mechanisms Controlling Formation and Evolution of Nanostructures in a Seed-mediated Synthesis. Laure Bisson^{1,2}, Cedric Boissiere¹, Clement Sanchez¹, Cecile Thomazeau² and Denis Uzio²; ¹Catalyse et Séparation, Institut Français du pétrole, Vernaison, France; ²Laboratoire Chimie de la Matière Condensée, UPMC, Paris, France.

Recently, the synthesis of metallic anisotropic nanoobjects has been of great interest. Controlling their size and shape induces interesting modification of their optical, electronic and catalytic properties and opens new possibilities for applications in photonics, electronic devices, chemical sensing, catalysis, drug delivery... Metallic nanoparticles are used as the active phase for heterogeneous catalysts, because of their unique catalytic properties. Today the link between nanoparticles size and catalytic properties has been thoroughly described. However a current issue in catalysis research is to determine whether a specific crystallographic plane of the metallic nanoparticle is responsible for the activity and selectivity properties in a structure sensitive reaction [1,2]. Following this purpose, metallic nanoparticles with specific morphologies showing highly selective catalytic properties have been studied [3]. In the present work, Palladium nanostructures are prepared by a seeding growth approach in a surfactant mediated aqueous medium, based on a method reported for the synthesis of Au nanoparticles [4]. The Pd⁰ nanoparticles obtained present various morphologies : rods, tetrahedra and/or bipyramides, cubes, hexagonal shaped polyhedra. The synthesis of these nanoparticles, the study of their growth mechanism and their evolution in the reaction medium will be presented. The factors affecting the formation of these nanoparticles have been investigated and it is demonstrated that the size and nature of Palladium seeds play an important role. A detailed transmission electron microscopy study associated with high resolution observations of the Pd nanoobjects in the "seeding" step and evolving with time in the "growth" step provided evidence that the nucleation and growth of these particles is dominated by an aggregative mechanism. This mechanism is to the best of our knowledge reported for the first time for a controlled growth synthesis of metallic nanoparticles in an aqueous medium. TEM images show that there is an homogeneous nucleation leading to nuclei, cohabiting with seeds injected from the first step. We propose a model of formation of the various particle morphologies driven by the self-assembling of these two populations of spherical particles, taking into account the role of the surfactant and the size and nature of the seed. Moreover, upon ageing the particles undergo a ripening process, yielding to spherical particles. This process can be attributed to an oxidative etching of Pd⁰ particles. [1] Che, M., Bennett, C.O., *Advances in Catalysis*, 1989, 36, p. 55. [2] Somorjai, G.A., Jacobs, P.W., *Journal of Molecular Catalysis A: Chemical*, 1998, 131, p. 5. [3] Narayanan, R., El-Sayed, M.A., *Journal of the American Chemical Society*, 2004, 126, p. 7194. [4] Jana, N.R., Gearheart, L., Murphy, C.J., *Journal of Physical Chemistry B*, 2001, 105, p. 4065.

DD16.27

Low Density Aerogels and Foams: Self-assembled Macroscopic Structures Controlled on the Nanometer Scale. John Joseph Karnes, Streit John and Nicole Petta; Schafer Corporation, Livermore, California.

We have synthesized a variety of low density materials using a broad spectrum of synthesis techniques, including sol-gel hydrolysis-condensation, formation of high internal phase emulsions, and epoxide ring opening reactions. The synthesized gels/foams, when treated to the proper drying procedure (such as critical point drying), result in materials with fascinating physical and aesthetic properties. The composition of these materials may arise from organic or metallic precursors while easily maintaining a bulk density of less than 100mg/cc. Our work focuses primarily on the organic, but we have also used these techniques to produce aerogels of other elements including silicon, nickel, and chromium. We shall report our ability to control the properties of these materials by tuning synthesis and processing parameters. For example, by varying the pore size of these materials, from <5nm to the micron range, we can control the transparency/opacity of the aerogels. We have also demonstrated the ability to cast these materials into molds of various shapes and produce flat aerogel films as thin as 100microns. The durability and machinability of these materials will be discussed. These aerogels and foams can be synthesized to be robust enough to be processed by conventional machining techniques.

DD16.28

Formation of Zinc Layered Double Hydroxide in Colloidal ZnO Nanoparticles Dazhi Sun¹, Minhao Wong², Nobuo Miyatake³ and Hung-Jue Sue¹; ¹Mechanical Engineering Department, Texas A&M University, College Station, Texas; ²Kaneka Corporation, Takasago, Hyogo, Japan; ³Kaneka Texas Corporation, Pasadena, Texas.

Colloidal ZnO nanoparticles with sizes ranging from 2-5 nm have been synthesized by adding zinc acetate methanol solution into KOH/methanol solution. Zinc layered double hydroxide (Zn-LDH) was found to exist in the precipitates from the ZnO sol of early stage. The formation of Zn-LDH in ZnO colloids was investigated. It was found that Zn-LDH formation was greatly affected by reactant concentrations, reacting time, and temperature. The growth of ZnO nanoparticles and the structural transformation of acetate zinc hydroxide to spherical ZnO nanocrystals by solvent evaporation were monitored via X-ray diffraction and transmission electron microscopy. Our results suggest that solvent evaporation is an effective approach to remove layered double hydroxide from the ZnO nanocrystals.

DD16.29

IB Element Doped p-ZnO Nanorods and their Optical Properties. Ji-Won Choi¹, Jung-Wook Lee¹, Heung-Chun Park¹, Hyunmi Hwang², Jaeyong Lee² and Won-Kook Choi¹; ¹Thin Film Materials Research Center, Korea Institute of Science and Technology, Seoul, South Korea; ²Department of Physics, Yonsei University, Seoul, South Korea.

ZnO has substantial advantages including wide bandgap, large exciton binding energy, and specific optical properties and the room temperature lasing action of nanorod array of ZnO has demonstrated that the functional design of ZnO nanomaterials in a highly oriented and ordered array is of crucial importance for the development of display and illumination devices. However, growth of reliable p-type ZnO to produce long lasting and robust devices is still under debate. In this study, IB element doped p-ZnO nanorods embedded in anodic alumina membranes were grown on n-Si and n-SiC single crystal substrate by rf magnetron sputtering method. The morphology and photoluminescent characteristics of well ordered nanorods were investigated by scanning electron microscopy, x-ray diffraction and photoluminescence.

DD16.30

In-Situ Core/Shell Structured FePt/ZnFe2O4 Magnetic Nanoparticles Ki-Eun Kim and Yun-Mo Sung; Materials Sci. & Eng., Korea University, Seoul, South Korea.

FePt magnetic nanoparticles have been intensively studied due to its bright future for high-density data storage applications. They show high magnetocrystalline anisotropy when they have L10 (FCT) structure, which is a critical issue in tailoring the high-density data storage devices. However, as-prepared FePt nanoparticles show disordered FCC phase which is paramagnetic, and in general, the transformation from the disordered FCC to the ordered L10 phase occurs above 550 oC, which is high enough to cause serious sintering problems for the FePt

nanoparticles. Much effort has been poured to reduce the phase transformation temperature for example doping of Ag, Au, Cu, etc., and the increase in the vacancy concentration at the FePt lattices was proposed as a ruling mechanism. In this study, Zn-doped FePt nanoparticles were successfully synthesized using polyol and thermolysis methods. As-prepared nanoparticles were annealed at 400 °C for 30 min to obtain the ordered L10 phase. The as-prepared and the annealed Zn-doped FePt nanoparticles were identified as in the disordered FCC and the ordered L10 structure, respectively using x-ray diffraction (XRD). Also, formation of ZnFe₂O₄ phase was identified in the annealed nanoparticles. High-resolution transmission electron microscopy (HRTEM) results show that the annealed nanoparticles maintained their original hexagonal array as the as-prepared ones did. Also, the annealed ones showed formation of FePt/ZnFe₂O₄ core/shell structure, which was identified using HRTEM, selected area electron diffraction (SAED), and energy dispersive x-ray spectroscopy (EDS). The transformation behavior of the disordered FCC to the ordered L10 phase was investigated by differential scanning calorimetry (DSC), and the variation in the endothermic peak temperatures was monitored according to the DSC scan rates. The peak temperatures corresponding to the DSC scan rates were used for Kissinger analysis, a non-isothermal kinetics, and the activation energy for the phase transformation was obtained for the FePt nanoparticles doped with different amount of Zn. The nanoparticles with higher Zn content showed lower transformation temperature and lower activation energy barrier most probably due to the increased vacancy concentration in the FePt matrix. Magnetic properties of nanoparticles were investigated using vibrating-sample magnetometry (VSM), and FePt/ZnFe₂O₄ core/shell nanoparticles showed increased coercivity compared to the pure FePt, which could be possible due to the magnetic coupling interaction between the FePt core and the ZnFe₂O₄ shell. The Zn addition into the FePt matrix could contribute not only to lowering the phase transformation temperature by approximately 150 °C to suppress sintering of nanoparticles, but also to enhancing its magnetic properties. Also, the ZnFe₂O₄ shell forming during the annealing process could act as a barrier layer preventing sintering of FePt nanoparticles at 400 °C.

DD16.31

Structural Control of Carbon Nanowalls and Their Properties as a Transparent Conducting Material Suguru Noda, Rie Nishimoto, Hisashi Sugime, Susumu Inasawa, Yoshiko Tsuji and Yukio Yamaguchi; Department of Chemical System Engineering, The University of Tokyo, Tokyo, Japan.

Carbon forms a variety of nanostructures with unique properties. Since the recent discovery of carbon nanowalls (CNWs) or carbon nanosheets [1], their synthesis methods and their applications to field emitters have been studied by several groups. CNWs can be grown by plasma enhanced chemical vapor deposition (PE-CVD) without catalysts, but the growth conditions and the resulting structures vary from group to group. In this work, we investigated the effect of growth conditions on CNW structures, tried to control the structure by controlling the nucleation and growth steps, and examined their properties as a transparent conducting material. CNWs were grown on quartz glass substrates by a cold-wall PE-CVD reactor from C₂H₄ at around 800 K with a r.f. power of 150 W. Its growth nature depended largely on the C₂H₄ pressure; deposition hardly occurred at a pressure lower than 0.13 kPa, CNWs grew after a incubation time around 10 min at 0.13-0.2 kPa, and they grew without any incubation at 0.27 kPa and above. CNWs grown at 0.27 kPa and above for 5 min typically had a transparency around 80 % and a sheet resistance of 5-10 kΩ/sq. The CNW structures were observed by a field emission scanning electron microscope, and they proved to have a networked structure with a few nanometer wall thickness and a several tens nanometer spacing. When we consider their application to a transparent conducting material, enlarging these dimensions is important because the number of grain boundaries, and thus the electrical resistance, among the walls can be reduced. For this purpose, we examined a three-step-growth process, i.e. seeding, etching and regrowth, only by changing the gas pressures. By switching the gas from C₂H₄ to H₂, CNWs can be easily etched. CNWs with a 80 % transparency were mostly etched in 1 min by H₂ plasma at 0.8 kPa, resulting into small CNWs isolated each other. Then we switched the gas from H₂ to C₂H₄/H₂ mixture to mildly grow these "seeds" without additional nucleation of CNWs. The spacing among CNWs increased by a factor of 2-3, but the sheet resistance did not change so much. To improve the electrical conducting property, control of other structures such as crystalline defects and hydrogen inclusion will be important as well. [1] Y. Wu, et al., Adv. Mater. 14, 64 (2002).

DD16.32

Expansion and Characterization of Mesostructures in Aerosol-generated Particles. Malin Sorensen¹, Juan Jose Valle-Delgado², Robert Corkery¹ and Peter Alberius¹; ¹Institute for Surface Chemistry, Stockholm, Sweden; ²Department of Chemistry, Surface Chemistry, Royal Institute of Technology, Stockholm, Sweden.

A systematic study on the impact of a non-volatile organic swelling agent on the mesostructure of aerosol generated particles was done. The Pluronic block copolymer F127 ((EO)₁₀₆(PO)₇₀(EO)₁₀₆) was used as template and polypropylene glycol (PPG M.W 3000) was used as swelling agent. Overall the well ordered 2D hexagonal (*p6mm*) mesostructure expanded roughly linearly, about 15%, before transforming into mesocellular foam. The study of meso/macroporous materials is not straight forward when it comes to a quantification of absolute pore volumes. A new method aiming at determining the exact mass and thereby the porosity of individual particles is under development. Atomic force microscope (AFM) cantilevers are used as "balances". By probing the shift in resonance frequency of the cantilevers, with and without particles attached, the mass of individual particles can be extracted and total porosity calculated. Techniques such as X-ray diffraction (XRD), nitrogen adsorption and transmission electron microscopy (TEM) were used to investigate the impact of PPG on the expansion and order of the structure. Geometrical models of the expansion were derived to interpret the extracted results. This enabled us to explain the impact of the swelling agent on the well ordered 2D hexagonal mesostructure and the transformation to the foam structure.

DD16.33

Vertically Aligned Growth and Characterization of III-Nitride Nanowires and Heterostructure Nanowires. George T Wang¹, A. Alec Talin¹, J. Randall Creighton¹, Donald J. Werder², Elaine Lai¹, Richard J. Anderson¹ and Ilke Arslan¹; ¹Sandia National Laboratories, Albuquerque, New Mexico; ²Los Alamos National Laboratory, Los Alamos, New Mexico.

Nanowires based on the direct bandgap semiconductor Group III nitride (AlGaInN) materials system have attracted attention as potential building blocks in optoelectronics, sensing, and electronics. We have employed a VLS-based metal-organic chemical vapor deposition process to synthesize highly aligned arrays of single-crystalline GaN nanowires on 2-inch diameter sapphire and GaN substrates without the use of a patterned template. SEM and TEM analysis indicate that the nanowires share a common [11-20] growth orientation and have aligned facets, with a majority of the nanowires lacking a catalyst cluster at the tip. We have found a strong correlation between growth temperature and the optical and electrical properties of the nanowires, which we propose is due to carbon incorporation from the metal-organic source. The effects of substrate and catalyst preparation on the ordered growth will be also discussed. Building on our growth technique, aligned radial heterostructure nanowire arrays

consisting of a GaN cores and various III-nitride shell materials, including AlGaIn and AlN, were synthesized and characterized. Our results show that the presence of the AlGaIn and AlN shell layers in the core-shell nanowires have significant effects on the nanowire transport properties, when compared to GaN nanowires. Additionally, characterization of the heterostructure nanowires via 3D STEM tomography and spatially resolved photoluminescence will be presented. Sandia is a multiprogram laboratory operated by Sandia Corporation, a Lockheed Martin Company, for the United States Department of Energy under contract DE-AC04-94AL85000.

DD16.34

Synthesis of 1D Nanorods of Phthalocyanine Using Porous Alumina as a Template and Magnetic Control of the Molecular Orientation During Solidification. Seichi Takami, Yasuhiro Shirai, Yutaka Wakayama and Toyohiro Chikyow; Advanced Electronic Materials Center, National Institute for Materials Science, Tsukuba, Ibaraki, Japan.

Conjugated molecules are expected as a key component to establish organic electronics. Many researchers study the controlled growth of well-ordered solids of organic molecules to realize better electrical properties. In addition to the vacuum deposition of thin films, we believe that the fabrication of nanorods with controlled molecular orientation should be developed as a building block for miniaturized devices. Antiferromagnetic organic molecules are aligned under applied magnetic field. Based on this property, we propose the synthesis of 1D nanorods of phthalocyanine, whose molecular orientation in the nanorods was controlled by an applied magnetic field during solidification. In this presentation, we show the synthesis of the 1D nanorods of phthalocyanine molecules using anodized porous alumina as a template and the control of molecular orientation by applying 5T magnetic field during solidification. We also discuss the effect of pore wall surface of the porous alumina on the molecular orientation.

DD16.35

CoP-based Material as a Catalyst for Carbon Nanotube Via Formation at 400C Guo-Dung Chen, Tri-Rung Yew and Chung-Min Tsai; Materials Science and Engineering, National Tsing-Hua University, Hsinchu, Taiwan, Taiwan.

This paper presents the investigation of electroless CoP-based material as a catalyst for carbon nanotube (CNT) via formation at 400C. Electroless CoP-based material was not only used as a barrier cap for Cu wiring, but also as a catalyst for CNT growth. To increase CNT density for low resistance via formation, it requires dense and small catalysts for CNT synthesis. The electroless plating process of CoP-based materials was optimized to provide a proper surface morphology and Co distribution for dense CNT synthesis. The CNTs were synthesized by chemical vapor deposition. The surface morphology of CoP-based materials was inspected by atomic force microscopy (AFM). The Raman spectra were used to characterize the CNTs. Scanning electron microscopy (SEM) and transmission electron microscopy (TEM) were also employed to characterize the CoP-based catalyst and CNTs. Besides, a Cu/low-k dual damascene test structure was used for CNT synthesis to measure via resistance and investigate its feasibility for future CMOS interconnect via application.

DD16.36

Study on the Growth of ZnO Micro and Nano-structures at Low Temperature and Atmospheric Pressure. Monica Morales¹, B. Claflin^{1,2}, G. C. Farlow¹ and D. C. Look^{1,2}; ¹Physics, Wright State University, Dayton, Ohio; ²Semiconductor Research Center, Wright State University, Dayton, Ohio.

Deposition of ZnO from the vapor in flowing carrier gases has been studied for use in the growth of micro- and nano-structures. We have investigated how variations in the carrier gas composition, gas flow rate and the position of the substrate control the formation and the morphology of the nanostructures. The source material was either Zn powder or Zn acetate. These were either evaporated (powder) or decomposed (acetate) in the temperature range 500°C to 650°C in flowing Ar plus oxygen at atmospheric pressure. It was found that precise control of the gas composition, gas flow rate, and growth time were key to reliable deposition. It was also found that Zn powder must be washed in HCl followed by distilled water to achieve reliable deposition at the lower temperatures. Scanning electron microscopy (SEM) images of samples grown from a Zn acetate source show porous films forming within 1 cm from the source, to micron-sized chimneys forming at 5 cm from the source, to 100-nm dispersed crystals at 7 cm or greater distance from the source. SEM images of samples grown from a Zn powder source show forested needles approximately 100 nm in diameter by 1 micron long. Photoluminescence measurements from these samples show a dominant line at 3.36 eV with additional features at 3.32 and 3.37 eV. The line widths are ~ 3.5 meV, indicating good quality material. The usual green-band emission is also observed. Electronic transport measurements were unsuccessful, presumably because the films were not continuous.

DD16.37

Synthesis of Zinc-Blende CdSe Core Based Type I (Core)Shell and (Core) Double Shell Quantum Dots and Their Optical Properties. Sung Jun Lim, Yongwook Kim and Seung Koo Shin; Chemistry, Pohang University of Science and Technology, Pohang, Kyungbuk, South Korea.

Highly luminescent zinc-blende CdSe quantum dots (QDs) of various sizes were synthesized by adopting the injection-free method(1) with some modifications. CdSe QDs were overcoated with wider band-gap semiconductor shells such as CdS, ZnS, and ZnSe. The shell thickness was controlled while suppressing the self-nucleation of the shell materials during overcoating. All three inorganic shells improve the photoluminescence quantum yield (QY), but induce the red-shift of both the absorption and emission maxima. The organic passivation with thiols reduces QY, however the amount of reduction varies with shell materials. All zinc-blende (core)shell QDs were overcoated with additional ZnS layers and made water-soluble and their optical properties were studied. (1) Y.A.Yang, H.Wu, K.R.Williams, and Y.C.Cao, Angew.Chem.Int.Ed. 44 (2005) p. 6712

DD16.38

Novel Approach to the Synthesis of Mn-doped CdSe Nanocrystals. Woo-Chul Kwak and Yun-Mo Sung; Materials Sci. & Eng., Korea University, Seoul, South Korea.

Colloidal CdSe and Mn:CdSe nanocrystals were successfully prepared by the paraffin oil-based inverse micelle process. The nanocrystals were identified to have zinc-blende structure instead of common wurtzite by X-ray diffraction (XRD). Energy dispersive x-ray spectroscopy (EDS) and inductively coupled plasma (ICP) analyses reveal the ~4.0 atomic % Mn concentration. The Mn doping in the CdSe lattices was evidenced by electron paramagnetic resonance (EPR) result which shows six separated peaks around 330 mT, corresponding to Mn. The size and shape of the nanocrystals were investigated by high-resolution transmission electron microscopy (HRTEM), and the crystallinity was confirmed using selected

area electron diffraction (SAED) analysis. Large difference was observed in the particle size of each system, and the incorporated Mn atoms significantly contribute to nanocrystal growth during synthesis. The blue shift in UV-visible absorption and photoluminescence (PL) emission spectra reveal that band gap increases with Mn incorporation into the CdSe lattices due to the high energy band gap of MnSe.

DD16.39

Water-soluble TOPO-Free All Zinc-Blende Structure (Core)Shell Quantum Dots: Synthesis, Characterization and Fluorescence Tagging on Biomolecules. Yongwook Kim, Sung Jun Lim, Min-Soo Suh, Hye Jin Ham, Hye-Joo Yoon, Bonghwan Chon, Taiha Joo and Seung Koo Shin; Dept. of chemistry, POSTECH, Pohang, South Korea.

All zinc-blende structure (CdSe)ZnS (core)shell quantum dots (QDs) were synthesized in octadecene in the absence of tryoctylphosphine oxide (TOPO). QDs were made water-soluble by ligand exchange with functionalized thiols, such as 3-mercaptopropionic acid (MPA), 3-mercaptopropanol (MPO) and aminoethanethiol (AET). In TOPO-free environment, the QDs surface was covered with thiol ligands only. The hydrodynamic radii of water-soluble QDs were measured by dynamic light scattering (DLS). In all three cases, no aggregates were formed at room temperature. The absorption and photoluminescence (PL) spectra were taken and the PL lifetimes were measured by femto-second time-correlated single photon counting (TCSPC). Each water-soluble functional group was successfully conjugated with biomolecules (protein, DNA) and small molecules by applying various bioconjugate chemistry. QD-biomolecule conjugates were characterized by gel electrophoresis and purified by column chromatography. Both nonspecific binding and biocompatibility were studied in vitro.

DD16.40

Roles of Pre-Laser-Ablation of Mn in Growth of ZnO Nanorods by Chemical Vapor Deposition Takashi Hirate, Hiroshi Miyashita and Tomomasa Satoh; Electronics and Informatics Frontiers, Kanagawa University, Yokohama, Japan.

We studied on a role of laser ablation in fabrication of ZnO nanorods by chemical vapor deposition (CVD) combined with laser ablation of Mn. Metal Zn vapor and O₂ gas are used as precursors to synthesize ZnO and N₂ is used as carrier gas. The Mn pellet is placed near a Si(111) substrate in a deposition chamber and ablated by a pulsed Nd:YAG laser beam (10 shots/sec, 0.04 J/shot). In this study, the laser ablation of Mn is performed in advance of growth of ZnO nanorods by CVD (pre-laser-ablation), i.e., after the laser ablation of Mn for 1 sec to 1 min, O₂ is introduced into a deposition chamber and ZnO nanorods are grown only by CVD for 3 min. The growth conditions are as follows. The growth temperature is 550 degree C. The growth pressure is 27 Pa. O₂ flow rate is 1.5 SCCM. We mainly studied on dependency of morphology of ZnO nanorods on the pre-laser-ablation time, and it was found that the pre-laser-ablation is an effective method to analyze a growth mechanism of nanorods. When no pre-laser-ablation is performed, randomly oriented nanorods with 20 nm averaged diameter and 250 nm averaged length are grown with very low number density of 4 per squared microns. The dispersions in diameter, length and growth direction are very large. When the pre-laser-ablation is performed for only 1 sec, however, ZnO nanorods with 64 nm diameter and 500 nm length are uniformly grown, and the number density is about 50 per squared micron. The directions of nanorods, however, are not so uniform. When the pre-laser-ablation is performed for 5 sec, well aligned ZnO nanorods with 40 nm diameter and 650 nm length are uniformly grown, and the number density is about 120 per squared micron. Comparing with the results of 1 sec of pre-laser-ablation, thinner and longer nanorods are grown with well aligned direction and the number density is over the double. A ZnO nucleation layer that is formed continuously between ZnO nanorods and Si substrate is observed, although it is not formed in the case of 1 sec pre-laser-ablation. When the pre-laser-ablation is performed for 30 sec, well aligned ZnO nanorods with 75 nm diameter and 800 nm length are uniformly grown, and the number density is about 70 per squared micron. The thickness of nucleation layer is 170 nm. When the pre-laser-ablation is performed for 1 min, the morphology of nanorods and the thickness of nucleation layer are almost same as those when the pre-laser-ablation time is 30 sec. We consider from the experimental results as followings. Any species of Mn that is laser-ablated and reached on the substrate play a role of 'nucleus' for growth of ZnO nanorods. The direction of nanorod grown from this nucleus may be random and the collisions between initial nanorods are occurred. This region may be a nucleation layer. As the results of collisions the growth of nanorods with oblique growth direction is stopped and only the nanorods with vertical growth direction continue to grow.

DD16.41

PLA-CVD Growth of Vertically Aligned Carbon Nanotube Arrays. Zuqin Liu¹, Alex Puretzky^{1,2}, David Styers-Barnett¹, Chris Rouleau^{1,2}, Gyula Eres^{1,2} and David Geohegan^{1,2}; ¹Center for Nanophase Materials Sciences, Oak Ridge National Laboratory, Oak Ridge, Tennessee; ²Materials Science and Technology Division, Oak Ridge National Laboratory, Oak Ridge, Tennessee.

Pulsed laser-assisted chemical vapor deposition (PLA-CVD) has been developed to synthesize carbon nanotubes (CNTs) in localized regions on substrates. The precise temporal and spatial delivery of pulsed laser irradiation on substrates offers the potential to grow lateral nanotubes of different lengths and vertically-aligned forests of different heights on different locations of the same substrate, as well as a method to systematically investigate nucleation efficiency and onset times, and growth kinetics. Using variable pulse-width Nd:YAG laser heating of catalyst-coated substrates in methane gas mixtures and in situ pyrometry (with 2 ms resolution) previously we reported the synthesis of discrete single-walled carbon nanotubes (SWNTs) by PLA-CVD at growth rates up to 100 microns/second, faster than reported by any other technique. Single, 50-ms laser pulses were shown to grow micron-long SWNTs directly between prefabricated electrodes for the deterministic synthesis of field-effect transistors. Here, the PLA-CVD nucleation and growth kinetics of vertically aligned carbon nanotube arrays (VANTAs) are reported. For nucleation and growth kinetics studies, relatively large (1mm-diameter) laser spots of Gaussian intensity distribution are utilized. The radial temperature gradient away from the spot center is utilized to determine the optimal growth conditions for the VANTAs, and to investigate the variation in the diameter and density of the CNTs at different locations. The application of PLA-CVD to synthesize structures of varying height is demonstrated. Research sponsored by the Divisions of Scientific User Facilities (laser direct writing) and Materials Sciences and Engineering (growth kinetics measurements), Office of Basic Energy Sciences, U.S. Department of Energy, under contract DE-AC05-00OR22725 with Oak Ridge National Laboratory, managed and operated by UT-Battelle, LLC.

DD16.42

Fabrication Of Metallic Chromium Nano- And Micro-Structures By Gas Phase Reaction. Luis A Valentin, Luis F Fonseca and Oscar Resto; Physics, University of Puerto Rico, San Juan, Puerto Rico.

Magnetic conductive nanostructures are of main importance for the development of devices in new technologies as spintronics. We report the fabrication of novel micro and nano structures of metallic chromium. The nano- rods and tubes were grown on a p-type Si wafer. The reaction takes

place in a stainless steel reactor maintaining the temperature near 1000°C for several hours. Metallic Zinc that is added to the reactor appears to play a crucial role for the synthesis of the Cr structures. The characterization of the nano- and microtubes included: HRTEM, EELS spectrum analysis, mapping, electron diffraction, X-ray fluorescence and XPS spectroscopies. Details of the morphology and composition of the structures will be presented as well as the proposed growth mechanism.

DD16.43

A Study of the Effects of Electrolyte on the Formation of Porous Alumina Loosineh Avakians, Lynn Trahey and Angelica Stacy; Chemistry, University of Berkeley California, Berkeley, California.

Porous anodic alumina (PAA) templates are commonly used in synthesizing nanowires of materials that are potentially useful as quantum wires. These templates are made by the anodization of aluminum in acidic solutions. The goal of this project is to study the effects of varying the electrolyte choice and concentration on the formation of PAA templates. Although effects of electrolytes such as oxalic, sulfuric and phosphoric acids are well known to researchers, it is desired to investigate the templates in new electrolyte environments that may result in enhancements of pore wall functionalities and dimensions. Therefore, new electrolytes with differing conjugate bases have been studied to determine their potential to serve as pore forming electrolytes. Scanning electron microscopy has been used to study the morphologies of PAA films produced under a variety of controlled conditions.

DD16.44

Understanding the Growth Mechanism of Single-Walled Carbon Nanotubes Using "Spin-on-Catalyst" Method. Seung Min Kim¹, Mark Pender², Tyson C. Back³, Allison Jacques², Benji Maruyama² and Eric A. Stach¹; ¹School of Materials Engineering and Birck Nanotechnology Center, Purdue University, West Lafayette, Indiana; ²Materials & Manufacturing Directorate, Air Force Research Laboratory, Wright-Patterson Air Force Base, Ohio; ³Materials Engineering, University of Dayton, Dayton, Ohio.

In order for single-walled carbon nanotubes (SWCNTs) to be incorporated as building blocks in future electronics, it is necessary to control their structure, as this is known to strongly affect their electronic properties. The primary motivation of our work is to investigate the exact growth mechanisms during catalytic chemical vapor deposition (CCVD) of SWCNTs. Specific physical and chemical mechanisms of interest include catalytic reaction of metal catalysts with hydrocarbon sources and the nucleation and growth of SWCNTs from metal catalysts. These processes are in fact of broader interest as they can affect more general catalytic activity, and are thus of substantial basic and industrial importance. Recently, several in-situ experiments[1] using specially designed transmission electron microscopes (TEMs) have revealed significant features of CNT growth, which are not observed in normal ex-situ images. However, more systematic in-situ experiments with higher spatial resolution are still needed to clarify several controversial observations, and thus fully understand the exact growth mechanism of SWCNTs created by CCVD. For successful in-situ TEM experiments with high spatial resolution images of the catalyst and nanotube structure, two requirements should be satisfied. First, movement of catalysts during SWCNT growth should be minimized to allow more careful characterization of their evolving structure. Second, the concentration of catalysts must be well controlled to allow individual tube growths to be studied from start to finish. The spin-on-catalyst (SOC) method, which has been demonstrated in prior research[2], is well matched to these requirements. In these experiments, SWCNTs were successfully produced using a high temperature reduction of commercially available Fe(NO₃)₃ particles in an amorphous SiO_x film on Si substrate. We will present details of the sample preparation method based on the SOC approach. Additionally, we will show that these same films are suitable for SWCNT growth by CCVD. Although characterization of the phase and sizes of the catalysts by X-ray photoelectron spectroscopy (XPS) and atomic force microscopy (AFM) were reported in the prior work[2], these are indirect methods and we demonstrate that measurement errors native to these techniques alter the prior conclusions. By utilizing electron diffraction and high resolution images combined with electron energy loss spectroscopy (EELS), we have shown that the catalyst particles are in fact smaller than was realized (of order 2 - 7 nm) and that they are mostly composed of iron oxide, not iron silicide. We anticipate presenting preliminary results from the growth of SWCNTs in-situ to environmental-cell TEM (E-TEM), with a focus on understanding the inter-relationship between the catalyst structure and resulting nanotube chirality. [1] S. Helveg, et al, Nature, 427, 426(2004) / M. Lin, et al., Nano Lett., 6, 449(2006). [2] M. J. Pender, et al, Chem. Mater., 16, 2544(2004).

DD16.45

Low Temperature Synthesis of Thick Diamond Films based on Low Power CVD Techniques. Xinpeng Wang, Physics, University of Puerto Rico, Rio Piedras Campus, San Juan, Puerto Rico.

Novel Chemical Vapor Deposition (CVD) set has been designed and installed that includes heater, bias voltage, thermocouple, controllers for gas flow, gas composition, and gas pressure. Advantage of this CVD is that all parameters such as temperature, bias voltage and gas flux can be independently controlled. At the condition of substrate temperature down to 2000°C, thick diamond film has grown with growth rate of 30 nm per hour. Both AC and DC power supplies have been employed and electric power used for heating hot filament for CVD is less than 60W. All these conditions are very different from traditional hot filament CVD techniques for synthesis of crystalline diamond films. Both scanning electron microscope (SEM) and Raman scattering spectroscopy have been used for characterizing the samples. Experimental results indicate that the temperature of hot filament, the gas flow rate, and strength of bias electric field will obviously affect the nanostructured surface of the samples.

DD16.46

Abstract Withdrawn

DD16.47

Abstract Withdrawn

DD16.48

Controlled Growth of Heterophase TiO₂ Nanowires via CVD Jung-Chul Lee and Yun-Mo Sung; Materials Sci. & Eng., Korea University, Seoul, South Korea.

TiO₂ is a wide-band gap semiconductor showing wide range of applications, including photocatalysts, gas and humidity sensors, and photochemical solar cells. The photocatalytic efficiency of TiO₂ is greatly influenced not only by its crystalline structure, such as brookite, anatase, and rutile, but also by its morphological features. With the development of nanotechnology, nanostructured TiO₂ is finding wider applications. Several research results reveal that one-dimensional TiO₂ nanostructures can be synthesized by a template sol-gel method, a relatively new chemical procedure. With this approach TiO₂ nanotubes in polycrystalline anatase were successfully synthesized. However, this wet-chemistry based template method not only arrives at the polycrystalline structures, but also causes contamination problems, which seriously deteriorate physical and chemical properties of TiO₂. Furthermore, so far no one has reported the synthesis and characterization of TiO₂ NW's having mixed crystalline phases of anatase and rutile via chemical vapor deposition (CVD). Heterophase TiO₂ NW's were successfully grown all over quartz and sapphire substrates by CVD using Ti powder and liquid TiCl₄ at a substrate temperature of 700 °C. X-ray diffraction (XRD) was performed to analyze crystallinity of the TiO₂ NW's. The morphological features of the TiO₂ NW's were characterized by field emission scanning electron microscopy (FESEM). High-resolution transmission electron microscopy (HRTEM) and energy dispersive x-ray spectroscopy (EDS) analysis performed on the individual NW's indicates that the nanowires are well-defined TiO₂ with mixed phases of anatase and rutile. Photocatalytic efficiency was investigated for the TiO₂ NW's measuring the decomposition rates of methylene blue solution, and it was discussed based upon variation in the phase composition and morphological features of the TiO₂ NW's.

SESSION DD17: Synthesis and Characterization of Nanoscale Materials II

Chairs: Xiao-Min Lin and Horst Weller

Friday Morning, April 13, 2007

Room 2001 (Moscone West)

8:30 AM *DD17.1

Synthesis of Luminescent and Magnetic Nanoparticles and their Use in Materials- and Life Sciences Horst Weller, Physical Chemistry, University of Hamburg, Hamburg, Germany.

This talk describes recent developments in the synthesis and characterization of semiconductor and metal nanoparticles. Results on the growth kinetics and the control of size, shape and surface chemistry will be addressed. Examples for 2D and 3D self assembly of nanoparticles are given. We report on the formation of colloidal crystals from semiconductor and magnetic nanoparticles as well as on the formation of ordered films using various coating techniques. Moreover we present measurements on the size-dependent magnetic properties of nanoparticles. We also report on the use of nanoparticles for biological and medical applications which include a robust coating with biocompatible polymers and embedding nanoparticles in polymer vesicles. Examples on the improvement of magnetic resonance imaging using tailored superparamagnetic nanoparticles are given.

9:00 AM DD17.2

Synthesis of Crystalline BaTiO₃ Nanocrystals with Surface Capping Ligands and Self-Assembly of Nanocrystals. Zhuoying Chen^{1,2}, Jiaqing He³, Yimei Zhu³ and Stephen O'Brien^{1,2}; ¹Applied Physics and Applied Math, Columbia University, New York, New York; ²Columbia Materials Research Science and Engineering Center (MRSEC), Columbia University, New York, New York; ³Center for Functional nanomaterials, Brookhaven National Laboratory, Upton, New York.

A new nonhydrolytic method for the preparation of well-crystallized size-tunable barium titanate (BaTiO₃) nanocrystals capped with surface ligands is reported. A combination of alcohols and carboxylic acids with alkyl chains were employed in order to effect size and morphological controls. Nanocrystals of barium titanate with diameters of 6-10 nm (capped with decanoic acid), 3-5 nm (capped with oleic acid), 10-20 nm (a nanoparticle and nanorod mixture capped with oleyl alcohol) and 2-3 nm (capped with oleyl alcohol) were synthesized, and can be readily dispersed into nonpolar solvents such as hexane. Techniques including XRD, TEM, SAED and HREM confirm the crystallinity and morphology. One important goal of the project is the incorporation of ferroelectric or high k dielectric nanoparticles into multicomponent self-assembled superlattices. Preliminary binary self-assembly experiments are carried out using nanocrystals of iron oxide, lead selenide, gold, and barium titanate.

9:15 AM DD17.3

Synthesis, Characterisation and Understanding of the Crystal Growth Mechanism in PbS Nanocrystals Deborah Berhanu¹ and Paul O'Brien²; ¹The School of Chemistry and the School of Materials, The University of Manchester, Manchester, United Kingdom; ²The School of Chemistry and the School of Materials, The University of Manchester, Manchester, United Kingdom.

There is considerable interest in developing simple, inexpensive and environmentally benign protocols to grow metal chalcogenide nanomaterials for practical purposes. Semiconductor nanocrystals of PbS are particularly well investigated for telecommunication and biological applications as it exhibits luminescence in the Near IR region. Consequently quantum dots based on semiconductors of group IV-VI materials are particularly appealing.¹ Factors effecting this include the relatively small bulk band gaps (PbS 0.41 eV, PbSe 0.28eV) and strong quantum size effects due to the large Bohr radii of both electrons and holes. We have demonstrated a simple "soft-hydrothermal" route to nanocrystalline PbS and CdS nanoparticles, using air-stable crystalline complexes as single-source precursors.² This technique was further investigated for the preparation of lead chalcogenide nanocrystals using microwave systems. The "soft-hydrothermal" approach involves a single-step "one-pot" protocol that appeals to chemists and others in the field, providing potential for development of nanomaterials using limited resources. This straightforward technique was used in the present study to investigate the crystal growth mechanism in PbS nanocrystals. 1. I. Kang and F.W. Wise, J. Opt. Soc. Am. B, 1997, 14 (7), 1632. 2. D. Berhanu, K. Govender, D. Smyth-Boyle, M. Archbold, D.P. Halliday and P. O'Brien, Chem. Commun., 2006, in press.

9:30 AM DD17.4

Synthesis and Spectroscopic Studies of Doped II-VI Chalcogenide Quantum Dots Paul Irving Archer, Daniel R Gamelin and Nick S Norberg; Chemistry, University of Washington, Seattle, Washington.

Abstract: The challenge of doping colloidal II-VI chalcogenide semiconductor quantum dots (QDs) is addressed through new preparations and spectroscopic analysis. The use of electronic absorption and magnetic circular dichroism (MCD) spectroscopies as probes of 3d transition metal

dopant speciation in $TM^{2+}:AE$ QDs (where $TM = Co^{2+}, Mn^{2+}$, etc.; $A = Zn^{2+}, Cd^{2+}$; $E = S^{2-}, Se^{2-}$) will be described. Recent results relating to giant excitonic Zeeman splittings (ΔE_{Zeeman}) and size-dependent charge transfer photoionization processes in doped semiconductor nanocrystals will be presented and discussed with respect to potential applications of doped semiconductor nanostructures.

9:45 AM DD17.5

Oxide-supported Metal Nanoparticles and their Applications. Nanfeng Zheng and Galen D. Stucky; Department of Chemistry and Biochemistry, University of California, Santa Barbara, California.

Metal nanoparticles exhibit unique chemical properties that differ from those of their bulk materials and enable them to find distinct applications in catalysis and chemical sensing. For example, although bulk gold is considered catalytically inactive, gold nanoparticles with size less than 10 nm exhibit high catalytic activities towards different types of reactions. In order to be efficient catalysts, however, metal nanoparticles should not sinter during catalytic processes. Putting metal nanoparticles on oxide supports represents one of effective methods to stabilize the metal nanoparticles. The challenge remains of designing oxide-supported metal nanoparticles with well-defined parameters (e.g., particle size, size distribution, loading content, type of support). We have now successfully developed general and unique synthetic routes not only to monodisperse metal nanoparticles but also to efficient oxide-supported metal nanoparticle catalysts. The prepared catalysts exhibit attractive catalytic properties towards selective oxidation of alcohols, aldehydes and alkenes by using air or oxygen as an oxidant under mild conditions.

10:00 AM DD17.6

Ultra Large Scale and Green Synthesis of Monodisperse Magnetite Nanocrystals. Cafer T. Yavuz^{1,2}, Jessica Cox⁴, Carmen Suchecki⁵, Angelina Tran⁴ and Vicki L. Colvin^{1,2,3}; ¹Chemistry Dept., Rice University, Houston, Texas; ²Center for Biological and Environmental Nanotechnology (CBEN), Rice University, Houston, Texas; ³Chemical Engineering, Rice University, Houston, Texas; ⁴Rice University, Houston, Texas; ⁵Northwestern University, Evanston, Illinois.

Magnetite (Fe_3O_4) nanocrystals were synthesized in size distributions below 10% and in mass quantities. We present the first reactor that would produce highly monodisperse and uniform magnetite nanocrystals 1g/hour. The most environmental friendly (green) synthesis was reported for high quality nanocrystals. Cost of manufacturing of magnetite nanocrystals cut down to industrial standards.

10:30 AM DD17.7

Position-Controlled Doping of Semiconductor Nanocrystals Y. Charles Cao, Yongan Yang, Ou Chen and Alexander Angerhofer; Chemistry, University of Florida, Gainesville, Florida.

The ability to precisely control the doping of semiconductor nanocrystals can create an opportunity for producing functional materials with new properties, which are of importance to applications such as biomedical diagnosis, solar cells, and spintronics. This opportunity has stimulated research efforts to develop synthetic methods to incorporate dopants into a variety of colloidal semiconductor nanocrystals. It has been found that nanocrystals with dopants inside their crystal lattice can exhibit different properties from those with dopants on their surface. However, less is known on the fundamental question of whether different dopant positions inside nanocrystals can affect physical properties of doped nanocrystals. Herein, we report a new doping approach, using a three-step synthesis to produce high-quality Mn-doped CdS/ZnS core/shell nanocrystals. This approach allows the precise control of Mn radial position and doping level in core/shell nanocrystals. Based on this synthetic advance, we have demonstrated that optical properties of Mn-doped nanocrystals indeed depend on Mn radial positions inside the nanocrystals. In addition, we have synthesized nanocrystals with a room-temperature Mn-emission quantum yield of 56%, which is nearly twice as high as that of the best Mn-doped nanocrystals reported previously. Nanocrystals with such a high-emission quantum yield are very important to applications such as nanocrystal-based biomedical diagnosis.

10:45 AM DD17.8

Surface Passivation Effects on Optical and Material Characteristics of Silicon Nanocrystals by High Pressure Water Annealing and Forming Gas Annealing. Hiroyuki Sanda, Maria Makarova, Jenna Hagemeyer, James McVittie, Jelena Vuckovic and Yoshio Nishi; Electrical Engineering Department, Stanford University, Stanford, California.

Silicon based photonics is gaining considerable research attention since this technology can realize silicon light emitting devices. Nanocrystalline silicon is a promising candidate to achieve such devices because of the efficient photoluminescence (PL) of silicon nanocrystals (Si-nc) and because of the fabrication compatibility with CMOS processing. Currently, the exact mechanism of the emission, the condition to achieve high quantum efficiency and the procedures for effective surface passivation are all active research topics. In this work, Si-nc was fabricated by sputtering and high temperature annealing in a SiO_2 matrix. Post Si-nc formation treatments investigated here included both high-pressure water vapor annealing (HWA) and forming gas annealing (FGA). HWA is of interest since it is an effective surface passivation process for porous silicon, while FGA is the classic silicon passivation process. The optical and material characteristics of the nc-Si were measured and compared before and after HWA and FGA by PL, ellipsometry, X-ray photoelectron spectroscopy (XPS), and infrared absorption spectroscopy, for the first time. We co-sputtered Si and SiO_2 onto a silicon substrate without rotation so that an across substrate gradient of Si in SiO_2 was achieved. The samples were then annealed using the following processes: high temperature annealing at 1100°C for 1 hour in N_2 , the same 1100°C annealing followed by FGA at 400°C for 30 minutes, and the same 1100°C annealing followed by HWA at 2.6MPa and 260°C for 5 hours. The excess Si content in the SiO_2 matrix ranges from 1 atomic % (at%) to 27 at% across the wafer by XPS. The PL intensity in the range of 600-1000nm is maximized at the position with an excess Si of 8 at%. As the excess Si decreases from 8 at%, the PL intensity decreases because of the reduction of the nc-Si density. On the other hand, as the excess Si increases from 8 at%, the PL intensity decreases probably because the crystal size is too large to emit photons. Both HWA and FGA are shown to enhance the PL intensity by about 3 times at the 8 at% excess Si position, for the first time, suggesting that both processes passivate surface dangling bonds of the nc-Si with hydrogen. In addition, the peak wavelength of the PL spectrum, 775nm, shifts to 750nm after HWA, while it stays the same after FGA. This result suggests that water molecules oxidize Si-nc during HWA. Although, the oxidation states of Si are widely distributed from Si^{0+} to Si^{4+} after the sputter deposition by the Si 2p XPS analysis, Si^{0+} and Si^{4+} dominate after annealing at 1100 °C because of the phase separation to Si and SiO_2 . XPS depth profiling shows that the excess Si content is uniform across the film thickness after the 1100 °C annealing, suggesting the slow Si diffusion in SiO_2 . Transmission electron microscopy (TEM) observation and electron spin resonance (ESR) measurement are in progress and will be discussed at the meeting.

11:00 AM DD17.9

Optical Properties of Chromophoric Thiol Coated Nanoparticles Prepared by Place Exchange Reactions. Wojciech Haske, Michal Malicki, Seth R. Marder and Joseph W. Perry; Chemistry and Biochemistry, Georgia Institute of Technology, Atlanta, Georgia.

Silver and gold nanoparticles, with diameters of 8 ± 2 nm and 11 ± 2 nm respectively, have been synthesized on a large scale in the presence of primary amines and have been found to undergo facile modification with thiolated ligands by a place exchange reaction at room temperature. The rate of the place exchange reaction has been monitored via fluorescence quenching of thiolated chromophores upon attachment to the metal nanoparticles. The reaction is fast and monitoring of the fluorescence allows one to monitor the exchange process from an early stage of the reaction. The fluorescence intensity decay as a function of time is bi-exponential suggesting two different adsorption-desorption pathways or processes. Chromophoric thiol, present at a roughly stoichiometric quantity needed to provide 100% coverage, was consumed almost quantitatively (>90%). TEM images show that the size distribution of silver nanoparticles changes upon place exchange but the size of gold nanoparticles is not significantly affected by the reaction. The optical properties of chromophoric thiol coated metal nanoparticles were investigated by using UV-visible absorption and fluorescence spectroscopy. The chromophoric thiols used were N-(12-dodecylthiol) carbazole (DTC), N,N'-Bis(3-methylphenyl)-N,N'-diphenylbenzidine dodecyloxythiol (TPDDT) and N,N'-Bis(3-methylphenyl)-N,N'-diphenylbenzidine propyloxythiol (TPDPT). Carbazoles are well known to form excimers in solution at high concentration or in polymers such as polyvinyl carbazole. Although, the surface concentration of carbazoles on the nanoparticles is very high, fluorescence spectra of carbazole modified silver and gold nanoparticles show no excimer emission. Quenching of the monomer emission is observed relative to that in dilute solution. For carbazole modified Au and Ag nanoparticles the fluorescence yield is factor of 100 and 10 time smaller than that for the free ligand in solutions, respectively. TPDDT coated gold nanoparticles show much lower fluorescence quenching than for carbazole and the fluorescence is twice as strong for gold as for silver nanoparticles. The fluorescence properties and photophysical mechanisms for the studied chromophoric thiol coated particles will be discussed.

11:15 AM DD17.10

Electric Field-Driven Route for Nanocrystal Synthesis Dong Soo Yun¹ and Angela M Belcher^{1,2}; ¹Materials Science, MIT, Cambridge, Massachusetts; ²Biological Engineering Division, MIT, Cambridge, Massachusetts.

To date, nanoparticle synthesis has been successfully demonstrated via either aqueous or non-aqueous solvents. Although metallic oxides are optimal materials for a wide variety of applications, the high equilibrium temperature ($T_e > 200^\circ\text{C} \sim 600^\circ\text{C}$) of phase formation makes their direct nanoparticle synthesis as well as single crystal oxide growth difficult at room temperature using pure aqueous solution. Little research has been done on metal oxides and metallic compounds using surfactant-free aqueous solvents because it is more difficult to make nanoparticles with well-controlled nanocrystalline properties such as crystallinity, shape, size and oxidation under these conditions. Here, we present a new method that uses high electric fields to form both polycrystalline and single crystal metal oxides, such as hafnium oxide, zirconium oxide, Iridium oxide, and iron oxide. Conditions for this synthesis include aqueous solution in less than one minute at room temperature without any additional processing steps. Non-aqueous solvent-mediated metal oxide, such as hafnium oxide and iron oxide single crystals, were also synthesized using this method. The quality of these materials suggest that this is an appropriate method for nanoparticle synthesis of pure metals and metallic compounds using surfactant-free aqueous solutions at room temperature without reducing agents. In addition, the synthesis of multi-component oxides of high equilibrium temperature ($T_e > 200^\circ\text{C}$) such as $\text{Hf}(\text{Zr},\text{Al})\text{O}_2$, was demonstrated at room temperature with reactions times under 5 minutes. These materials are not readily formed using traditional nanoparticle synthesis methods.

11:30 AM DD17.11

Galvanic Replacement Reaction on Multiply-twinned Ag Nanoparticles in an Organic Medium. Xianmao Lu¹, Marquez-Sanchez Manuel³ and Younan Xia¹; ¹Department of Chemistry, University of Washington, Seattle, Washington; ²Chemical Engineering, University of Texas at Austin, Austin, Texas; ³INEST Group, Philip Morris USA, Richmond, Virginia.

A variety of noble metal hollow nanostructures with tunable SPR can be synthesized with galvanic replacement reaction in aqueous solution by using sacrificial Ag templates and oxidizers composed of desired metals, such as Au, Pd, or Pt. Although we have reported a mechanistic study on the galvanic replacement reaction between Ag nanocubes and HAuCl_4 in an aqueous medium, it is still not clear how Ag multiply-twinned particles (MTPs) behave when they react with HAuCl_4 in an organic medium. Due to the rich vacancy and grain boundary defects and the rapid diffusion rate of atoms in small particles, the galvanic replacement process of Ag MTPs is expected to quite differently from that of single-crystal Ag nanocubes. Herein we present a systematic study on the galvanic replacement reaction between Ag MTPs ($d < 20\text{nm}$) and HAuCl_4 in an organic solvent. We closely monitored both morphological and spectral changes as the molar ratio of HAuCl_4 to Ag was increased. The details of reaction were found to be different from previous observations on single-crystal nanocubes and cubooctahedrons - the replacement reaction resulted in the formation of alloy nanorings and nanocages from Ag MTPs with a decahedral or icosahedral shape. The SPR peak of resultant hollow structures can be shifted to 740 nm, a wavelength sought by many biomedical applications. The effects of capping ligands and AgCl precipitate on the replacement reaction were also investigated.

11:45 AM DD17.12

Heterostructured Nanoparticles Directly Synthesized from Gas Phase YunHao Xu¹, Jianmin Bai^{1,2} and Jian-Ping Wang¹; ¹Department of Electrical and Computer Engineering, University of Minnesota, Minneapolis, Minnesota; ²Research Institute of Magnetic Materials, Lanzhou University, Lanzhou, Gansu, China.

Heterostructured nanoparticles are highly desirable in applications such as medical imaging, drug delivery, thermal cancer treatment and etc., which combine different properties of the individual component structure into one single nanoparticle and have possible enhancement of each properties [1-3]. Different from the previous two-step method used in both the chemical approach [4, 5] and physical vapor deposition approach [6], a "one-step" method is developed to synthesize heterostructured nanoparticles direct from gas phase. An integrated nanoparticle deposition system is used to fabricate the heterostructured nanoparticles in this study, which employs a vacuum based nanocluster deposition technique [7]. A magnetron sputter gun and a cooling chamber are the main components of the nanocluster source, where the magnetron gun is used to generate the atoms for particle formation and the whole process of heterostructured nanoparticle formation happened inside the cooling chamber. It has been demonstrated that a variety of heterostructures can be produced by using the method, including core-shell, multi-core-multi-shell, dumbbell, and sphere with

nodules. The heterostructure is formed by controlling the initial conditions of atom generating and the thermal environment in the nanocluster source. The initial conditions such as homogeneity and composition will affect the nucleation process at the beginning of particle formation. The initial conditions can be controlled by changing the sputtering conditions in the nanocluster source, where the atoms for particle formation are generated from. The thermal environment in the nanocluster source is related to the plasma density, density of sputtered atoms, pressure and carrier gas flow rate. Density of sputtered atoms is related to current used for sputtering. Pressure is adjusted by balancing the carrier gas flow rate and pumping speed. Results have been obtained from different materials systems including Co and Au [8], Fe and Ag [9], FeCo and Si [10], and FeCo and Au/Ag/Cu. Composition distribution and magnetic properties of the heterostructured nanoparticles have been characterized. [1] V. Skumryev, et al, Nature 423, 850 (2003). [2] E. Prodan, et al, Nano Lett. 3, 1411 (2003). [3] H. Kim, et al, J. AM. CHEM. SOC. 127, 544 (2005). [4] L. Jin, et al, J. Sol. Stat. Chem. 159, 26 (2001). [5] M. Chen, et al, J. Appl. Phys. 93, 7551 (2003). [6] J. Bai, J.-P. Wang, Appl. Phys. Lett., 87, 152502 (2005). [7] Y.H. Xu, et al, J. Appl. Phys. 97, 10J305 (2005) [8] Y.H. Xu, J.-P. Wang, Nano Lett., submitted for publication, 2006 [9] Y.H. Xu, et al, to be published. [10] J. Bai, et al, Nanotechnology, submitted for publication, 2006

SESSION DD18: Synthesis and Characterization of Nanoscale Materials III

Chairs: Masaru Kuno, Xiao-Min Lin, Ruth Pachter and Moonsub Shim

Friday Afternoon, April 13, 2007

Room 2001 (Moscone West)

1:30 PM DD18.1

Directed Synthesis of High-aspect-ratio Single crystal PbTe nanorods. Arup Purkayastha¹, Qingyu Yan¹, Darshan D Gandhi¹, Binay Singh¹, Theodarian Borca-Tasciuc² and Ganapathiraman Ramanath¹; ¹Department of Materials Science and Engineering, purkaa@rpi.edu, Troy, New York; ²Mechanical Aerospace and Nuclear Engineering, Rensselaer Polytechnic Institute, Troy, New York.

PbTe is a very important material for many applications such as thermoelectric refrigeration and power generation systems, photoconductive device components and infrared detectors. Nanostructuring is an attractive strategy to increase the thermoelectric figure of merit ZT by reaping the benefits of boundary scattering-induced thermal conductivity decrease and quantum-confinement-induced electrical conductivity increase. For example, quantum dot superlattices of PbSeTe/PbTe film exhibit ZT = 1.6, compared to ZT = 0.4 for bulk PbTe. An even higher ZT could be expected by introducing confinement in two dimensions, i.e., in nanorods and nanowires. Although sono-electrochemical synthesis of PbTe nanorods have been reported, the nanorod length is very small (100-200 nm), limiting its use for device fabrication. Here, we demonstrate a new solvothermal approach to direct the large scale sequential synthesis of ultra long 1-12 nm long single crystal PbTe nanorods with a diameter of ~60-250 nm by converting Te nanotubes of similar dimensions. The nanorod aspect ratio is between 10 to 36, which is the highest reported for PbTe. The Te nanotubes were prepared by solvothermal reduction of tellurium in the presence soft templates L-cystein ethylester dihydrochloride and cetyl ether (brij 52) in ethylene glycol. In situ reaction of the Te nanotubes with Pb salts and hydrazine, which serves as the reducing agent, converts the Te nanotubes into PbTe nanorods. The nanorod aspect ratio is inherited from the aspect ratio for the tellurium rods. X-ray diffraction, and energy dispersive X-ray spectroscopy (EDS) reveal the presence of near stoichiometric (50-50) trigonal PbTe phase. The Te nanotube length, and hence that of the nanorods can be adjusted by changing the concentration of cetyl ether and reaction temperature during Te nanotube synthesis. High resolution transmission electron diffraction analyses reveal that each PbSe rod is a single crystals with low defect concentration. In addition to the mechanism of PbTe nanorod formation, we will present the Seebeck coefficient and electrical conductivity of films of the PbTe nanostructures and individual nanorods.

1:45 PM DD18.2

Interfacial Synthesis of Platinum Nanowire Networks, Yujia Song¹, Robert M. Garcia^{1,2}, Rachel M. Dorin^{1,2}, Haorong Wang^{1,2}, Yan Qiu^{1,2} and John A. Shelnutt^{1,3}; ¹Nanostructure and Semiconductor Physics, Sandia National Laboratories, Albuquerque, New Mexico; ²Chemistry, Chemical & Nuclear Engineering, and Biology Department, The University of New Mexico, Albuquerque, New Mexico; ³Department of Chemistry, University of Georgia, Athens, Georgia.

Platinum nanowire networks are obtained via interfacial chemical reaction of platinum complex in chloroform with sodium borohydride in water under vigorous stirring. These wires range from 2 to 5 nm in diameter and are polycrystalline with junctions at every 10-20 nm in length on average. The key to the synthesis is to take advantage the unique environment brought about by the water/oil/surfactant interface. Platinum complexes were transferred from water phase to chloroform phase by dissolving surfactant in chloroform. Surprisingly, at a certain ratio between platinum salt and surfactant, the transfer of platinum to chloroform is complete as monitored by UV-vis spectra. Since control experiments in the absence of the water/oil interface conducted in either water or chloroform phase lead to platinum nanomaterials with different morphologies from the nanowire networks, it is expected that the interfacial environment plays a crucial role for the formation of the interconnected platinum nanowires. A possible mechanism is suggested. This new form of platinum is characterized by transmission and scanning electron microscopy, electron and X-ray diffraction, cyclic voltammetry, and nitrogen adsorption. The materials possess a high surface area (35 m²/g) and random pores in the range of 2 to 10 nm. This synthetic approach is simple, general, and can be used to prepare a variety of metal nanomaterials. For example, by control of the synthetic parameters, palladium nanoKoosh balls and gold nanowires can be obtained. These nanomaterials are expected to have a wide range of potential applications, including as catalysts. Sandia is multiprogram laboratory operated by Sandia Corporation, a Lockheed Martin Company, for the United States Department of Energy's National Nuclear Security Administration under Contract DEAC04-94AL85000.

2:00 PM DD18.3

Synthesis of Si/Ge Nanowire Heterostructures for Strain-Controlled Bandstructure Modification. Teresa J. Clement¹, David J. Smith², Jeff Drucker³ and S. Thomas Picraux^{1,4}; ¹School of Materials, Arizona State University, Tempe, Arizona; ²Center for Solid State Science, Arizona State University, Tempe, Arizona; ³Department of Physics and Astronomy, Arizona State University, Tempe, Arizona; ⁴Los Alamos National Laboratory, Los Alamos, New Mexico.

Strain in axial and core-shell Si/Ge nanowire heterostructures, grown via the vapor-liquid-solid mechanism, provides a unique opportunity for controlling bandstructures of specific nanostructures. The heterostructure growth process combines *in situ* gold seed evaporation on atomically clean Si (111) surfaces, *in situ* growth from Si and Ge gaseous precursors - either silane or disilane - germane or digermane, and real-time monitoring of nanowire growth via optical reflectometry. (Di)silane or (di)germane precursor selection adds an additional control by which we are

able to grow specific heterostructures - axial or core-shell. We show axial heterowires form more easily by catalyzing silane or germane at the Au eutectic seed, while core-shell heterowires grow more easily by stabilizing lateral growth using disilane or digermane. Our recently demonstrated strain mapping of nanowires based on geometric phase analysis of high resolution transmission electron microscopy (HRTEM) lattice imaging reveals the expected large strains present at the heteroepitaxial interfaces of these nanowires. The measured strain state of axial and core-shell heterostructure nanowires quantitatively correlates with that predicted using finite element, continuum elasticity modeling. For core-shell heterostructures, the relative strain between the core and shell depends on the core-to-shell diameter ratio. This strain partitioning provides the opportunity to use this ratio for strain engineering the electronic properties of the NW heterostructure. Using simple deformation potential-based electronic structure modeling, we demonstrate that the bandgap of a <111> oriented Ge core may be tuned over a much larger range than that of a Si core due to the position of the conduction band valleys in the Brillouin zone. Similar analysis applied to Si and Ge strained discs in axial heterostructures indicate the formation of quantum dots with large tunnel barriers will be possible. Our results combine optical reflectometry and strain-mapping to systematically design and reproducibility control the formation of novel Si/Ge heterostructured nanowires.

2:15 PM DD18.4

Synthesis of Epitaxially Aligned Ge/Si Core-shell Nanowires. Irene A. Goldthorpe¹, Joshua B. Ratchford², Christopher E.D. Chidsey² and Paul C. McIntyre¹, ¹Department of Materials Science and Engineering, Stanford University, Stanford, California; ²Department of Chemistry, Stanford University, Stanford, California.

Depositing a Si film around a Ge nanowire (NW) creates a structure with additional advantageous properties beyond that of a single element Si or Ge NW. A heteroepitaxially grown shell may allow for engineering of strain in both the shell and the inner core. Moreover, the valence band offset may allow confinement of holes to the core, reducing the influence of surface defects in carrier scattering for p-type NWs. The Ge-core/Si-shell arrangement is desirable for the higher carrier mobilities of Ge and the superior properties of SiO₂ passivation. In this work, vertically aligned Ge/Si core-shell NWs have been synthesized by CVD. First, Ge NWs were heteroepitaxially grown on Si(111) substrates; the NW diameter was controlled through the use of monodisperse Au nanoparticles as the catalysts. Silane was then used to deposit the shell. The Au remaining on the Ge NW tips is problematic since (i) the Au can catalyze unwanted Si NW growth and (ii) the Au particles at the NW tips diffuse into the structure at the temperatures required to obtain single crystalline Si shells. Our experiments have investigated a wet chemical etching procedure for Au removal from the Ge NWs with a KI/I₂-based solution. This solution does not appear to etch the NW surface, allowing a heteroepitaxial shell to be obtained following the etching procedure. We have also researched the deposition conditions which dictate whether three-dimensional Si islands or a continuous amorphous, polycrystalline, or crystalline Si film forms around the Ge cores during the subsequent Si growth step, and these results will be summarized.

2:30 PM DD18.5

Diameter Dependence of Interfacial Abruptness in Si/Si_{1-x}Ge_x Heterostructure Nanowires Grown via Vapor-Liquid-Solid Growth. Trevor Edward Clark^{1,2}, Elizabeth C. Dickey^{1,2}, Kok-Keong Lew^{1,2}, Pramod Nimmatoo^{1,3}, Ling Pan¹ and Joan M. Redwing^{1,2,3}, ¹Materials Science and Engineering, Penn State, University Park, Pennsylvania; ²Materials Research Institute, Penn State, University Park, Pennsylvania; ³Chemical Engineering, Penn State, University Park, Pennsylvania.

Si/Si_{1-x}Ge_x heterostructure nanowires (hNWs) have potential as components in high performance electronic, photonic and thermoelectric devices. Successful implementation in such devices, however, requires the ability to modulate the axial composition of the wire and form abrupt interfaces. In the vapor-liquid-solid (VLS) process, crystallization occurs from the liquid phase, consequently changes in wire composition are dependent on the ability to rapidly vary the liquid-phase composition. In this study, we investigate interfacial abruptness in Si/Si_{1-x}Ge_x hNWs grown via gold-mediated VLS growth in a low pressure chemical-vapor-deposition reactor. The hNWs are grown using SiH₄ and GeH₄ precursor gases in an H₂ carrier gas on oxidized Si wafers coated with thin (<2nm) Au films. The resultant hNWs have diameters between 10 and 120 nm. Compositional profiles of the hNWs are obtained via intensity profiles from high-angle annular dark-field scanning transmission electron microscopy (HAADF STEM). Radial profiles reveal that the leading edge of the Si/Si_{1-x}Ge_x interface is non-planar with a parabolic shape (Ge enrichment along the central axis of the hNWs). Axial profiles reveal that the leading edge (when GeH₄ is added to the inlet gas) can be modeled by an error function. This suggests that the shape and abruptness of this interface is dictated by Ge diffusion from a finite source into a semi-infinite medium. Profiles from the trailing edges (GeH₄ removed from inlet gas) can be modeled by an exponential decay. The abruptnesses of both edges are dependent on diameter, with the abruptness improving with decreasing diameter. The known duration for synthesis of each block also enables determination of the respective growth rates. The growth rates have a negative diameter-dependence consistent with a Gibbs-Thomson effect. The ramifications of these results on axial doping of hNWs grown via VLS will be discussed.

2:45 PM DD18.6

Growth and Electrical Properties of Epitaxial Silicon Nanowires grown by Vapor-Liquid-Solid Growth on (111)Si Substrates Sarah M. Dilts¹, Rebeca C. Diaz², Chad M. Eichfeld¹, Bangzhi Liu¹, Suzanne E. Mohney¹, Theresa S. Mayer² and Joan M. Redwing^{1,2}, ¹Materials Science and Engineering, Penn State University, University Park, Pennsylvania; ²Electrical Engineering, The Pennsylvania State University, University Park, Pennsylvania.

High density arrays of epitaxially-oriented silicon nanowires (SiNWs) are of interest for the fabrication of vertical wrap-gate nanowire transistors. These structures have traditionally been fabricated by the vapor-liquid solid technique using Au thin films deposited on (111)Si substrates and SiCl₄ as the source gas for wire growth. In this process, epitaxial orientation of the nanowires is believed to be promoted by a combination of high growth temperature (~900°C) and the presence of HCl, which acts to etch oxide from the substrate surface. Our initial studies have focused on investigating the effect of growth conditions on wire orientation, structure and growth rate with the aim of developing a better understanding of the role of growth chemistry in this process. Silicon nanowire arrays were fabricated using 1 nm Au thin films deposited on (111)Si substrates in an atmospheric pressure hot-wall quartz tube reactor using SiCl₄ as the source gas in an H₂ carrier gas. Wire orientation was found to be strongly dependent on the growth temperature with ~ 80% of the SiNWs being <111> oriented perpendicular to the substrate at 900°C but dropping to ~18% at 800°C. At low SiCl₄ partial pressures (P_{SiCl₄}), the growth rate of the wires increases with increasing P_{SiCl₄} reaching a maximum of ~ 3 µm/min at P_{SiCl₄} of 3.7 Torr.

Beyond this point, the growth rate begins to decrease with increasing P_{SiCl_4} due to a shift in gas phase chemistry which promotes the reverse HCl etching reaction similar to what is observed in thin film deposition. The resistivity of nominally undoped SiNWs grown under these conditions was studied using four-point measurements carried out on individual SiNWs released from the substrate by ultrasonic agitation and assembled onto pre-patterned back-gated test structures using field-assisted assembly. Nominally undoped SiNWs grown on p-type (111)Si substrates ($\rho=1-15\ \Omega\text{-cm}$) were determined to be p-type with a room-temperature resistivity on the order of $800\ \Omega\text{-cm}$, indicating the presence of unintentional acceptors in the nanowires. By using high resistivity ($\rho=2000-10000\ \Omega\text{-cm}$) (111)Si substrates, the wire resistivity increased approximately one order of magnitude, indicating that dopants in the substrate are incorporated in the wires during growth and contribute, in part, to the background electrical properties of the nanowires.

3:30 PM DD18.7

Atomic, Electronic, and Three-Dimensional Characterization of Core/Shell Nitride Nanowires. Ilke Arslan¹, Alec Talin¹, Francois Leonard¹ and George T. Wang²; ¹Sandia National Laboratories, Livermore, California; ²Sandia National Laboratories, Albuquerque, New Mexico.

Semiconductor nanowires are being developed as nanoscale building blocks for a variety of new nano-device applications. With these new developments comes a need for sophisticated characterization of the materials properties of the nanowires. The traditional technique of two dimensional (2-D) transmission electron microscopy (TEM), which has thus far been useful for the study of single crystals where the third dimension is uniform, is no longer sufficient to characterize the complex, three dimensional (3-D) structures that define nanotechnology. Therefore, to gain a full understanding of the structure-property relationships of the nanowires, we use a combination of atomic-resolution imaging, atomic-resolution electron energy-loss spectroscopy (EELS), energy dispersive x-ray (EDX) spectroscopy, and three dimensional imaging in the scanning transmission electron microscope (STEM). In particular, it is important to understand the morphology of the nanowires in 3-D since their materials properties are controlled by their 3-D shape and size. The relatively new technique of STEM tomography that we highlight in this paper allows us to reconstruct nanostructures with a resolution approaching 1nm in all three spatial dimensions. Here we present a comprehensive study of GaN/AlN core/shell nanowires, which could have applications in nanophotonics and high mobility nanoelectronics. Using STEM tomography, we are able to directly image the size, shape and morphology of the nanowires in three dimensions. Interestingly, while prior conductivity measurements indicate that the GaN/AlN nanowires are more conductive than GaN in general, there are some cases in which GaN/AlN nanowires of the same length and diameter can be insulating. Our results suggest that this may be due to a discontinuity of the GaN core observed in some of the nanowires, leading to a bamboo-like structure. We will present a detailed analysis comprising 2-D STEM images and 3-D tomograms (providing nanowire morphology) as well as the complementary information from EELS and EDX spectra (providing nanowire compositional analysis). Work at Sandia is supported by the Department of Energy, under contract DE-AC04-94AL85000.

3:45 PM DD18.8

Selective Plating on n-Type Silicon Nanowires for Junction Delineation and Nanostructure Fabrication Chad M. Eichfeld^{1,2}, Carolyn Wood^{2,3}, Sarah M. Dilts¹, Bangzhi Liu¹, Joan M. Redwing^{1,2} and Suzanne E. Mohny^{1,2}; ¹Department of Materials Science and Engineering, Pennsylvania State University, University Park, Pennsylvania; ²Center for Nanoscale Science, Pennsylvania State University, University Park, Pennsylvania; ³Department of Physics, Illinois Institute of Technology, Chicago, Illinois.

The in situ growth of p-n junctions in silicon nanowires enables the fabrication of a variety of nanoscale electronic devices. We have developed a method for selective coating of Au onto the n-type segments of silicon nanowire p-n junctions, providing feedback into the study of the growth of nanowire homojunctions. Selective plating allows for quick verification of the position of p-n junctions along the nanowire using scanning or transmission electron microscopy, and it allows for measurement of the length of the p- and n-type segments. Dopant modulated silicon nanowires were fabricated using Au-catalyzed vapor-liquid-solid growth using SiH₄ as the source gas and PH₃ for n-type doping. Nanowires were fabricated with multiple n+ segments of increasing length that were grown between nominally 1 μm long p- segments. Segments of n-type silicon as short as 100 nm in nanowires that were 100 nm in diameter have been plated. Selective plating is furthermore attractive for placing Au catalyst at preset locations along a silicon nanowire for subsequent vapor-liquid-solid growth. The electrochemical mechanism for the selectivity of the plating process is also discussed.

4:00 PM DD18.9

Springs, Rings, and Spirals of Rutile-Structured Tin Oxide Nanobelts. Rusen Yang and Zhong Lin Wang; Materials Science and Engineering, Georgia Institute of Technology, Atlanta, Georgia.

Synthesis of nanomaterials with well controlled size, morphology and chemical composition has attracted increasing interests, because those novel nanostructured materials are crucial for exploring the chemical and physical properties of those materials originating from their shape, decreased dimension size and crystallographic structure. Wurtzite structured ZnO has been synthesized in the formation of single-crystalline nanorings, nanosprings and nanospiral, [1, 2] which was proposed to be related to the non-central symmetry of wurtzite structure and the spontaneous polarization. In agreement to the polarization induced growth model, we have discovered for the first time the formation of single-crystalline SnO₂ springs, rings and spirals [3]. All of the SnO₂ nanostructures were synthesized using a solid-vapor process in a horizontal tube furnace and their composition, morphology and crystallographic structure were confirmed by EDS, SEM and TEM. A detail analysis showed that the growth of those nanomaterials could be also understood on the basis of polar surfaces of the rutile-structured SnO₂. The SnO₂ nanobelts that made of the ring/spring grew along $\sim[0-11]$ with dominant $\pm(011)$ polar side surfaces. Bending of the belt to form a ring can decrease the electrostatic energy from the spontaneous polarization. The minimization of the total energy contributed by electrostatic polarization energy and elastic deformation energy determines the final morphology of the SnO₂ nanobelt, resulting in the formation of the ring, multiply looped spiral or even helical structure. [1] (a) X.Y. Kong; Z.L. Wang, Nano Lett. 3 (2003) 1625-1631. (b) X.Y. Kong; Z.L. Wang; Appl. Phys. Lett. 84 (2004) 975-977. (c) X.Y. Kong; Y. Ding; R.S. Yang; Z.L. Wang, Science, 303 (2004) 1348-1351. (d) R.S. Yang; Y. Ding; Z.L. Wang, Nano Lett. 4 (2004) 1309-1312 [2] R.S. Yang, Z.L. Wang, J. Am. Chem. Soc. 128 (2006) 1466-1467.

4:15 PM DD18.10

Synthesis and Characterization of Novel Nanostructured Thermoelectric Materials. Xiaofeng Qiu^{1,2} and Clemens Burda^{1,2}; ¹Center for Chemical Dynamics and Nanomaterials Research, Case Western Reserve University, Cleveland, Ohio; ²Chemistry, Case Western Reserve

University, Cleveland, Ohio.

We demonstrated the successful synthesis of Bi₂Se₃ heterostructure nanowires and PbTe nanorods via a novel sonoelectrochemical method in aqueous solution at room temperature, which are very promising building blocks for future thermoelectric devices. By using electrochemical analysis, we found that the ligand to cation ratio played a very important role in the determination of the product purity. Our sonoelectrochemical setup provides sufficient parameters to fine tune the structure of the product. Besides Bi₂Se₃ and PbTe, the sonoelectrochemical technique can also be applied for the synthesis of other promising nanomaterials. Thus, this method can be a very powerful new tool for nanoscientists to prepare novel building blocks for future nanostructure-based devices. Besides the sonoelectrochemical approach, we also developed a wet chemical method to fabricate nanostructured Bi₂Se₃ thin films. The morphologies and coverage of the thin film can be varied. The transport properties of the thin film were studied and an improved Seebeck coefficient was obtained. This method shows a promising way to prepare nanostructured thermoelectric thin films and provide scientists in the field with a possible solution for fabricating better thermoelectric devices.

4:30 PM DD18.11

Synthesis of Diameter-controlled Bismuth Nanowires using Porous Anodic Alumina Template Coated by Atomic Layer Deposition.

Kyungeun Lee, Bo Kyung Ahn, Sihyeong Kim, Changdeuck Bae and Hyunjung Shin; School of Advanced Materials Engineering, Kookmin University, Seoul, South Korea.

We present a strategy for the fabrication of Bi nanowires with precisely controlled diameter. Our approach combines template-directed atomic layer deposition (ALD) technique with electrochemical deposition that allows atomic-level control over pore diameters in the original templates and thus over the diameter of metal nanowires. Various oxide layers of ZrO₂, TiO₂ or Al₂O₃ onto anodic aluminum oxide (AAO) templates with the pores of ~60 nm in diameter were deposited to reduce the size of pores. Ultra-precision control over the wall thickness of the oxide nanotubes is already shown in our research group [1]. The controlled diameters of the inner pores in oxide coated AAO templates were 53, 44, and 36 nm, respectively. Surface treatment of the inner walls of the oxide nanotubes was conducted to make them hydrophilic to enhance the diffusion of Bi precursor ions during the electrochemical deposition. It is noted that the fabrication of the Bi nanowires in ZrO₂-coated nanopores is more effective than that in TiO₂. Diameters of the fabricated Bi nanowires correspond to the sizes of pores. We choose Bi as a model material in which the quantum confinement of electrons can be clearly observed as a function of wire diameter. Transport properties as functions of Bi nanowires' diameters are discussed. Acknowledgement This work was supported by the Center for Nanostructured Materials Technology of the Korean Ministry of Science and Technology (M105K0010026-06K1501-02610). [1] H. Shin, D.-K. Jeong, J. Lee, M. M. Sung, J. Kim, Adv. Mater. 2004, 16, 1197.

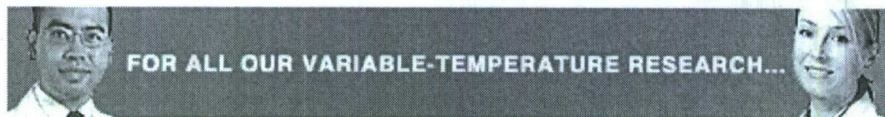
4:45 PM DD18.12

High Aspect Ratio Nanowires: New Opportunities in Synthesis and Assembly Byron Gates, Nazanin Mabrhan-Shafiee, Nathanael Sieb and Elham Majidi; Chemistry, Simon Fraser University, Burnaby, British Columbia, Canada.

New opportunities exist in the synthesis and assembly of high aspect ratio nanowires. It is, hypothetically, much easier to incorporate individual nanowires rather than nanorods into the appropriate test devices to characterize electrical properties of the nanostructured material. Standard lithography tools could be used to pattern the appropriate electrodes for characterizing high aspect ratio nanowires. The appropriate choice of synthetic techniques is, however, essential to achieve nanowires with the necessary aspect ratios for incorporation into these test devices. This presentation will cover recent advances in the development of solution phase synthesis of these nanostructures. Solution phase techniques were chosen, in part, for the ease of incorporating dopants, versatility of surface modification, and simplicity of scaling-up the synthesis to large quantities. Assembly of these nanostructures is increasingly challenging as the aspect ratio also increases. Techniques are presented that address the issues of dispersion, entanglement, and placement of these nanowires into well-defined patterns.



World-Class Surface Metrology Instruments
SPM/AFMs | Profilometers | Interferometers



FOR ALL OUR VARIABLE-TEMPERATURE RESEARCH...



WE APPLY NANOMANUFACTURING TECHNOLOGY

APPLY NOW



© 1995-2008, Materials Research Society 506 Keystone Drive, Warrendale, PA, 15086-7573, USA
Phone: 724 779.3003, Fax: 724 779.8313, Email: [Customer Service](#), [Member Service](#), [Feedback](#)